

Mission of the Global Monitoring Division:

To acquire, evaluate, and make available accurate, long-term records of atmospheric gases, aerosol particles, and solar radiation in a manner that allows the causes of change to be understood.

Conference Website:

<http://www.esrl.noaa.gov/gmd/annualconference/>

Purpose of the Global Monitoring Annual Conference:

To bring together preeminent scientists to discuss the latest findings in climate research and how to integrate science, observations and services to better serve society.

Terms of use:

Material in this document may be copied without restraint for library, abstract service, educational, or personal research purposes. All other uses are prohibited without prior consent from authors.

This report may be cited as:

45th Global Monitoring Annual Conference, 2017 Program and Abstracts Booklet,
NOAA Earth System Research Laboratory, Global Monitoring Division

This report compiled and distributed by:

NOAA Earth System Research Laboratory
Global Monitoring Division
325 Broadway, R/GMD1
Boulder, CO 80305
<http://www.esrl.noaa.gov/gmd>



UNITED STATES DEPARTMENT OF COMMERCE
National Oceanic and Atmospheric Administration
Office of Oceanic and Atmospheric Research
Earth System Research Laboratory
325 Broadway – David Skaggs Research Center
Boulder, Colorado 80303-3337

NOAA Earth System Research Laboratory **45th Global Monitoring Annual Conference**

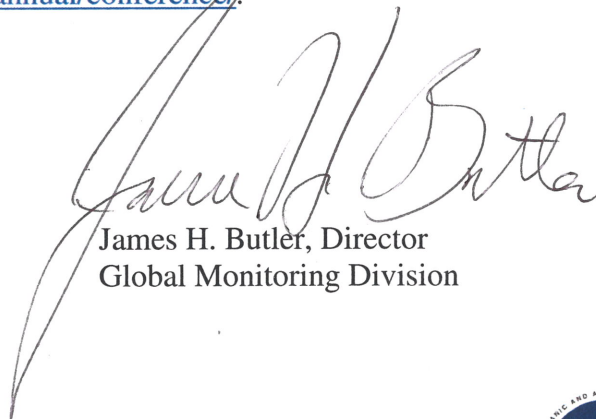
May 23-24, 2017
Boulder, Colorado

45 years! We have a mixed sense of pride and amazement that the 2017 Global Monitoring Annual Conference marks the 45th time we have convened researchers from around the world to discuss the latest observations, measurement techniques, data interpretation, and network operations in a collaborative and small setting.

The Global Monitoring Division of NOAA's Earth System Research Laboratory welcomes you to the 2017 conference. Hosting this annual gathering is a hallmark of GMD and highlights our dedication to the global research community to collectively improve our knowledge base practices. Year-in and year-out, the goal of the conference remains steadfast, to create a forum for thoughtful and lively discussion on research from sustained measurement records and what it takes to understand them.

Long-term records are critical for understanding complex climate system variables and the effort truly requires the expertise of a global community. Thank you for joining us! We look forward to the discussions and hope you agree that the 45th Global Monitoring Annual Conference is informative, inspiring, and relevant to the most pressing questions facing society today.

The conference agenda and abstracts from all presentations and posters at the conference are available at <http://www.esrl.noaa.gov/gmd/annual/conference/>.



James H. Butler, Director
Global Monitoring Division



NOAA Atmospheric Baseline Observatories

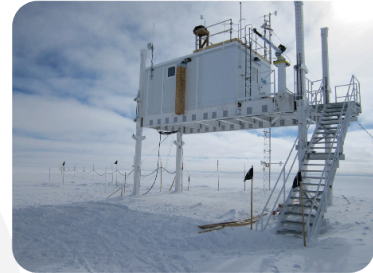
Barrow, Alaska



Trinidad Head, California



Summit, Greenland



Mauna Loa, Hawaii

American Samoa



South Pole

Barrow, Alaska (est. 1973), 71.32° North, 156.61° West

Trinidad Head, California (est. 2002), 41.05° North, 124.15° West

Mauna Loa, Hawaii (est. 1957), 19.53° North, 155.57° West

Cape Matatula, American Samoa (est. 1974), 14.24° South, 170.56° West

South Pole, Antarctica (est. 1957), 90.00° South, 24.80° West

Summit, Greenland (est. 2010), 72.58° North, 38.48° West

NOAA ESRL GLOBAL MONITORING ANNUAL CONFERENCE 2017

David Skaggs Research Center, Room GC-402
325 Broadway, Boulder, Colorado 80305 USA

Tuesday Morning, May 23, 2017 AGENDA

(Only presenter's name is given; please refer to abstract for complete author listing.)

		Page No.
07:00	Registration Opens in GC-402 - lunch orders and posters collected at registration table	
07:30 - 08:15	Morning Snacks - coffee, tea, fruit, bagels and donuts served	
Session 1	Welcome, Keynote Address & Highlights — Chaired by Russell C. Schnell	
08:15 - 08:30	Welcome and Conference Overview <i>James H. Butler (NOAA Earth System Research Laboratory, Global Monitoring Division (GMD))</i>	-
08:30 - 09:00	Keynote Address - Climate, Melting Ice And Rising Seas: Observing and Understanding to Reduce Risks <i>Richard B. Alley (The Pennsylvania State University, Department of Geosciences, and Earth and Environmental Systems Institute)</i>	1
09:00 - 09:15	Highlighted Speaker - Implications of the Continued Increase in Atmospheric Methane Burden <i>Edward J. Dlugokencky (NOAA Earth System Research Laboratory, Global Monitoring Division (GMD))</i>	2
09:15 - 09:30	Highlighted Speaker - Black Carbon Measurements at Cape Grim, Tasmania <i>Fabienne Reisen (Commonwealth Scientific and Industrial Research Organisation (CSIRO), Oceans and Atmosphere, Aspendale, Australia)</i>	3
09:30 - 09:45	Highlighted Speaker - Ozone, Aerosol and Carbon Gases at the Mt. Bachelor Observatory <i>Dan Jaffe (University of Washington)</i>	4
9:45 - 10:15	Morning Break & Group Photo on the Stage	
Session 2	Carbon Cycle & Greenhouse Gases - Global Observations — Chaired by Stefan Schwietzke	
10:15 - 10:30	How We Know that Human Activities Are Driving Climate Change <i>Pieter P. Tans (NOAA Earth System Research Laboratory, Global Monitoring Division (GMD))</i>	5
10:30 - 10:45	Sources of Systematic Differences in Global CO ₂ Inverse Model Results <i>Benjamin Gaubert (National Center for Atmospheric Research (NCAR), Atmospheric Chemistry Observations and Modeling Laboratory)</i>	6
10:45 - 11:00	10 Years of Observation for Greenhouse Gases by Commercial Airlines In the CONTRAIL Project <i>Yousuke Sawa (Meteorological Research Institute, Tsukuba, Japan)</i>	7
11:00 - 11:15	Nitrous Oxide Emissions Estimated with the Carbon Tracker-Lagrange North American Regional Inversion Framework <i>Cynthia Nevison (Institute of Arctic and Alpine Research (INSTAAR), University of Colorado)</i>	8
11:15 - 11:30	Vertical Gradients in Atmospheric CO ₂ as a Constraint on Southern Ocean Fluxes <i>Kathryn McKain (Cooperative Institute for Research in Environmental Sciences (CIRES), University of Colorado)</i>	9
11:30 - 11:45	Toward Improvement on Estimation of North American CO ₂ Fluxes from CarbonTracker-Lagrange: A High-Resolution Regional Inverse Modeling System for Assimilating Atmospheric CO ₂ <i>Lei Hu (Cooperative Institute for Research in Environmental Sciences (CIRES), University of Colorado)</i>	10
11:45 - 12:00	Multi-species Atmospheric Inversion of Sectoral Greenhouse Gas Emissions in the Indianapolis Urban Environment <i>Brian Nathan (The Pennsylvania State University, Department of Meteorology)</i>	11
12:00 - 13:00	Catered Lunch - Outreach Classroom GB-124 (pre-payment of \$12.00 at registration)	

NOAA ESRL GLOBAL MONITORING ANNUAL CONFERENCE 2017

David Skaggs Research Center, Room GC-402
325 Broadway, Boulder, Colorado 80305 USA

Tuesday Afternoon, May 23, 2017 AGENDA

(Only presenter's name is given; please refer to abstract for complete author listing.)

Page No.

Session 3	Global Radiation — Chaired by Allison McComiskey	
13:00 - 13:15	Surface Energy Budget Process Relationships as a Means for Evaluating Model Performance in Central Greenland <i>Matthew Shupe (Cooperative Institute for Research in Environmental Sciences (CIRES), University of Colorado)</i>	12
13:15 - 13:30	Drivers and Environmental Responses to the Changing Annual Snow Cycle of Northern Alaska <i>Christopher J. Cox (Cooperative Institute for Research in Environmental Sciences (CIRES), University of Colorado)</i>	13
13:30 - 13:45	Arctic Heat Waves: Towards Quantifying the Role of Atmospheric Dynamics <i>Robert S. Stone (Science and Technology Corporation)</i>	14
13:45 - 14:00	Changing Air Quality in the Southeast U.S. and Potential Implications for Regional Solar Radiation Budget <i>James Patrick Sherman (Appalachian State University, Department of Physics and Astronomy)</i>	15
14:00 - 14:15	Surface-measured Trends of Aerosol Optical Depth as an Indicator of Stratospheric Aerosol Trends <i>John Augustine (NOAA Earth System Research Laboratory, Global Monitoring Division (GMD))</i>	16
14:15 - 14:30	The Hazy Space Between Cloud and Aerosol <i>Chuck Long (Cooperative Institute for Research in Environmental Sciences (CIRES), University of Colorado)</i>	17
14:30 - 14:45	Two Centuries of Volcanic Aerosols Derived from Lunar Eclipse Records, 1805-2015 <i>Richard A. Keen (University of Colorado, Emeritus, Department of Atmospheric and Oceanic Sciences)</i>	18
14:45 - 15:15	Afternoon Break	
Session 4	Carbon Cycle & Greenhouse Gases - Isotopes — Chaired by Arlyn Andrews	
15:15 - 15:30	Detecting Trends in Fossil Fuel Emissions with $^{14}\text{CO}_2$ in the Presence of Transport Errors and Biased Inventories <i>Sourish Basu (Cooperative Institute for Research in Environmental Sciences (CIRES), University of Colorado)</i>	19
15:30 - 15:45	Optical Detection of Radiocarbon (^{14}C) Below Modern Levels by Cavity Ring-down Spectroscopy <i>Adam J. Fleisher (National Institute of Standards and Technology (NIST))</i>	20
15:45 - 16:00	Unexpected and Significant Biospheric CO_2 Fluxes in the Los Angeles Basin Indicated by Atmospheric Radiocarbon ($^{14}\text{CO}_2$) <i>John B. Miller (NOAA Earth System Research Laboratory, Global Monitoring Division (GMD))</i>	21
16:00 - 16:15	Constraining Biospheric Exchange Processes Over North America by Joint Assimilation of Atmospheric CO_2 and $\delta^{13}\text{C}$ <i>Ivar R. van der Velde (Cooperative Institute for Research in Environmental Sciences (CIRES), University of Colorado)</i>	22
16:15 - 16:30	Gaseous Reference Materials to Underpin Measurements of Amount Fraction and Isotopic Composition of Greenhouse Gases <i>Paul Brewer (National Physical Laboratory, Teddington, United Kingdom)</i>	23
16:30 - 16:45	Calibration Strategies for FTIR and Other IRIS Instruments for Accurate $\delta^{13}\text{C}$ and $\delta^{18}\text{O}$ Measurements of CO_2 in Air <i>Joële Viallon (Bureau International des Poids et Mesures (BIPM), Sèvres, France)</i>	24
17:00 - 20:00	Poster Session (DSRC Cafeteria) with appetizers and refreshments	

Keynote Address - Climate, Melting Ice and Rising Seas: Observing and Understanding to Reduce Risks

R.B. Alley

The Pennsylvania State University, Department of Geosciences, and Earth and Environmental Systems Institute, University Park, PA 16802; 814-863-1700, E-mail: rba6@psu.edu

Sea-level rise is ongoing from thermal expansion of the ocean, melting mountain glaciers, small changes in the great ice sheets, and perhaps from changing groundwater storage. Climate history shows strongly that past rises in CO₂ have driven warming that forced sea-level rise, supporting physical understanding and models that additional rise is almost unavoidable, with amount and rate depending especially on carbon dioxide (CO₂) emissions. Large deviations from the mean rise can occur locally, due to the effects of changes in winds and currents, as well as local ground motion from tectonic processes, ongoing response to the end of the ice age, local withdrawal or injection of fluids, and other processes. Thus, providing policymakers and the public with actionable assessments and projections of local mean rise and risks of extrema requires multifaceted, accurate measurement and modeling spanning atmosphere, ocean, ice and the not-so-solid Earth. The potential exists for threshold-crossing behavior in ice sheets causing rapid ice-cliff failure (see Figure) that could greatly increase sea-level rise - we may plan for less than a meter in the next century or so with an uncertainty smaller than the mean, and instead get several meters. The research required to assess the associated risks overlaps with that for smaller rise but includes many additional issues. Costs of sea-level rise likely are notably super-linear, increasing perhaps as the square of the rise, or some other power greater than one. Perhaps non-intuitively, this in turn means that ice-sheet collapse would increase the societal costs associated with rise from other sources, and thus increase the value of knowledge of the full suite of processes affecting sea level. Great challenges remain to model these processes and provide accurate projections, especially near tipping points, for the full range of possible forcings. Maintenance and extension of key observational datasets on atmosphere, ocean and ice will help guide process-based studies and enable model improvements through data assimilation, greatly advancing understanding and societally useful projections.



Figure 1. The ~100 m-high calving front of Jakobshavn Glacier, Greenland is near failure. Retreat in West Antarctica could generate even higher cliffs with faster failure, driving rapid sea-level rise. Photo by R. Alley.

Highlighted Speaker - Implications of the Continued Increase in Atmospheric Methane Burden

E.J. Dlugokencky¹, M.J. Crotwell^{2,1}, A.M. Crotwell^{2,1}, P.M. Lang¹, L. Bruhwiler¹, A.Q. Wang¹ and K. Thoning¹

¹NOAA Earth System Research Laboratory, Global Monitoring Division (GMD), Boulder, CO 80305; 303-497-6228, E-mail: ed.dlugokencky@noaa.gov

²Cooperative Institute for Research in Environmental Sciences (CIRES), University of Colorado, Boulder, CO 80309

Measurements of methane (CH_4) from weekly air samples collected in GMD's cooperative global air sampling network provide an important constraint on the global CH_4 budget. In 2016, atmospheric CH_4 continued to increase, and the average rate of increase during 2014 to 2016 was ~ 11 ppb yr^{-1} . In contrast, the growth rate of atmospheric CH_4 was near-zero from 1999 to 2006. While atmospheric CH_4 's current rate of increase is still lower than it was in the early-1980s, emissions are likely greater now than any time since NOAA measurements began in 1983. Figure 1 shows emissions estimated from a 1-box mass balance using the observed global annual mean burden and annual increase combined with an estimate of CH_4 's lifetime. With the assumption of no trend in lifetime, we found no trend in emissions from 1984-2006 (blue circles and dashed line). This result contrasts with Emission Database for Global Atmospheric Research (EDGAR) anthropogenic emissions plus a fixed amount for natural emissions (red triangles), which shows a significant trend driven mostly by increased production and use of fossil fuels. In 2007, our estimate of emissions from the observations increased above the 1984-2006 trend, then increased further starting in 2014. We've identified changing tropical emissions related to precipitation as a likely major contributor to the renewed increase in atmospheric CH_4 , but many additional processes must also be involved. The details of the causes, although still not known, are important for CH_4 's future impact on climate.

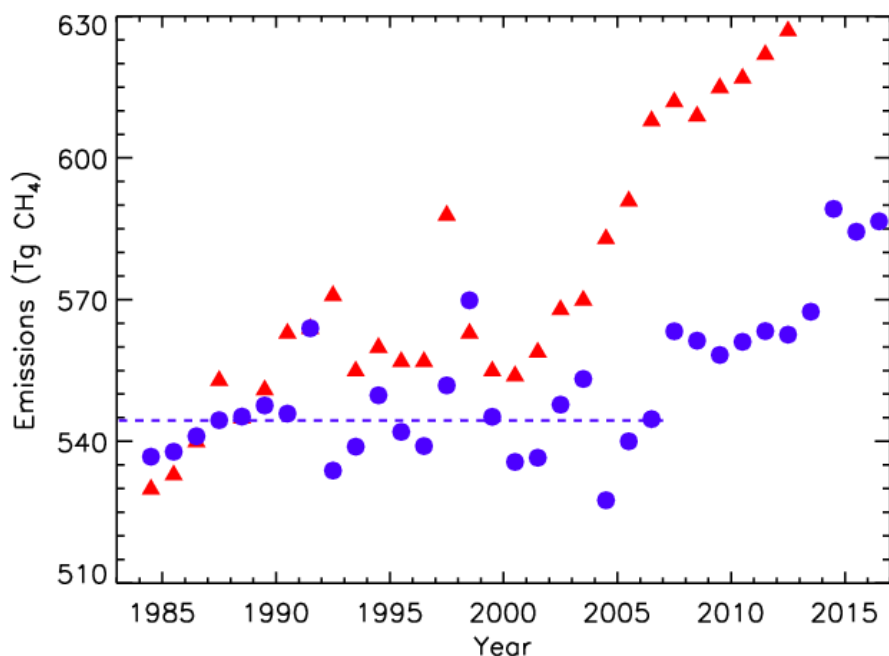


Figure 1. Total global CH_4 emissions determined from observations (blue) and from EDGAR inventory plus fixed natural emissions (red). Observation-based estimates are based on mass balance using CH_4 global annual means and annual increase and a constant lifetime of 9.1 yr to calculate loss. The dashed line is a straight line fitted to the annual emissions from 1984-2006 (slope = 0 ± 0.6 Tg CH_4 yr^{-1} ; 95% CI). We add 245 Tg CH_4 yr^{-1} natural emissions to EDGAR's anthropogenic emissions to get total global emissions.

Highlighted Speaker - Black Carbon Measurements at Cape Grim, Tasmania

F. Reisen, J. Gras, J. Ward and M. Keywood

Commonwealth Scientific and Industrial Research Organisation (CSIRO), Oceans and Atmosphere, Aspendale, Australia; +61-3-9239-4435, E-mail: fabienne.reisen@csiro.au

Black carbon (BC) measurements have been made at Cape Grim, on the northwest coast of Tasmania, using a Mutli-Angle Absorption Photometer (MAAP) since 2007. In 2015 a Photoacoustic Extinctionmeter (DMT PAX-870 nm) that measures absorption and scattering at 870 nm and a Tricolor Absorption Photometer (TAP-NOAA/Brethel) that measures absorption at 467, 528 and 652 nm were installed at Cape Grim.

Here we report on the BC observations made at Cape Grim between 2011 and 2017. Monthly median BC concentrations ranged from 3-33 ng/m³ with lowest levels measured in summer and highest levels measured in winter. Daily BC concentrations ranged from 0.07 to 4483 ng/m³; the very high BC concentrations were measured during the Tasmanian fires in January and February 2016. As a result of the extensive fires in January and February impacting on the measurement site at Cape Grim, the yearly averaged concentration for 2016 was 61 ng/m³, approximately twice the yearly averaged BC concentrations measured in previous years. Taking into consideration all wind directions, the main contributors to BC at Cape Grim were northern Tasmania and Melbourne eastern Victoria, with low BC concentrations measured during baseline conditions (marked by white lines in Figure 1).

The presentation will also report on comparisons between BC concentrations measured from 2015 and 2017 using three different BC measurement instruments (MAAP, PAX and TAP).

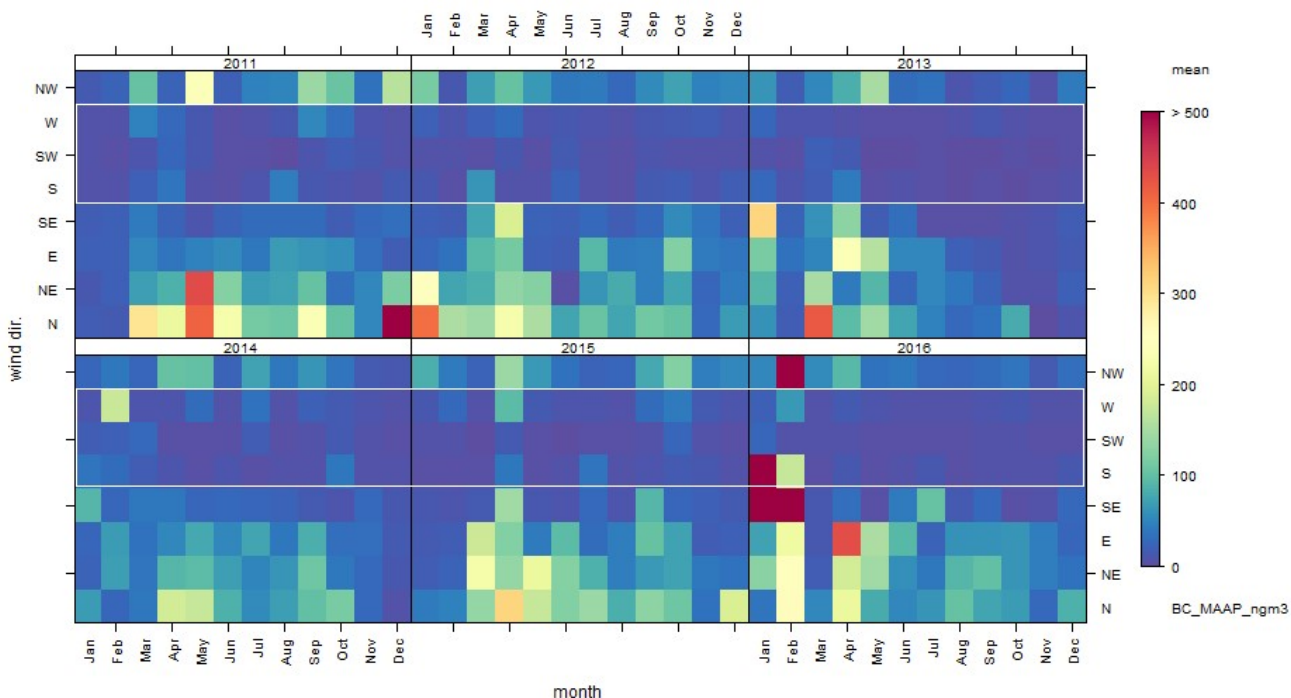


Figure 1. Monthly mean BC concentrations measured at Cape Grim between 2011 and 2017 as a function of wind direction. Baseline conditions are marked by white lines.

Highlighted Speaker - Ozone, Aerosol and Carbon Gases at the Mt. Bachelor Observatory

D. Jaffe¹, J. Hee¹, A.E. Andrews² and J. Kofler^{3,2}

¹University of Washington, Seattle, WA 98105; 425-352-5357, E-mail: djaffe@uw.edu

²NOAA Earth System Research Laboratory, Global Monitoring Division (GMD), Boulder, CO 80305

³Cooperative Institute for Research in Environmental Sciences (CIRES), University of Colorado, Boulder, CO 80309

Mt. Bachelor Observatory (MBO) is a high elevation (2.8 km a.s.l.) research site located on the summit of Mt. Bachelor in Central Oregon. The site was started by the University of Washington in 2004, with a focus on ozone (O₃), aerosols and related trace species. Figure below shows an aerial view of Mt Bachelor. Over the past 14 years our research has focused on O₃, aerosols, mercury and carbon cycle gases. In this presentation I will focus on some of our newest results such as:

1. Trends and causes for inter-annual variations in O₃ and aerosols;
2. Relationship between carbon cycle gases, O₃, aerosols and transport patterns;
3. Aerosol size distributions in biomass burning plumes and long-range transported pollution;
4. New observations of aerosol absorption and black carbon using multiple tools;
5. Improving our methods to characterize the boundary layer and free troposphere.

In this presentation, I will give an overview of MBO gas and aerosol observations over the past 14 years, with a focus on the new results given above.



Figure 1. Mt. Bachelor in Central Oregon. The observatory is located on the summit.

How We Know That Human Activities Are Driving Climate Change

P.P. Tans

NOAA Earth System Research Laboratory, Global Monitoring Division (GMD), Boulder, CO 80305;
303-497-6678, E-mail: pieter.tans@noaa.gov

There are multiple types of independent observations that make a compelling case: The increases in greenhouse gases that we observe are caused entirely by human activities. Focusing on carbon dioxide, CO₂ emissions from fossil fuel burning and cement production are larger than net uptake by all ecosystems in the northern hemisphere during the growing season. The contrast with the past, both recent and distant, is striking. CO₂ is now 45% higher than before the industrial revolution. Half of all cumulative emissions since the pre-industrial have occurred since 1990. The current multi-year average rate of increase is above 2 ppm/year, which is about 200 times faster than what natural processes were able to do when the Earth climbed out of the last ice age between 17,000 and 11,000 years ago. The isotopic composition of atmospheric CO₂ is changing, ruling out that the observed increase can be due to volcanic processes or to an oceanic source. Therefore the source of the added CO₂ must be organic. Atmospheric oxygen is decreasing confirming that colossal amounts of something are being oxidized. Measurements of ¹⁴CO₂ demonstrate that the organic matter being burned is very old. The difference in CO₂ mole fraction between the two hemispheres has been increasing over the last five decades, in rough proportion to the global rate of fossil fuel burning. These are observations, they are not predictions and do not depend on any models. Enhanced heat retention by the added greenhouse gases now stands at 1.25% of all solar radiation absorbed by the Earth system.

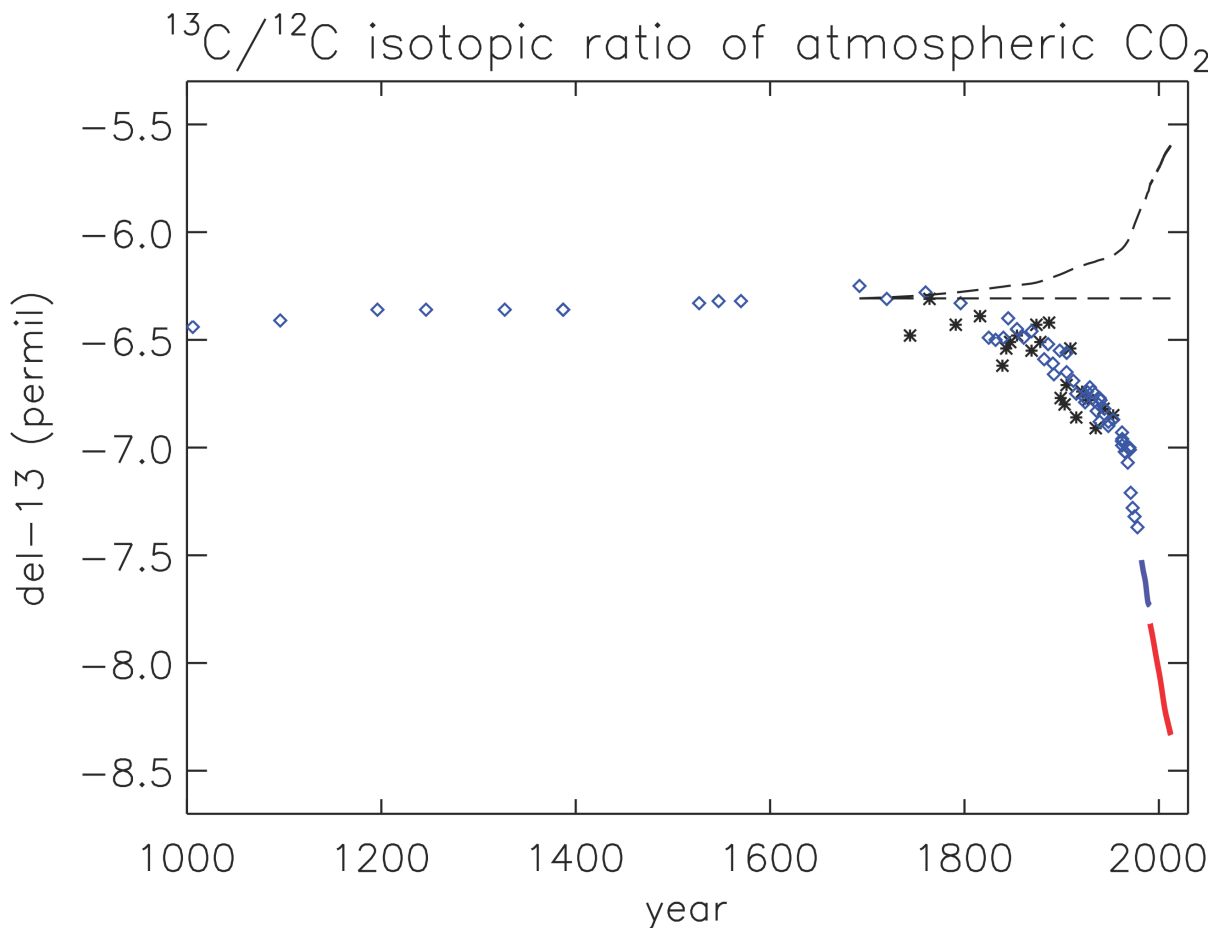


Figure 1. Ice core and firn data from CSIRO, direct atmospheric measurements from NOAA and University of Colorado/INSTAAR.

Sources of Systematic Differences in Global CO₂ Inverse Model Results

B. Gaubert¹, B.B. Stephens², A.R. Jacobson^{3,4}, S. Basu^{3,4}, F. Chevallier⁵, C. Roedenbeck⁶, P.K. Patra⁷, T. Saeki⁷, I. van der Laan-Luijkx⁸, W. Peters⁸, D. Schimel⁹ and The HIPPO science team¹⁰

¹National Center for Atmospheric Research (NCAR), Atmospheric Chemistry Observations and Modeling Laboratory, Boulder, CO 80307; 303-497-1488, E-mail: gaubert@ucar.edu

²National Center for Atmospheric Research (NCAR), Earth Observing Laboratory, Boulder, CO 80307

³Cooperative Institute for Research in Environmental Sciences (CIRES), University of Colorado, Boulder, CO 80309

⁴NOAA Earth System Research Laboratory, Global Monitoring Division (GMD), Boulder, CO 80305

⁵Laboratoire des Sciences du Climat et de l'Environnement (LSCE), Institut Pierre-Simon Laplace, Orme des Merisiers, France

⁶Max Planck Institute (MPI) for Biogeochemistry, Jena, Germany

⁷Japan Agency for Marine-Earth Science and Technology (JAMSTEC), Department of Environmental Geochemical Cycle Research, Yokohama, Japan

⁸Wageningen University, Department of Meteorology and Air Quality, Wageningen, The Netherlands

⁹NASA Jet Propulsion Laboratory, California Institute of Technology, Pasadena, CA 91109

¹⁰Harvard University, Department of Earth and Planetary Sciences, Cambridge, MA 02138

Current estimates of the global carbon budget are informed by surface flux estimates from atmospheric inverse models. It is essential to quantify the uncertainty in inverse flux calculations through comparison with independent observations. We have compared a suite of state-of-the-art inverse flux estimates [MACC (v14r2), Jena (s04_v3.8), CT2016, CTE2016, ACTM (with IEA or CDIAC emissions) and TM5-4DVar] to carbon dioxide (CO₂) concentration profiles from the HIPPER Pole-to-Pole Observations (HIPPO) aircraft campaigns (2009-2011, Wofsy et al. 2011), to assess the dependence of their results on differences in vertical mixing and to identify other drivers of remaining model spread. To reconstruct annual and seasonal distributions for different altitudes and latitudes, we have sampled the models along the HIPPO flight tracks and fitted the binned values with a combination of an offset from a prescribed trend and 2 harmonics. The modelled CO₂ fields agree well with HIPPO observations, in particular for annual mean vertical gradients in the Northern Hemisphere. Although the models differ in inverse approaches, assimilated observations, prior fluxes, and transport, their large-scale fluxes are in closer agreement than in the previous TransCom3 experiment where only the transport model varied. The dependence of northern extratropical annual fluxes on northern hemisphere vertical mixing appears less important than in TransCom3.

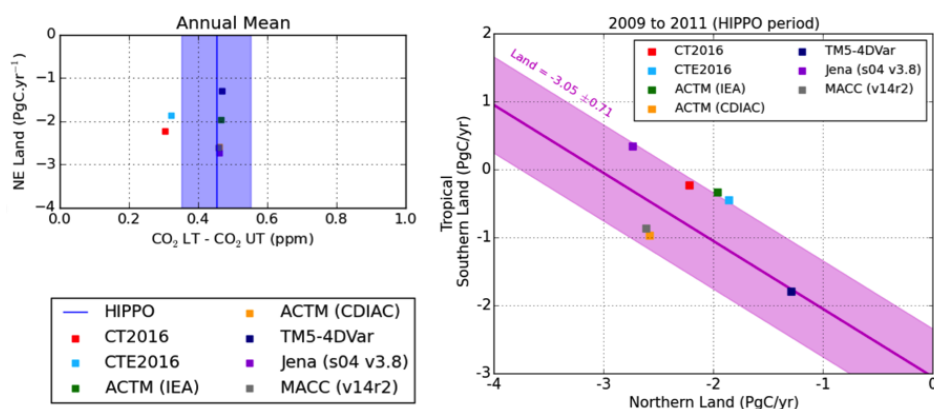


Figure 1. Left panel: Annual mean vertical gradient of CO₂ between the lower troposphere (LT, surface to 700 hPa) and upper troposphere (UT, 700 to 400 hPa), measured by HIPPO (blue line) with an uncertainty range of 0.1 ppm and for each inversion (square). The Northern Extratropical land net flux (2009 to 2011) is plotted on the Y axis. Right panel: this same quantity is shown on the X axis and the remaining land net flux (tropics and southern hemisphere) is shown on the Y axis. The pink line shows the Global Carbon Project 2016 estimates for the same period with reported uncertainty.

10 Years of Observation for Greenhouse Gases by Commercial Airlines in the CONTRAIL Project

Y. Sawa¹, T. Machida², H. Matsueda¹, Y. Niwa¹, T. Umezawa^{3,2}, K. Tsuboi¹, K. Katsumata², H. Eto⁴, D. Goto⁵, S. Morimoto⁶ and S. Aoki⁶

¹Meteorological Research Institute, Tsukuba, Japan; +81-29-853-8538, E-mail: ysawa@mri-jma.go.jp

²National Institute for Environmental Studies, Tsukuba-City, Ibaraki, Japan

³Max Planck Institute (MPI) for Chemistry, Mainz, Germany

⁴Japan Airlines, Tokyo, Japan

⁵National Institute of Polar Research (NIPR), Tokyo, Japan

⁶Tohoku University, Sendai, Japan

Since 2005, we have conducted an observational project for atmospheric greenhouse gases using passenger aircraft of the Japan Airlines (JAL) named Comprehensive Observation Network for TRace gases by AirLiner (CONTRAIL). The CONTRAIL deploys three measurement programs. (1) Successful operation of Continuous CO₂ Measuring Equipment (CME) over the past 10 years has delivered more than 7 million *in situ* carbon dioxide (CO₂) data points from over 10,000 flights between Japan and Europe, Australia, North America, and Asia. (2) Automatic Air Sampling Equipment (ASE) has collected more than 5,000 air samples in the upper troposphere mainly over the Western Pacific (i.e. flight tracks between Australia and Japan) since 1993 when the previous JAL observation project was initiated. (3) In April 2012, we started monthly flask samplings in the upper troposphere or lower stratosphere at high latitudes over the Eurasian continent during flights between Europe and Japan. These air samples were analyzed for various greenhouse gases such as methane, nitrous oxide or sulfur hexafluoride.

The 10-year CME observations enabled us to well-characterize spatiotemporal variations of CO₂ in wide regions of the globe especially the Asia-Pacific regions, and we present some of such examples. We found enhanced CO₂ growth rates of about 3 ppm/year during 2012-2013, although we need to consider the influence of irregular observation density in flight routes and time. Another example of an inter-annual variation is that we observed vertical CO₂ profiles significantly different over Singapore between October 2014 and October 2015. The elevated CO₂ in the lower troposphere in 2015 is attributable to the massive burnings in Indonesia.

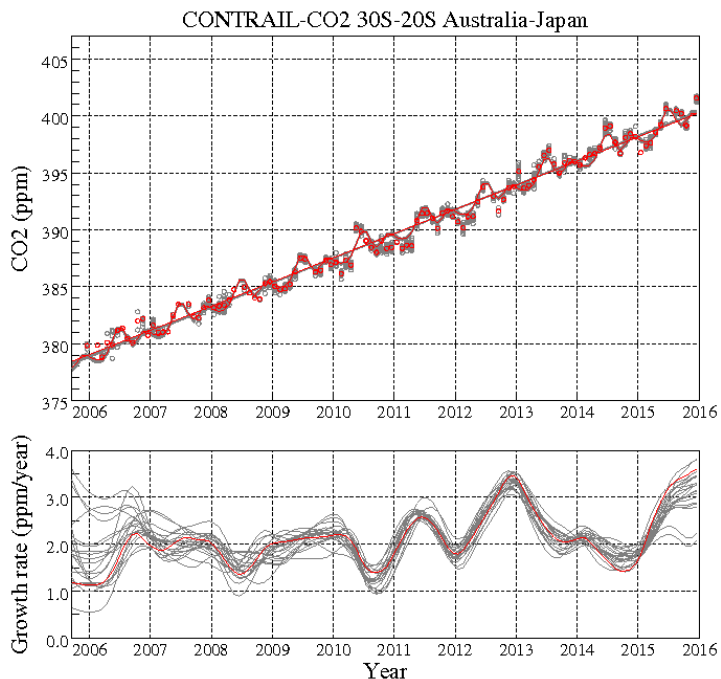


Figure 1. Observed CO₂ mixing ratios and growth rates at about 10 km for the latitude of 30S-20S during the flights between Australia and Japan. Red color shows mean values with all available data, while gray colors show those calculated from 20 cases with using only 30% of data by random collections.

Nitrous Oxide Emissions Estimated with the Carbon Tracker-Lagrange North American Regional Inversion Framework

C. Nevison¹, A.E. Andrews², K. Thoning², E.J. Dlugokencky², C. Sweeney^{3,2}, L. Hu^{3,2}, E. Saikawa⁴, J. Benmergui⁵ and S. Miller⁶

¹Institute of Arctic and Alpine Research (INSTAAR), University of Colorado, Boulder, CO 80309; 303-492-7924, E-mail: Cynthia.Nevison@colorado.edu

²NOAA Earth System Research Laboratory, Global Monitoring Division (GMD), Boulder, CO 80305

³Cooperative Institute for Research in Environmental Sciences (CIRES), University of Colorado, Boulder, CO 80309

⁴Emory University, Department of Environmental Sciences, Atlanta, GA 30322

⁵Harvard University, Cambridge, MA 02138

⁶Stanford University, Stanford, CA 94305

North American nitrous oxide (N_2O) emissions of 1.5 ± 0.2 Tg N/yr over 2008-2013 are estimated using the Carbon Tracker-Lagrange (CTL) regional inversion framework. The estimated N_2O emissions are largely consistent with the Emission Database for Global Atmospheric Research (EDGAR) global inventory and with the results of global atmospheric inversions. Emissions are strongest from the Midwestern corn/soybean belt, which accounts for about 25% of the total North American N_2O source. The emissions are maximum in late spring/early summer, consistent with a nitrogen fertilizer-driven source, but also show a late winter spike consistent with freeze-thaw effects. Interannual variability in emissions across the primary months of fertilizer application is positively correlated to mean soil moisture and precipitation. The estimated N_2O flux from the Midwestern corn/soybean belt and the more northerly U.S./Canadian wheat belt corresponds to 3.8-4.6% and 1.4-3.5%, respectively, of total synthetic + organic N fertilizer applied to those regions.

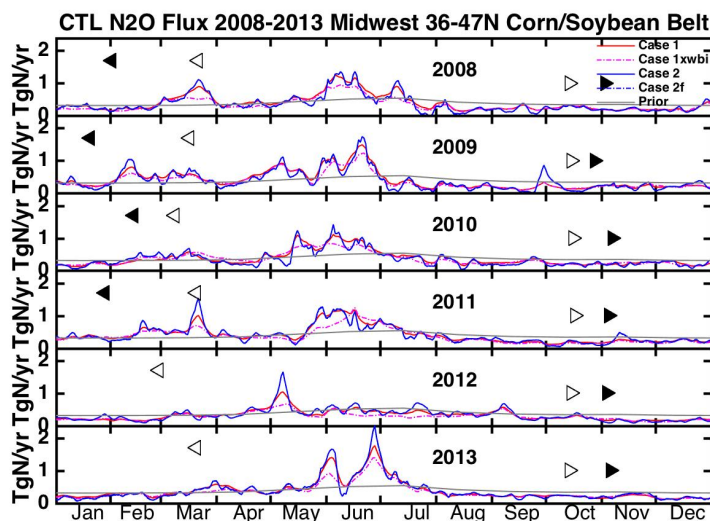


Figure 1. Posterior N_2O flux integrated over the Midwestern corn/soybean belt (36° to $47^\circ N$, 102° to $80^\circ W$, in grids where 5% or more of land area was planted in corn and/or soybean). Cases 1 (red) and 2 (blue) are defined based on different model-data mismatch and prior flux uncertainty covariance parameters and use a best guess prior derived from Saikawa *et al.* [2014], while Case 2f (blue dash) uses a flat prior. The magenta dashed line shows Case 1xwbi, in which N_2O data from West Branch, Iowa were omitted from the inversion. Left and right facing triangles show the approximate day when soil temperature climbs above $0^\circ C$ and drops below $10^\circ C$ ($50^\circ F$), respectively. Solid and open triangles reflect mean soil temperature integrated over the southern (36° to $41.5^\circ N$) and northern (41.5° to $46^\circ N$) half, respectively, of the Midwestern Corn/Soybean belt. In 2012 and 2013, no $0^\circ C$ crossing symbol is plotted for the southern half of the belt because the mean soil temperature remained above freezing.

Vertical Gradients in Atmospheric CO₂ as a Constraint on Southern Ocean Fluxes

K. McKain^{1,2}, C. Sweeney^{1,2}, B.B. Stephens³, A.R. Jacobson^{1,2}, M. Long⁴, E.A. Kort⁵ and P.K. Patra⁶

¹Cooperative Institute for Research in Environmental Sciences (CIRES), University of Colorado, Boulder, CO 80309; 303-497-6229, E-mail: kathryn.mckain@noaa.gov

²NOAA Earth System Research Laboratory, Global Monitoring Division (GMD), Boulder, CO 80305

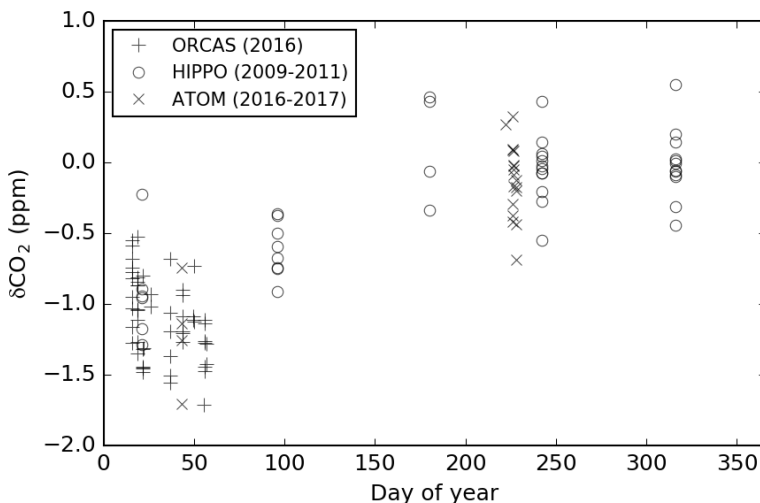
³National Center for Atmospheric Research (NCAR), Earth Observing Laboratory, Boulder, CO 80307

⁴National Center for Atmospheric Research (NCAR), Boulder, CO 80307

⁵University of Michigan, Ann Arbor, MI 48109

⁶Japan Agency for Marine-Earth Science and Technology (JAMSTEC), Department of Environmental Geochemical Cycle Research, Yokohama, Japan

The Southern Ocean plays an important role in the global carbon cycle and climate system, but net carbon dioxide (CO₂) flux into the Southern Ocean is difficult to model because it results from larger opposing and seasonally-varying fluxes due to thermally-forced outgassing and biological uptake. We present an analysis to constrain the seasonal cycle of net CO₂ exchange with the Southern Ocean and magnitude of summer uptake using the large-scale vertical gradient in atmospheric CO₂ as measured during three aircraft campaigns with coverage in the southern polar region. The Oxygen/nitrogen (O₂/N₂) Ratio and CO₂ Airborne Southern Ocean Study (ORCAS) was an airborne campaign that intensively sampled the atmosphere at 0-13 km altitude and 45-75 degrees south latitude in the austral summer (January-February) of 2016. The global airborne campaigns, the HIAPER Pole-to-Pole Observations (HIPPO) study and the Atmospheric Tomography Mission (ATom), provide additional measurements within the Antarctic Polar Cell from other seasons and multiple years. A compilation of vertical profile data from these campaigns provides a generalized description of the seasonal pattern of Southern Ocean air-sea fluxes and no evidence of large interannual variability in the seasonal pattern. The observed vertical gradients may also have significant contribution from long-range transport of terrestrial flux signals from northern latitudes. We use measurements of atmospheric methane (CH₄), which has no Southern Ocean source, a significant terrestrial source, and well-understood sink processes, to account for long-range transport in the observed CO₂ gradient. Comparison of observations and model simulations using multiple transport and flux models reveals a large spread in models' ability to reproduce the observed vertical gradient and seasonal cycle. We attempt to evaluate whether some model's tendency to underestimate the observed vertical gradient is due to too-small fluxes or too-large vertical mixing.



Toward Improvement on Estimation of North American CO₂ Fluxes from CarbonTracker-Lagrange: A High-Resolution Regional Inverse Modeling System for Assimilating Atmospheric CO₂

L. Hu^{1,2}, A.E. Andrews², K. Thoning², A.R. Jacobson^{1,2}, T. Nehrkorn³, M. Mountain³, A. Michalak⁴, V. Yavad⁵, Y. Shiga⁴, C. Sweeney^{1,2}, E.J. Dlugokencky², D. Worthy⁶, J.B. Miller², M. Fischer⁷, S. Biraud⁷ and P.P. Tans²

¹Cooperative Institute for Research in Environmental Sciences (CIRES), University of Colorado, Boulder, CO 80309; 303-497-5238, E-mail: lei.hu@noaa.gov

²NOAA Earth System Research Laboratory, Global Monitoring Division (GMD), Boulder, CO 80305

³Atmospheric and Environmental Research (AER), Inc., Lexington, MA 02421

⁴Carnegie Institution for Science, Department of Global Ecology, Stanford, CA 94305

⁵NASA Jet Propulsion Laboratory, California Institute of Technology, Pasadena, CA 91109

⁶Environment and Climate Change Canada, Toronto, Ontario, Canada

⁷Lawrence Berkeley National Laboratory (LBNL), Berkeley, CA 94720

NOAA's CarbonTracker is a global modeling system for deriving carbon dioxide (CO₂) exchange between the atmosphere and Earth's surface based on atmospheric CO₂ mole fraction measurements. It was developed in 2007 and has been providing an independent atmospheric perspective of CO₂ fluxes from natural ecosystems for comparison to inventory- and process-based flux products. Given recent advances in inverse modeling and atmospheric transport simulation, limitations in CarbonTracker's inversion setup and coarse resolution of atmospheric transport, however, may limit its ability to retrieve the most accurate carbon fluxes. Within NOAA, we have been developing a high-resolution regional inverse modeling system for improving estimation of North American CO₂ fluxes, CarbonTracker-Lagrange. In this system, we computed tracer-independent footprints using high-resolution Weather Research and Forecasting (WRF) meteorology. We further improved the inversion setup by solving for weekly scaling factors of 1° × 1° grid-scale fluxes with optimization of diurnal cycles of CO₂, whereas in CarbonTracker, it only optimizes weekly scaling factors of CO₂ fluxes from large ecoregions. Here, we will demonstrate that, in a synthetic-data experiment, results obtained from grid-scale inversions with optimization of diurnal cycles will reduce aggregation errors and improve estimation of North American CO₂ fluxes compared to inversion results obtained from only optimization of ecoregion-based fluxes (a CarbonTracker-like setup) (Fig. 1). We will further discuss the differences between fluxes derived from our new inversion system and those estimated from CarbonTracker using real atmospheric data for 2007 – 2014.

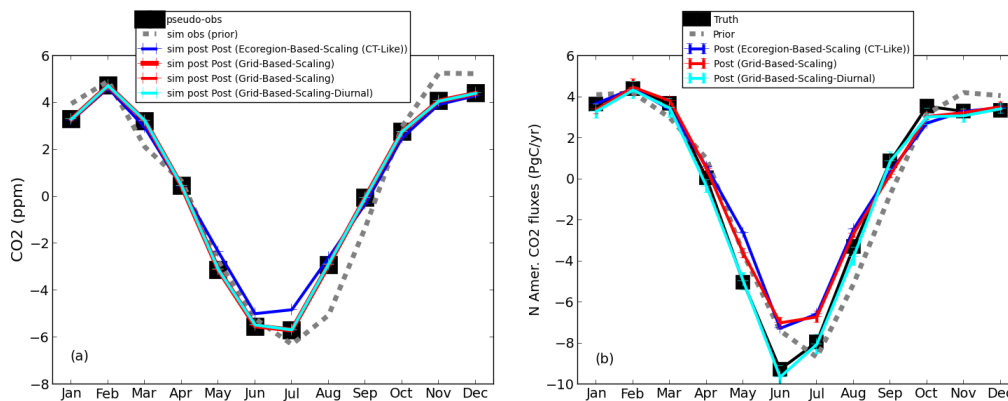


Figure 1. Observations (a) and fluxes (b) created and simulated in a synthetic-data experiment. Assumed true fluxes and the resulted average CO₂ mole fraction changes at NOAA's air sampling sites were indicated by black squares. Prior fluxes and the corresponding average CO₂ mole fraction changes were indicated by dashed lines. Posterior fluxes, derived from three different inversion setups: solving for ecoregion-based scaling factors (blue), solving for grid-based scaling factors (red), and solving for grid-based scaling factors with optimization of diurnal cycles of CO₂ (cyan), and their corresponding CO₂ mole fraction changes were noted by other colored lines.

Multi-species Atmospheric Inversion of Sectoral Greenhouse Gas Emissions in the Indianapolis Urban Environment

B. Nathan¹, T. Lauvaux¹, J. Turnbull^{2,3}, K. Gurney⁴ and C. Sweeney^{5,3}

¹The Pennsylvania State University, Department of Meteorology, University Park, PA 16802; 814-863-8320, E-mail: bjn5178@psu.edu

²GNS Science, National Isotope Centre, Lower Hutt, New Zealand

³NOAA Earth System Research Laboratory, Global Monitoring Division (GMD), Boulder, CO 80305

⁴Arizona State University, Tempe, AZ 85287

⁵Cooperative Institute for Research in Environmental Sciences (CIRES), University of Colorado, Boulder, CO 80309

A high-resolution atmospheric inversion system has been developed to quantify urban-scale carbon dioxide (CO₂) emissions over Indianapolis, IN. However, emissions estimates need to be decomposed into their constituent economic source sector contributions to be of great benefit to policymakers. We show here that, with the assistance of flask measurements of multiple trace gases, sectoral emissions can be retrieved at the city scale. With five automated flask samplers collecting weekly samples across the Indianapolis urban environment from 2012 to 2015, we demonstrate the benefits and limitations of directly calculating inverse emissions of fossil-fuel CO₂ (CO₂ff) source sectors with the aid of trace gases, assuming known CO₂ff-to-gas ratios for each sector. Analyses of Bayesian inversion results are first performed in a pseudodata framework built with the Hestia inventory product. We determine the required density of measurements and the characteristics of the trace gases able to separate sectoral contributions. In the second part, we present a real-data source sector inversion for traffic emissions (including off-road combustion engines) calculated using flask measurements of CO₂ff, carbon monoxide (CO) and acetylene (C₂H₂). Our results suggest that sectoral emissions require multiple trace gases with varying CO₂ff-to-gas ratios to quantify each sector accurately. With the appropriate combination of atmospheric tracers, we show that sectoral emissions of CO₂ff can be constrained by urban-scale inversions providing key information for monitoring and verifying mitigation policies at the city level.

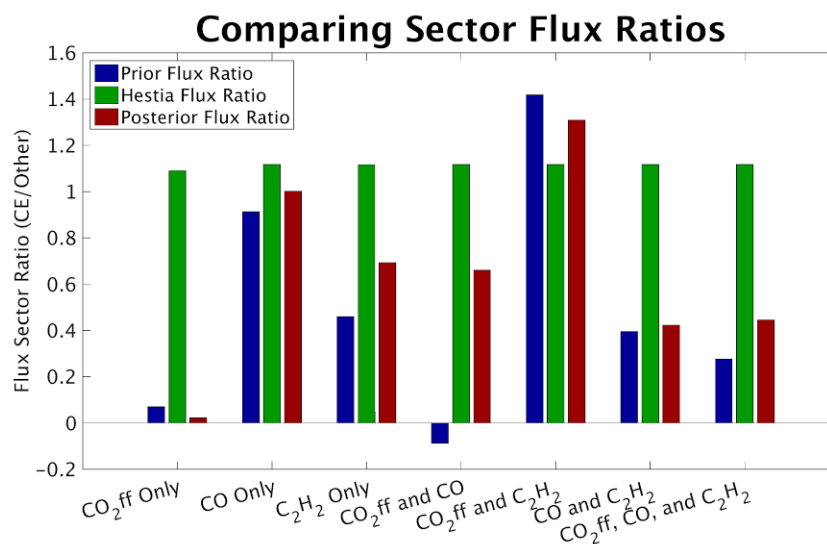


Figure 1. Ratio between combustion engine (traffic and off-road) emissions and the other sectors (airport, commercial, industrial, railroad, residential, and energy production) based on Hestia (in green), perturbed Hestia (a priori in blue), and after inversion (a posteriori in red). The different cases correspond to various combinations of atmospheric flask measurements of carbon dioxide (CO₂ff derived from ¹⁴CO₂), CO and C₂H₂ used in the different inversions over Indianapolis.

Surface Energy Budget Process Relationships as a Means for Evaluating Model Performance in Central Greenland

M. Shupe^{1,2}, N. Miller^{1,2}, C.J. Cox^{1,2} and O. Persson^{1,2}

¹Cooperative Institute for Research in Environmental Sciences (CIRES), University of Colorado, Boulder, CO 80309; 303-497-6471, E-mail: matthew.shupe@noaa.gov

²NOAA Earth System Research Laboratory, Physical Sciences Division (PSD), Boulder, CO 80305

The Greenland Ice Sheet (GIS) plays important roles in the global climate system, impacting sea-level rise, northern hemisphere circulation patterns, and potentially the ocean thermohaline circulation. Variability in the GIS mass budget is of utmost importance and is the result of numerous processes including surface melt, runoff, and precipitation. Within the context of a warming Arctic, surface melt is increasing dramatically. It is therefore essential to understand the key processes that control variability in the surface temperature and ultimately surface melt. The surface energy budget, comprised of radiative, turbulent, and conductive heat fluxes, represents the balance of energy at the surface and largely determines the surface temperature variability. To represent the surface energy budget and melt in current and future climates, numerical models must be able to accurately represent variability in the surface energy budget, including the partitioning of energy into individual terms and the key atmospheric drivers. This presentation draws upon a comprehensive set of surface and atmosphere measurements made at Summit, Greenland to examine the key terms of the surface energy budget. Variability in surface radiation is found to be largely driven by the solar cycle and by the presence of clouds. Changes in surface radiation elicit responses in the surface temperature, turbulent sensible and latent heat fluxes, and conductive heat flux. Relationships are developed that relate the radiative forcing terms and responding terms as they manifest over a full annual cycle. These relationships are then used to evaluate how surface energy budget processes are represented in model and reanalysis products, including ERA-Interim, CFSv2, and the new CESM.

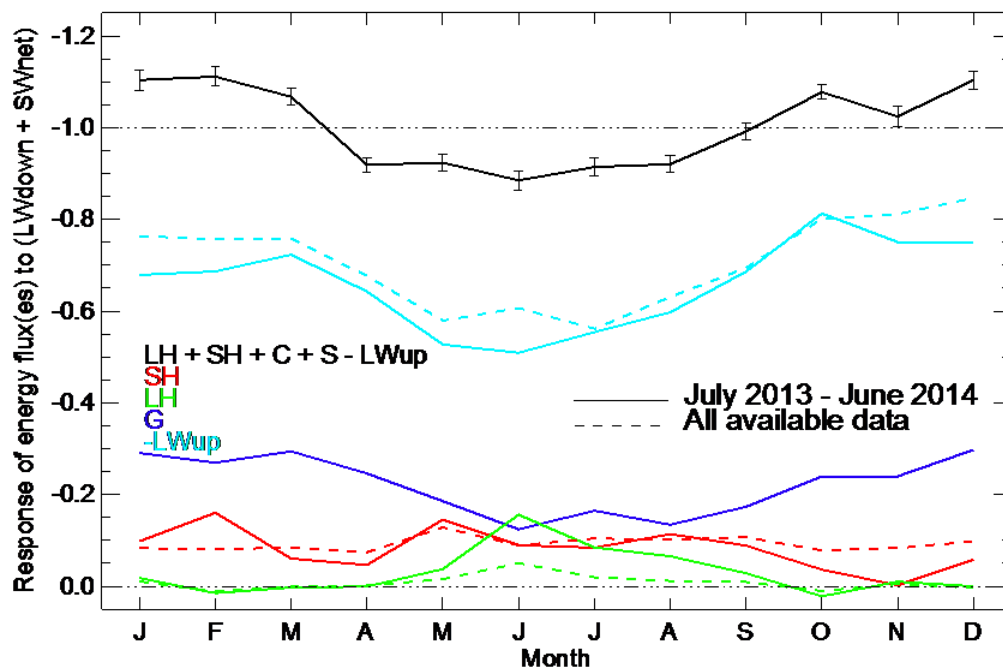


Figure 1. Monthly "slopes" showing the responses of individual energy budget terms to radiative forcing. Here the "forcing" terms are the net shortwave (SWnet) and downwelling longwave (LWdown) fluxes. The "responding" terms are the latent heat (LH), sensible heat (SH), ground heat (G), and upwelling longwave radiation (LWup), which is a proxy for surface temperature.

Drivers and Environmental Responses to the Changing Annual Snow Cycle of Northern Alaska

C.J. Cox^{1,2}, R.S. Stone^{3,4}, D.C. Douglas⁵, D. Stanitski⁴, G. Divoky⁶, G.S. Dutton^{1,4}, C. Sweeney^{1,4}, J.C. George⁷ and D. Longenecker^{1,4}

¹Cooperative Institute for Research in Environmental Sciences (CIRES), University of Colorado, Boulder, CO 80309; 303-497-4518, E-mail: christopher.j.cox@noaa.gov

²NOAA Earth System Research Laboratory, Physical Sciences Division (PSD), Boulder, CO 80305

³Science and Technology Corporation, Boulder, CO 80305

⁴NOAA Earth System Research Laboratory, Global Monitoring Division (GMD), Boulder, CO 80305

⁵USGS Alaska Science Center, Juneau, AK 99801

⁶Friends of Cooper Island, Seattle, WA 98112

⁷Department of Wildlife Management, North Slope Borough, Barrow, AK 99723

Linkages between atmospheric, ecological and biogeochemical variables in the changing Arctic are analyzed using long-term measurements at the NOAA/GMD Barrow Atmospheric Baseline Observatory (BRW) near Utqiagvik (formerly Barrow), Alaska. Two key variables are the date when snow disappears in spring, as determined primarily by atmospheric dynamics, precipitation, air temperature, winter snow accumulation and cloud cover, and the date of onset of snowpack in autumn that is additionally influenced by ocean temperature and sea ice extent. In 2015 and 2016 the snow melted early at Utqiagvik due mainly to anomalous warmth during May attributed to atmospheric circulation patterns, with 2016 being the earliest on record. These years are discussed in the context of a 115-year snowmelt record at Utqiagvik with trends toward earlier melting since the mid-1970s (-2.86 days/dec) and later snow onset in autumn (+4.6 days/dec). The impacts of a lengthening snow-free season on regional phenology, soil temperatures, fluxes of gases from the tundra, and relationships to regional sea ice conditions are discussed. For example, at nearby Cooper Island, where a colony of seabirds, Black Guillemots, have been monitored since 1975, timing of egg laying is correlated with Utqiagvik snowmelt with 2015 and 2016 being the earliest years. Better understanding of these interactions is needed to predict the annual snow cycles in the region at seasonal to decadal scales, and to anticipate coupled environmental responses.

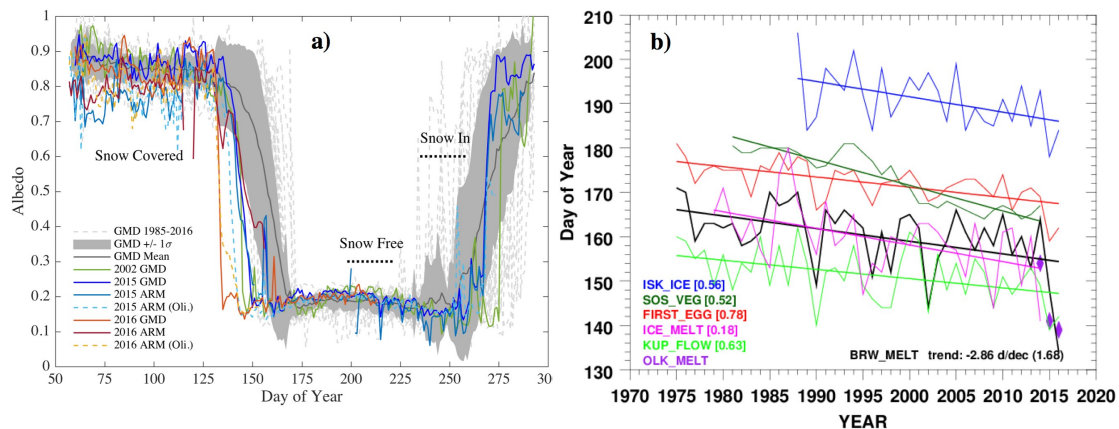


Figure 1. (a) BRW daily mean albedo 1987-2016 and select years from BRW, DoE-ARM NSA, and Oliktok (ARM). (b) BRW snowmelt dates and dates of other spring onset metrics: ice-out at Isaktoak Lagoon (ISK_ICE), onset of flow >10K cfs in the Kuparuk River (KUP_FLOW), start of the vegetative based on NDVI (SOS_VEG), first Black Guillemot egg (FIRST_EGG), mean melt onset over nearby sea ice (ICE_MELT), Oliktok snowmelt dates (diamonds). Correlations (r) with BRW snowmelt dates in brackets.

Arctic Heat Waves: Towards Quantifying the Role of Atmospheric Dynamics

R.S. Stone^{1,2}, C.J. Cox^{3,4} and D. Stanitski²

¹Science and Technology Corporation, Boulder, CO 80305; 303-444-4748, E-mail: robstephston@gmail.com

²NOAA Earth System Research Laboratory, Global Monitoring Division (GMD), Boulder, CO 80305

³Cooperative Institute for Research in Environmental Sciences (CIRES), University of Colorado, Boulder, CO 80309

⁴NOAA Earth System Research Laboratory, Physical Sciences Division (PSD), Boulder, CO 80305

The climate of northern Alaska is influenced by synoptic-scale pressure systems centered in the North Pacific and Beaufort Sea, the Aleutian Low (AL) and Beaufort Sea Anticyclone (BSA), respectively. The NOAA/GMD Barrow Atmospheric Baseline Observatory (BRW) is strategically located for monitoring regional changes in climate in response to variations in atmospheric dynamics. In recent years, anomalously warm springtime conditions have contributed to earlier snow and ice melt in the vicinity of BRW. Arctic heat waves have occurred during both spring and winter, contributing to the record low sea ice extent observed during the 2016/2017 winter. At BRW, abnormal warmth was experienced during May 2015 (a record high) and again in 2016, when record early snowmelt occurred. January 2017 also tied the historic record for warmth at BRW.

The role of atmospheric circulation is investigated, in particular the advection of heat and moisture into the Arctic from the North Pacific. Heat waves in Alaska occur when the BSA weakens and the AL shifts westward, establishing a gradient in air pressure with a high pressure ridge to the east. The relative strengths and positions of these features determine if and when Pacific air flows into the Arctic. To quantify the potential for warm-air advection associated with the juxtaposition of the AL and BSA, an index referred to as ALBSA, is defined on the basis of the difference between east-west (E-W) and north-south (N-S) pressure gradients. Gradients between specified points are expressed in terms of differences in geopotential height at the 850 hPa pressure level using NCAR/NCEP Reanalysis

fields: (<https://www.esrl.noaa.gov/psd/cgi-bin/data/composites/printpage.pl>). Case studies are presented to illustrate the relationship of the 2015/2016 May heat waves at BRW with positive values of ALBSA (Figure 1), and also the near-record warmth of January 2017. We find that early years of snowmelt at BRW correlate with high values of the May E-W component of ALBSA. That is, warm air advection plays a significant role in determining when the spring-to-summer transition occurs on the North Slope of Alaska. In turn, early snowmelt initiates a number of ecological responses, including an increase in the net radiation budget, greening of the tundra, permafrost thaw and enhanced methane flux.

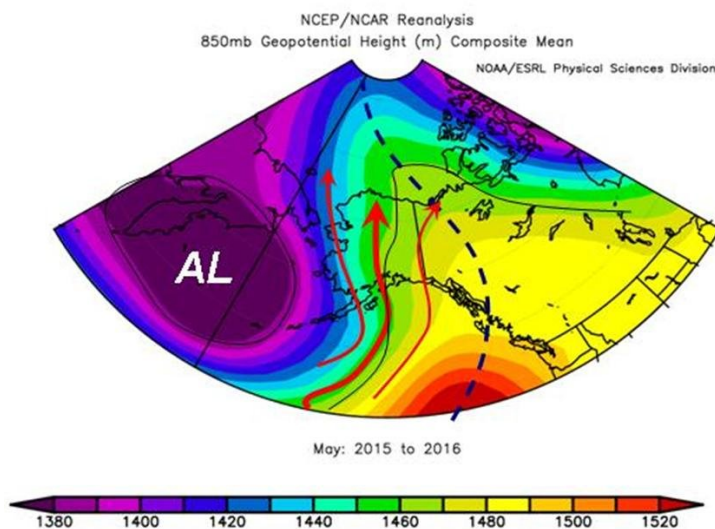


Figure 1. Mean May 850 hPa geopotential height field, averaged for 2015 and 2016 (source: NCEP/NCAR Reanalysis). Red arrows show schematically the advection of air from the north Pacific into the Arctic as a result of an east-west pressure gradient established between the Aleutian Low (AL) and high pressure ridge (dashed line) extending into the Beaufort Sea.

Changing Air Quality in the Southeast U.S. and Potential Implications for Regional Solar Radiation Budget

J.P. Sherman

Appalachian State University, Department of Physics and Astronomy, Boone, NC 28608; 828-262-2438, E-mail: shermanjp@appstate.edu

Numerous publications have discussed the potential role of aerosols in the Southeast (SE) U.S. ‘warming hole’ during the 20th century. However, long-term measurements of aerosol optical depth (AOD) made by NASA’s Moderate Resolution Imaging Spectrometer (MODIS), aboard the polar-orbiting Terra and Aqua satellites reveal decreasing trends in aerosol loading over the SE U.S. Trend studies from surface-based NASA AERONET and NOAA/ESRL network sites also show decreases in AOD (Li et al., 2014; Yoon, 2012) and lower tropospheric aerosol light scattering coefficient (Collaud-Coen et al., 2013) over much of the U.S. However, there were a lack of network sites in the SE U.S. during these study periods and satellite-based estimates of aerosol direct radiative effect in the background SE U.S. may be overestimated (Sherman and McCommiskey, 2017), in addition to a negative MODIS AOD bias (~ 0.03) over the AERONET site at Appalachian State University (APP; Sherman et al., 2016). The APP facility is home to the only co-located NOAA/ESRL, NASA AERONET, and (beginning 2016) NASA MPLNET sites in the SE U.S., with continuous measurements of aerosol radiative and microphysical properties initiated in June 2009. Though the 8-year record at APP is slightly less than that required for analysis of statistically-significant aerosol trends (Collaud-Coen), several apparent trends are evident that are both consistent with and advance results from previous studies. MODIS-measured AOD above APP from 2001-2016 reveals a decrease in AOD, which is supported by the 6.5 years of AOD measurements as part of AERONET. Lower tropospheric light scattering and absorption (measured as part of NOAA/ESRL) are both decreasing at similar rates, leading to little change in single-scattering albedo. The decreases are modulated by months with large wildfire influence, which could become more frequent in a warmer, drier, climate. Hemispheric backscatter fraction (proxy for sub-micron aerosol size distribution) is increasing, indicating a trend toward smaller particles. Aerosol number concentrations show a smaller change over the 8-year period, indicating that changes in aerosol size distribution are likely the primary contributor to lower light scattering at APP.

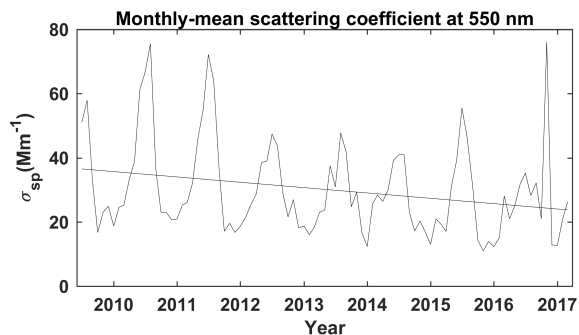


Figure 1. Time series of monthly-mean PM₁₀ aerosol light scattering coefficient at 550 nm.

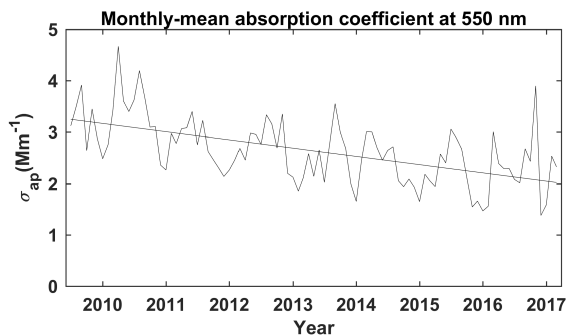


Figure 2. Time series of monthly-mean PM₁₀ aerosol light absorption coefficient at 550 nm.

Surface-measured Trends of Aerosol Optical Depth as an Indicator of Stratospheric Aerosol Trends

J. Augustine

NOAA Earth System Research Laboratory, Global Monitoring Division (GMD), Boulder, CO 80305;
303-497-6415, E-mail: john.a.augustine@noaa.gov

Measurements of aerosol optical depth (AOD) at five wavelengths in the visible and near infrared have been made at GMD's U.S. SURFRAD sites in concert with surface radiation budget measurements for the past 20 years. This valuable dataset has been used to assemble a modern AOD climatology for the U.S., quantify the second indirect effect of aerosols, and assess the mean surface radiative forcing of aerosols. AOD time series from each SURFRAD station show recurring features such as a minimum in winter, maximum in summer, and a secondary maximum in Spring from strong baroclinic springtime storms in the U.S. and the transport of Asian dust from similar storms in the dry regions of northwest China and Mongolia. An unexpected feature is that all stations show a slow increase of their annual AOD minimum from the beginning of the dataset (1997) to about 2011, followed by a dramatic decrease to the present (see figure). Given that AOD minima represent a very clean troposphere, could those trends in AOD minima be indicative of trends in stratospheric aerosol loading? Until the early 2000s, the general belief was that only explosive equatorial volcanoes affected aerosol loading in the stratosphere. Proof of the contribution of minor extratropical volcanic eruptions to stratospheric aerosols came with the launch of the Cloud-Aerosol Lidar with Orthogonal Polarization (CALIOP) space-borne lidar in 2006. Time series of CALIOP data averaged over the northern hemisphere (30°N - 60°N) show distinct trajectories of plumes from several northern hemisphere eruptions entering the stratosphere between 2006 and 2011, and a dramatic clearing thereafter. The influence of each plume lasted only on the order of months but sequential eruptions within that period kept the stratosphere populated with volcanic aerosol. When compared to the magnitude of stratospheric AOD, the ground-based AOD minima are greater because they include background-level tropospheric aerosol loading. However, the trends of the surface-based AOD minima show a similar behavior as trends of stratospheric AOD. AOD minima from stations with more turbid atmospheres are noisier and show trend magnitudes that differ from those in the stratosphere. However, trends in annual AOD minima from cleanest SURFRAD site (Desert Rock, Nevada) match those of stratospheric aerosol quite well and may serve as a useful proxy.

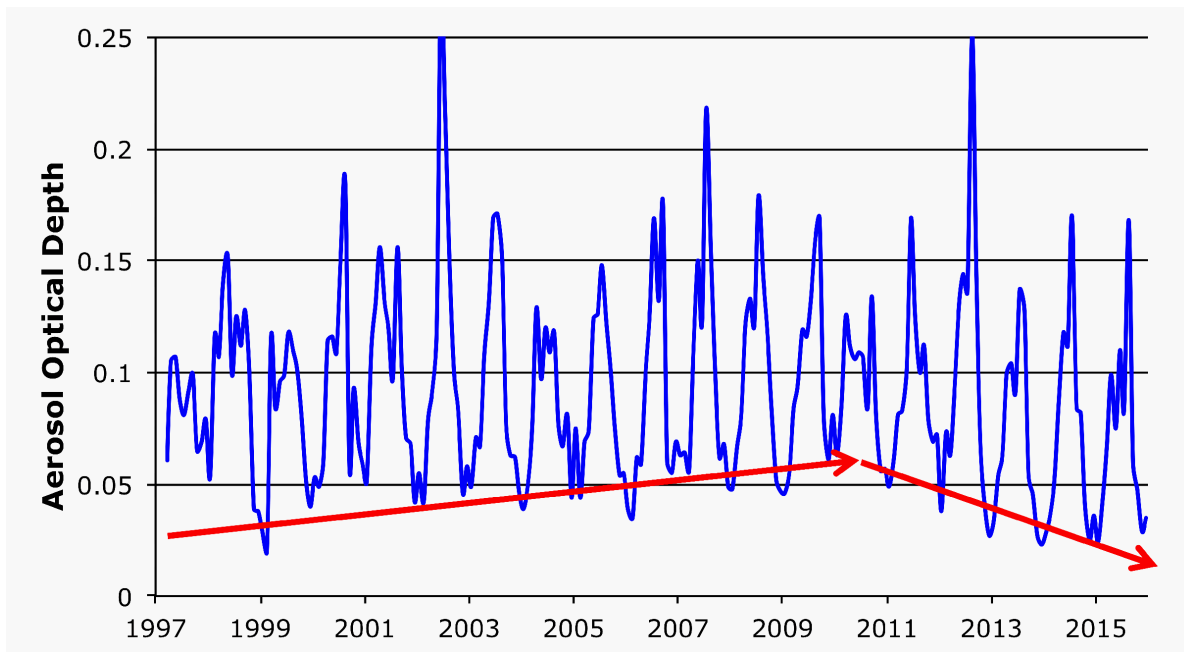


Figure 1. Time series monthly mean 500 nm aerosol optical depth for the Table Mt., Colo. SURFRAD site. Red arrows indicate direction of trends of AOD minima.

The Hazy Space between Cloud and Aerosol

C. Long^{1,2}, J. Calbo³, J. Augustine², A. McComiskey² and J. González³

¹Cooperative Institute for Research in Environmental Sciences (CIRES), University of Colorado, Boulder, CO 80309; 303-497-6056, E-mail: chuck.long@noaa.gov

²NOAA Earth System Research Laboratory, Global Monitoring Division (GMD), Boulder, CO 80305

³University of Girona, Girona, Spain

The definition of what is and is not a cloud is not well defined for markedly optically-thin situations of condensed water in the atmospheric column. For aerosols, we tend to think mostly in terms of small dry particles of low optical depths. The transition zone between our common perceptions of "aerosol" and "cloud" is a bit hazy at best. We take a look at this transitional loading that has been coined the "twilight zone" to determine the frequency of occurrence and importance using several surface-based observing techniques. Sensitivity analyses are applied on sky camera images, and broadband and spectral radiometric measurements, taken at Girona (Spain) and Boulder (CO, USA).

Results. Sky cameras

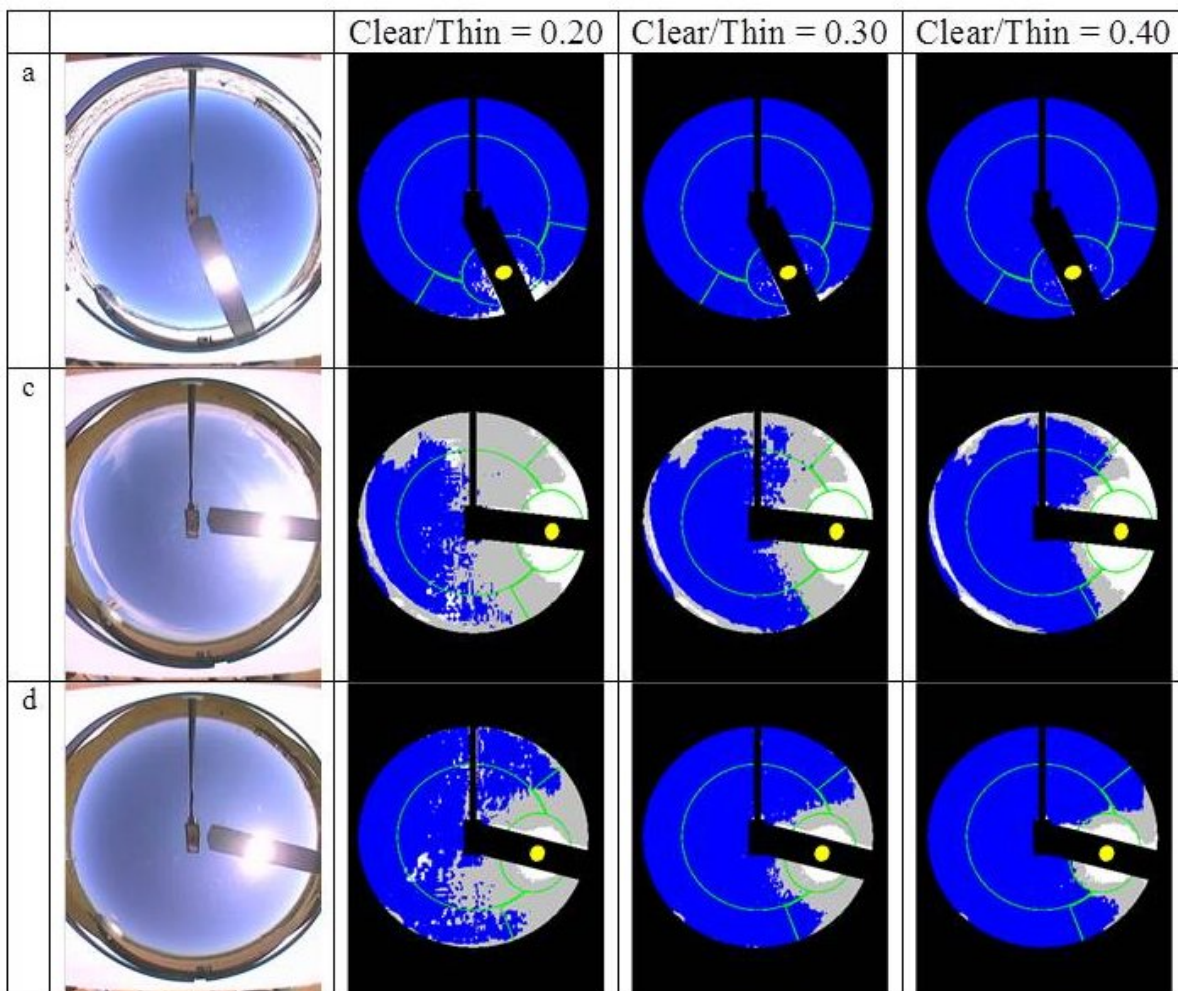


Figure 1. Examples of testing various processing thresholds for classifying cloud/no clouds for three different "haziness" conditions.

Two Centuries of Volcanic Aerosols Derived from Lunar Eclipse Records, 1805-2015

R.A. Keen

University of Colorado, Emeritus, Department of Atmospheric and Oceanic Sciences, Boulder, CO 80309; 303-642-7721, E-mail: richard.keen@colorado.edu

About once per year, on average, the moon is totally eclipsed; the moon is then illuminated by sunlight refracted into the umbra, primarily by the stratosphere. Stratospheric aerosols can affect the brightness of the eclipsed moon, and climatically significant, visible-band, global aerosol optical depth (AOD) can be directly measured from the difference between observed and predicted brightness.

In 2004, Hofmann et al. summarized five decades of stratospheric aerosol observations, “Surface-Based Observations of Volcanic Emissions to the Stratosphere”, in *Volcanism and the Earth’s Atmosphere*, Geophysical Monograph 139, American Geophysical Union. Among the records were lunar eclipse AOD, updated at the 2015 and 2016 NOAA Global Monitoring Annual Conferences (GMAC):

https://www.esrl.noaa.gov/gmd/publications/annual_meetings/2015/abstracts/100-150401-A.pdf and

http://www.esrl.noaa.gov/gmd/publications/annual_meetings/2015/posters/P-48.pdf , and

https://www.esrl.noaa.gov/gmd/publications/annual_meetings/2016/abstracts/121-160425-C.pdf and

https://www.esrl.noaa.gov/gmd/publications/annual_meetings/2016/posters/P60-Keen.pdf

Using eclipse observations published in the historic literature, the AOD time series has been extended back to 1805. Some climatically significant implications of this AOD record:

There was more volcanic effect on the climate during 1915-1962, and less from 1820-1882, than previously determined by Dust Veil (DVI) and Volcanic Explosivity Indices and other estimates. The largest DVI event, Cosigüina in 1835, is demoted to a minor event in the eclipse AOD record. Since 1979, volcanoes are responsible for a half of the observed warming (MSU Satellite temperatures). Volcanic forcing has not increased since 1996, ruling out volcanoes out as a cause of the 19-year pause.

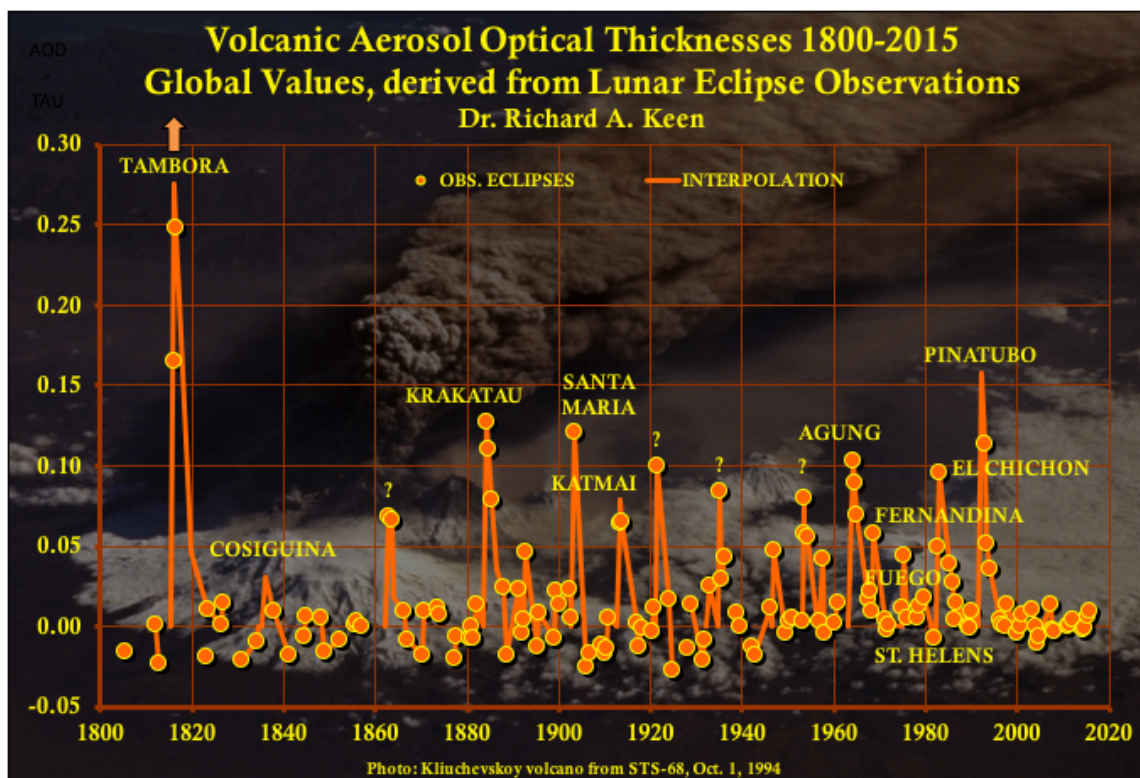


Figure 1. Global Volcanic Aerosol climate forcing from Lunar Eclipse observations, 1805-2015.

Detecting Trends in Fossil Fuel Emissions with $^{14}\text{CO}_2$ in the Presence of Transport Errors and Biased Inventories

S. Basu^{1,2}, J.B. Miller² and S. Lehman³

¹Cooperative Institute for Research in Environmental Sciences (CIRES), University of Colorado, Boulder, CO 80309; 303-834-5361, E-mail: sourish.basu@noaa.gov

²NOAA Earth System Research Laboratory, Global Monitoring Division (GMD), Boulder, CO 80305

³Institute of Arctic and Alpine Research (INSTAAR), University of Colorado, Boulder, CO 80309

In earlier work, we developed an atmospheric inversion framework to estimate regional emissions of fossil fuel carbon dioxide (CO_2) by assimilating atmospheric measurements of CO_2 and $^{14}\text{CO}_2$ [Basu et al., 2016]. We showed that given a realistic network of $\sim 5,000$ $^{14}\text{CO}_2$ observations per year located primarily over North America, our framework could estimate monthly U.S. national totals to within a few percent, and the annual national total to within 1%. We also showed, however, that the absolute accuracy of our estimate was strongly dependent on the atmospheric transport model used, an Achilles' heel of all atmospheric inversions.

Here we investigate whether the interannual variability of emissions derived from our framework is less sensitive to biases in the atmospheric transport model than are the absolute annual estimates themselves. Specifically, we evaluate whether it is possible to derive robust estimates of decade long trends in fossil fuel emissions using biased atmospheric transport, and test the sensitivity of trend detection capabilities to the design of the observational network. These issues relate directly to the feasibility of verifying national emission trajectories pledged by countries within their Intended Nationally Determined Contributions (INDCs) at United Nations Framework Convention on Climate Change's 21st Conference of the Parties (UNFCCC COP21) climate summit.

Preliminary results show that given a network of $\sim 5,000$ observations per year, we can robustly estimate U.S. national emission trends, even when starting from a "first guess" emission inventory without a trend and with biased atmospheric transport. We also show how far our estimated trends deviate from the truth under the "current best case" scenario of assimilating 1,000 observations per year, and how a badly informed prior ($\sim 40\%$ bias) affects those estimate.

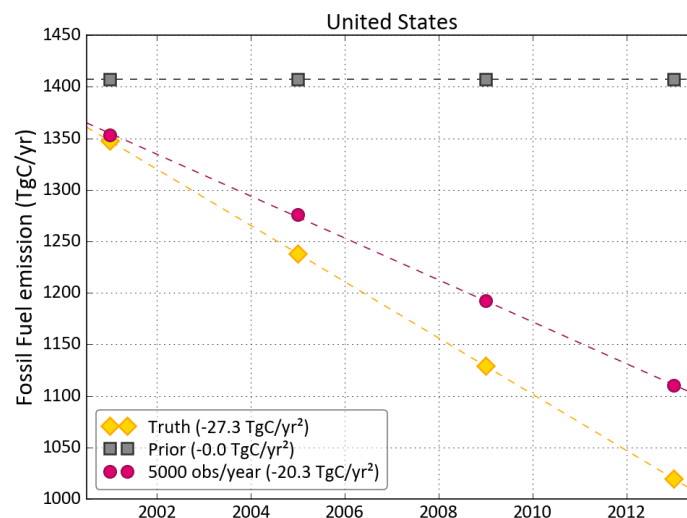


Figure 1. Preliminary results from our trend detection experiment. In our Observing System Simulation Experiments (OSSE), the "nature run" or "true" fossil fuel emissions had a negative trend, while the first guess or "prior" emissions did not. Our inversion system could recover part of that trend with 5000 $^{14}\text{CO}_2$ observations per year (primarily over North America). Efforts to minimize the trend detection error are in progress.

Optical Detection of Radiocarbon (^{14}C) Below Modern Levels by Cavity Ring-down Spectroscopy

A.J. Fleisher, D.A. Long, Q. Liu and J.T. Hodges

National Institute of Standards and Technology (NIST), Gaithersburg, MD 20880; 301-975-4864, E-mail: adam.fleisher@nist.gov

We report the optical detection of radiocarbon (^{14}C) in biogenic carbon dioxide (CO_2) samples with a fraction modern carbon of $F < 1$ using a mid-infrared laser spectrometer. The table-top instrument operates on the principles of cavity ring-down spectroscopy in the linear absorption regime by measuring the mole fraction of absorbers $\chi = (\int \alpha(\nu) d\nu) / (cnS)$, where c is the speed of light, n is the total number density, S is the absorption line strength, α is the measured absorption coefficient, and ν is the laser frequency. The absorption coefficient α is related to the time constant of the optical resonator in the presence of molecular absorbers τ by the simple equation $\alpha = 1/(c\tau) - 1/(c\tau_0)$, where τ_0 is the empty-cavity time constant. The optical detection of radiocarbon by linear absorption spectroscopy is therefore fundamentally different from the seminal laser experiments based on non-linear saturated absorption cavity ring-down (SCAR). Measurements of χ_{14} for biogenic and petrogenic CO_2 samples, respectively, were used to determine the limits of our first-generation radiocarbon spectrometer capable of definitively distinguishing samples of CO_2 with $F < 1$.

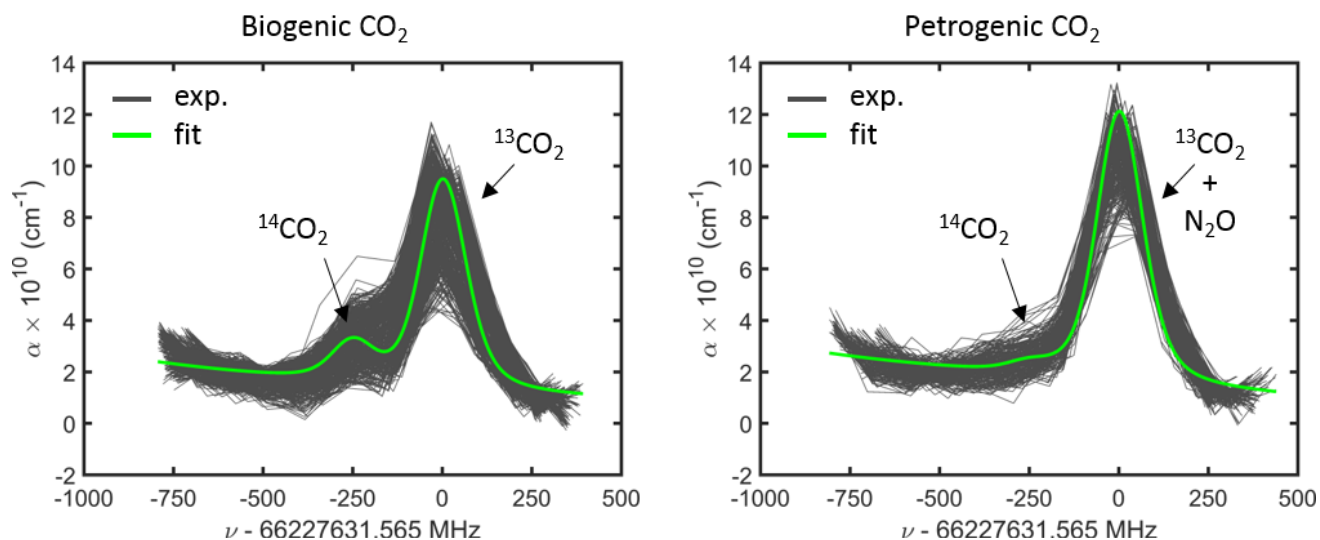


Figure 1. Left. Spectrum of radiocarbon dioxide ($^{14}\text{CO}_2$) for a biogenic sample of CO_2 with $F = 0.86$. Right. Spectrum of a petrogenic sample of CO_2 with $F = 0$. Fraction modern (F) was independently measured for each sample by a commercial accelerator mass spectrometry laboratory. Nearby $^{13}\text{CO}_2$ and N_2O interferences were mitigated by reducing the sample temperature to $T = 220$ K. The spectrometer comprises a quantum cascade laser, fast optical switch, high-finesse optical resonator and cold cell, low-noise photoreceiver, analog-to-digital converter, and computer software for signal processing.

Unexpected and Significant Biospheric CO₂ Fluxes in the Los Angeles Basin Indicated by Atmospheric Radiocarbon (¹⁴CO₂)

J.B. Miller¹, S. Lehman², K.R. Verhulst³, V. Yadav³, C. Miller³, R. Duren³, S. Newman⁴ and C. Sloop⁵

¹NOAA Earth System Research Laboratory, Global Monitoring Division (GMD), Boulder, CO 80305; 303-497-7739, E-mail: john.b.miller@noaa.gov

²Institute of Arctic and Alpine Research (INSTAAR), University of Colorado, Boulder, CO 80309

³NASA Jet Propulsion Laboratory, California Institute of Technology, Pasadena, CA 91109

⁴California Institute of Technology, Pasadena, CA 91125

⁵Earth Networks, Inc., Germantown, MD 20876

Cities account for about 70% of global fossil fuel-carbon dioxide (CO₂) emissions, and with urban populations rising, it will become imperative to accurately account for urban emissions. Fossil fuel-CO₂ emissions are typically estimated using economic statistics on fuel consumption, and while accurate at national and annual scales, the errors are unknown at urban scales. It is therefore important to develop independent methods of estimating emissions for cities. Atmospheric CO₂ measurement networks in several urban areas have recently been established, but CO₂ alone can not distinguish biospheric and fossil contributions. Using measurements of atmospheric ¹⁴CO₂, the gold standard for identifying fossil fuel emissions in the atmosphere, we will show that CO₂-only methods can lead to substantial biases in fossil fuel-CO₂ emissions detection.

Here, we report results of an air sampling network for radiocarbon (¹⁴C) measurements within the Los Angeles monitoring network. These ¹⁴CO₂ measurements are part of NOAA's larger effort to measure radiocarbon for fossil fuel-CO₂ identification at regional (~102 – 103 km) scales throughout the U.S., but the Los Angeles sites are concentrated spatially and exhibit much larger CO₂ and ¹⁴CO₂ signals than at any other measurement site. Mid-day CO₂ enhancements above background at our three sites in Los Angeles averaged 16 ppm, but ¹⁴CO₂ data reveal that only ~ 75% of the enhancement resulted from fossil fuel combustion. Thus, the remaining 25% originated from biospheric sources. We will quantify the contributions of possible sources to this unexpectedly large (and seasonally varying) biospheric contribution. Finally, we will discuss the implications of these results for urban emissions monitoring using surface and space-based approaches and also explore the benefits of improving fossil fuel detection by using atmospheric measurements of CO₂, CO, ¹⁴CO₂, and other tracers.

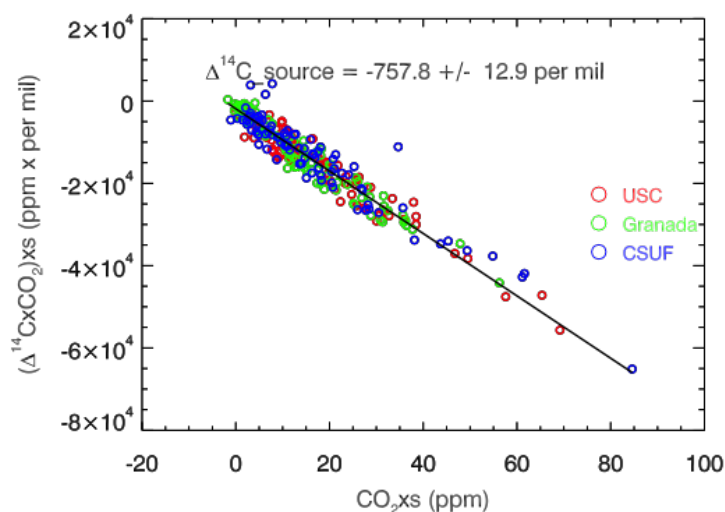


Figure 1. Correlation between enhancements over background of CO₂ and ¹⁴CO₂ at three sites in the Los Angeles Basin: U. of Southern California, Granada Hills, and Cal. State Fullerton. The slope of the correlation should be -1000 for a purely fossil fuel CO₂ signal, but the deviation shows a ~ 25% contribution from biospheric sources.

Constraining Biospheric Exchange Processes over North America by Joint Assimilation of Atmospheric CO₂ and δ¹³C

I.R. van der Velde^{1,2}, J.B. Miller², W. Peters³, A.E. Andrews² and P.P. Tans²

¹Cooperative Institute for Research in Environmental Sciences (CIRES), University of Colorado, Boulder, CO 80309; 303-497-5591, E-mail: ivar.vandervelde@noaa.gov

²NOAA Earth System Research Laboratory, Global Monitoring Division (GMD), Boulder, CO 80305

³Wageningen University, Department of Meteorology and Air Quality, Wageningen, The Netherlands

Droughts can cause widespread decline of carbon uptake by plants, which respond to droughts by reducing their stomatal aperture to limit water loss. Given the complex feedbacks that exist between the terrestrial biosphere and climate, the future of the land carbon sink remains uncertain in a world where droughts may be more extreme and frequent. However, the isotopic ratio of ¹³C/¹²C in atmospheric carbon dioxide (CO₂) (reported as δ¹³C in ‰), which we measure, provides insight into climate-carbon coupling. This is because photosynthesis imposes distinctive isotopic fractionation patterns upon atmospheric δ¹³C. Variations of δ¹³C in the atmosphere reflect spatially coherent changes in stomatal conductance and/or in the relative contributions from C3 (e.g. forests) and C4 (e.g. maize) plant growth, but as shown in Fig. 1, we cannot simulate δ¹³C accurately with our biosphere model. In an effort to improve biosphere models, we have developed an inverse model capable of assimilating δ¹³C and CO₂ data. In this system we estimate the magnitude of isotopic fractionation during photosynthesis. This could help us better understand the biogeochemical interactions between the atmosphere and vegetation, and help us to improve parameterization of the main controls of carbon exchange in biosphere models.

We focus on CO₂ and ¹³CO₂ flux estimation over North America using a dense synthetic data set for both tracers and a Lagrangian particle dispersion model WRF-STILT. By comparing modeled with pseudo ‘observed’ CO₂ and δ¹³C data at surface sites we can optimize our prior flux estimates derived from a biosphere model. We will present comparisons between our optimized values and those observed, and discuss the current strengths and shortcomings of our framework. We find that our system can retrieve meaningful signals in isotopic fractionation when the total CO₂ budget is fairly well determined in a first step. In addition, we mainly get information on isotopic fractionation upwind of sites, which tends to represent a large fraction of the productivity of the continent. Unlike for CO₂, these regional fractionation estimates would be adequate, because we are most interested in the relationship between isotopic fractionation and stomatal response in plants during droughts.

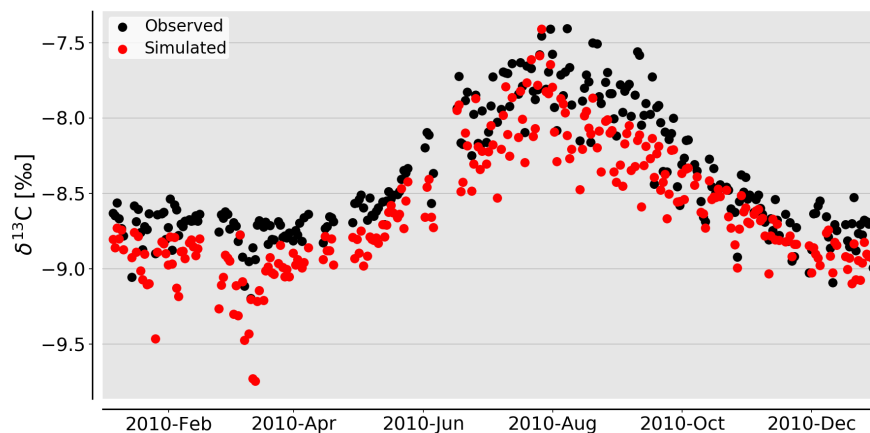


Figure 1. Observed δ¹³C (black) together with simulated δ¹³C driven by SiBCASA model fluxes (red) for Park Falls Wisconsin. The seasonal cycle of δ¹³C is anti correlated with CO₂. Less negative values indicate the atmosphere is more enriched with ¹³CO₂ relative to ¹²CO₂ during the growing season due to photosynthetic fractionation [data provided by INSTAAR].

Gaseous Reference Materials to Underpin Measurements of Amount Fraction and Isotopic Composition of Greenhouse Gases

P. Brewer, D. Worton, R. Pearce and K. Resner

National Physical Laboratory, Teddington, Middlesex, United Kingdom; +44 (0) 20 8943 6007, E-mail: paul.brewer@npl.co.uk

The European Metrology Research Programme HIGHGAS project has led to significant advances in the development of high accuracy, SI traceable, gaseous reference materials of carbon dioxide (CO₂), methane (CH₄), nitrous oxide (N₂O) and carbon monoxide (CO). Research has focussed on driving the uncertainty of the reference materials towards the World Meteorological Organization (WMO) compatibility goals and monitoring their stability. Improvements have been achieved by optimising passivation chemistry used in cylinder treatment, reducing the uncertainty in the gravimetry of the matrix components and making high-accuracy quantification of target impurities in the matrix gas.

In addition, a capability to fully characterise the isotopic composition of the CO₂ in the reference materials has been developed to account for measurement biases introduced by instrumentation detecting only certain isotopologues. The data shows that knowledge of the CO₂ composition is crucial for addressing commutability issues from preparing synthetic reference materials but also for assigning the correct atomic weight for the calculation of gravimetrically prepared mixtures, which can change the amount fraction by as much as 4.4 nmol/mol.

This work has provided the framework for new research priorities focussed on developing gaseous reference materials of CO₂ and N₂O for underpinning measurements of stable isotopes to infer their origin in the atmosphere. A new infrastructure is proposed that will deliver international CO₂ reference materials with traceability to the VPDB primary standard, to meet the increasing demand. New international gaseous N₂O reference materials will also be developed with stated uncertainties. The research will develop new field-deployable spectroscopy and initiate SI traceability of the international CO₂ isotope ratio scale by re-measuring the absolute isotope ratios by gas-source isotope ratio mass spectrometry (IRMS).

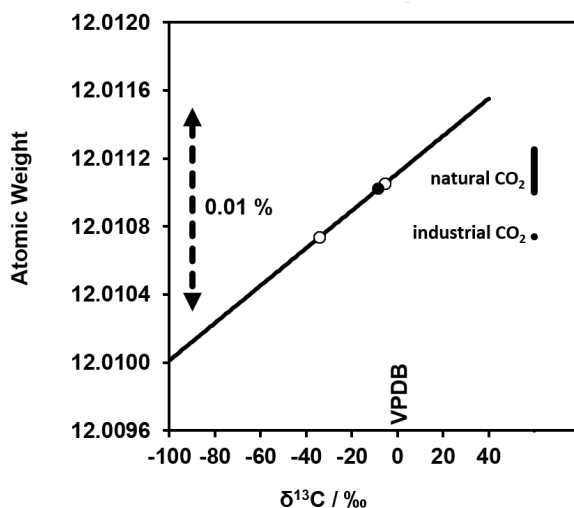


Figure 1. Atomic weight of carbon plotted as a function of the proportion of ¹³C present, denoted by the delta scale, where VPDB has a $\delta^{13}\text{C}$ value of zero. The difference in atomic weight for naturally occurring CO₂ compared to the CO₂ purified by an industrial process is shown and their difference on the δ scale. The filled circle shows the measurement of a standard referenced to the WMO scale using IRMS. The open circles show IRMS measurements of the CO₂ purified by an industrial process (with the most negative δ value) and the same gas spiked with pure ¹³CO₂, both diluted to ambient amount fractions with synthetic air.

Calibration Strategies for FTIR and Other IRIS Instruments for Accurate $\delta^{13}\text{C}$ and $\delta^{18}\text{O}$ Measurements of CO_2 in Air

E. Flores¹, J. Viallon¹, P. Moussay¹, D.W.T. Griffith² and R.I. Wielgosz¹

¹Bureau International des Poids et Mesures (BIPM), Sèvres, France; +33-1-45-07-62-70, E-mail: jviallon@bipm.org

²University of Wollongong, Wollongong, Australia

Over recent years the introduction of Isotope Ratio Infrared Spectroscopy (IRIS), based on various spectroscopic techniques, has advanced stable isotope analysis in the atmosphere, allowing *in situ* field measurements of the isotope ratio of carbon dioxide (CO_2) in air, performed in real time directly on the air sample without separation of CO_2 from air. These instruments also need to be calibrated with CO_2 in air standard mixtures, applying calibration strategies which exploit the specificity of IR absorption spectroscopy, namely its dependency on individual isotopologues amount fraction in the sample.

The BIPM has developed a novel methodology to calibrate a Fourier Transformed Infrared (FTIR) spectrometer using only two standards of CO_2 in air with different mole fractions but identical isotopic composition. A complete uncertainty analysis was performed and measurements of $\delta^{13}\text{C}$ and $\delta^{18}\text{O}$ with standard uncertainties of 0.09 ‰ and 1.03 ‰, respectively, were demonstrated, at a nominal CO_2 mole fraction of 400 $\mu\text{mol mol}^{-1}$ in air. A different strategy was chosen for another IRIS system (Thermo Delta Ray) which makes use of two standards of CO_2 in air of known but differing $\delta^{13}\text{C}$ and $\delta^{18}\text{O}$ isotopic composition, reaching standard uncertainties of 0.18 ‰ and 0.48 ‰, for $\delta^{13}\text{C}$ and $\delta^{18}\text{O}$ measurements, respectively. Both calibration strategies were validated using a set of five Primary Reference Gas Mixtures of CO_2 in whole air or synthetic air in the mole fraction range of 378-420 $\mu\text{mol mol}^{-1}$, prepared and/or value assigned either by the National Institute of Standards and Technology (NIST) or the National Physical Laboratory (NPL). The standards were prepared using pure CO_2 obtained from different sources, namely: combustion; Northern Continental and Southern Oceanic Air and a gas well source, with $\delta^{13}\text{C}$ values ranging between -35 ‰ and -1 ‰. All measurements were compared with values assigned independently on the same samples by Isotope Ratio Mass Spectrometry (IRMS) at the Max Planck Institute for Biogeochemistry Jena (MPI-Jena), providing the traceability to the VPDB- CO_2 scale for $\delta^{13}\text{C}$ and $\delta^{18}\text{O}$.

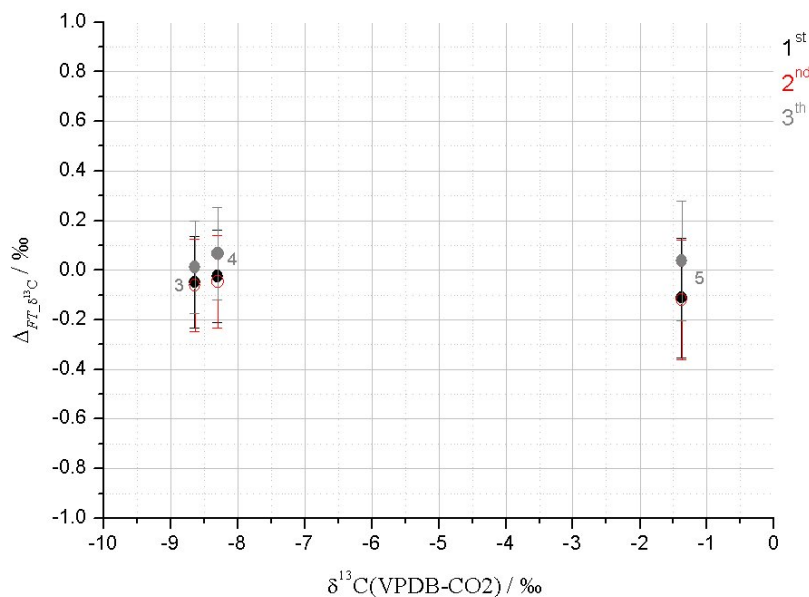


Figure 1. Difference between $\delta^{13}\text{C}$ values of the three samples evaluated by FTIR and by IRMS, as measured three times. The error bar represents the expanded uncertainty at a 95% level of confidence.

NOAA ESRL GLOBAL MONITORING ANNUAL CONFERENCE 2017

David Skaggs Research Center, Room GC-402
325 Broadway, Boulder, Colorado 80305 USA

Wednesday Morning, May 24, 2017 AGENDA

(Only presenter's name is given; please refer to abstract for complete author listing.)

07:00	Registration Opens in GC-402 - lunch orders collected at registration table	
07:30 - 08:00	Morning Snacks - coffee, tea, fruit, bagels and donuts served	
		Page No.
Session 5	Carbon Cycle & Greenhouse Gases - Methane & Carbon Monoxide — Chaired by John B. Miller	
08:00 - 08:15	Model Simulations of Atmospheric Methane and Their Evaluation Using AGAGE/NOAA Surface and IAGOS-CARIBIC Airborne Observations, 1997-2014 <i>Carl Brenninkmeijer (Max Planck Institute (MPI) for Chemistry, Atmospheric Chemistry Division, Mainz, Germany)</i>	25
08:15 - 08:30	Little Evidence for Significant Increases of CH ₄ Emission in the U.S. Over the Past Decade <i>Xin Lan (Cooperative Institute for Research in Environmental Sciences (CIRES), University of Colorado)</i>	26
08:30 - 08:45	Using Observations to Understand Regional Methane Budgets <i>Neil Harris (Cranfield University, Cranfield, United Kingdom)</i>	27
08:45 - 09:00	Separation of Methane Emissions from Biogenic Sources and Natural Gas Based on CH ₄ , C ₂ H ₆ and NH ₃ Column Observations in the Colorado Front Range <i>Natalie Kille (Cooperative Institute for Research in Environmental Sciences (CIRES), University of Colorado)</i>	28
09:00 - 09:15	Dual Frequency Comb Measurements of Greenhouse Gases Over Boulder <i>Eleanor Waxman (National Institute of Standards and Technology (NIST))</i>	29
09:15 - 09:30	Improved Mechanistic Understanding of Natural Gas Methane Emissions from Spatially Resolved Aircraft Measurements <i>Stefan Schwietzke (Cooperative Institute for Research in Environmental Sciences (CIRES), University of Colorado)</i>	30
9:30 - 10:00	Morning Break	
Session 6	Ozone, Water Vapor & Aerosols — Chaired by Irina Petropavlovskikh & Patrick Sheridan	
10:00 - 10:15	Rapid Desiccation of the Stratosphere in 2016: Connection to an Anomalous Change in the QBO <i>Dale F. Hurst (Cooperative Institute for Research in Environmental Sciences (CIRES), University of Colorado)</i>	31
10:15 - 10:30	Stratospheric Ozone at South Pole Begins to Show Signs of Improvement in the Yearly Ozone Hole <i>Bryan J. Johnson (NOAA Earth System Research Laboratory, Global Monitoring Division (GMD))</i>	32
10:30 - 10:45	Out of the SHADOZ: Impacts and Uncertainties of Ozonesonde Reprocessing <i>Jacquelyn Witte (Science Systems and Applications, Inc. (SSAI))</i>	33
10:45 - 11:00	Global Ozone Trends: First Results from the Tropospheric Ozone Assessment Report (TOAR) <i>Audrey Gaudel (Cooperative Institute for Research in Environmental Sciences (CIRES), University of Colorado)</i>	34
11:00 - 11:15	Surface Ozone in the Northern Front Range and the Influence of Oil and Gas Development on Ozone Production During FRAPPÉ/DISCOVER-AQ <i>Lucy Cheadle (Cooperative Institute for Research in Environmental Sciences (CIRES), University of Colorado)</i>	35
11:15 - 11:30	Impacts of Increasing Aridity and Wildfires on Aerosol Loading in the Intermountain Western U.S. <i>A. Gannet Hallar (University of Utah)</i>	36
11:30 - 11:45	Measurements of the Boundary Layer at Mauna Loa Observatory, Hawaii <i>John Barnes (Cooperative Institute for Research in Environmental Sciences (CIRES), University of Colorado)</i>	37
11:45 - 12:00	Ground-based and Aircraft Observations of Greenhouse Gases, Aerosols, and Other Trace Species Carried Out in Siberia, Russia <i>Mikhail Arshinov (V.E. Zuev Institute of Atmospheric Optics, Siberian Branch, Russian Academy of Science (IAO SB RAS), Tomsk, Russia)</i>	38
12:00 - 13:00	Catered Lunch - Outreach Classroom GB-124 (pre-payment of \$12.00 at registration)	

NOAA ESRL GLOBAL MONITORING ANNUAL CONFERENCE 2017

David Skaggs Research Center, Room GC-402
325 Broadway, Boulder, Colorado 80305 USA

Wednesday Afternoon, May 24, 2017 AGENDA

(Only presenter's name is given; please refer to abstract for complete author listing.)

		Page No.
Session 7	Halocarbons & Other Trace Gases — Chaired by James W. Elkins	
13:00 - 13:15	The Continued Slowdown in the Decline of Atmospheric CFC-11 <i>Stephen A. Montzka (NOAA Earth System Research Laboratory, Global Monitoring Division (GMD))</i>	39
13:15 - 13:30	Possible Influences of Stratospheric Transport Variability on Emission Estimates of Long-lived Trace Gases <i>Eric Ray (Cooperative Institute for Research in Environmental Sciences (CIRES), University of Colorado)</i>	40
13:30 - 13:45	Variability in Inter-hemispheric Exchange Inferred from Tropospheric Measurements of SF ₆ <i>Brad D. Hall (NOAA Earth System Research Laboratory, Global Monitoring Division (GMD))</i>	41
13:45 - 14:00	On the Emissions of HCFCs and CFCs Potentially Related to HFC Production <i>Martin K. Vollmer (Swiss Federal Laboratories for Materials Science and Technology, Empa, Dübendorf, Switzerland)</i>	42
14:00 - 14:15	European Emissions of the Powerful Greenhouse Gases Hydrofluorocarbons Inferred from Atmospheric Measurements and Their Comparison with Annual National Reports to UNFCCC <i>Michela Maione (University of Urbino, Department of Basic Sciences and Foundations, Urbino, Italy)</i>	43
14:15 - 14:30	Establishing Regular Measurements of Halocarbons at Taunus Observatory <i>Tanja Schuck (Goethe University, Institute for Atmospheric and Environmental Sciences, Frankfurt, Germany)</i>	44
14:30 - 15:00	Afternoon Break	
Session 8	Carbon Cycle & Greenhouse Gases - Remote Sensing — Chaired by Sourish Basu	
15:00 - 15:15	What Have We Learned About the Carbon Cycle from GOSAT and OCO-2? <i>David F. Baker (Cooperative Institute for Research in the Atmosphere (CIRA), Colorado State University)</i>	45
15:15 - 15:30	Assimilating NASA's Atmospheric Composition Observations in the GEOS Earth System Model <i>Steven Pawson (NASA Goddard Space Flight Center (GSFC))</i>	46
15:30 - 15:45	Using GEOS-5 Aerosols to Inform the OCO-2 CO ₂ Retrieval <i>Robert R. Nelson (Colorado State University, Department of Atmospheric Science)</i>	47
15:45 - 16:00	Amazonian GPP Estimated from Satellite-observed Carbonyl Sulfide Mixing Ratios <i>Timothy W. Hilton (University of California at Merced)</i>	48
16:00 - 16:15	Five-year Survey of the U.S. Natural Gas Flaring Observed from Space with VIIRS <i>Mikhail Zhizhin (Cooperative Institute for Research in Environmental Sciences (CIRES), University of Colorado)</i>	49
16:15 - 16:30	Analysis on the Spatiotemporal Distribution of OCO-2 XCO ₂ Over South Korea <i>Gawon Kim (National Institute of Meteorological Sciences, Seogwipo-si, South Korea)</i>	50
16:30 - 16:45	An Update on OCO-2 at the End of Prime Mission <i>Christopher W. O'Dell (Cooperative Institute for Research in the Atmosphere (CIRA), Colorado State University)</i>	51
16:45	Closing Remarks - Dr. James Butler, Director (NOAA/ESRL Global Monitoring Division)	

Model Simulations of Atmospheric Methane and Their Evaluation Using AGAGE/NOAA Surface and IAGOS-CARIBIC Airborne Observations, 1997-2014

P. Zimmermann¹, C. Brenninkmeijer¹, A. Pozzer¹, P. Jöckel² and J. Lelieveld²

¹Max Planck Institute (MPI) for Chemistry, Atmospheric Chemistry Division, Mainz, Germany; +49-(0)-176 478 176 67, E-mail: carl.brennkmeijer@mpic.de

²German Aerospace Center (DLR), Institute of Atmospheric Physics, Oberpfaffenhofen-Wessling, Germany

The global budget and trend of atmospheric methane (CH_4) have been simulated with the ECHAM/MESSy Atmospheric Chemistry (EMAC) model (T106, 90 hybrid pressure levels, ~ 500 m vertical in the Upper Troposphere Lower Stratosphere (UTLS), 2-min time steps, troposphere nudged towards ECMWF data) for the period 1997 through 2014, distinguishing eleven CH_4 source categories. Simulated CH_4 has been compared to observations from selected AGAGE and NOAA surface stations and 327 intercontinental Civil Aircraft for Regular Investigation of the atmosphere Based on an Instrument Container (CARIBIC) flights. The surface data give long-term consistent time series, whereas the aircraft data cover different parts of the globe for different periods and effects specific for the UTLS have to be dealt with. Source-segregated station simulation results have been rearranged to optimally fit in sum the station records, especially with respect to the inter-hemispheric CH_4 -gradient (ΔNS). The resulting redistribution represents an emission scenario which is suitable to explain the considered observations.

Tagged simulations with the eleven initial source categories were carried out to analyze the composition of the observed global CH_4 burden and derive steady state CH_4 lifetimes from the different sources. In this model configuration, without any CH_4 - H_2O feedback, the atmospheric CH_4 abundance is linearly dependent on the source strength and thus allows a posteriori rescaling of individual emissions with proportional effects on the corresponding inventories. Aiming for an observation consistent ΔNS , Amazon wetland emissions had to be enhanced by 30.57 Tg/y with compensating reduction of Northern Hemisphere fossil fuel related emissions. The correspondingly rescaled tagged results were superimposed without affecting the global mass balance. By including two additional (tagged) sources, one representing natural emissions (South America) and one shale gas production related emissions (North America), their potential role in growing CH_4 concentrations since 2007 has been investigated.

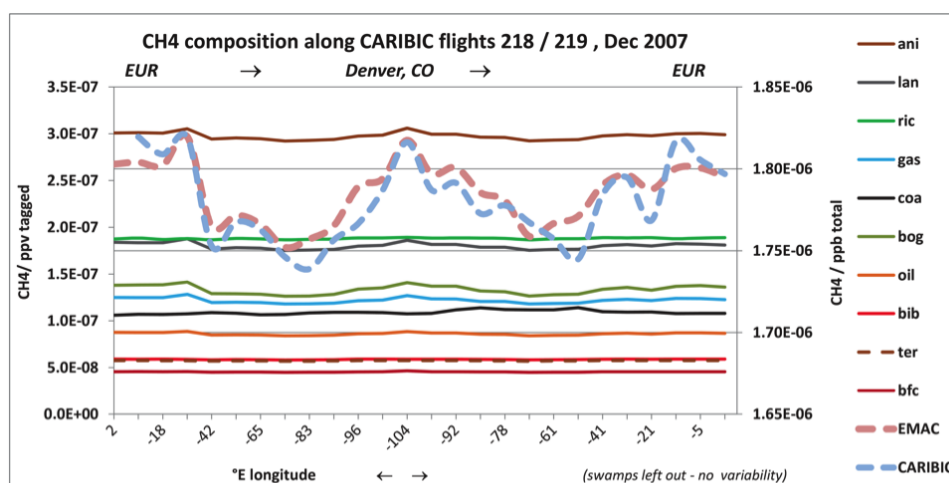


Figure 1. Example showing the different contributions (tagged, left) to the CH_4 burden (right) at cruise altitude of the CARIBIC observatory for 2 sequential flights, namely FRANKFURT-DENVER-FRANKFURT. The model values (red dashed) match the measurements (blue) which for a large part took place in the stratosphere (http://projects.knmi.nl/campaign_support/CARIBIC/171207/tsecPV07121712.gif). The discrepancy in symmetry is due to the time shift and slight differences in the actual flight corridor followed. Generally the model slightly dampens low values observed in tropopause folds due to limited resolution (about 500 m vertical).

Little Evidence for Significant Increases of CH₄ Emission in the U.S. over the Past Decade

X. Lan^{1,2}, P.P. Tans², C. Sweeney^{1,2}, A.E. Andrews², E.J. Dlugokencky², P. Lang², M.J. Croswell^{1,2}, B.R. Miller^{1,2}, S.A. Montzka², J. Kofler^{1,2}, K. McKain^{1,2} and S. Wolter^{1,2}

¹Cooperative Institute for Research in Environmental Sciences (CIRES), University of Colorado, Boulder, CO 80309; 347-276-3889, E-mail: xin.lan@noaa.gov

²NOAA Earth System Research Laboratory, Global Monitoring Division (GMD), Boulder, CO 80305

Recent studies on whether methane (CH₄) emissions from oil and natural gas (ONG) operations in the U.S. have significantly increased are still inconclusive. To provide observational evidence we carefully analyzed the *in situ* CH₄ measurements from the NOAA Global Greenhouse Gas Reference Network (GGGRN) for the best estimates of CH₄ trends for 2006-2016. Methane data from 11 aircraft sites and 9 surface/tower sites across the U.S. were included in this study. Variations of sampling frequencies in different seasons were taken into account for accurate trend detection. We found that most of our sites had similar CH₄ trends of ~ 6.5 ppb/yr, which was comparable with the recent global background CH₄ trend from the Mauna Loa Atmospheric Baseline Observatory. By utilizing the vertical gradient (planetary boundary layer relative to high altitude data), we have the ability to detect significant increase of surface emissions larger than 7-10% over the study period from most of our sites. However, statistically-significant increases were only found at the Southern Great Plains site in Oklahoma (SGP, downwind of the Eagle Ford, Barnett Shale and Woodford ONG fields) and the Dahlen sites in North Dakota (DND, downwind of the Bakken ONG field), which indicated influences from regional ONG activities. Ethane (C₂H₆) measurements from SGP (C₂H₆ measurements were not available at DND) and propane (C₃H₈) measurements from both SGP and DND exhibited significant increasing trends. Linear correlations were well identified for surface C₃H₈ and CH₄ enhancements at SGP, relative to observations at higher altitudes. However, by applying the observed enhancement ratios of surface C₃H₈ /CH₄ and the C₃H₈ trends (as indicator for ONG emissions) on CH₄ trend estimates, we would infer much larger surface CH₄ trends than what we actually observed at these two sites. When using C₂H₆, i-pentane, n-pentane, or n-butane data, we also infer much larger surface CH₄ trends. We found that the fat-tailed distribution of these hydrocarbon data and the changing enhancement ratios over time are likely responsible. This discrepancy suggests that using a constant enhancement ratio is not likely a reliable approach to compute CH₄ emission trends from ONG.

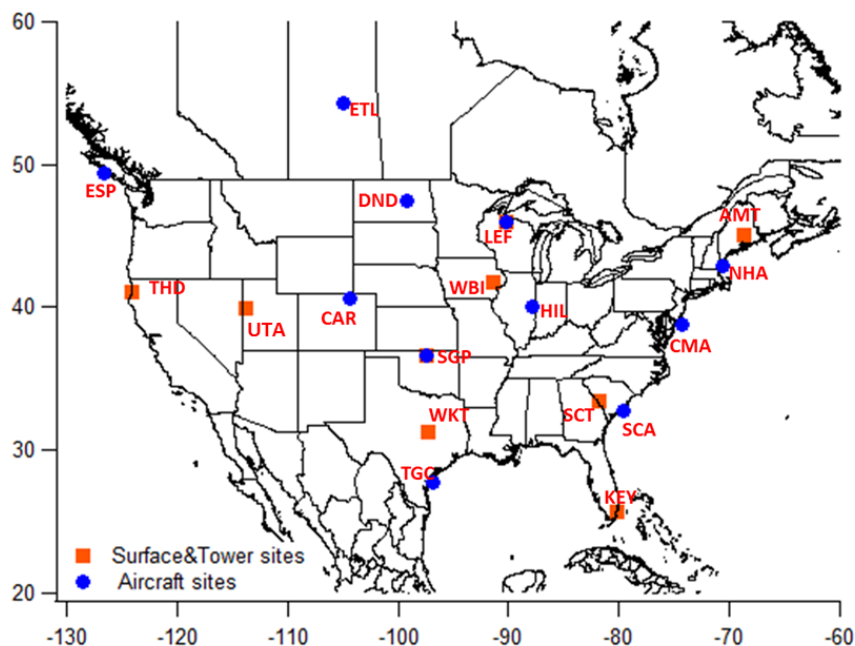


Figure 1. Long-term monitoring sites from the NOAA GGGRN.

Using Observations to Understand Regional Methane Budgets

N. Harris¹, A. Robinson², S. Connors², S. Riddick², R. Skelton², A. Manning³ and partners in the GAUGE project⁴

¹Cranfield University, Cranfield, United Kingdom; +44-1234-758155, E-mail: neil.harris@cranfield.ac.uk

²Cambridge University, Cambridge, United Kingdom

³UK Meteorological Office, Exeter, United Kingdom

⁴UK Natural Environment Research Council GAUGE (Greenhouse gAs Uk and Global Emissions) Project, United Kingdom

There is a growing need for comparisons between emission estimates produced using bottom-up and top-down techniques at high spatial resolution. In response to this, a proof of concept study has been performed in which developed an inversion approach to estimate methane (CH_4) emissions for a region (East Anglia) in the South East of the U.K. (~100 x 150 km) at high spatial resolution. We present results covering a 1-year period (June 2013 - May 2014) in which atmospheric CH_4 concentrations were recorded at 1-2 minute time-steps at four locations within the region of interest. Precise measurements were obtained using gas chromatography with flame ionisation detection (GC-FID) at three of the sites; the fourth used a PICARRO Cavity Ring-Down Spectrometer (CRDS). These observations, coupled with the U.K. Met Office's Lagrangian particle dispersion model, NAME, were used within the InTEM inversion system to produce the CH_4 emission fields. Realistic county emissions estimates in East Anglia were produced, which compare well with those of the U.K. National Atmospheric Emissions Inventory (NAEI).

In parallel a study of hot-spot emissions from a landfill near Cambridge was conducted with reasonable agreement being found emission estimates using the WindTrax dispersion model, a Gaussian Plume model and the NAME InTEM approach described above. We conclude that while the regional NAME InTEM approach provides real information about the location of hot-spot emissions, more work is needed to improve the uncertainties associated with the emission estimates. Bayesian approaches in which hot-spot locations are included in the prior show potential in this regard.

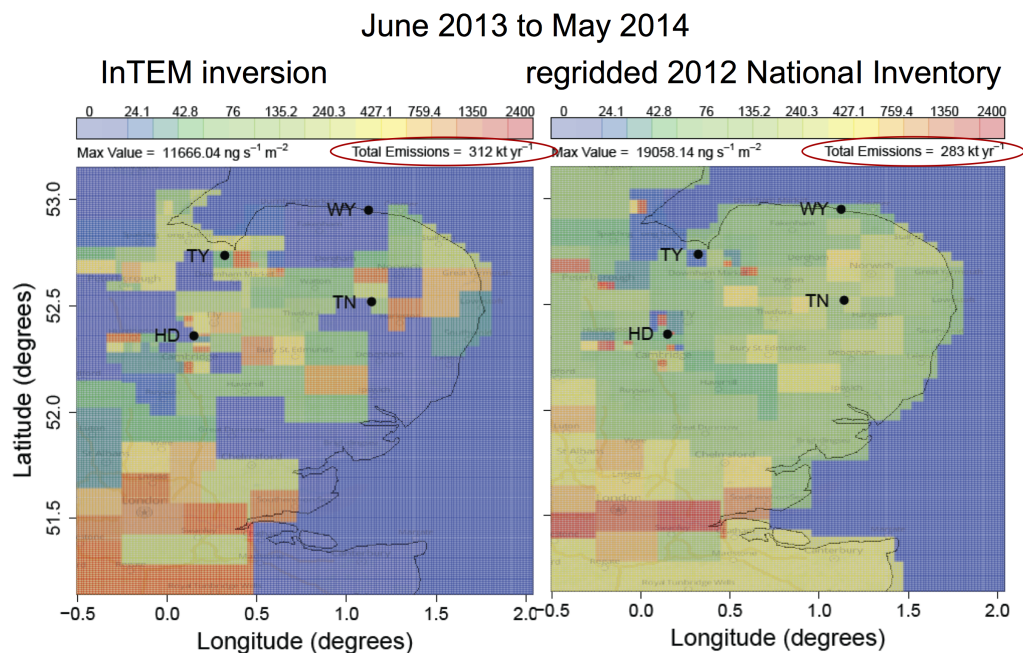


Figure 1. Estimated emissions of CH_4 in East Anglia from: (left) InTEM inversion of CH_4 measurements at marked sites; and (right) U.K. NAEI for 2012.

Separation of Methane Emissions from Biogenic Sources and Natural Gas Based on CH_4 , C_2H_6 and NH_3 Column Observations in the Colorado Front Range

N. Kille¹, R. Chiu¹, M. Frey², F. Hase², M. Sha², T. Blumenstock² and R. Volkamer³

¹Cooperative Institute for Research in Environmental Sciences (CIRES), University of Colorado, Boulder, CO 80309; 303-735-2235, E-mail: natalie.kille@colorado.edu

²Institute for Meteorology and Climate Research, Karlsruhe Institute of Technology, Campus Alpin, Karlsruhe, Germany

³University of Colorado, Department of Chemistry and Biochemistry, Boulder, CO 80309

Methane (CH_4) in the Northern Colorado Front Range is emitted from biogenic sources such as concentrated animal feeding operations (CAFOs) and natural gas production and storage. In March 2015 we deployed a network of five Fourier Transform Spectrometers (FTS) to characterize the regional-scale CH_4 dome in the Colorado Front Range based on vertical column measurements. Three EM27sun FTS measured CH_4 , oxygen (O_2) and water vapor columns at Eaton, CO, inside the dome and at two boundary sites; University of Colorado mobile Solar Occultation Flux measured ethane (C_2H_6), ammonia (NH_3), and H_2O at Eaton, CO, and a NCAR high-resolution FTS measured all gases at Boulder, CO. The column averaged dry air mole fractions $X\text{CH}_4$, $X\text{C}_2\text{H}_6$, and $X\text{NH}_3$ were determined using O_2 columns for air mass factor normalization, and background column was subtracted to derive column enhancements over background, $dX\text{CH}_4$, $dX\text{C}_2\text{H}_6$, $dX\text{NH}_3$ at Eaton, CO. Eaton is located both near CAFOs and at the northern edge of oil and natural gas production wells of the Denver-Julesburg Basin. Our approach for source apportioning methane employs a linear regression analysis that explains $dX\text{CH}_4$ in terms of $dX\text{C}_2\text{H}_6$ as tracer for natural gas sources, and $dX\text{NH}_3$ as tracer for CAFO emissions.

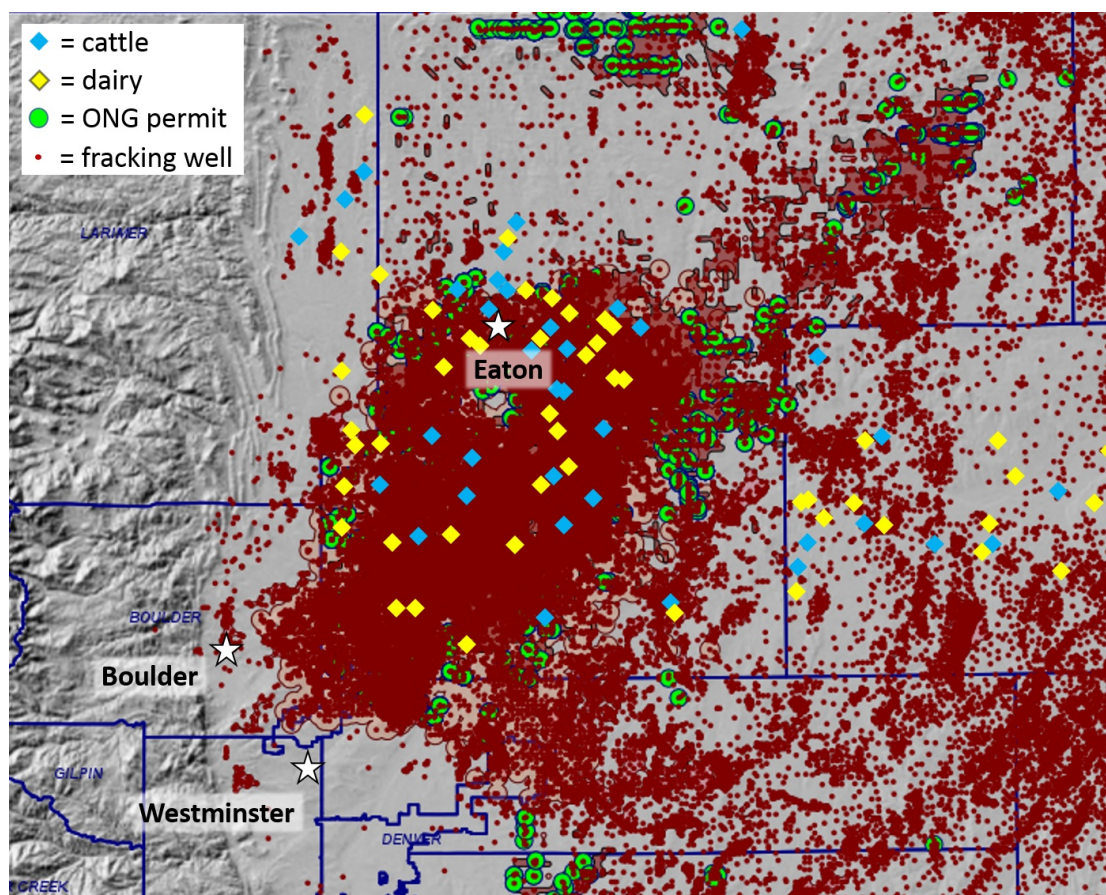


Figure 1. Map showing the measurement sites Eaton, Boulder, and Westminster, as well as CAFO and fracking locations.

Dual Frequency Comb Measurements of Greenhouse Gases over Boulder

E. Waxman¹, K. Cossel¹, G.W. Truong^{1,2}, F. Giorgetta¹, W. Swann¹, S. Coburn³, R. Wright³, G.B. Rieker³, I. Coddington¹ and N. Newbury¹

¹National Institute of Standards and Technology (NIST), Boulder, CO 80305; 303-497-4483, E-mail: eleanor.waxman@nist.gov

²Crystalline Mirror Solutions, Santa Barbara, CA 93101

³University of Colorado, Department of Mechanical Engineering, Boulder, CO 80309

Dual frequency comb spectroscopy (DCS) is a new technique that combines the precision of laser-based measurements with the broad spectral bandwidth of traditional incoherent spectroscopic techniques, resulting in a portable instrument with broad spectral bandwidth, high spectral resolution (0.0067 cm^{-1}), absolute frequency accuracy, and rapid data acquisition. We have compared two dual frequency comb instruments over a 2-km round-trip open-air path behind NIST. We find that the two instruments agree to better than 0.6 ppm carbon dioxide (CO_2), 7 ppb methane (CH_4), and 36 ppm water vapor (H_2O) over a two-week period of near-continuous measurements. We also compared the frequency comb measurements against a nearly co-located Picarro and find that they agree to better than 3.4 ppm CO_2 and 17 ppb CH_4 . We attribute these discrepancies primarily to differences between the HIGH-resolution TRANsmission molecular absorption (HITRAN) database and the World Meteorological Organization scale. We also present preliminary frequency comb data measured over the city of Boulder showing strong enhancements in CO_2 relative to background measurements allowing us to estimate traffic emissions from the city.

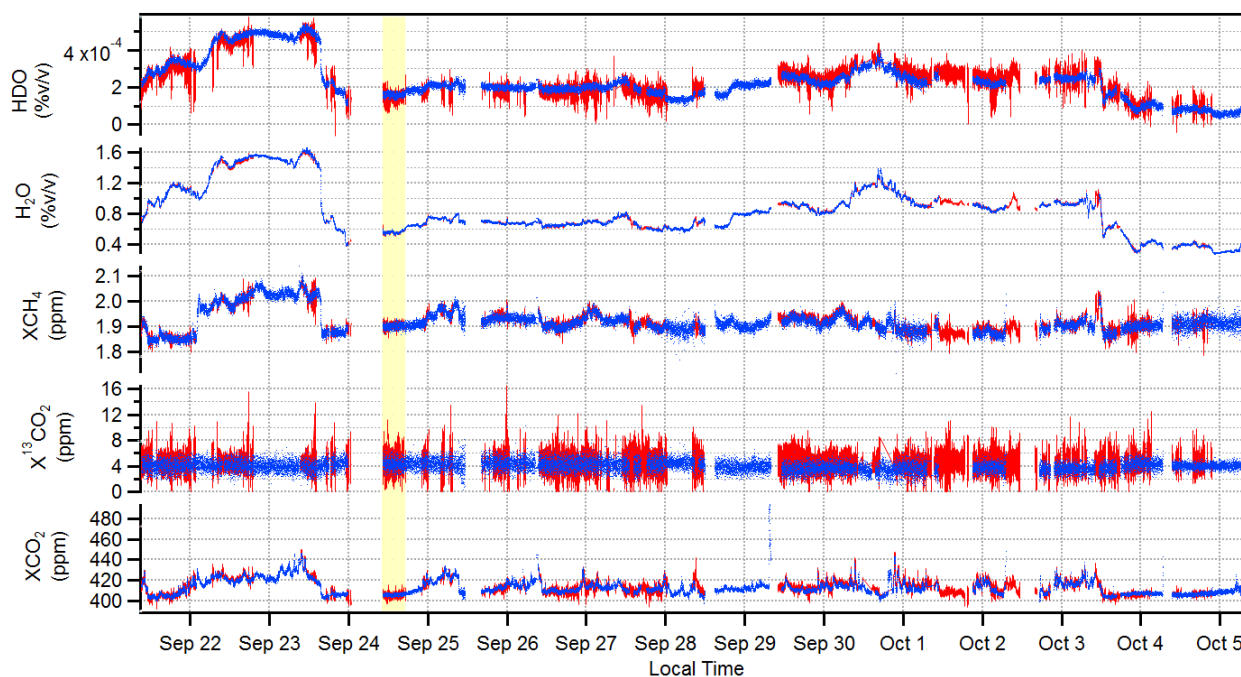


Figure 1. Comparison of two dual comb spectroscopy instruments over a 2-km round-trip path behind NIST showing excellent agreement between the two instruments. Blue: DCS A. Red: DCS B. There is more noise on DCS B data because the instrument had lower power reaching the detector.

Improved Mechanistic Understanding of Natural Gas Methane Emissions from Spatially Resolved Aircraft Measurements

S. Schwietzke^{1,2}, G. Petron^{1,2}, S. Conley^{3,4}, C. Pickering⁵, I. Mielke-Maday^{1,2}, E.J. Dlugokencky², P.P. Tans², T. Vaughn⁵, C. Bell⁵, D. Zimmerle⁵, S. Wolter^{1,2}, C.W. King⁶, A.B. White⁶, T. Coleman^{1,6}, L. Bianco^{1,6} and R.C. Schnell²

¹Cooperative Institute for Research in Environmental Sciences (CIRES), University of Colorado, Boulder, CO 80309; 303-497-5073, E-mail: stefan.schwietzke@noaa.gov

²NOAA Earth System Research Laboratory, Global Monitoring Division (GMD), Boulder, CO 80305

³Scientific Aviation, Roseville, CA 95661

⁴University of California at Davis, Davis, CA 95616

⁵Colorado State University, Fort Collins, CO 80523

⁶NOAA Earth System Research Laboratory, Physical Sciences Division (PSD), Boulder, CO 80305

Confidence in basin-scale methane (CH_4) emission estimates from oil and gas (O&G) operations hinges on an in-depth understanding, objective evaluation and continued improvements of both top-down (e.g. aircraft measurement based) and bottom-up (e.g. component-/facility-level measurements and engineering calculations) approaches. Enhancing the spatio-temporal resolution of top-down and bottom-up methods may allow improved reconciliation analysis of reported differences in O&G related CH_4 emission estimates. This presentation summarizes the first spatially-resolved CH_4 emission estimates from an aircraft mass balance in the U.S. Fayetteville shale gas play for 10 km x 60 km sub-regions. Refinements of the aircraft mass balance method were needed to reduce the number of potential methodological biases (e.g. data and methodology). The refinements include an in-depth exploration of the definition of upwind conditions and their impact on calculated downwind CH_4 enhancements and total CH_4 emissions, and taking into account small but non-zero vertical and horizontal wind gradients in the boundary layer. Optimal meteorological conditions and employment of multiple measurement platforms led to reduced uncertainty estimates compared to some previous studies. We identify higher emitting sub-regions, and localize repeating emission patterns as well as differences between days. In addition, we use spatio-temporally resolved NG industry reported activity data for the specific flight periods to offer explanations for the observed spatio-temporal CH_4 emission patterns. The increased resolution of the top-down calculation will for the first time allow for a spatially resolved comparison with a high resolution bottom-up CH_4 emission estimate based on facility-level emission measurements, concurrent activity data and other data sources.

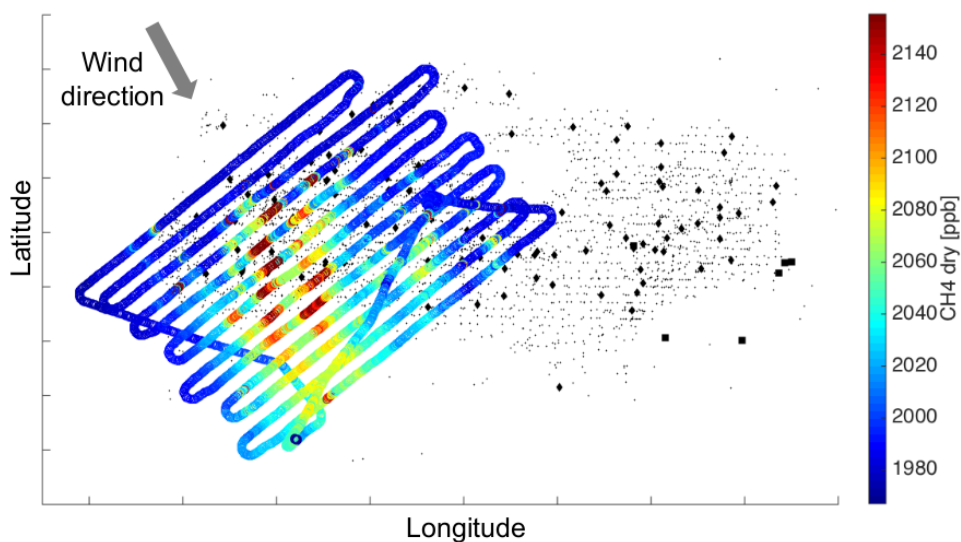


Figure 1. Raster flight pattern over parts of the Fayetteville shale gas basin and resulting methane levels indicate higher emitting sub-regions. A single flight example is shown as part of multiple flights in other parts of the basin, as well as repeats.

Rapid Desiccation of the Stratosphere in 2016: Connection to an Anomalous Change in the QBO

D.F. Hurst^{1,2}, S.M. Davis^{1,3}, K.H. Rosenlof³, E.G. Hall^{1,2} and A.F. Jordan^{1,2}

¹Cooperative Institute for Research in Environmental Sciences (CIRES), University of Colorado, Boulder, CO 80309; 303-497-7003, E-mail: Dale.Hurst@noaa.gov

²NOAA Earth System Research Laboratory, Global Monitoring Division (GMD), Boulder, CO 80305

³NOAA Earth System Research Laboratory, Chemical Sciences Division (CSD), Boulder, CO 80305

The quasi-periodic cycle of alternating westerly and easterly zonal winds in the tropical stratosphere, better known as the quasi-biennial oscillation (QBO), alters the stratospheric distributions of water vapor, ozone and other trace gases. The switch between QBO phases manifests itself as changes in tropical upwelling and the temperature of the tropical stratosphere. These inter-annual QBO changes have occurred in a fairly repeatable way since records began in 1953, with one exception: the 2015/2016 cycle. At the end of 2015, easterly winds had begun their expected downward propagation in the tropics, reaching 15 hPa by early 2016. However, in January 2016 this normal progression was curtailed by an anomalous upward displacement of the existing westerlies between 15 and ~30 hPa, and easterly winds suddenly appeared at ~30 hPa. These “early” easterlies continued their downward propagation during 2016, cooling the tropical tropopause and dramatically decreasing water vapor in the tropical lower stratosphere.

Annual and inter-annual variations in tropical lower stratospheric water vapor are generally attributed to the seasonal and QBO-induced cycles of tropical tropopause temperatures, respectively (see Figure 1). Extremes in these variations occur when the annual and inter-annual cycles of tropical coldpoint temperatures are constructively superimposed. In 2016 the cooling of the tropical tropopause by “early” QBO easterlies was augmented by the normal seasonal cooling during the latter half of the year. Tropical tropopause temperatures dropped 2.5°C during 2016 and tropical lower stratospheric water vapor mixing ratios fell 1.9 ppmv, 40% of the average December mixing ratio at 83 hPa. The strongest dry tropical anomalies, spanning the Indian Ocean from Africa to Indonesia, may have been intensified by enhanced convection driven by La Niña conditions. By December 2016 the desiccated tropical air had been transported poleward and upward, drying the subtropical lower stratosphere and advecting a dry layer to higher altitudes.

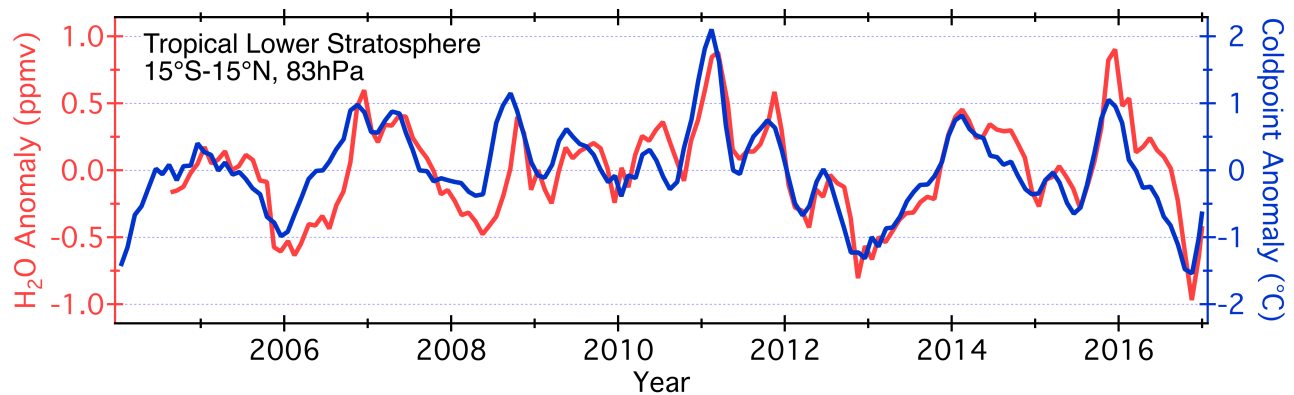


Figure 1. Water vapor anomalies in the tropical lower stratosphere are based on monthly zonal averages of Aura Microwave Limb Sounder retrievals (red). Tropical coldpoint temperature anomalies, based on the MERRA2 reanalysis (blue), slightly precede and correspond well with the water vapor anomalies. There were rapid and large declines in both anomalies during 2016.

Stratospheric Ozone at South Pole Begins to show Signs of Improvement in the Yearly Ozone Hole

B.J. Johnson¹, P. Cullis^{2,1}, C.W. Sterling^{2,1}, G. McConville^{2,1}, J. Booth¹ and I. Petropavlovskikh^{2,1}

¹NOAA Earth System Research Laboratory, Global Monitoring Division (GMD), Boulder, CO 80305; 303-497-6942, E-mail: bryan.johnson@noaa.gov

²Cooperative Institute for Research in Environmental Sciences (CIRES), University of Colorado, Boulder, CO 80309

Slight improvement in the severity of the September to mid-October ozone hole over South Pole Station, Antarctica is shown in the balloon-borne ozonesonde averaged data in Figure 1. The total column ozone average in the recent 5-year period 2012-2016 shows a slight upward shift by mid-September compared to the 1991-2011 average, but remains below the early 1986-1990 average total column line. This early period represents the first 5 years of ozonesonde measurements at South Pole, during a time when equivalent effective stratospheric chlorine was increasing rapidly. The NOAA Ozone Depleting Gas Index (ODGI) peaked over Antarctica by 2002. The steady decline in the ODGI should mean less severe ozone holes are expected each year. However, substantial natural year-to-year variability in the Antarctic polar vortex and total column ozone caused by variability in dynamical conditions are observed at South Pole and make it difficult to detect a definite trend towards full recovery. The Dobson spectrophotometer 1964-1981 median shown in Figure 1, before stratospheric ozone depletion was observed, provides a glimpse of what full recovery should look like when total column ozone remains above 220 Dobson units (DU) into October.

Ozonesonde profiles showed one other slight improvement. The September depletion rate in the 14-21 km layer dropped to 3 Dobson Units (DU) per day falling below the 1991-2011 range of 3.0 – 4.0 DU/day.

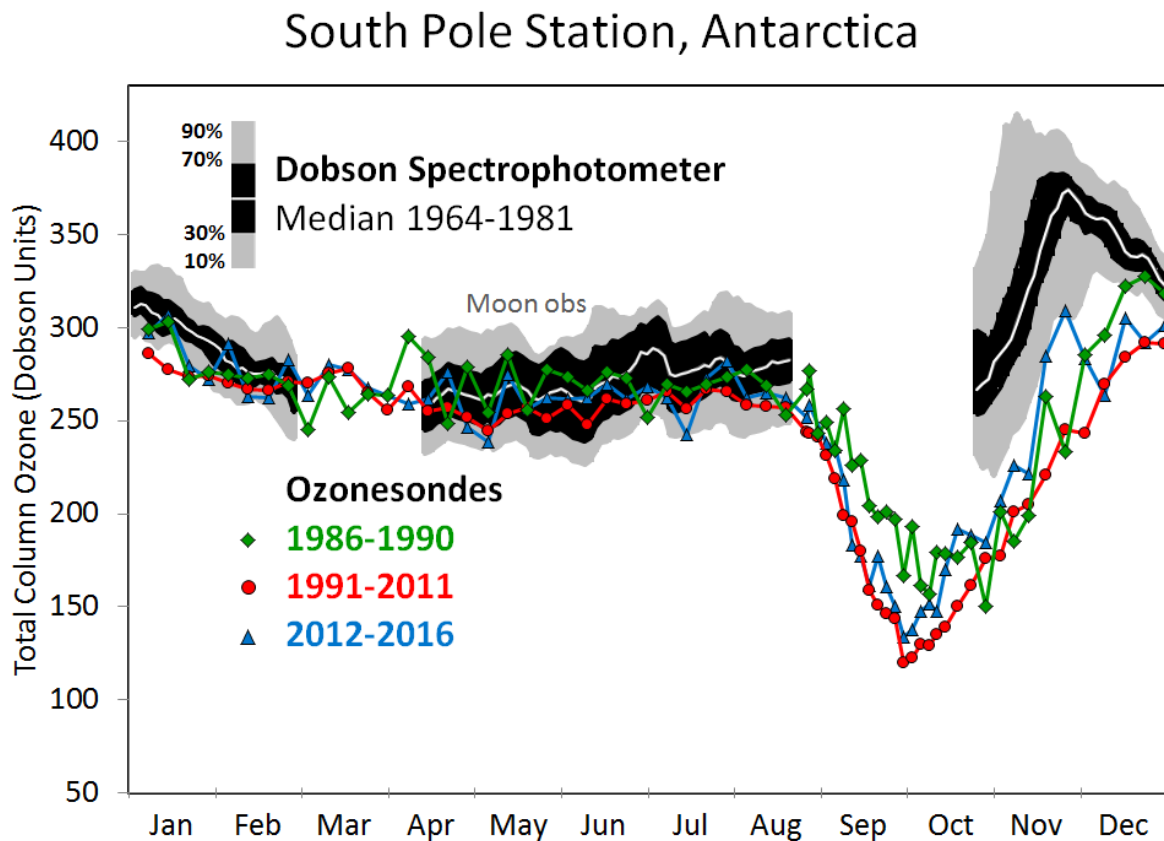


Figure 1. South Pole Station total column ozone averages from Dobson and ozonesonde measurements.

Out of the SHADOZ: Impacts and Uncertainties of Ozonesonde Reprocessing

J. Witte^{1,2}, A.M. Thompson², M. Fujiwara,³ S. Ogino⁴, A. Jordan^{5,6}, B.J. Johnson⁶, C.W. Sterling^{5,6} and N. Komala⁷

¹Science Systems and Applications, Inc. (SSAI), Lanham, MD 20706; 301-614-5991, E-mail: jacquelyn.witte@nasa.gov

²NASA Goddard Space Flight Center (GSFC), Atmospheric Chemistry and Dynamics Laboratory, Greenbelt, MD 20771

³Hokkaido University, Sapporo, Hokkaido, Japan

⁴Japan Agency for Marine-Earth Science and Technology (JAMSTEC), Yokosuka, Natsushimacho, Japan

⁵Cooperative Institute for Research in Environmental Sciences (CIRES), University of Colorado, Boulder, CO 80309

⁶NOAA Earth System Research Laboratory, Global Monitoring Division (GMD), Boulder, CO 80305

⁷Indonesian Institute of Aeronautics and Space (LAPAN), Jakarta, Indonesia

The SHADOZ (Southern Hemisphere ADditional OZonesondes) network is a NASA/GSFC project in collaboration with NOAA/ESRL/GMD, and international partners from Asia, Africa and Europe to archive long-term electrochemical concentration cell (ECC) ozonesonde records from tropical stations since 1998. There are currently over 6000 ozonesonde profiles in the SHADOZ database, with 14 stations having records for at least 10 years. Like many long-term sounding projects, SHADOZ is characterized by variations in operating procedures, instrumentation, and data processing. These contribute to measurement uncertainty and may limit the reliability of deriving ozone profile trends from the soundings. Recent advances in reprocessing methods and post processing software, such as Skysonde (a NOAA/GMD product), have led to a comprehensive reprocessing of SHADOZ ozonesonde data records. We present an evaluation of the first reprocessing of ozone profile records from the Watukosek-Java, Indonesia and Hanoi, Vietnam stations in the SHADOZ archive. The NOAA/GMD operational guidelines and Strato software system has been employed for the entire data record at Java and the first half of Hanoi's record before switching to a Vaisala system. Methods for homogenizing these long-term ozone records are discussed and preliminary estimates of ozone uncertainty are shown. Satellite overpass data from Aura Ozone Monitoring Instrument (OMI) and Microwave Limb Sounder (MLS) are used as reference measurements to study the impact of reprocessing at the Java and Hanoi stations.

SHADOZ Sites: <https://tropo.gsfc.nasa.gov/shadoz>



Figure 1. Map of SHADOZ stations.

Global Ozone Trends: First Results from the Tropospheric Ozone Assessment Report (TOAR)

A. Gaudel^{1,2}, O. Cooper^{1,2}, G. Ancellet³, I. Petropavlovskikh^{1,4}, A. Thompson⁵, V. Thouret⁶ and J. Witte^{7,5}

¹Cooperative Institute for Research in Environmental Sciences (CIRES), University of Colorado, Boulder, CO 80309; 303-497-6563, E-mail: audrey.gaudel@noaa.gov

²NOAA Earth System Research Laboratory, Chemical Sciences Division (CSD), Boulder, CO 80305

³Laboratoire Atmosphères, Milieux, Observations Spatiales-Institute Pierre Simon Laplace (LATMOS-IPSL), National Center for Scientific Research (CNRS), Université Pierre et Marie Curie, Université d, Paris, France

⁴NOAA Earth System Research Laboratory, Global Monitoring Division (GMD), Boulder, CO 80305

⁵NASA Goddard Space Flight Center (GSFC), Atmospheric Chemistry and Dynamics Laboratory, Greenbelt, MD 20771

⁶Laboratoire d'Aérodynamique, The National Center for Scientific Research (CNRS), and Université Paul Sabatier Toulouse III, Toulouse, France

⁷Science Systems and Applications, Inc. (SSAI), Lanham, MD 20706

Tropospheric ozone (O_3) is a greenhouse gas and pollutant detrimental to human health and crop and ecosystem productivity. Since 1990 a large portion of the anthropogenic emissions that react in the atmosphere to produce O_3 have shifted from North America and Europe to Asia. This rapid shift, coupled with limited O_3 monitoring in developing nations, has left scientists unable to answer the most basic questions: Is ozone continuing to decline in nations with strong emission controls? To what extent is O_3 increasing in the developing world? International Global Atmospheric Chemistry's (IGAC) Tropospheric Ozone Assessment Report (TOAR) has been designed to answer these questions and this presentation will show the first results from the TOAR-Climate initiative, summarizing global trends of tropospheric O_3 , but focusing on regions where observations are the most developed: North America, Europe and East Asia. In this study, *in situ* ground-based instruments, the In-service Aircraft for a Global Observing System (IAGOS), ozonesondes and lidar are combined to provide an up-to-date picture of tropospheric O_3 changes from the surface to the tropopause since the 1990s.

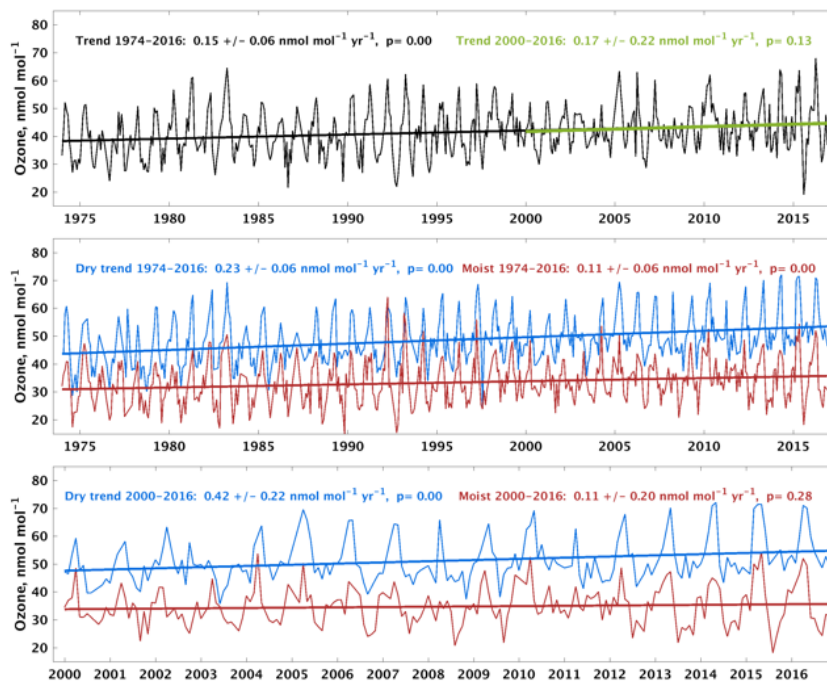


Figure 1. a) Nighttime monthly median ozone values at Mauna Loa Observatory calculated with all available data for months with at least 50% data availability, January 1974 – December 2016. b) Same as in a) but for data split into dry (dewpoint less than the climatological monthly 40th percentile) and moist (dewpoint greater than the climatological monthly 60th percentile) categories. A dry or moist category in any given month must have a sample size of at least 24 individual hourly nighttime observations. c) As in b) but for 2000-2016.

Surface Ozone in the Northern Front Range and the Influence of Oil and Gas Development on Ozone Production During FRAPPÉ/DISCOVER-AQ

L. Cheadle^{1,2}, S.J. Oltmans³, G. Petron^{1,2}, R.C. Schnell², E.J. Mattson⁴, S.C. Herndon⁵, A.M. Thompson⁶, D. Blake⁷ and A. McClure-Begley^{1,2}

¹Cooperative Institute for Research in Environmental Sciences (CIRES), University of Colorado, Boulder, CO 80309; 206-271-9224, E-mail: lucy.cheadle@noaa.gov

²NOAA Earth System Research Laboratory, Global Monitoring Division (GMD), Boulder, CO 80305

³Retired from NOAA Earth System Research Laboratory, Global Monitoring Division (GMD), Boulder, CO 80305

⁴Colorado Department of Public Health and Environment (CDPHE), Denver, CO 80246

⁵Aerodyne Research Inc., Billerica, MA 01821

⁶NASA Goddard Space Flight Center (GSFC), Atmospheric Chemistry and Dynamics Laboratory, Greenbelt, MD 20771

⁷University of California at Irvine, Department of Chemistry, Irvine, CA 92697

The results of this study demonstrate that high concentrations of ozone (O_3) in the northern Front Range of Colorado are not limited to the urban Denver area; high O_3 is observed in rural areas where oil and gas activity is the primary source of O_3 precursors. On individual days, oil and gas precursors can contribute in excess of 30 ppb to O_3 growth and could lead to exceedances of the Environmental Protection Agency (EPA) standards. Data used in this study was gathered from continuous surface O_3 monitors as well as additional flask measurements and mobile laboratories that were part of the Front Range Air Pollution and Photochemistry Experiment (FRAPPÉ) and Deriving Information on Surface conditions from Column and Vertically Resolved Observations Relevant to Air Quality (DISCOVER-AQ) field campaign of July and August, 2014. Overall O_3 levels during the summer of 2014 were lower than in 2013, likely due to cooler and damper weather than an average summer. This study determined the average O_3 mixing ratio on summer days with limited photochemical production within the boundary layer to be approximately 45 ppb. Mobile laboratory and flask data collected on July 23, August 3, and August 13, 2014 provide representative case studies of different O_3 formation environments in and around Greeley. Observations of a number of gases (including methane, ethane, carbon monoxide, nitrous oxide (NO_x)) measured along with O_3 are used to identify possible sources of O_3 precursor emissions that could contribute to O_3 formation. The July 23 survey demonstrated low O_3 enhancement while the August 3 and August 13 surveys recorded O_3 at 30 ppb or more above concentrations on days with limited photochemical production. August 3 is an example of both high oil and gas emissions and high agricultural emissions. August 13 demonstrates high oil and gas emissions, low agricultural emissions, and carbon monoxide measurements that were well correlated with ethane from oil and gas, suggesting an oil and gas related activity as a potential NO_x and O_3 precursor source.

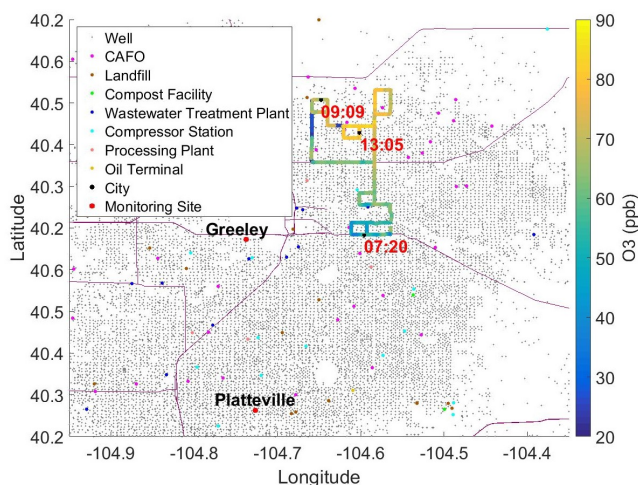


Figure 1. Map of mobile laboratory O_3 measurements on August 13, 2014.

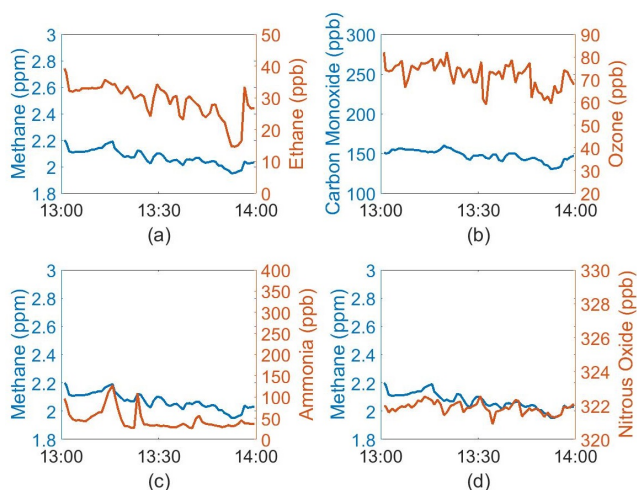


Figure 2. Time series of gaseous species from mobile laboratory on August 13, 2014.

Impacts of Increasing Aridity and Wildfires on Aerosol Loading in the Intermountain Western U.S.

A.G. Hallar^{1,2}, N. Molotch³, E. Andrews^{4,5}, J.J. Michalsky^{4,5}, R. Peterson^{1,2}, B. Livneh⁴, J. Hand⁶, D. Lowenthal² and I.B. McCubbin²

¹University of Utah, Salt Lake City, UT 84112; 970-819-0968, E-mail: Gannet.Hallar@dri.edu

²Storm Peak Laboratory, Desert Research Institute, Steamboat Springs, CO 80488

³University of Colorado, Department of Geography, Boulder, CO 80309

⁴Cooperative Institute for Research in Environmental Sciences (CIRES), University of Colorado, Boulder, CO 80309

⁵NOAA Earth System Research Laboratory, Global Monitoring Division (GMD), Boulder, CO 80305

⁶Cooperative Institute for Research in the Atmosphere (CIARA), Colorado State University, Fort Collins, CO 80521

Feedbacks between climate warming, land surface aridity, and wildfire derived aerosols represent a large source of uncertainty in future climate predictions. Here, long-term observations of aerosol optical depth (AOD), surface level aerosol loading, fire-area burned, and hydrologic simulations are used to show that regional scale increases in aridity and resulting wildfires have significantly increased summertime aerosol loading in remote high-elevation regions of the Intermountain West of the U.S. Surface summertime organic aerosol loading and total AOD were both strongly correlated ($p < 0.05$) with aridity and fire area burned at high-elevation sites across major western U.S. mountain ranges. These results demonstrate that surface level organic aerosol loading is dominated by summertime wildfires at many high-elevation sites. This analysis provides new constraints for climate projections on the influence of drought and resulting wildfires on aerosol loading. These empirical observations will help better constrain projected increases in organic aerosol loading with increased fire activity under climate change.

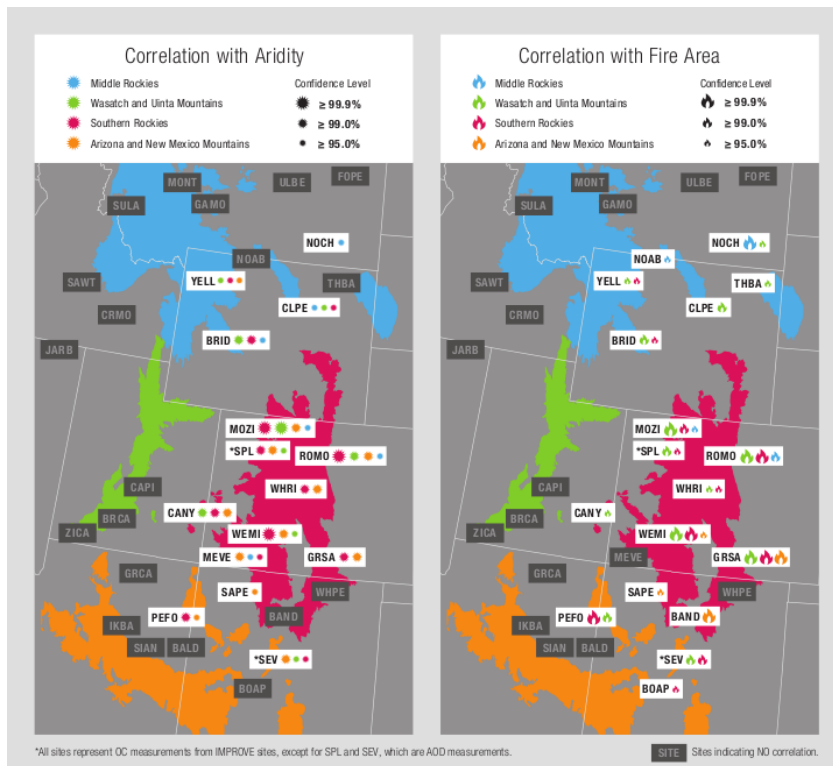


Figure 1. The correlation between summertime annual organic aerosol loading (OC) or AOD across the Intermountain West and (a) annual summertime aridity (b) total fire area burned across the Intermountain West. White boxes denote sites where a significant correlation [$p < 0.05$] was observed. The color indicates the specific mountain range. Dark grey boxes represent sites where no correlation was observed.

Measurements of the Boundary Layer at Mauna Loa Observatory, Hawaii

J. Barnes^{1,2} and N.C.P. Sharma³

¹Cooperative Institute for Research in Environmental Sciences (CIRES), University of Colorado, Boulder, CO 80309; 720-684-9143, E-mail: John.E.Barnes@noaa.gov

²NOAA Earth System Research Laboratory, Global Monitoring Division (GMD), Boulder, CO 80305

³Central Connecticut State University, Department of Physics and Engineering Physics, New Britain, CT 06053

The NOAA Mauna Loa Atmospheric Baseline Observatory (MLO) is an atmospheric monitoring station on the North side of Mauna Loa Volcano (4169 m summit) located at an altitude of 3396 m. The bright sun, dark lava surface, and the seven percent grade of the mountain create a surface radiation wind that changes from upslope in the daytime to downslope after sunset. This radiation wind has a magnitude of 2.5-3.0 m/s. The off-island wind interacts with the mountain to create a barrier wind which is about 80% of the off-island windspeed. The radiation wind dominates when the off-island winds are low, and opposite is true when the off-island winds are strong. Temperature inversions form at sunset in the first 50 meters above the ground. Aerosol profiles, measured with a unique technique called CLidar, or camera lidar, often increase with altitude and show a peak between 60 and 160 meters. Nephelometer measurements on the tower verified a 40% increase between 10 and 38 meters. The aerosol generally decreases to upper tropospheric values with a distinct change in the rate of decrease at 600 m above the ground. At night the region between the aerosol peak and 600 m is often flowing upslope, counter to the downslope surface flow. The source of the air in this counter flow region is not well understood, but appears to come from levels below the station altitude at least occasionally. This possibly would impact the interpretation of some of the air samples taken during this period. A period in the winter of 2015-2016 was investigated to compare the different energy contributions to the diurnal cycle. For an average clear day the solar contribution was 6.6 kW*Hr/m^2 . The energy stored in the lava was estimated by burying temperature loggers and was 3.5 kW*Hr/m^2 and 0.06 kW*Hr/m^2 was stored in the air. The blackbody (greybody) radiation from the lava surface was 6.0 kW*Hr/m^2 over the 24 hour period.

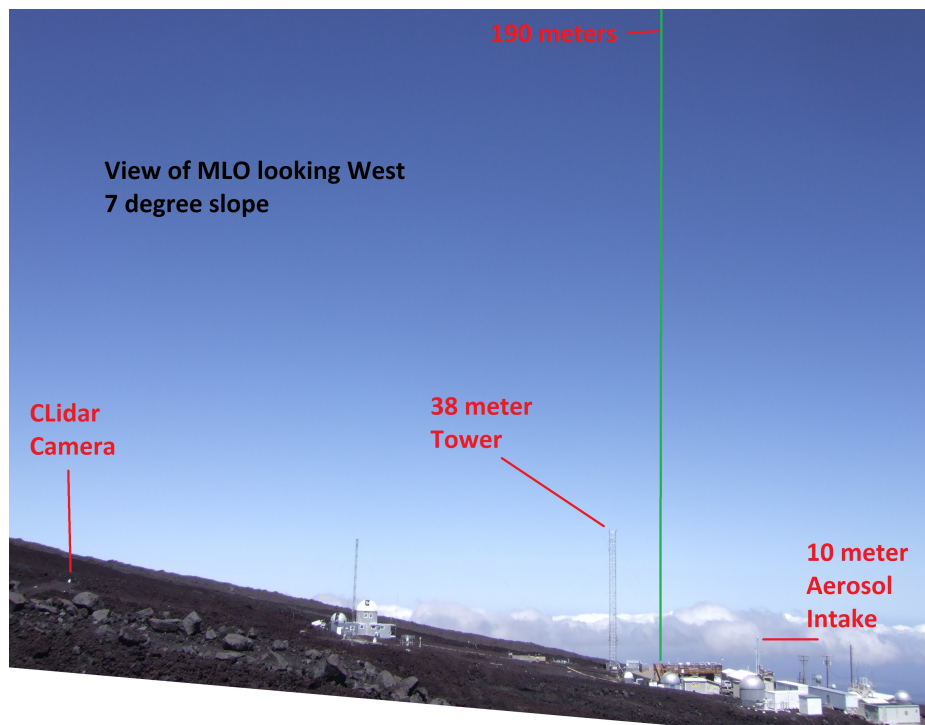


Figure 1. View of Mauna Loa Observatory showing the layout of the station on the dark lava, the position of the lidar laser (green beam) imaged by the CLidar camera, and the tower.

Ground-based and Aircraft Observations of Greenhouse Gases, Aerosols, and other Trace Species Carried out in Siberia, Russia

M. Arshinov¹, B.D. Belan¹, M.V. Panchenko¹, T. Machida², M. Sasakawa², S. Maksyutov², P. Ciais³, J.-D. Paris³, P. Nedelec⁴, J.-M. Cousin⁴, G. Athier⁴, Y.S. Balin¹, I.E. Penner¹, G.P. Kokhanenko¹, K. Law⁵, G. Ancellet⁵, J. Pelon⁵, P.N. Antokhin¹, D.K. Davydov¹, A.V. Fofonov¹, G.A. Ivlev¹, A.V. Kozlov¹, O.A. Krasnov¹, D.A. Pestunov¹, G.N. Tolmachev¹, D.V. Simonenkov¹ and D.G. Chernov¹

¹V.E. Zuev Institute of Atmospheric Optics, Siberian Branch, Russian Academy of Science (IAO SB RAS), Tomsk, Russia; +7-3822-49-28-94, E-mail: michael@iao.ru

²National Institute for Environmental Studies, Tsukuba-City, Ibaraki, Japan

³Laboratoire des Sciences du Climat et de l'Environnement (LSCE), Orme des Merisiers, France

⁴Laboratoire d'Aérodologie, The National Center for Scientific Research (CNRS), and Université Paul Sabatier Toulouse III, Toulouse, France

⁵LATMOS, Université Pierre et Marie Curie and Centre National de la Recherche Scientifique (CNRS), Paris, France

Siberia covers a vast area of the land surface of the Northern Hemisphere (NH). Its various ecosystems are very sensitive to a climate change, so investigation of the atmospheric composition in this region is of great importance for understanding land-atmosphere exchange processes and possible feedbacks in the whole NH. In spite of recognizing the problem, continuous and comprehensive measurements are still lacking. In order to understand what happens in Siberia, the Institute of Atmospheric Optics of the Siberian Branch of the Russian Academy of Science (IAO SB RAS) combined its own efforts with several institutions from Japan and France to fill up the gap in observational data. Here, we present some results of long-term and large-scale cooperative studies of the Siberian airshed undertaken over the past two decades.

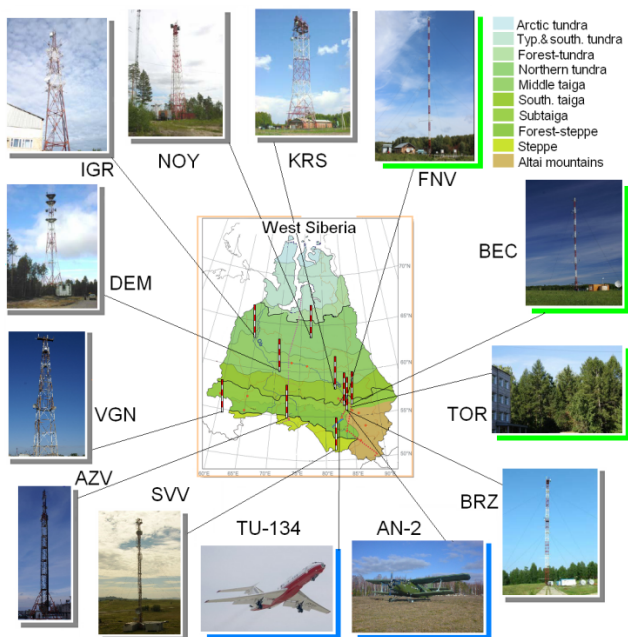


Figure 1. Joint NIES-IAO ground-based network for GHG monitoring (JR-STATION; gray shade), IAO own stations (aerosols and trace gases; green shade), Joint NIES-IAO regional aircraft observations of GHG (blue shade).

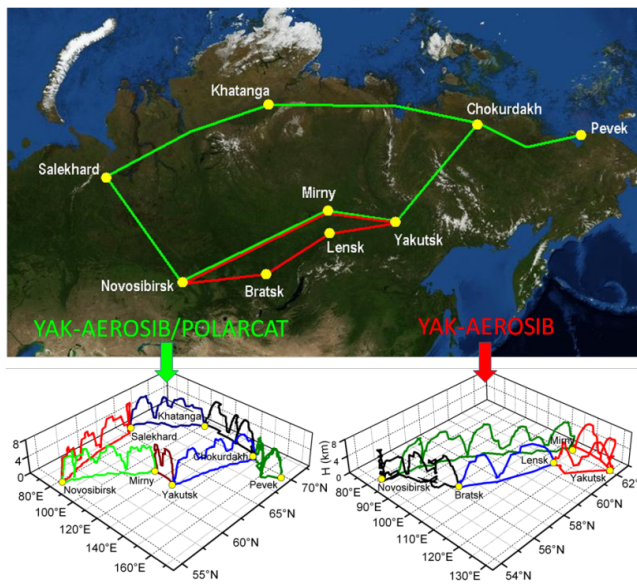


Figure 2. Map of flight routes and a pattern of the large-scale airborne campaigns (IAO-LSCE-LA-LATMOS): YAK-AEROSIB – 2006 (2 campaigns), 2007, 2008, 2010, 2012, 2013); YAK-AEROSIB/POLARCAT – 2008.

The Continued Slowdown in the Decline of Atmospheric CFC-11

S.A. Montzka¹, G.S. Dutton^{2,1}, P. Yu^{3,2}, R.W. Portmann³, E. Ray^{2,3}, F.L. Moore^{2,1}, D. Nance^{2,1}, B.D. Hall¹, C. Siso^{2,1}, J. Daniel³, B. Miller^{2,1}, D. Mondeel^{2,1}, L. Kuijpers⁴, L. Hu^{2,1} and J.W. Elkins¹

¹NOAA Earth System Research Laboratory, Global Monitoring Division (GMD), Boulder, CO 80305; 303-497-6657, E-mail: Stephen.A.Montzka@noaa.gov

²Cooperative Institute for Research in Environmental Sciences (CIRES), University of Colorado, Boulder, CO 80309

³NOAA Earth System Research Laboratory, Chemical Sciences Division (CSD), Boulder, CO 80305

⁴Eindhoven Centre for Sustainability, Technical University Eindhoven, Eindhoven, Netherlands

The atmospheric decline of CFC-11 since 2002 has been difficult to reconcile with reported global production being essentially zero since 2007. In the absence of production we would have expected the “bank” of CFC-11 (produced but not-yet-emitted chemical) to have diminished, a slow decline in global emissions, an accelerating decline in global mean mole fraction, and a north-to-south mole fraction approaching zero. Instead, measurements from multiple instruments at GMD from 2002 to 2012 show that the atmospheric CFC-11 decline did not accelerate over this period but remained steady at -2.2 ± 0.2 ppt/yr in both hemispheres, implying unchanging global emissions throughout that decade. Conceivably these results could be explained by a slowly changing emission rate of CFC-11 from in-use applications (the bank), but this cannot readily explain the striking 50% slowdown in the atmospheric decline of CFC-11 observed since 2012 to -1.1 ppt/yr. This slowdown was also coincident with a 50% increase in the measured hemispheric mole fraction difference (north – south). These observations imply a substantial increase in the flux of CFC-11 in the northern hemisphere, although the underlying cause of these changes remains unclear. Here we consider the observations with multiple 3-D model simulations (CESM1-WACCM) using dynamics specified by MERRA, MERRA2 or GEOS5 to diagnose the observations to investigate if they reflect substantial changes in broad-scale atmospheric mixing process, an increase in emissions nearly a decade after reported global production ceased, or a combination of both influences.

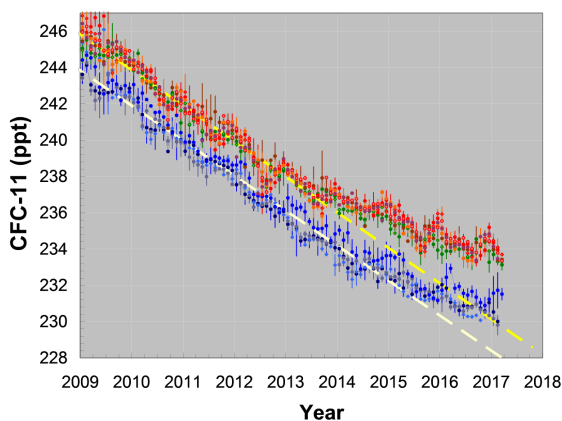


Figure 1. Monthly mean mole fractions of CFC-11 at northern hemispheric sites (red and green points) and southern hemispheric sites (blue points) since 2009 as measured from flasks by gas chromatography with mass spectrometry detection. Dashed lines are fits to northern (yellow) and southern (white) hemispheric means during 2004 to 2013.

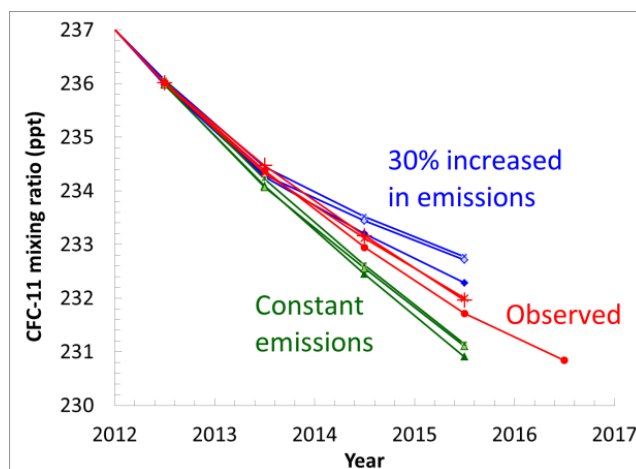


Figure 2. Observed and simulated annual mean mole fractions of CFC-11 in recent years. Results from three different measurement systems at NOAA (red) are compared to 3-D simulations using the CESM1-WACCM model and three different representations of reanalyzed meteorology (MERRA, MERRA2, and GEOS5) with constant emissions after 2012 (green lines) and a 30% increase in emissions in 2014 and 2015 compared to the 2002-2012 mean (blue lines).

Possible Influences of Stratospheric Transport Variability on Emission Estimates of Long-lived Trace Gases

E. Ray^{1,2}, J. Daniel², S.A. Montzka³, R.W. Portmann², P. Yu^{2,1}, K.H. Rosenlof², F.L. Moore^{1,3}, G.S. Dutton^{1,3}, J.W. Elkins³ and D. Mondeel^{1,3}

¹Cooperative Institute for Research in Environmental Sciences (CIRES), University of Colorado, Boulder, CO 80309; 303-497-7628, E-mail: eric.ray@noaa.gov

²NOAA Earth System Research Laboratory, Chemical Sciences Division (CSD), Boulder, CO 80305

³NOAA Earth System Research Laboratory, Global Monitoring Division (GMD), Boulder, CO 80305

We use surface measurements of a number of long-lived trace gases, including chlorofluorocarbons (CFC-11, CFC-12) and nitrous oxide (N_2O), and a 3-box model to estimate the influences of interannual variability in bulk stratospheric transport characteristics on emission estimates of these trace gases. The results suggest that stratospheric transport variability such as due to the Quasi-Biennial Oscillation, decadal scale trends, anomalous shifts in stratospheric circulation strength such as around the years 2000 and 2014, and shifts in Southern Hemisphere versus Northern Hemisphere stratospheric circulation can all affect emission estimates of long-lived trace gases. We compare the 3-box model derived bulk stratospheric transport characteristics to the variability in stratospheric satellite measurements, residual circulation estimates and global model simulations to check for consistency. The implications of fully accounting for stratospheric variability in emission estimates of long-lived trace gases can be significant, including for those gases monitored by the Montreal Protocol and/or of climatic importance.

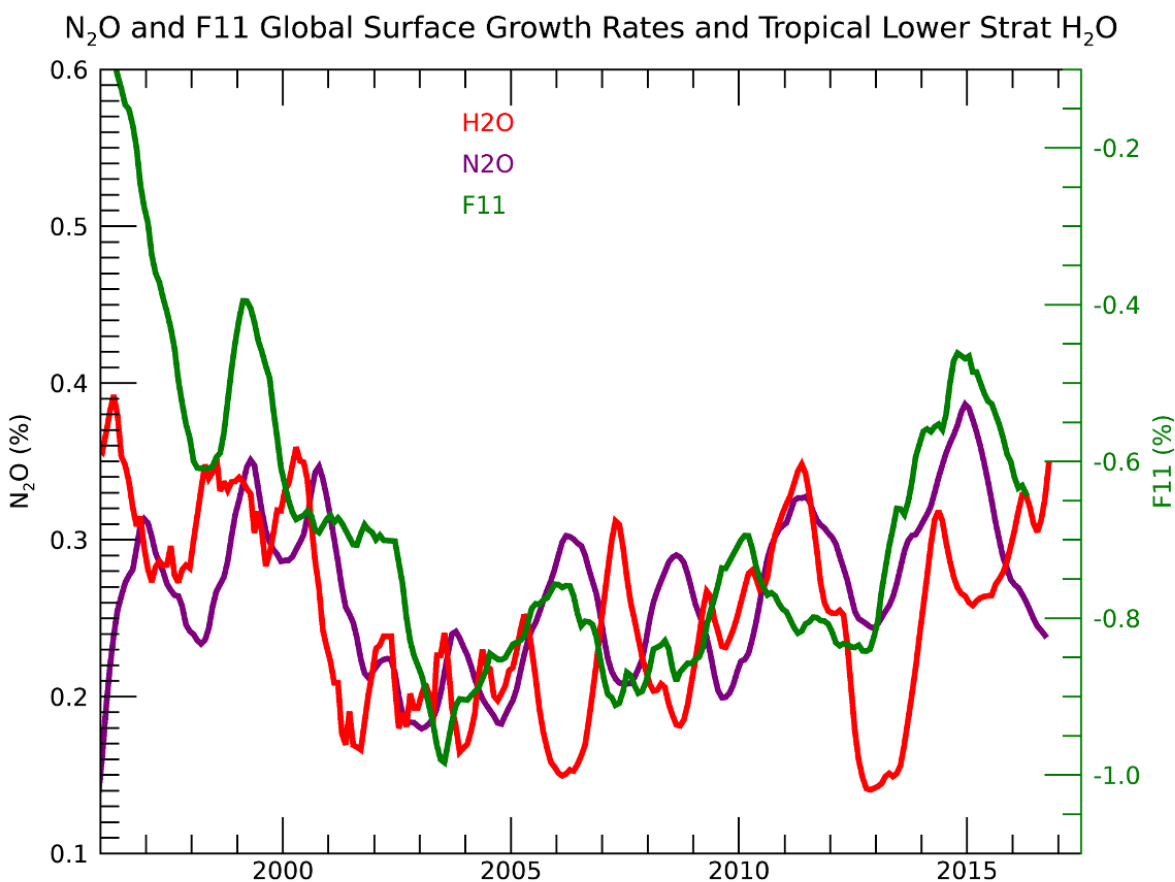


Figure 1. Time series of the global surface growth rates of CFC-11 (green) and N_2O (purple) based on NOAA/GMD measurements, and the anomaly of tropical lower stratospheric water vapor (red) from the SWOOSH data set.

Variability in Inter-hemispheric Exchange Inferred from Tropospheric Measurements of SF₆

B.D. Hall¹, E.J. Dlugokencky¹, G.S. Dutton^{2,1}, D. Nance^{2,1}, D. Mondeel^{2,1} and J.W. Elkins¹

¹NOAA Earth System Research Laboratory, Global Monitoring Division (GMD), Boulder, CO 80305; 303-497-7011, E-mail: Bradley.Hall@noaa.gov

²Cooperative Institute for Research in Environmental Sciences (CIRES), University of Colorado, Boulder, CO 80309

With a long atmospheric lifetime (~850 yr) and no known tropospheric or stratospheric loss processes, sulfur hexafluoride (SF₆) is useful as a tracer of large-scale atmospheric transport. The latitudinal gradient has been used to assess model transport, in terms of both inter-hemispheric exchange, as well as mean transport time, or tropospheric “age of air”. We derive an inter-hemispheric exchange time, τ_{ex} , from global surface measurements of SF₆. We find an annual cycle with a minimum in late Northern Hemisphere summer and maximum in spring. Some years show a bi-modal cycle, as depicted in some atmospheric models, with a second maximum occurring in fall/winter. We also see inter-annual variability, with some years showing relatively slower exchange than others. Climate drivers, such as El Niño Southern Oscillation (ENSO), and their possible affect on τ_{ex} inter-annual variability and associated impacts on trace gas distributions are examined.

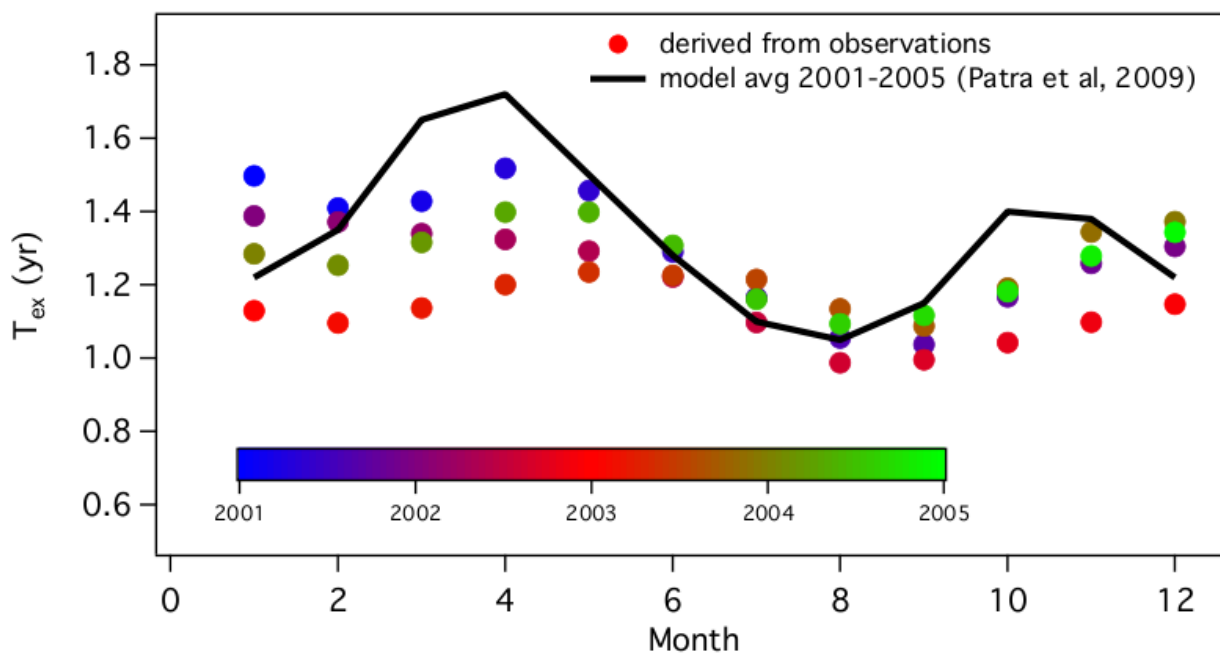


Figure 1. Annual cycle of inter-hemispheric exchange time derived from surface measurements of SF₆ (symbols) and a mean model result over the same period from Patra et. al, 2009 [Atmos. Chem. Phys., 9, 1209–1225, 2009].

On the Emissions of HCFCs and CFCs Potentially Related to HFC Production

M.K. Vollmer¹ and the AGAGE Team²

¹Swiss Federal Laboratories for Materials Science and Technology, Empa, Dübendorf, Switzerland; 41-58-765-42-42, E-mail: martin.vollmer@empa.ch

²Advanced Global Atmospheric Gases Experiment (AGAGE) Team

Based on the Montreal Protocol on Substances That Deplete the Ozone Layer there is a general ban on the use of chlorofluorocarbons (CFCs) since 2010, and an ongoing phase-out for hydrochlorofluorocarbons (HCFCs). The regulations are in place for 'emissive' use and essentially apply to end-products in refrigeration, foam blowing, fire retardants and as solvents. The regulations do not apply to the use of these chemicals as feedstock or process agents. Leakage of CFCs and HCFCs process agents during production of hydrofluorocarbons (HFCs) may lead to detectable changes in the atmosphere.

Recent studies have shown the presence of HCFC-133a ($\text{CF}_3\text{CH}_2\text{Cl}$) and HCFC-31 (CH_2ClF) in the atmosphere, two compounds, for which no purposeful use is known. Speculations are in place on their atmospheric presence from emissions during HFC manufacture. We present updated atmospheric records of HCFC-133a and HCFC-31 and derive emissions based on the AGAGE (Advanced Global Atmospheric Gases Experiment) 12-box model. HCFC-133a atmospheric abundances and emissions have reversed multiple times over the past decades. In contrast, HCFC-31 has declined over the past years to ~ 0.1 ppt (parts-per trillion, nmol/mol) in the northern hemisphere.

We also provide evidence for increased growth of CFCs, in particular CFC-115. An atmospheric history for this compound is derived from archived air samples and *in situ* measurements at AGAGE stations. 12-box model calculations show a decline in the global growth rates of CFC-115 from a maximum of 0.45 ppt/yr in the late 1980s to 0.005 ppt/yr in 2009 but a re-increasing growth to 0.02 ppt/yr in the last years. If we assume this increase to be solely due to a change in emissions then these are globally increasing from ~ 0.6 kt/yr in 2009 to ~ 0.9 kt/yr in 2015. A source of CFC-115 is identified as impurity in the refrigerant HFC-125 for which CFC-115 is an intermediate in one possible production path. Also, high-resolution CFC-115 measurements from the Asian AGAGE stations show increasing pollution events (frequency and magnitude) advected to the sites over the past years. The records are used in a FLEXPART regional model simulation to identify source regions of CFC-115 emissions. Our analysis shows 'hot-spot' emissions from the Asian mainland, which may explain some of the enhanced atmospheric growth.

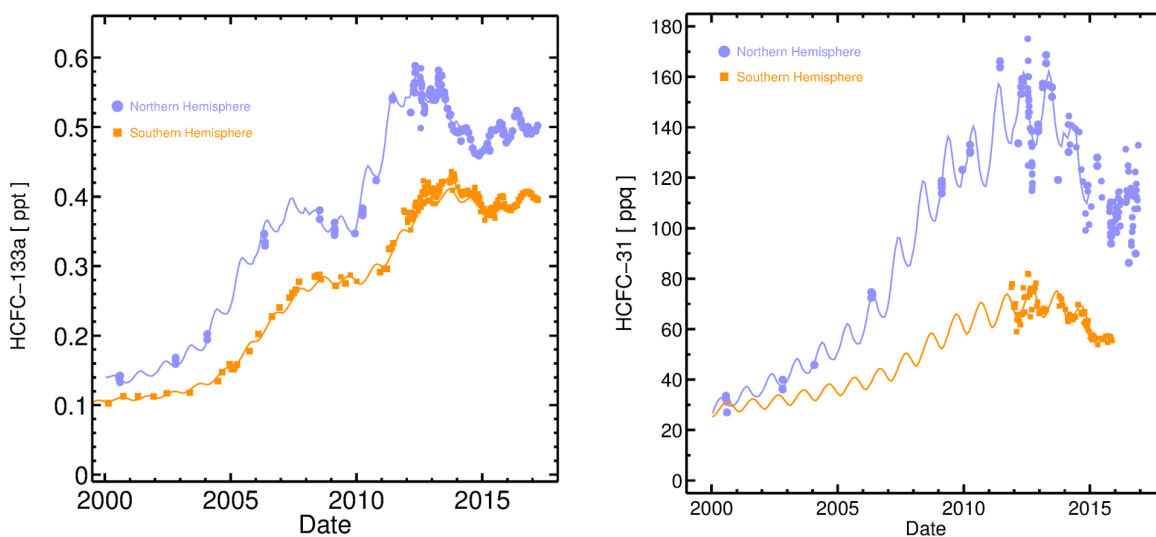


Figure 1. Atmospheric records of HCFC-133a (left) and HCFC-31 (right) (updated from Vollmer et al., 2015 and Schoenenberger et al., 2015)

European Emissions of the Powerful Greenhouse Gases Hydrofluorocarbons Inferred from Atmospheric Measurements and Their Comparison with Annual National Reports to UNFCCC

M. Maione^{1,2}, F. Graziosi¹, J. Arduini¹, F. Furlani¹, U. Giostra¹, P. Cristofanelli², X. Fang³, O. Hermanssen⁴, C. Lunder⁴, Greet Janssens-Maenhout⁵, S. O'Doherty⁶, S. Reimann⁷, N. Schmidbauer⁴, M.K. Vollmer⁷ and D. Young⁶

¹University of Urbino, Department of Basic Sciences and Foundations, Urbino, Italy; +39-0722-303-316, E-mail: michela.maione@uniurb.it

²Institute of Atmospheric Sciences and Climate, National Research Council of Italy, Bologna, Italy

³Massachusetts Institute of Technology, Center for Global Change Science, Cambridge, MA 02139

⁴Norwegian Institute for Air Research (NILU), Oslo, Norway

⁵European Commission Joint Research Centre, Institute for Environment and Sustainability, Ispra, Italy

⁶University of Bristol, School of Chemistry, Bristol, United Kingdom

⁷Swiss Federal Laboratories for Materials Science and Technology, Empa, Dübendorf, Switzerland

Hydrofluorocarbons (HFCs) are powerful greenhouse gases (GHG) introduced after the phase-out of the ozone depleting chlorinated gases required by the Montreal Protocol (MP). The climate benefit of reducing the emissions of HFCs led to the Kigali amendment to the MP calling for developed countries to start to phase-down HFCs by 2019 and for developing countries to freeze between 2024 and 2028, to avoid half a degree Celsius of warming by the end of the century. HFCs are also controlled under the Kyoto Protocol of the United Nations Framework Convention on Climate Change (UNFCCC). Annex I parties to the Convention submit annual national GHG inventories based on a bottom-up approach. Top-down methodologies based on atmospheric measurements can be used in support to the inventory compilation. We used atmospheric data from four European sites combined with the FLEXPART dispersion model and a Bayesian inversion method, to derive emissions of nine HFCs from the European Geographic Domain and from twelve regions within it, then comparing our results with the annual reports of European countries to the UNFCCC, as well as with the EDGAR database. Despite some discrepancies when considering the single compounds and countries, an overall agreement is found when comparing aggregated data, which between 2008 and 2014 are on average 84.2 against the 95.1 Tg-CO₂-eq.yr⁻¹ reported to UNFCCC. In agreement with other studies, the gap at the global level between bottom-up estimates of Annex I countries and total global top-down emissions should be essentially due to emissions from non-reporting countries (non-Annex I).

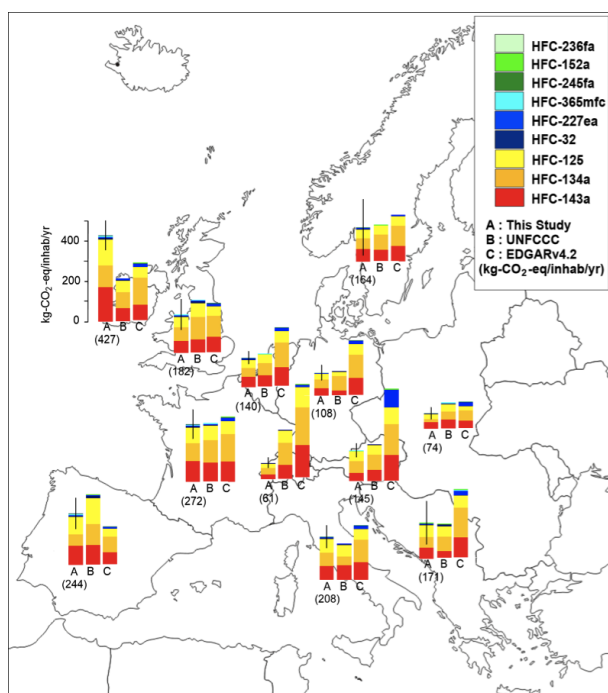


Figure 1. Per-capita emissions from twelve macro-areas in the European Geographic Domain. Emissions, given in kg-CO₂-eq.y⁻¹.inhabitants⁻¹, are averaged over 2008-2014 for the inversion results (columns A) and the IPCC country reports (columns B). EDGAR data (columns C) are averaged over 2008-2010.

Establishing Regular Measurements of Halocarbons at Taunus Observatory

T. Schuck, F. Lefrancois, F. Gallmann and A. Engel

Goethe University, Institute for Atmospheric and Environmental Sciences, Frankfurt, Germany;
+49-69-798-40249, E-mail: schuck@iau.uni-frankfurt.de

In late 2013 an ongoing whole air flask collection program was started at the Taunus Observatory (TO) in central Germany. Being a rural site in close vicinity to the densely populated Rhein-Main area with the city of Frankfurt, Taunus Observatory allows assessment of local and regional emissions but due to its altitude of 825m also regularly experiences background conditions (Figure 1). With its large capture area, halocarbon measurements at the site have the potential to improve the database for estimation of regional and total European halogenated greenhouse gas emissions.

Currently, flask samples are collected weekly for analysis using a Gas Chromatography Mass Spectrometry (GC-MS) system at Frankfurt University employing a quadrupole as well as a time-of-flight (TOF) mass spectrometer. The TOF instrument yields full scan mass information and allows for retrospective analysis of so far undetected non-target species. For quality assurance, additional samples are collected approximately bi-weekly at the Mace Head Atmospheric Research Station (MHD) in parallel with sampling for NOAA's Halocarbons & other Atmospheric Trace Species (HATS) flask sampling program. Samples get analyzed in Frankfurt following the same measurement procedure as TO flask samples. Thus the TO time series can be linked to both the *in situ* Advanced Global Atmospheric Gases Experiment (AGAGE) measurements and the NOAA flask sampling program at MHD. In 2017 it is planned to supplement the current flask sampling by employing an *in situ* GC-MS system with a TOF mass spectrometer at the site, thus increasing the measurement frequency.

We will present the time series of selected halocarbons recorded at Taunus Observatory. While there is good agreement of baseline mixing ratios between TO and MHD, measurements at TO are regularly influenced by elevated halocarbon mixing ratios (Figure 2). An analysis of HYSPLIT trajectories for the existing time series revealed significant differences in halocarbon mixing ranges depending on air mass origin.

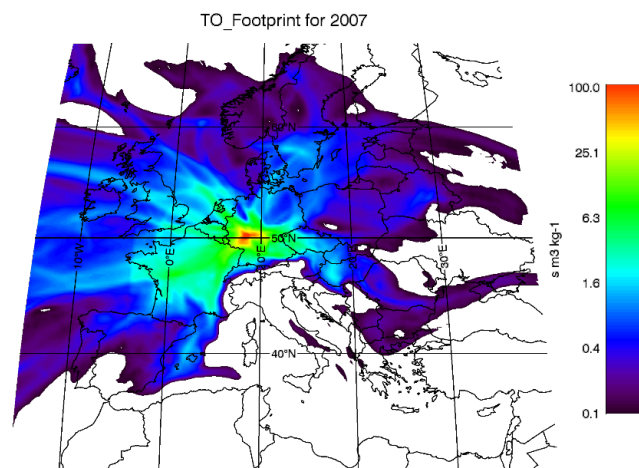


Figure 1. Footprint of the Taunus Observatory. Air masses are influenced by regional emissions (red/yellow area) but the site also regularly experiences a maritime influence from the northwest (courtesy D. Brunner).

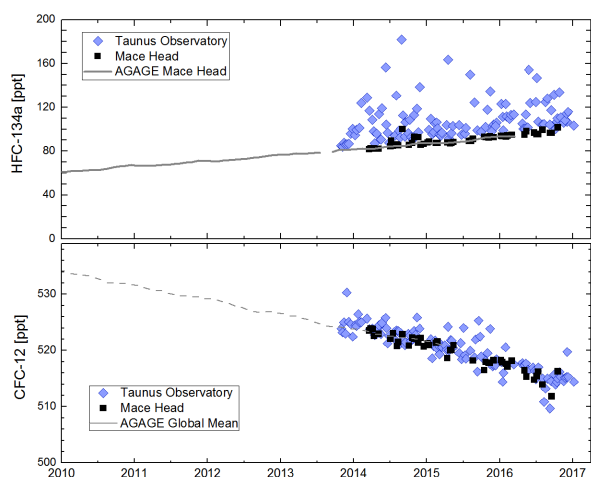


Figure 2. Time series of HFC-134a (top) and CFC-12 (bottom) at Taunus Observatory and Mace Head. HFC-134a is still widely used in air conditioning thus showing an increasing trend and strongly varying mixing ratios at TO. Usage of CFC-12 is phased out; it exhibits decreasing mixing ratios and comparable variability at TO and MHD.

What Have We Learned About the Carbon Cycle from GOSAT and OCO-2?

D.F. Baker¹, A. Jacobson^{2,3} and S. Crowell⁴

¹Cooperative Institute for Research in the Atmosphere (CIRA), Colorado State University, Fort Collins, CO 80521; 303-497-6999, E-mail: David.F.Baker@noaa.gov

²Cooperative Institute for Research in Environmental Sciences (CIRES), University of Colorado, Boulder, CO 80309

³NOAA Earth System Research Laboratory, Global Monitoring Division (GMD), Boulder, CO 80305

⁴University of Oklahoma, Norman, Oklahoma 73019

Many of the science questions posed by the Greenhouse Gases Observing Satellite (GOSAT) and Orbiting Carbon Observatory (OCO-2) projects require that carbon dioxide (CO₂) estimates retrieved from satellite observations be interpreted using atmospheric CO₂ models. To this end, the OCO-2 project has assembled a large team of modelers, representing the most important ensemble of models since TransCom. With two full years of OCO-2 data in hand and 8 years of GOSAT data, we can now assess how constraints from these instruments are helping to answer fundamental questions about the global carbon cycle. Primary among these is how increased observational coverage in low latitudes is refining our understanding of the carbon balance in the tropics. The recent El Niño gives us a rare opportunity to explore this, as assimilation of satellite data yields a distinctly different picture of this perturbation to the carbon cycle compared to assimilation of traditional *in situ* data. We also report on progress towards assessing and understanding biases in satellite retrievals, and how over-constraining the models with data refines our estimates of uncertainties deriving from transport error and inversion methodology.

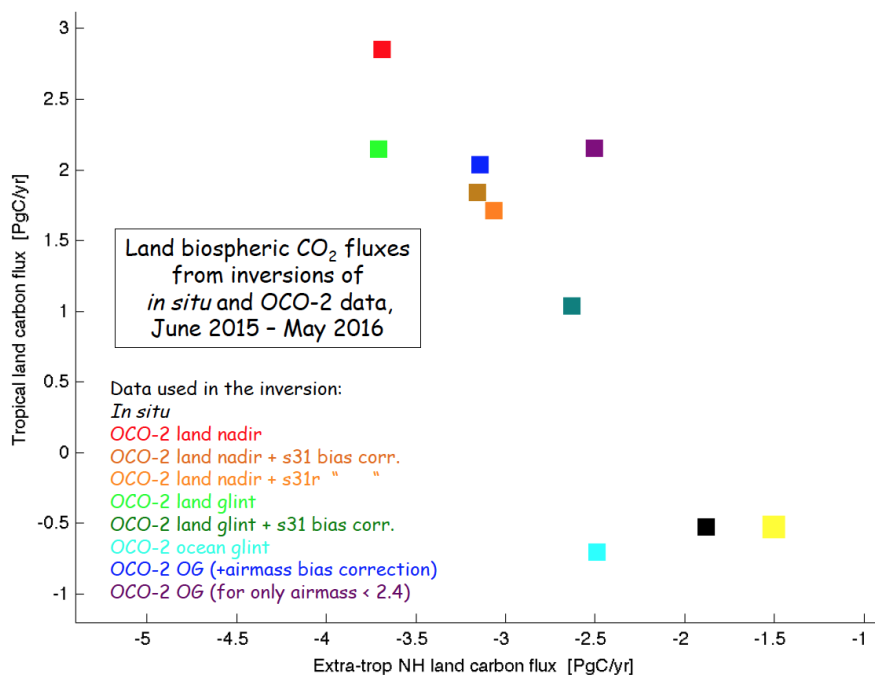


Figure 1. The partition of the land biospheric CO₂ flux (extra-tropical Northern Hemisphere vs. tropics & Southern Hemisphere) for June 2015 - May 2016, from global flux inversions of *in situ* data (black) and various types of data from the Orbiting Carbon Observatory (OCO-2) satellite (colors). Different modes of OCO-2 data (land nadir, land glint, ocean glint) have been used in separate inversions to assess consistency, with different post-hoc bias corrections applied. Despite some scatter due to uncertainties in the proper bias correction to use, the satellite data consistently show that the tropical land regions released from 1.5 to 2.5 more PgC/yr during this span, which coincided with a strong El Niño, than is given by the *in situ* data. A single atmospheric transport model (PCTM) and inversion scheme (Baker 4Dvar) is used in all cases.

Assimilating NASA's Atmospheric Composition Observations in the GEOS Earth System Model

S. Pawson¹, L. Ott¹, A. Chatterjee¹, A. Darmenov¹, A. da Silva¹, D. Jacob², C. Keller¹, E. Knowland¹, M. Long², T. Oda¹, J.E. Nielsen¹, K. Wargan¹ and B. Weir¹

¹NASA Goddard Space Flight Center (GSFC), Greenbelt, MD 20771; 301-614-6159, E-mail: Steven.Pawson-1@nasa.gov

²Harvard University, Cambridge, MA 02138

The Goddard Earth Observing System (GEOS) modeling and assimilation system is used to support NASA's Earth Observations. Built using the Earth System Modeling Framework, GEOS includes coupled modules to represent physical, chemical and biological processes in the Earth System. Global applications span spatial scales as fine as a few km and temporal scales from hours to months and decades. Routine products include weather analyses and forecasts, seasonal analyses and forecasts, and reanalyses. Research products include global, high-resolution simulations and studies of observational impacts in current and future systems. Built around the FV3 dynamical core, GEOS routinely includes simulations, analyses and forecasts of atmospheric composition, using data from NASA's EOS satellite fleet (Terra, Aqua, and Aura) and other sources. Modern-Era Retrospective Analysis for Research and Applications 2 (MERRA-2) is the first global reanalysis that includes aerosols and ozone from research instruments. GEOS is used to support NASA's carbon-cycle science, including assimilation of Orbiting Carbon Observatory 2 (OCO-2) data. Reactive chemistry studies began with a focus on the climate impacts of ozone change and is now transitional to studies of air pollution and its impacts. This talk will give an overview of this work, with remarks on its relevance to Next Generation Global Prediction System (NGGPS) and other activities within NOAA.

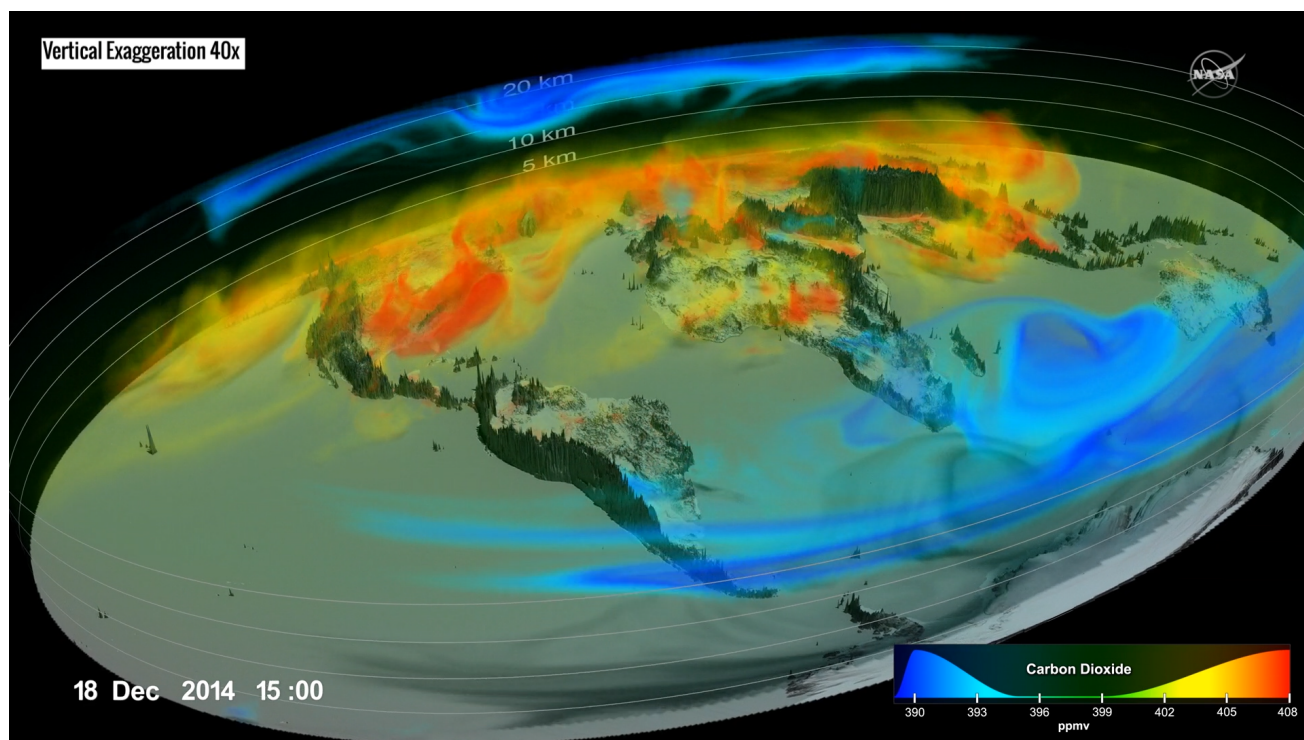


Figure 1. Assimilated 3D carbon dioxide (CO_2) fields on 13 Dec 2014. The assimilation combines retrievals of total-column CO_2 from the OCO-2 instrument with GEOS model forecasts. Blue colors represent low concentrations (~ 393 ppmv and lower), associated with biospheric uptake near the surface and aged air in the stratosphere, while reds represent high concentrations (403 ppmv and higher), associated with transport from regions of strong emissions.

Using GEOS-5 Aerosols to Inform the OCO-2 CO₂ Retrieval

R.R. Nelson¹ and C.W. O'Dell²

¹Colorado State University, Department of Atmospheric Science, Fort Collins, CO 80523; 763-354-8411, E-mail: rnelson@atmos.colostate.edu

²Cooperative Institute for Research in the Atmosphere (CIARA), Colorado State University, Fort Collins, CO 80521

The primary goal of Orbiting Carbon Observatory 2 (OCO-2) is to use hyperspectral measurements of reflected near-infrared sunlight to retrieve column mean carbon dioxide (CO₂) with the accuracy and precision needed to improve our estimates regional carbon fluxes. These accuracy requirements can only be met, however, if the light path modification effects of clouds and aerosols are taken into account. The current OCO-2 aerosol parameterization is simplistic and the corresponding retrieved aerosol information compares poorly to AERONET. In this work, we create a more complex aerosol parameterization to better inform the CO₂ retrieval algorithm. Specifically, we evaluate the impact of 3D aerosol fields from the Goddard Earth Observing System Model, Version 5 (GEOS-5) on the retrieved column mean CO₂ from OCO-2. By fitting a Gaussian profile to the GEOS-5 aerosol profiles and ingesting them with low uncertainty into retrieval algorithm we hope to better constrain the retrieval and reduce errors in X_{CO₂}. Here, we present results of a comparison between the retrieved X_{CO₂} measurements and Total Carbon Column Observing Network (TCCON). Future studies include modifying the OCO-2 retrieval algorithm to be able to ingest full GEOS-5 vertical profiles of aerosol as well as addressing the bias by incorporating a stratospheric aerosol component from temporally and spatially averaged Cloud-Aerosol Lidar and Infrared Pathfinder Satellite Observations (CALIPSO) measurements.

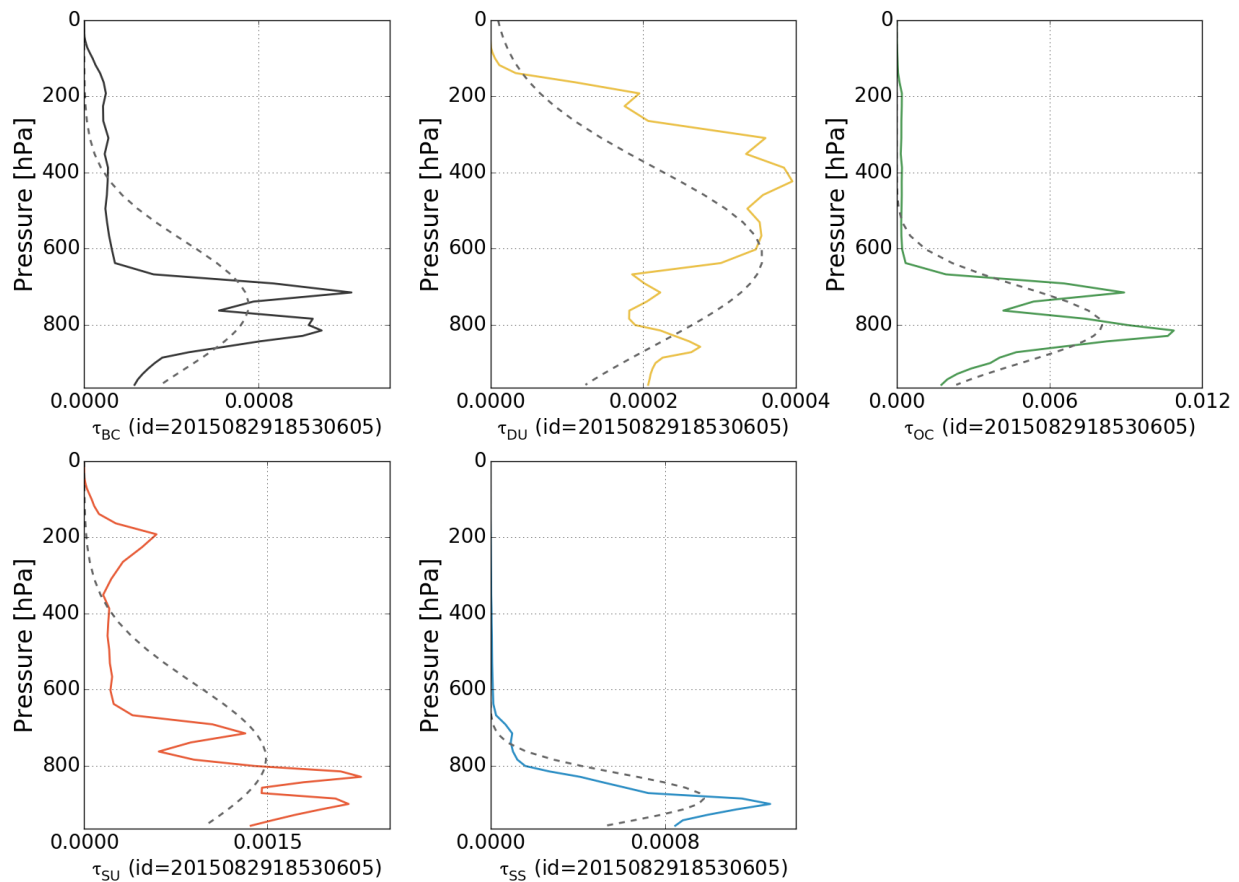


Figure 1. Example of fitting Gaussians to the GEOS-5 aerosol profiles in order to ingest them into the OCO-2 retrieval algorithm.

Amazonian GPP Estimated from Satellite-observed Carbonyl Sulfide Mixing Ratios

J. Stineciper¹, L. Kauai², J. Worden², I.T. Baker³, J. Berry⁴, T.W. Hilton¹ and J.E. Campbell¹

¹University of California at Merced, Merced, CA 95343; 559-977-3840, E-mail: jstineciper@ucmerced.edu

²NASA Jet Propulsion Laboratory, California Institute of Technology, Pasadena, CA 91109

³Colorado State University, Department of Atmospheric Science, Fort Collins, CO 80523

⁴Carnegie Institution for Science, Department of Global Ecology, Stanford, CA 94305

In recent decades gross primary production (GPP) has annually removed roughly 25% of anthropogenic carbon dioxide from the atmosphere. Global GPP magnitude and spatial attribution are highly uncertain, making these terrestrial biosphere-atmosphere carbon cycle feedbacks a first-order uncertainty in future climate predictions. The Brazilian Amazon contributes a large proportion of that uncertainty, with Coupled Model Intercomparison Project Phase 5 (CMIP5) and TRENDY GPP model ensemble estimates diverging by a factor of three from minimum to maximum. Here we use Michelson Interferometer for Passive Atmospheric Sounding (MIPAS) satellite estimates of atmospheric carbonyl sulfide concentrations to constrain these GPP estimates to the mid-to-high end of the CMIP5/TRENDY range.

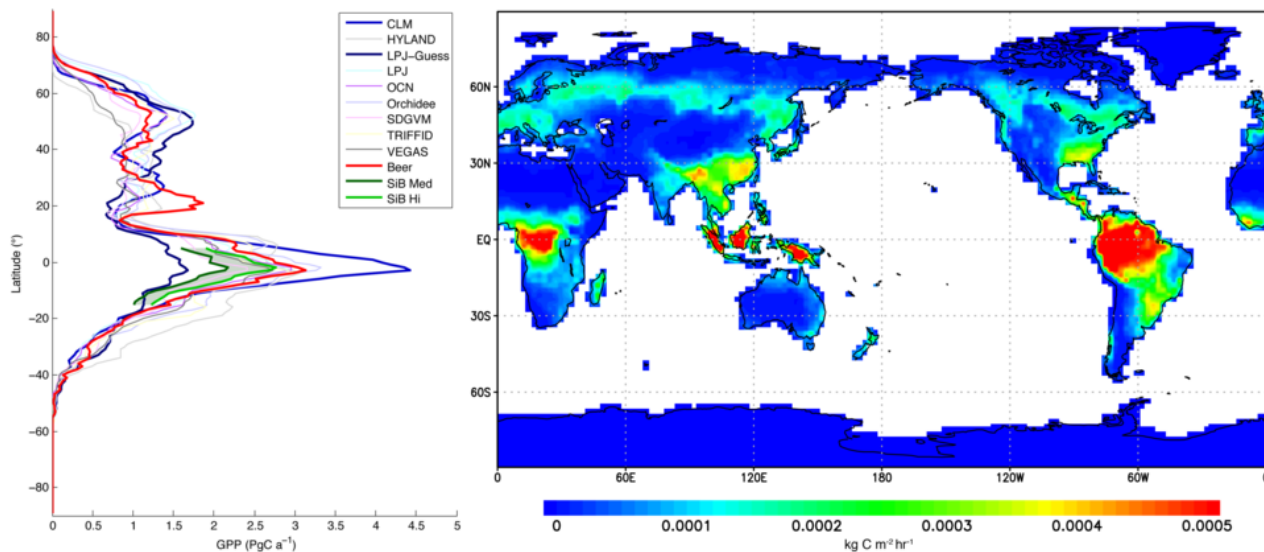


Figure 1. **Left:** Variation in terrestrial GPP by latitude. Bars have 1° width. Red line is approximate “data driven” line from Beer et al. (2010), scaled up by land areas in each grid cell. Dark and lighter green lines are SiB medium and SiB high estimates of GPP, calculated from linear trend between carbonyl sulfide (COS) plant uptake variable and SiB’s GPP variable. Blue CLM; Dark blue LPJ Guess. **Right:** map of annual average GPP in CLM (the high model). Units are kg C m⁻² hr⁻¹.

Five-year Survey of the U.S. Natural Gas Flaring Observed from Space with VIIRS

M. Zhizhin^{1,2}, C.D. Elvidge², K. Baugh^{1,2} and F. Hsu^{1,2}

¹Cooperative Institute for Research in Environmental Sciences (CIRES), University of Colorado, Boulder, CO 80309; 303-497-6385, E-mail: mikhail.zhizhin@noaa.gov

²NOAA National Environmental Satellite, Data, and Information Service (NESDIS), National Centers for Environmental Information (NCEI), Boulder, CO 80305

The five-year survey of natural gas flaring in 2012-2016 has been completed with nighttime Visible Infrared Imaging Radiometer Suite (VIIRS) data. The survey identifies flaring site locations, annual duty cycle, and provides an estimate of the flared gas volumes in methane equivalents. VIIRS is particularly well-suited for detecting and measuring the radiant emissions from gas flares through the collection of shortwave and near-infrared data at night, recording the peak radiant emissions from flares. The total flared gas volume is estimated at 140 +/-30 billion cubic meters (BCM) per year, corresponding to 3.5% of global natural gas production. While Russia leads in terms of flared gas volume (>20 BCM), the U.S. has the largest number of flares (8,199 of 19,057 worldwide). The two countries have opposite trends in flaring: while for the U.S. the peak was reached in 2015, for Russia it was the minimum. On the regional scale in the U.S., Texas has the maximum number of flares (3749), with North Dakota, the second highest, having one half of this number (2,003). The number of flares for most of the states has decreased in the last 3 years following the trend in oil prices. The presentation will compare the global estimates, and regional trends observed in the U.S. regions.

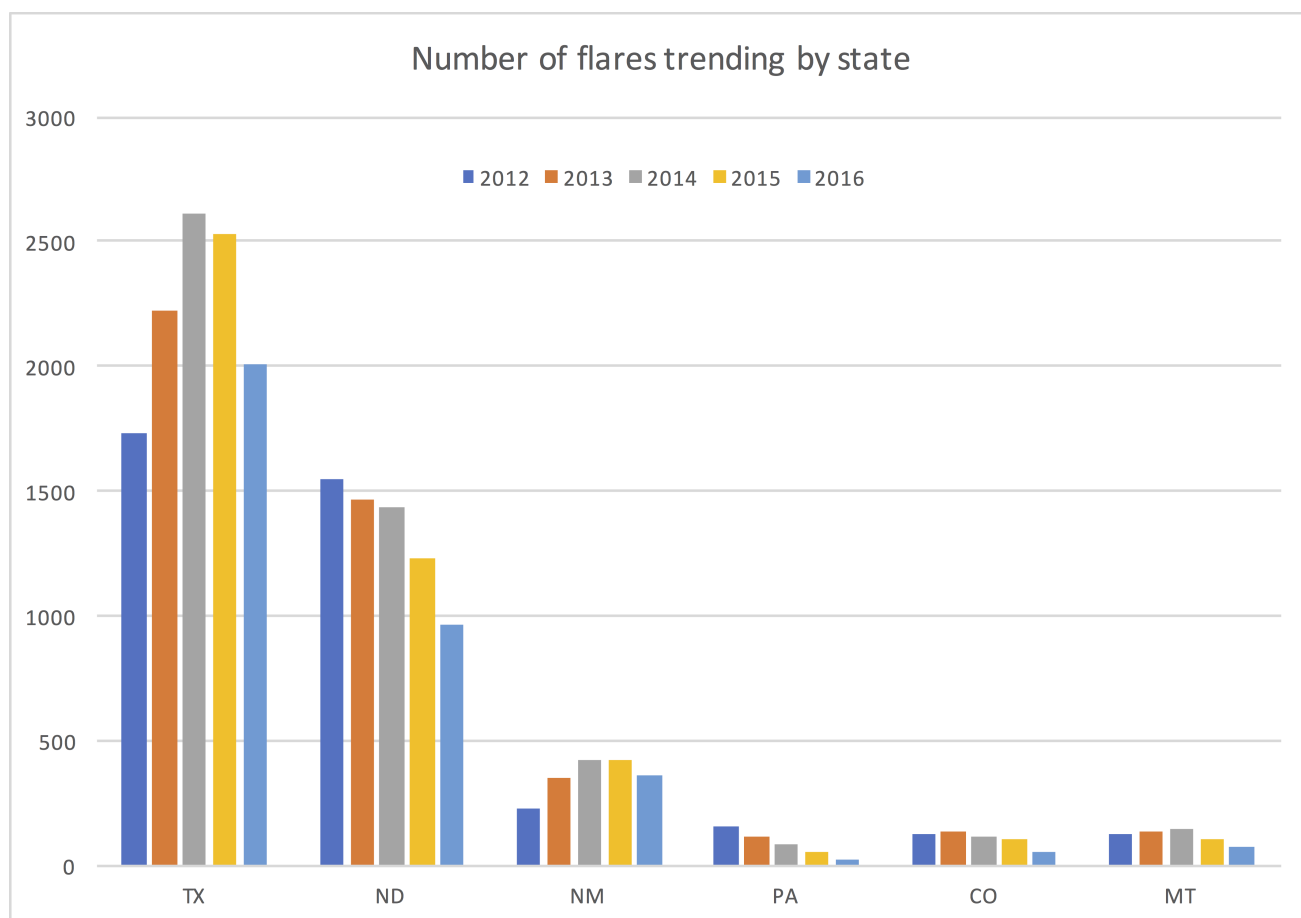


Figure 1. Number of flares trending in 2012-2016 for the U.S. states with more than 100 flares.

Analysis on the Spatiotemporal Distribution of OCO-2 XCO₂ over South Korea

G. Kim, Y. Oh, S.T. Kenea, J. Rhee, T. Goo and Y. Byun

National Institute of Meteorological Sciences, Seogwipo-si, Jeju-do, South Korea; +82-6-4780-6743, E-mail: kimgawon@korea.kr

Recently, satellite observations with wide coverage and high spatial resolution such as Orbiting Carbon Observatory-2 (OCO-2) have made it possible to study regional carbon dioxide (CO₂) distributions. In this study, we analyzed the spatiotemporal distribution of OCO-2 column-averaged dry air mole fractions (XCO₂) over South Korea (34°N-38°N, 124°E-130°E) from October 2014 to February 2017 to improve our understanding on CO₂ monitoring for the regional scale. Monthly mean Korea OCO-2 XCO₂s follow the annual cycle which can be characterized by low concentrations in summer and increases in winter [Figure 1(a)]. Fourier Transform Spectroscopy (FTS) XCO₂ in Anmyeon-do (AMY FTS, 36.54°N, 126.33°E) corresponds to OCO-2 XCO₂ with average difference of 0.21% (R=0.89). Surface CO₂ in Tae-ahn peninsula (36.73°N, 126.13°E) shows similar annual behavior to OCO-2 XCO₂ (R=0.92) but larger amplitude and higher concentration (average difference of 1.84%) because surface CO₂ is affected by more factors than the column-averaged CO₂. To find the spatial distribution of Korea OCO-2 XCO₂, 0.1°X0.1° grid mean OCO-2 XCO₂ anomalies during the whole research period were computed [Figure 1(b)]. Most of positive anomalies tend to be located near the big cities and the industrial regions. The regional differences presented in OCO-2 XCO₂ indicates that the enhancement of CO₂ due to the anthropogenic emitters is well reflected in OCO-2 XCO₂. However, CO₂ concentration varies not only by the human activity but also by the natural causes. Hence, to identify local anthropogenic sources in detail, comparison between the spatial distributions of OCO-2 XCO₂ and other satellite-observed anthropogenic gases over Korea is under investigating.

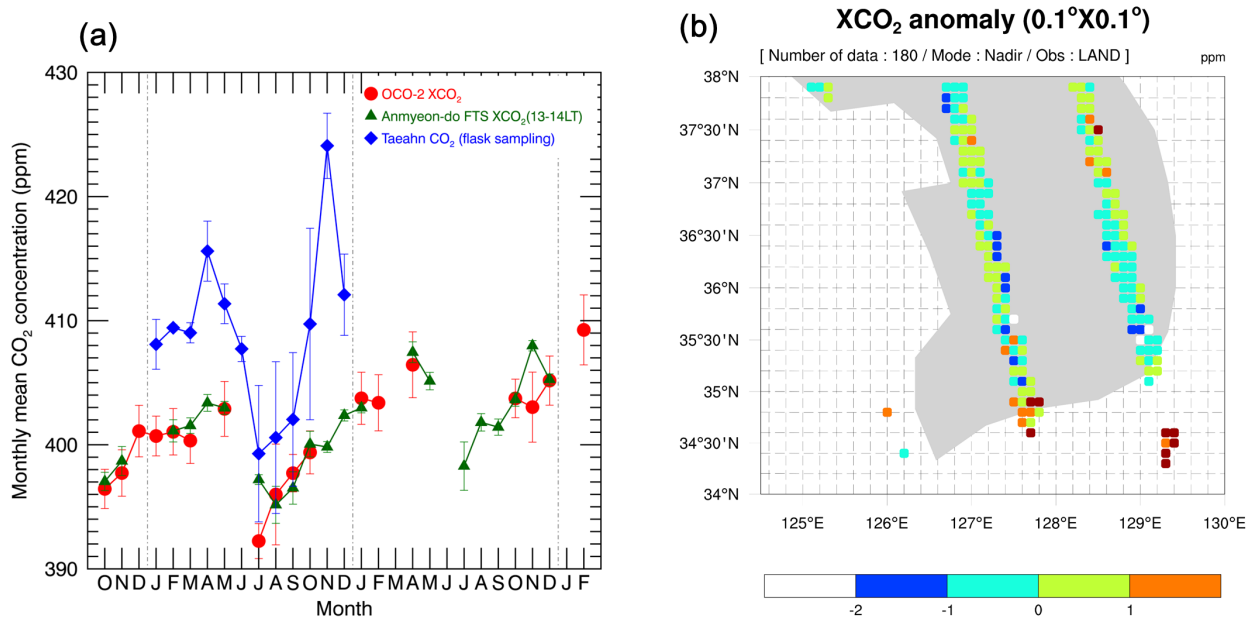


Figure 1. (a) Monthly mean concentration of OCO-2 XCO₂ (red), Anmyeon-do FTS XCO₂ (green) and Tae-ahn CO₂ (blue) for the period of October 2014-February 2017. Error bars indicate 1 standard deviation. (b) 0.1°X0.1° grid mean OCO-2 XCO₂ anomalies during the whole research period over Korea domain.

An Update on OCO-2 at the End of Prime Mission

C.W. O'Dell¹, D. Crisp², A. Eldering², M. Gunson², C. Frankenberg², P. Wennberg³ and D. Wunch³

¹Cooperative Institute for Research in the Atmosphere (CIARA), Colorado State University, Fort Collins, CO 80521; 970-491-8973, E-mail: christopher.odell@colostate.edu

²NASA Jet Propulsion Laboratory, California Institute of Technology, Pasadena, CA 91109

³California Institute of Technology, Pasadena, CA 91125

Space-based measurements of greenhouse gases have the potential to greatly add to our understanding of the state and evolution of the carbon cycle at increasingly finer scales, and of regions that are particularly difficult to monitor with more conventional methods. The NASA Orbiting Carbon Observatory-2 (OCO-2) completed its 2-year prime mission on October 16, 2016 and began its first extended mission. Since 6 September 2014, OCO-2 has been returning roughly 1.5 million measurements of column carbon dioxide (CO_2) (X_{CO_2}) per month, which have begun to yield new insights into carbon processes (Eldering et al., 2017). These include both recent insights into terrestrial carbon cycle changes induced by the 2015-16 El Niño, as well as rough proof-of-concept measurements of anthropogenic CO_2 from power plant to regional scales. OCO-2 data are also returning estimates of solar induce chlorophyll fluorescence (SIF), which provides a sensitive indicator of CO_2 uptake by the land biosphere. For CO_2 , the end-to-end performance of the instrument and retrieval algorithm is continuously validated through comparisons with X_{CO_2} estimates from TCCON (Figure 1) and other standards. Regional and seasonal biases still remain at a level of typically ~ 1 ppm. Improvements, especially over the ocean, are expected with the upcoming version 8 product, which includes a correction for trace amounts of upper-atmospheric aerosols, as well as numerous other minor improvements. SIF has been initially validated by direct comparisons to flux towers as well as to remote sensing measurements made via recent U.S.-based aircraft underflights. Together with the numerous space-based measurements systems currently in planning or recently deployed, such as TanSat, GOSAT-2, MicroCarb, OCO-3, and GeoCarb, the future currently seems bright for space-based greenhouse gas remote sensing.

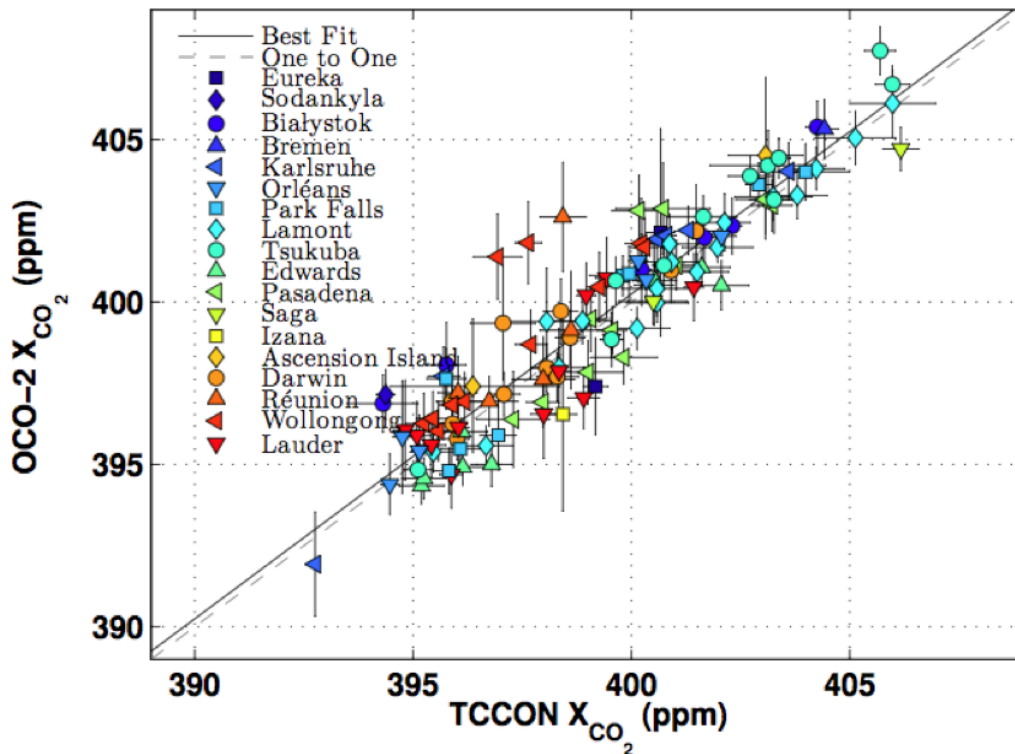


Figure 1. Comparison of OCO-2 X_{CO_2} to TCCON. [Adapted from Wunch et al., 2017.]

NOAA ESRL GLOBAL MONITORING ANNUAL CONFERENCE 2017

David Skaggs Research Center, Cafeteria
325 Broadway, Boulder, Colorado 80305 USA

Tuesday, May 23, 2017 17:00 - 20:00 POSTER SESSION AGENDA

(Only presenter's name is given; please refer to abstract for complete author listing.)

Arctic Monitoring

- P-1 ARM North Slope of Alaska Facilities: Unmanned Aerial Systems and Tethered Balloon Operations
Jasper Hardesty (Sandia National Laboratories)
- P-2 Seasonal Cycles of Aerosol Properties Across the North Slope of Alaska: Sources and Distributions from Utqiagvik (formerly Barrow) to Oliktok Point
Allison McComiskey (NOAA Earth System Research Laboratory, Global Monitoring Division (GMD))
- P-3 Observations of the Surface Radiation Budget and Cloud Radiative Forcing From Pan-Arctic Land Stations
Christopher J. Cox (Cooperative Institute for Research in Environmental Sciences (CIRES), University of Colorado)
- P-4 Asian Transport Influence on Greenland Crustal Aerosols
Nicholas Spada (University of California at Davis)
- P-5 Understanding the Impact of Biomass Burning on Ozone Conditions in the Arctic
Audra McClure-Begley (Cooperative Institute for Research in Environmental Sciences (CIRES), University of Colorado)
- P-6 Analysis of Near-surface Permafrost Monitoring Station Data from Alaska
Kang Wang (Institute of Arctic and Alpine Research (INSTAAR), University of Colorado)

Aerosols

- P-7 A Comparison of Photodiode and LED Based Sunphotometer-derived AOD with NASA AERONET
Ian Krintz (Appalachian State University, Department of Physics and Astronomy)
- P-8 Volatility of Materials Internally Mixed with Black Carbon from Biomass Burning
Kara Lamb (Cooperative Institute for Research in Environmental Sciences (CIRES), University of Colorado)
- P-9 Ambient Aerosol Extinction in Great Smoky Mountains National Park
Tim Gordon (Handix Scientific)
- P-10 Characterization of Transported Biomass-Burning Smoke from Indochina to Mt. Lulin Based on a Super Event in March of 2009
Sheng-Hsiang Carlo Wang (National Central University, Department of Atmospheric Sciences, Chung-Li, Taiwan)
- P-11 Aerosol Measurements Over Mauna Loa Observatory
Nimmi C. P. Sharma (Central Connecticut State University, Department of Physics and Engineering Physics)

Carbon Cycle & Greenhouse Gases - Methane & Carbon Monoxide

- P-12 Calibration and Field Testing of Cavity Ring-down Laser Spectrometers Measuring Methane Mole Fraction and the Isotopic Ratio of Methane, Deployed on Towers in the Marcellus Shale Region
Natasha Miles (The Pennsylvania State University, Department of Meteorology)
- P-13 Methane Source Attribution in the DJ Basin Using Mobile Surveys and Computational Analytics
Emmaline Atherton (St. Francis Xavier University, Antigonish, Canada)
- P-14 Temporal Variability in Methane at Indianapolis with Implications for the Urban Methane Flux Estimates
Nikolay Balashov (The Pennsylvania State University, Department of Meteorology)
- P-15 Stable Isotopes of Carbon Monoxide During Two Summers at Indianapolis, IN Show Significant Influence of Oxidized Biogenic Volatile Organic Compounds on the CO Budget
Isaac Vimont (Institute of Arctic and Alpine Research (INSTAAR), University of Colorado)
- P-16 Chemical Feedback from Decreasing Carbon Monoxide Emissions
Benjamin Gaubert (National Center for Atmospheric Research (NCAR), Atmospheric Chemistry Observations and Modeling Laboratory)

NOAA ESRL GLOBAL MONITORING ANNUAL CONFERENCE 2017

David Skaggs Research Center, Cafeteria
325 Broadway, Boulder, Colorado 80305 USA

Tuesday, May 23, 2017 17:00 - 20:00 POSTER SESSION AGENDA (Continued)

(Only presenter's name is given; please refer to abstract for complete author listing.)

Carbon Cycle & Greenhouse Gases - Measurements & Networks

- P-17 NOAA GMD'S Global Greenhouse Gas Reference Network Management, Logistics, and Importance
Eric Moglia (Cooperative Institute for Research in Environmental Sciences (CIRES), University of Colorado)
- P-18 NOAA Flask Measurements of Greenhouse and Trace Gases During the ACT-America Campaign
Bianca Baier (Cooperative Institute for Research in Environmental Sciences (CIRES), University of Colorado)
- P-19 Application of Observations from the Summer 2016 ACT-America Campaign to Constrain Modeled Regional CO₂ Concentrations and Fluxes
Brian Gaudet (The Pennsylvania State University, Department of Meteorology)
- P-20 Comparing Atmospheric CO₂ Measurements from Two Instruments at Baring Head, New Zealand
Sylvia Nichol (National Institute of Water and Atmospheric Research (NIWA), Wellington, New Zealand)
- P-21 Introduction of the NIMS Activities on a Carbon Cycle Study
Tae-Young Goo (National Institute of Meteorological Sciences, Seogwipo-si, South Korea)
- P-22 A Study of Diurnal and Seasonal Variations of Carbon Dioxide and Methane in the Eastern Highland Rim Region of Tennessee
Wilson K Gichuhi (Tennessee Technological University)
- P-23 Can We Detect the Conversion of the Harding Street Power Plant in Indianapolis from Coal to Natural Gas Using Tower-based CO₂ Mole Fraction Data Alone?
Nikolay Balashov (The Pennsylvania State University, Department of Meteorology)

Carbon Cycle & Greenhouse Gases - Modeling & Emissions

- P-24 The Role of Horizontal Grid Spacing on Transport and Mixing of Passive Tracers Over Complex Terrain
Gert-Jan Duine (University of Virginia)
- P-25 Evaluation of the Carbon Cycle in the CMIP5 Earth System Model ESM2G
Mark Leonard (Science and Technology Corporation)
- P-26 The Estimation of CO₂ Fluxes with a Coupled Meteorological and Tracer Transport Model
Vikram Khade (University of Toronto, Department of Physics, Toronto, Canada)
- P-27 Towards a Novel Integrated Approach for Estimating Greenhouse Gas Emissions in Support of International Agreements
Stefan Reimann (Swiss Federal Laboratories for Materials Science and Technology, Empa, Dübendorf, Switzerland)
- P-28 Quantification of NO_y and CO Emissions from Washington, D.C.-Baltimore During the WINTER Campaign
Olivia E. Salmon (Purdue University, Department of Chemistry)
- P-29 Analysis of Long-term Observations of NO_x and CO in Megacities and Application to Constraining Emissions Inventories
Gregory Frost (NOAA Earth System Research Laboratory, Chemical Sciences Division (CSD))
- P-30 Increased Propane Emissions from the United States
Lei Hu (Cooperative Institute for Research in Environmental Sciences (CIRES), University of Colorado)
- P-31 A Ten-Year (2006-2016) Record of Non-methane Hydrocarbons (NMHCs) in the Subtropical Marine Boundary Layer at the Cape Verde Atmospheric Observatory
Shalini Punjabi (University of York, Department of Chemistry, Wolfson Atmospheric Chemistry Laboratories (WACL), York, United Kingdom)
- P-32 Remote Tropical Island Mountaintop Measurements of Halogen Radicals and OVOCs
Theodore Koenig (University of Colorado, Department of Chemistry and Biochemistry)
- P-33 VOC Measurements Using Whole Air Sampling (WAS) During ATom-1
Isobel J Simpson (University of California at Irvine, Department of Chemistry)

NOAA ESRL GLOBAL MONITORING ANNUAL CONFERENCE 2017

David Skaggs Research Center, Cafeteria
325 Broadway, Boulder, Colorado 80305 USA

Tuesday, May 23, 2017 17:00 - 20:00 POSTER SESSION AGENDA (Continued)

(Only presenter's name is given; please refer to abstract for complete author listing.)

Halocarbons

- P-34 First Results of Tall Tower Surface-atmosphere N₂O Flux Measurements Over a Mixed Agricultural Region in Central Europe
László Haszpra (Hungarian Meteorological Service, Budapest, Hungary)
- P-35 The WMO-GAW-VOC Network with Contributions of AGAGE
Rainer Steinbrecher (Institute for Meteorology and Climate Research, Karlsruhe Institute of Technology, Campus Alpin, Karlsruhe, Germany)
- P-36 Twenty-Five Years of Airborne Observations of Ozone-Depleting and Climate-Related Gases in the Upper Troposphere and Lower Stratosphere
James W. Elkins (NOAA Earth System Research Laboratory, Global Monitoring Division (GMD))
- P-37 Sulfuryl Fluoride (SO₂F₂) Atmospheric Abundance and Trend from the GMD North American Tower and Aircraft Programs
Benjamin R. Miller (Cooperative Institute for Research in Environmental Sciences (CIRES), University of Colorado)
- P-38 Perfluoro-N-methylmorpholine (C₅F₁₁NO), a Persistent Greenhouse Gas: Laboratory Determination of Radiative Efficiency, Atmospheric Loss Processes and Global Warming Potential
François Bernard (Cooperative Institute for Research in Environmental Sciences (CIRES), University of Colorado)

Instrumentation - Lab & Field

- P-39 Development of Traceable Precision Dynamic Dilution Method to Generate Dimethyl Sulphide Gas Mixtures at Sub-nmol/mol for Ambient Measurement
Sangil Lee (Korea Research Institute of Standards and Science, Center of Gas Analysis, Daejeon, South Korea)
- P-40 Pressure Dependent CO₂ Enrichment in High-pressure Aluminum Cylinders
Michael F. Schibig (Early Postdoc.Mobility Fellow, Swiss National Science Foundation, Bern, Switzerland)
- P-41 Ensuring High-quality Data from NOAA'S GC-MS Perseus Instrument
Molly J. Crotwell (Cooperative Institute for Research in Environmental Sciences (CIRES), University of Colorado)
- P-42 High-precision, Continuous and Real-time Measurement of Atmospheric Oxygen Using Cavity Ring-down Spectroscopy
Jennifer Boulton (Picarro Inc.)
- P-43 Continuous, Regional Approach to Methane Source Detection and Sizing Using Dual Frequency Comb Laser Spectroscopy and Atmospheric Inversions
Caroline Alden (Cooperative Institute for Research in Environmental Sciences (CIRES), University of Colorado)
- P-44 2017 Cooperative Tower Network Overview and Insights
Jonathan Kofler (Cooperative Institute for Research in Environmental Sciences (CIRES), University of Colorado)
- P-45 Improvements to UCATS for the Atmospheric Tomography (ATom) Mission and Recent Results
Eric J. Hints (Cooperative Institute for Research in Environmental Sciences (CIRES), University of Colorado)
- P-46 Recent Methodological Advancements to the AirCore Atmospheric Profiler
Jonathan Bent (Cooperative Institute for Research in Environmental Sciences (CIRES), University of Colorado)
- P-47 NOAA Frost Point Hygrometer (FPH) Comparisons, Measurement Uncertainties and Recent Instrument Improvements
Emrys Hall (Cooperative Institute for Research in Environmental Sciences (CIRES), University of Colorado)

NOAA ESRL GLOBAL MONITORING ANNUAL CONFERENCE 2017

David Skaggs Research Center, Cafeteria
325 Broadway, Boulder, Colorado 80305 USA

Tuesday, May 23, 2017 17:00 - 20:00 POSTER SESSION AGENDA (Continued)

(Only presenter's name is given; please refer to abstract for complete author listing.)

Ozone & Water Vapor

- P-48 Homogenizing NOAA's Ozonesonde Data Set Improves Comparison with Satellite-derived Vertical Ozone Profiles
Chance W. Sterling (Cooperative Institute for Research in Environmental Sciences (CIRES), University of Colorado)
- P-49 SHADOZ (Southern Hemisphere Additional Ozonesondes) Network Report: Updates and Station Activities
Jacquelyn Witte (Science Systems and Applications, Inc. (SSAI))
- P-50 Ozone Vertical Profile Measurements in the Northern Front Range of Colorado in July-August 2014 During FRAPPE and DISCOVER-AQ
Samuel J. Oltmans (Retired from NOAA Earth System Research Laboratory, Global Monitoring Division (GMD))
- P-51 Influence of Stratospheric Intrusions on the Lower Free Tropospheric Ozone at Lulin Atmospheric Background Station
Chang-Feng Ou-Yang (National Central University, Department of Atmospheric Sciences, Chung-Li, Taiwan)
- P-52 Regional Trend Analysis of Surface Ozone Observations from Monitoring Networks in Eastern North America, Europe and East Asia
Kai-Lan Chang (National Research Council Post-Doc)
- P-53 Overview of the Long-term Ozone Trends and Uncertainties in the Stratosphere (LOTUS) SPARC Activity
Irina Petropavlovskikh (Cooperative Institute for Research in Environmental Sciences (CIRES), University of Colorado)
- P-54 Removal of Seasonal Bias from Dobson Spectrophotometer Records Using Reanalysis
Brandon Noirot (Cooperative Institute for Research in Environmental Sciences (CIRES), University of Colorado)
- P-55 Comparison of Ozone Retrievals from the Umkehr Reprocessing Version and Satellites
Koji Miyagawa (Guest Scientist at NOAA Earth System Research Laboratory, Global Monitoring Division (GMD))
- P-56 Differences Between the Reprocessed Dobson Total Ozone and Satellite Observation Records
Koji Miyagawa (Guest Scientist at NOAA Earth System Research Laboratory, Global Monitoring Division (GMD))
- P-57 Congregation of Vapors: Towards a Synoptic View of Water Vapor in Support of Airborne IR Astronomy
Jeffrey Van Cleve (SETI Institute)

Radiation

- P-58 A New Data Product for the NOAA Environmental UV-ozone Brewer Network (NEUBrew) Aerosol Optical Depth in the UV Spectral Region
Patrick Disterhoft (Cooperative Institute for Research in Environmental Sciences (CIRES), University of Colorado)
- P-59 Significant Improvements in Pyranometer Nighttime Offsets Using High-Flow, DC Ventilation
Mark C. Kutchenteiter (National Renewable Energy Laboratory (NREL))
- P-60 Analysis of Solar Radiation Measurements at BSRN Lulin Candidate Station
Nai-Ju Hsueh (National Central University, Department of Atmospheric Sciences, Chung-Li, Taiwan)

NOAA ESRL GLOBAL MONITORING ANNUAL CONFERENCE 2017

David Skaggs Research Center, Cafeteria
325 Broadway, Boulder, Colorado 80305 USA

Tuesday, May 23, 2017 17:00 - 20:00 POSTER SESSION AGENDA (Continued)

(Only presenter's name is given; please refer to abstract for complete author listing.)

Partner Stations & Meteorology

- P-61 A Length-Scale Analysis of Variance for Many Constituents from Aircraft, Satellite and Model Results During the 2013 SENEX Field Study
Stuart McKeen (Cooperative Institute for Research in Environmental Sciences (CIRES), University of Colorado)
- P-62 Continuous Long-term Monitoring of Atmospheric Key Species at the GAW Global Station Hohenpeissenberg
Dagmar Kubistin (Meteorological Observatory Hohenpeissenberg, German Meteorological Service, Hohenpeissenberg, Germany)
- P-63 Long-term Measurements from the GAW Cape Verde Atmospheric Observatory (CVAO)
J.R. Hopkins (University of York, National Centre for Atmospheric Science (NCAS), York, United Kingdom)
- P-64 Lanyu (Island) Station – New Horizons of the Western Pacific Ocean in Background Atmospheric Chemistry and Radiation Observations
Kun-Wei Lin (Central Weather Bureau, Observation Division, Taipei, Taiwan)
- P-65 Variability in the Onset of Summer Monsoon Over Vietnam
Nguyen Thi Lan Anh (Hanoi University of Natural Resources and Environment (HUNRE), Hanoi, Vietnam)
- P-66 Variability and Trends of Withdraw for the Summer Monsoon Over Vietnam
Phung Thi My Linh (Hanoi University of Natural Resources and Environment (HUNRE), Hanoi, Vietnam)
- P-67 Projections of Variability and Trends of Summer Monsoon Rainfall Over Vietnam
Nguyen Dang Mau (Vietnam Institute of Meteorology, Hydrology and Climate Change, Hanoi, Vietnam)
- P-68 Study of the Diurnal Cycle of Microphysical Properties of Clouds in the Amazon Basin Using GOES Measurements
André Cezar Pugliesi da Silva (Institute of Physics, University of São Paulo, São Paulo, Brazil)

Notes:

ARM North Slope of Alaska Facilities: Unmanned Aerial Systems and Tethered Balloon Operations

J. Hardesty, M. Ivey, D. Dexheimer, F. Helsel, D. Lucero, T. Houchens and A. Bendure

Sandia National Laboratories, Albuquerque, NM 87185; 505-844-8388, E-mail: joharde@sandia.gov

The Department of Energy Atmospheric Radiation Measurement program (ARM) North Slope of Alaska (NSA) Science Mission is to collect high latitude atmospheric data to refine climate models as they relate to the Arctic. The ARM NSA facilities have been operated by Sandia National Labs (Sandia) to provide scientific infrastructure and data to the international Arctic research community since 1997. The newest site was installed in 2013 at Oliktok Point, Alaska. The infrastructure at Oliktok is designed to be mobile and it may be relocated in the future to support other ARM science missions. Unmanned aerial system (UAS) and tethered balloon system (TBS) operations near Oliktok are enabled for all approved users by activating FAA-designated restricted air space (R2204) and international warning area (W220) activated by Sandia. UAS operations out of Barrow have also been done with FAA approval. The controlled airspaces at Oliktok Point provide for aerial measurements within a 4 nautical mile diameter around Oliktok Point, up to 7,000 feet altitude; and a 40 x 700 nautical mile corridor towards the North Pole, up to 20,000 feet altitude. Sandia operates a TBS program for atmospheric measurements in the Arctic. Test flights were begun in 2014, and TBS operations are evolving to provide regular Arctic data sets. The TBS collects high vertical resolution *in situ* atmospheric data and operates within clouds for data that improves understanding of Arctic atmospheric processes and to improve climate models. Data on aerosols, cloud properties, ice microphysics, thermodynamics and winds are now being collected and used. The TBS is also being tested to improve radar calibration for the ARM facilities. This poster will introduce recent and planned campaigns employing UAS and TBS at the ARM NSA facilities, examples of data and instrumentation, and future plans to improve or expand Arctic measurements and capabilities.

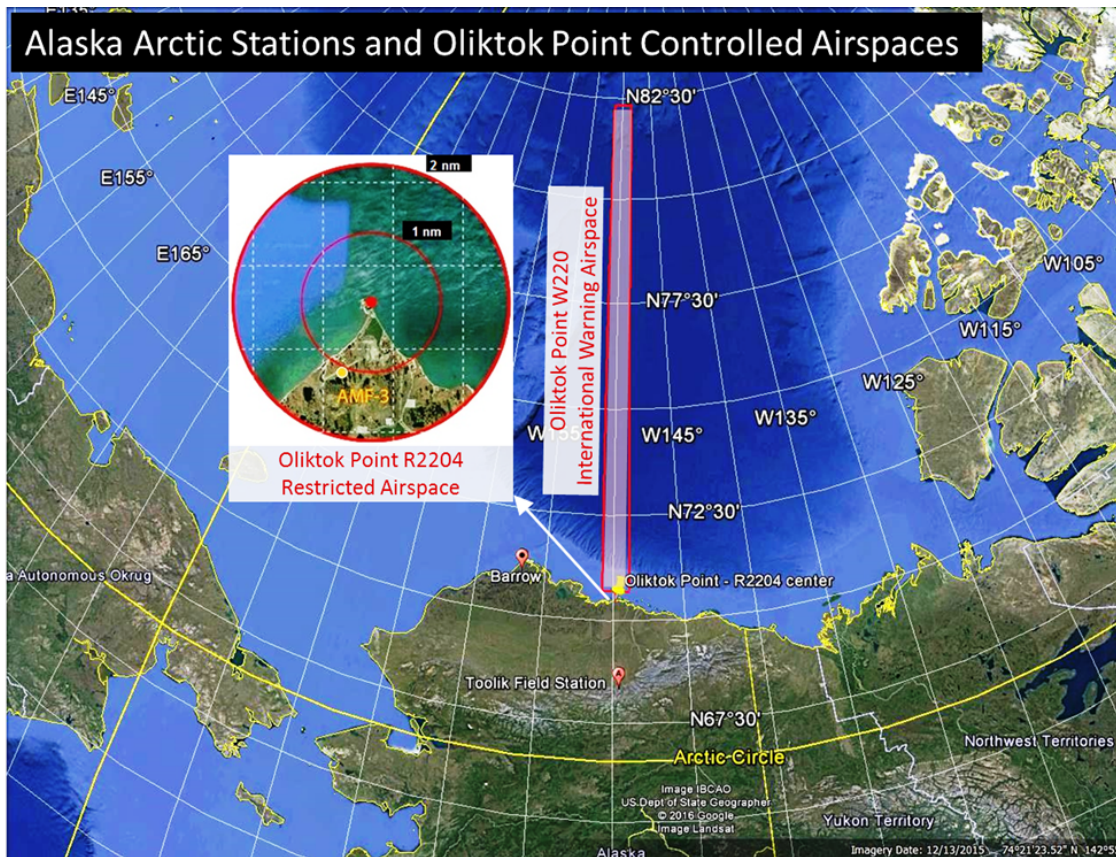


Figure 1. Alaska Arctic Stations and Oliktok Point Controlled Airspaces.

Seasonal Cycles of Aerosol Properties across the North Slope of Alaska: Sources and Distributions from Utqiagvik (formerly Barrow) to Oliktok Point

A. McComiskey¹, J. Creamean^{2,3}, G.D. Boer^{2,3}, M. Maahn^{2,3}, H. Telg^{2,1}, S. Tisina^{2,1}, P. Sheridan¹, A. Jefferson^{2,1} and R.S. Stone^{4,1}

¹NOAA Earth System Research Laboratory, Global Monitoring Division (GMD), Boulder, CO 80305; 303-497-6189, E-mail: allison.mccomiskey@noaa.gov

²Cooperative Institute for Research in Environmental Sciences (CIRES), University of Colorado, Boulder, CO 80309

³NOAA Earth System Research Laboratory, Physical Sciences Division (PSD), Boulder, CO 80305

⁴Science and Technology Corporation, Boulder, CO 80305

Recent studies indicate that negative aerosol radiative forcing in the Arctic has appreciably offset greenhouse gas warming and sea ice loss (Najafi et al. 2015, Gagne et al. 2015). At the same time, net forcing yields a warming of the Arctic region that is still much greater than the global average due to Arctic amplification mechanisms (Serreze and Barry 2011). The radiative forcing potential of aerosol is dictated by the source and evolution after emission, horizontal and vertical spatial distributions, and co-occurrence with surface cover and solar geometry, which have a high degree of variability at high latitudes. Characterizing aerosol property distributions relative to source is essential for predicting future Arctic climate system responses to other anthropogenic changes.

Here, we assemble aerosol measurements from a range of platforms and locations to assess how aerosol sources and properties distribute horizontally, vertically and temporally from the relatively pristine site of Utqiagvik to Oliktok Point on Prudhoe Bay. Airborne data are contextualized in a long-term, seasonal analysis of ground-based *in situ* and remote sensing observations of aerosol properties to evaluate the sources of aerosol in the boundary layer as compared to the free troposphere, and implications for the radiative forcing of aerosol is presented. Our findings establish patterns of aerosol properties consistent with known sources and transport patterns across the North Slope: more numerous, smaller particles surrounding Oliktok Point, likely from oil extraction activities; biomass burning aerosol aloft from long-range transport originating in boreal forests; and seasonal cycles of properties near the surface that reflect changing sources as surface cover and circulation pattern vary throughout the year.

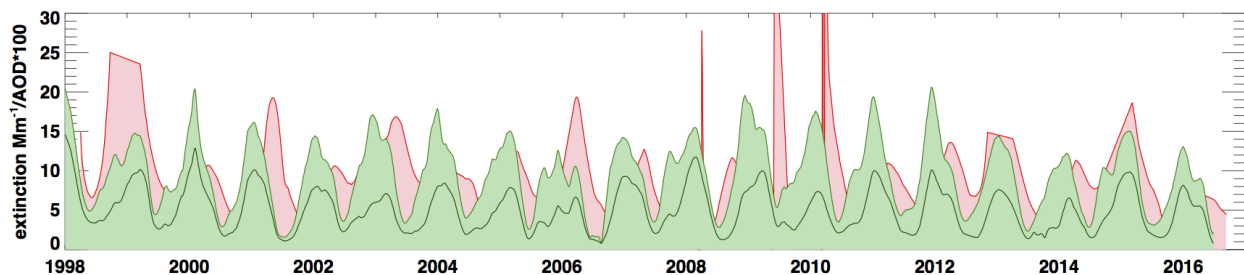


Figure 1. Seasonal cycles of ambient column (red) and dry surface (green) aerosol extinction at Utqiagvik, AK showing a persistent offset in the maximum each year. (Green: aerosol light extinction at 500 nm for particles < 10 μm measured *in situ* at the surface with a two month smoothing function; Dark Green line: extinction for particles < 1 μm ; Red: aerosol optical depth at 500 nm with a three month smoothing function).

Observations of the Surface Radiation Budget and Cloud Radiative Forcing From Pan-Arctic Land Stations

C.J. Cox^{1,2}, C.N. Long^{1,3}, T. Uttal², S. Starkweather^{1,2}, S.M. Crepinsek^{1,2}, M. Maturilli⁴, N. Miller^{1,5}, E.A. Konopleva-Akish^{6,2}, V.Y. Kustov⁷, K. Steffen⁸, G.D. Boer^{1,2}, A. McComiskey³ and R.S. Stone^{6,3}

¹Cooperative Institute for Research in Environmental Sciences (CIRES), University of Colorado, Boulder, CO 80309; 303-497-4518, E-mail: christopher.j.cox@noaa.gov

²NOAA Earth System Research Laboratory, Physical Sciences Division (PSD), Boulder, CO 80305

³NOAA Earth System Research Laboratory, Global Monitoring Division (GMD), Boulder, CO 80305

⁴Alfred Wegener Institute for Polar and Marine Research, Bremerhaven, Germany

⁵University of Colorado, Department of Atmospheric and Oceanic Sciences, Boulder, CO 80309

⁶Science and Technology Corporation, Boulder, CO 80305

⁷Arctic and Antarctic Research Institute (AARI), Saint Petersburg, Russia

⁸Swiss Federal Institute for Forest, Snow and Landscape Research WSL, Birmensdorf, Switzerland

High-quality, continuous, long-term observations of radiative fluxes are collected from land stations surrounding the Arctic Basin, including through the Baseline Surface Radiation Network (BSRN). The Radiation Working Group of the International Arctic Systems for Observing the Atmosphere (IASOA) is currently analyzing data acquired from Utqiagvik (Barrow), Alaska (1993-2016), Alert, Canada (2004-2016), Ny-Ålesund, Svalbard (1993-2016), Eureka, Canada (2007-2016), Tiksi, Russia (2011-2016), Oliktok Point, Alaska (2014-2016) and Summit, Greenland (2010-2012). The measurements include upwelling and downwelling longwave and shortwave fluxes, as well as direct and diffuse shortwave flux components, and surface meteorology. The observations are post-processed using the Radiative Flux Analysis method, which in addition to basic quality control provides value-added metrics such as cloud radiative forcing, optical depth and fractional sky cover. Inter-site comparisons are presented as well as temporal analyses of both the net surface radiation and individual components of the surface radiation budget.

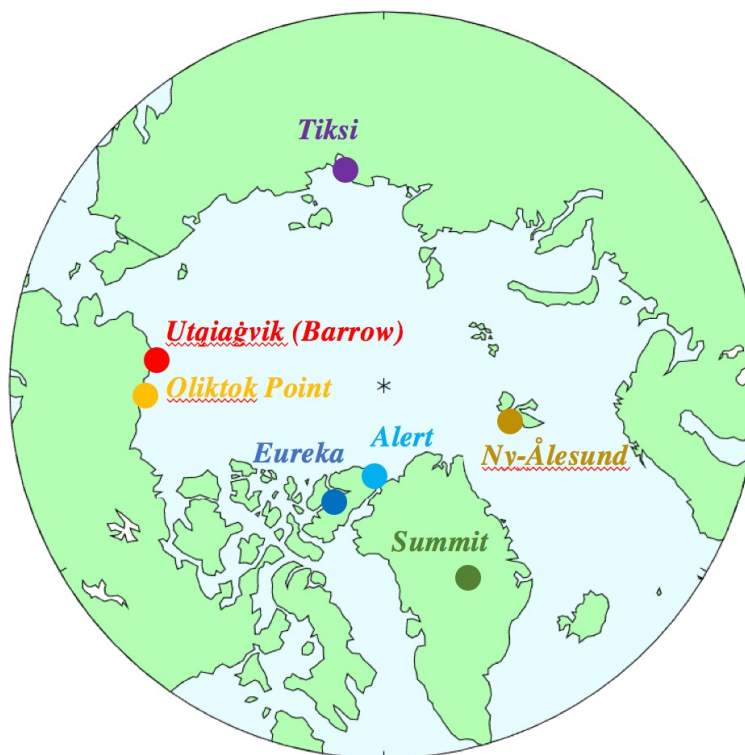


Figure 1. Stereographic map of the Arctic showing the locations of IASOA stations that are the focus of the analysis.

Asian Transport Influence on Greenland Crustal Aerosols

N. Spada and T. Cahill

University of California at Davis, Davis, CA 95616; 530-752-0933, E-mail: njspada@ucdavis.edu

Long-term sampling of size- and time-resolved particulate matter at the Greenland Summit Camp has provided important chemical speciation data for the Arctic regions. The continued use of DRUM (Davis Rotating-Unit for Monitoring, through 2021) sampling enables implementation of equipment and methodological upgrades that will increase sensitivity and reduce costs for the next 5 years as well as provide analysis for samples collected from 2014 to 2017. The key changes made include lengthening the time resolution bins from 6 hr to 12 hr samples, which will enhance detection of trace constituents by a factor of 4 and retain diurnal cycle resolution. Additionally, optical backscattering will be employed during optical analysis of collected samples in order to estimate single scattering albedo as a function of particle size. Recent efforts have focused on re-analysis and interpretation of samples collected from 2009 to 2013. Thus far, the most significant focus involved tracking crustal elemental signatures back to Asia. Annual dust storm events coupled with an arctic transport path have shown consistent spikes in industrial tracers (e.g. sulfur) and augmented elemental ratios (e.g. iron/calcium).

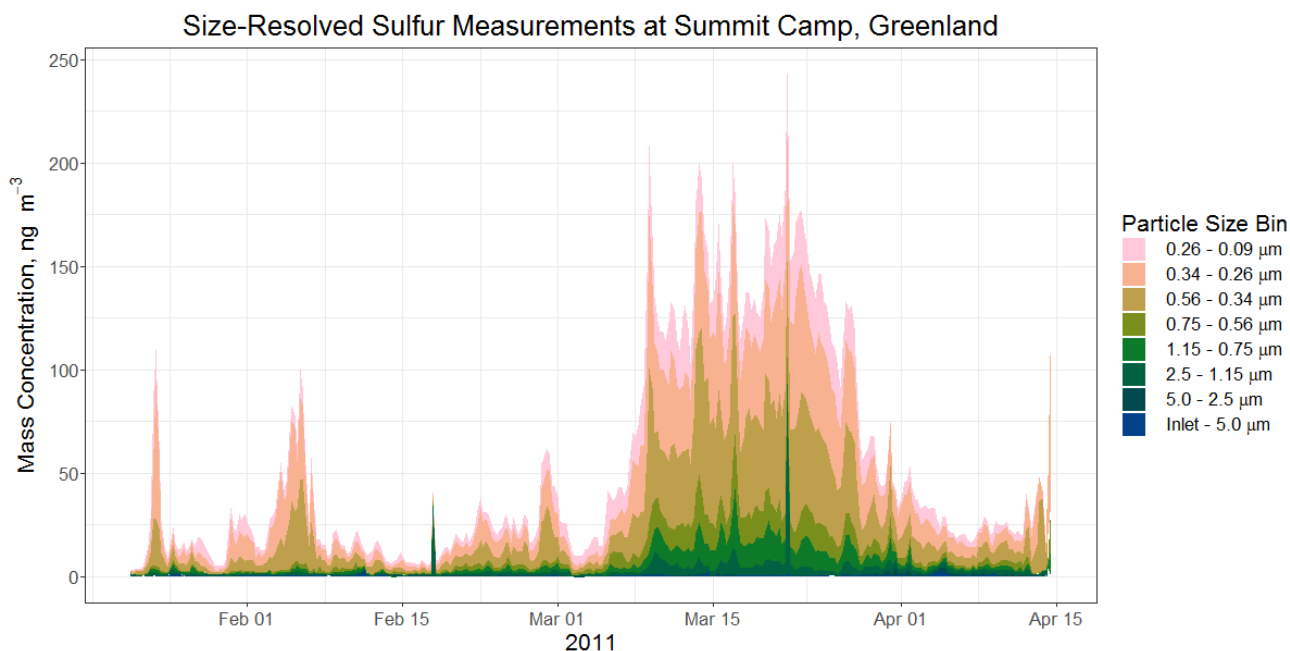


Figure 1. Stacked area mass concentrations (ng m^{-3}) of sulfur as a function of size (shown by color) and time (6 hr binning). Trajectory analysis using HYSPLIT indicates the spring enhancement of very fine sulfur may originate in Asia and transport through the Bering Sea.

Understanding the Impact of Biomass Burning on Ozone Conditions in the Arctic

A. McClure-Begley^{1,2}, S. Crepinsek^{1,3}, I. Petropavlovskikh^{1,2}, A.Y.^{1,2}, T. Uttal³, S.T.⁴, A. Jefferson^{1,2} and D. Helmig⁵

¹Cooperative Institute for Research in Environmental Sciences (CIRES), University of Colorado, Boulder, CO 80309; 303-497-6823, E-mail: Audra.mcclure@noaa.gov

²NOAA Earth System Research Laboratory, Global Monitoring Division (GMD), Boulder, CO 80305

³NOAA Earth System Research Laboratory, Physical Sciences Division (PSD), Boulder, CO 80305

⁴National Center for Atmospheric Research (NCAR), Boulder, CO 80307

⁵Institute of Arctic and Alpine Research (INSTAAR), University of Colorado, Boulder, CO 80309

Tropospheric ozone (O_3) is an atmospheric species formed by the reaction of precursor species [NO_x , carbon monoxide (CO), volatile organic compounds (VOC's)] in the presence of ultraviolet radiation and drives complex interactions which can result in impacts on atmospheric conditions in the Arctic. As an important greenhouse gas, O_3 has a significant influence on the photochemical characteristics, oxidation capacity, and radiative forcing of the atmosphere and at high levels has negative impacts on public health and overall ecosystem functioning. In the Arctic, tropospheric O_3 has variable characteristics in time and space. The Arctic O_3 conditions are strongly influenced by seasonal destruction events, Arctic haze, transport of pollution from Asia and influence from precursor compounds released from wildfires. Surface O_3 measurements have been made in the Arctic since 1973 (Barrow, Alaska) and have expanded spatially and temporally since. This study analyzes the relative impact of biomass burning on surface O_3 conditions from six Arctic measurement locations. The meteorological and chemical conditions of the atmosphere are examined to help explain variation in the Arctic surface O_3 conditions. Co-located measurements of meteorological conditions, carbon monoxide, and aerosol optical depth are used to understand the dominant sources of pollution, pollutant composition, and the interactions due to meteorological conditions that result in anomalies in the observed O_3 mixing ratios. However, there is still a need for additional information and measurements of chemical tracers to help discern the contributions of different pollutant sources to O_3 conditions. NOAA Hypslit back-trajectory analysis, satellite imagery, smoke verification models, and NCAR Community Earth System Model are used to interpret observations as a result of the limited geographical and temporal coverage of measurements required for attribution of pollution sources. Characterization of O_3 conditions is essential for understanding the spatial and temporal variation and behavior of O_3 as it relates to climate change in the Arctic.

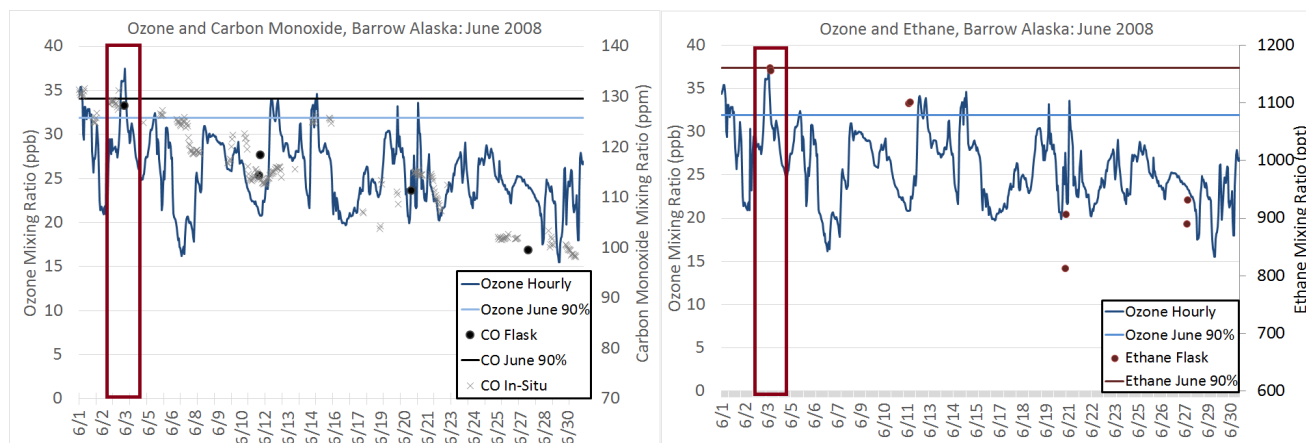


Figure 1. A case study of high O_3 measured from Barrow, Alaska on June 3, 2008 demonstrates the importance of co-located measurements, such as ethane (C_2H_6) and CO, for understanding the influence of biomass burning on ground-level O_3 conditions. Elevated CO, C_2H_6 , and O_3 provide insight to investigate the high ozone episode further with model, satellite, and back-trajectory analysis.

Analysis of Near-surface Permafrost Monitoring Station Data from Alaska

K. Wang¹, E. Jafarov², K. Schaefer³, V. Romanovsky⁴, W. Cable⁴, G.D. Clow^{5,1}, F. Urban⁵, M. Piper¹, C. Schwalm⁶, T. Zhang⁷, I. Overeem¹ and A. Kholodov⁴

¹Institute of Arctic and Alpine Research (INSTAAR), University of Colorado, Boulder, CO 80309; 303-359-4726, E-mail: Kang.Wang@colorado.edu

²Los Alamos National Laboratory, Los Alamos, NM 87545

³National Snow and Ice Data Center (NSIDC), Boulder, CO 80309

⁴Geophysical Institute Permafrost Laboratory, University of Alaska, Fairbanks (UAF), Fairbanks, AK 99775

⁵United States Geological Survey (USGS), Boulder, CO 80309

⁶Woods Hole Research Center, Falmouth, MA 02540

⁷Lanzhou University, College of Earth and Environmental Sciences, Lanzhou, Gansu, China

Recent observations of near-surface soil temperatures over the Circumpolar Arctic show continuing warming of the permafrost-affected soils. Rapid warming of the North Pole suggests amplified permafrost thaw with possible release of labile carbon stored within the first 3 m of permafrost into the atmosphere. Release of the currently frozen soil carbon to the atmosphere could accelerate and amplify anthropogenic climate warming. A consolidated near-surface permafrost dataset is needed to better understand the corresponding climate impact and constrain the permafrost thermal and spatial conditions in the land system models. In this study, we compile shallow ground temperature measurements collected by the U.S. Geological Survey (USGS) and the Geophysical Institute, University of Alaska Fairbanks (UAF) permafrost monitoring networks in Alaska. This dataset represents an initial effort in consolidating information on near-surface permafrost dynamics in the Northern Hemisphere. The Alaskan dataset includes air and ground temperature data, volumetric water content and snow depth measured since 1998. We used trend analysis to understand the dataset and recent permafrost thermal dynamics. The results of our analysis show the highest warming trend ($+0.30^{\circ}\text{C}/\text{yr}$) in the Alaska North Slope. We found strong relationship between the thermal offset at the ground surface and snow depths less 0.40 m. Based on the calculated linear trend projections we predict increase in near-surface temperature dynamics at 1 m in the range of $1.53\text{--}1.91^{\circ}\text{C}$ for the North Slope and stable warming (greater than 0°C) for the Interior over the next 20–25 years.

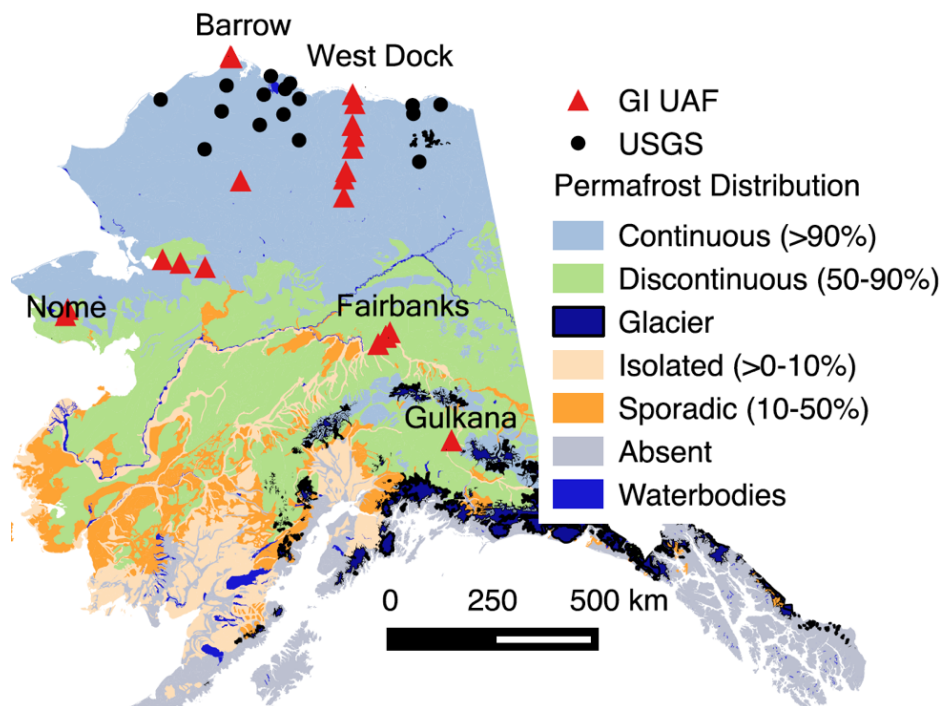


Figure 1. Locations of USGS and Geophysical Institute UAF permafrost monitoring stations in Alaska.

A Comparison of Photodiode and LED Based Sunphotometer-derived AOD with NASA AERONET

I. Krintz¹, J. Bokorney¹, S. Fischer², A. Nenow³ and J. Sherman¹

¹Appalachian State University, Department of Physics and Astronomy, Boone, NC 28608; 828-707-5735, E-mail: krintzia@appstate.edu

²Appalachian State University, Environmental Science, Boone, NC 28608

³Watauga High School, Boone, NC 28307

Regional and global studies of aerosol direct radiative forcing (DRF) and, more recently, surface-level particulate matter concentrations (PM_{2.5}), rely on aerosol optical depth (AOD) measurements from satellite-based platforms such as NASA's Moderate Resolution Imaging Spectroradiometer (MODIS) aboard Terra and Aqua due to near-global coverage daily. However, recent comparisons of MODIS-measured AOD with "ground-truth" AOD measurements at NASA AERONET sites located in mountainous regions around the world demonstrated a weaker agreement (Levy et al., 2010), with a small negative AOD bias over the Southern Appalachian Mountain Region (Sherman et al., 2016). To aid in validation of MODIS-retrieved AOD over these regions, networks of inexpensive handheld sunphotometers may be deployed to increase the spatial density of measurements where research-level instrumentation is otherwise unavailable (Brooks and Mims, 2001). Currently, few (if any) assessments of sunphotometer sensitivities or uncertainties have been conducted; to this end, the primary research goals are to quantify these unknowns and begin deployment to establish a mountainous citizen science network. Initial results from a multi-year comparison of AOD measured at Appalachian State University's NASA AERONET site with AOD measured by handheld sunphotometers using LEDs as detectors (Brooks and Mims, 2001) and a modified design using filtered photodiodes will be presented. A modified handheld sunphotometer with a microcontroller interface has been developed at Appalachian State to simplify data collection and transfer by citizen scientists; initial results of its performance are also presented.

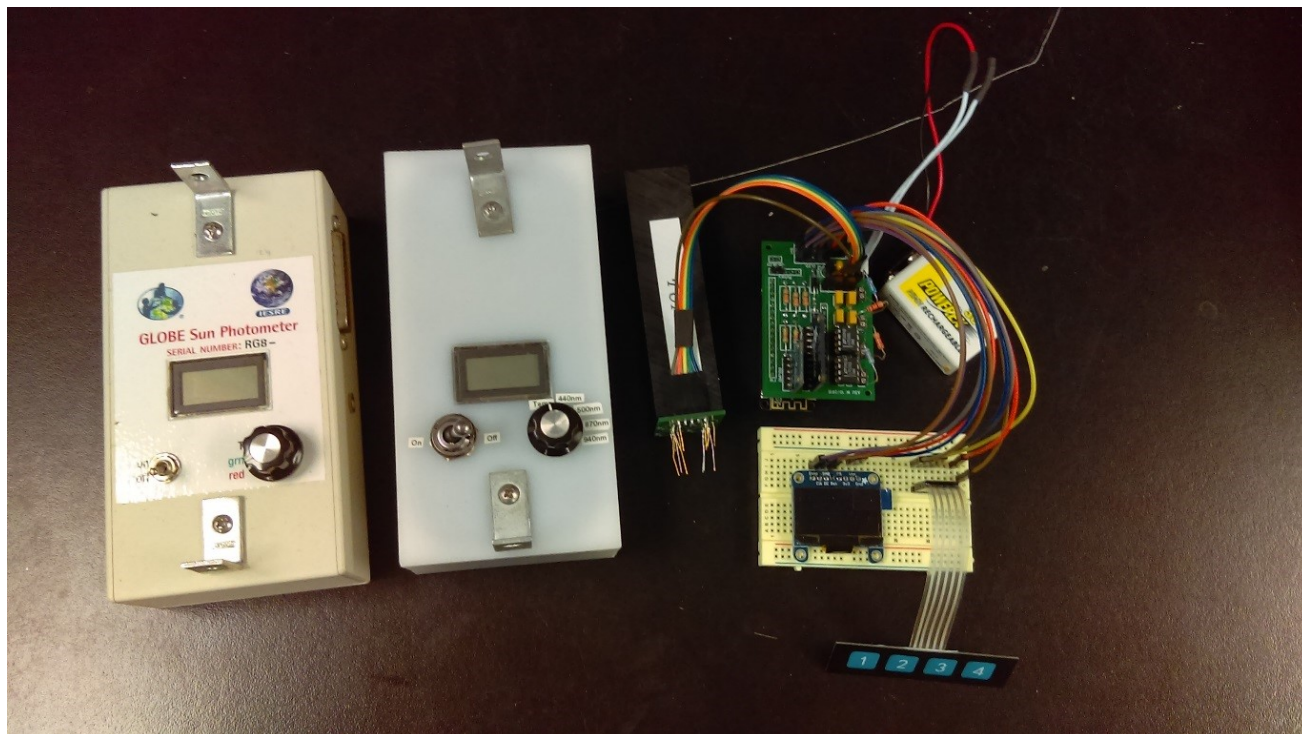


Figure 1. Three “generations” of sunphotometers have been used/developed at Appalachian State University. The first (left) is the GLOBE sunphotometer featuring LED detectors, followed by the filtered photodiode model (middle). The first microcontroller-based model is in the final stages of development (right).

Volatility of Materials Internally Mixed with Black Carbon from Biomass Burning

K. Lamb^{1,2}, H. Li³, A. May³, G. McMeeking⁴ and J. Schwarz²

¹Cooperative Institute for Research in Environmental Sciences (CIRES), University of Colorado, Boulder, CO 80309; 303-497-5256, E-mail: kara.lamb@noaa.gov

²NOAA Earth System Research Laboratory, Chemical Sciences Division (CSD), Boulder, CO 80305

³The Ohio State University, Columbus, OH 43210

⁴Handix Scientific, Boulder, CO 80301

Biomass burning (BB) is a huge source for black carbon (BC) containing aerosols to the troposphere. Both BC's absorption of light, and its lifetime in the atmosphere are affected by the amount of other materials internally mixed with it. These "coatings" can be formed of materials that condense onto the BC aerosol as the particles age in the atmosphere, or they can also occur at the time of emission. For BB, the properties of BC coatings (amount, composition) can potentially indicate differences in fuel types and/or burn conditions; e.g. burns producing more brown carbon have previously been associated with organic compounds with very low volatility (Saleh et al., 2014). Additionally, as pollution is transported from BB sources, it is diluted, leading to changes in gas/aerosol phase partitioning of intermediate volatility compounds. It is not yet known whether the volatility of the materials internally mixed with BC is the same as the volatility of the bulk aerosols. Measurements with a single particle soot photometer (SP2) during FireLab at the U.S. Department of Agriculture (USDA) Fire Sciences Lab in Missoula, MT provide a large data set of BC-specific information for a variety of fuels common to North American wildfires. Here, we examine the mixing state of BC aerosols for different fuel types in controlled laboratory burns. We also study the evolution of the internal mixing state and size distribution of the aerosols in chamber experiments simulating dilution of initially highly concentrated smoke plumes (See Fig. 1). To assess the changing composition of internally mixed materials on BC, as dilution and repartitioning occur, I investigate whether the volatility of the materials internally mixed with the BC does indeed differ from bulk aerosol, and to what extent the SP2 can constrain these effects.

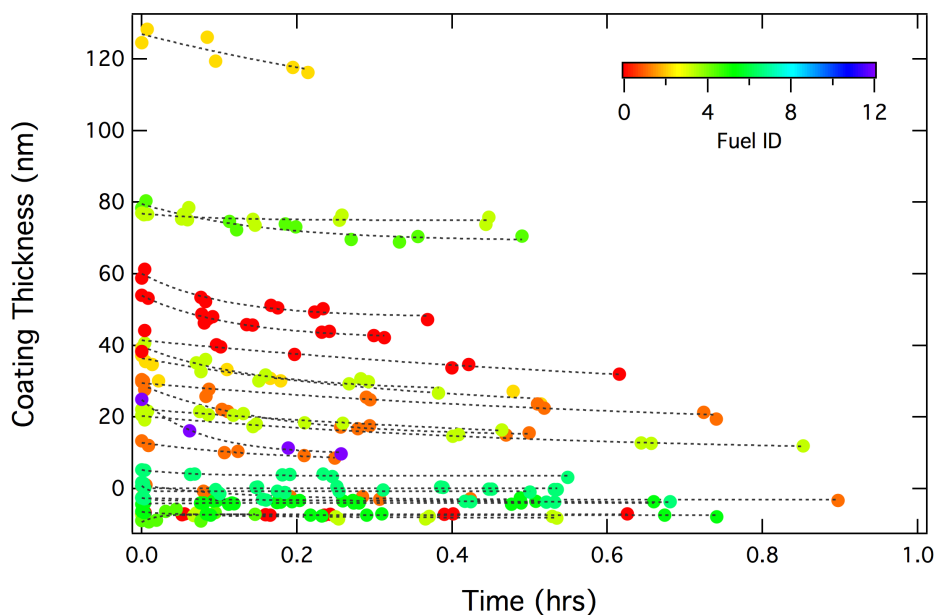


Figure 1. Evaporation of coatings on BC (4-6 fg cores) measured by the NOAA single-particle soot photometer during measurements of smoke inside a barrel from stack burns during Firelab. Smoke is initially drawn into the barrel near the beginning of the burn, and after the barrel is filled, it is closed off from the fire and continually diluted with filtered air. SP2 sampling occurs over typically 15 minutes during the dilution period. Initial coating thickness demonstrates large variability, and coatings evaporate faster at the beginning of the dilution.

Ambient Aerosol Extinction in Great Smoky Mountains National Park

T. Gordon¹, G. McMeeking¹, J. Renfro², E. McClure², A. Prenni³, T. Onasch⁴, A. Freedman⁴ and P. Chen¹

¹Handix Scientific, Boulder, CO 80301; 617-276-6445, E-mail: tim@handixscientific.com

²National Park Service, Gatlinburg, TN 37738

³National Park Service, Denver, CO 80225

⁴Aerodyne Research Inc., Billerica, MA 01821

The IMPROVE (Interagency Monitoring of Protected Visual Environments) program, which is tasked with monitoring visibility in U.S. National Parks and Wilderness Areas, relies on aerosol-induced light extinction reconstructed from speciated filter measurements and humidification growth factors. Under many atmospheric conditions reconstructed extinctions compare favorably with measurements; however, there are several possible sources of discrepancy. First, the IMPROVE reconstructions are based on 24-hour averaged filter measurements taken once every four days; thus, important transient events may not be well resolved. Second, at high relative humidities (RH) aerosol light extinction is very sensitive to RH perturbations; thus, under such conditions the humidification growth factors are highly uncertain.

The Open-Path Cavity Ringdown Spectrometer (OPCRDS) was designed to overcome the RH limitations of previous extinction instruments. The OPCRDS was recently deployed in the Great Smoky Mountains National Park (GSM), where the high RH and high photochemical activity typical in summer provided an opportunity to explore the upper limits of the aerosol hygroscopicity curve and the accuracies of both the IMPROVE extinction reconstruction algorithm and the GSM nephelometer used to validate reconstructed extinction. True ambient extinction measured by the OPCRDS and dry extinction measured by a traditional closed-cell extinction monitor were used to investigate the hygroscopicity of aerosol at GSM and the importance of coarse-mode particles to light extinction.

During the majority of the campaign the OPCRDS data agree closely with the GSM nephelometer and the reconstructed extinction. However, we observed discrepancies between scattering and ambient extinction due to coarse-mode particles, and several high RH events were not resolved by the reconstructed extinction. Finally, we found that the extinction calculated with the revised reconstruction algorithm (IMPROVE-2) was about 12% lower than the values calculated from the original algorithm and provided a slightly better fit to the OPCRDS data.

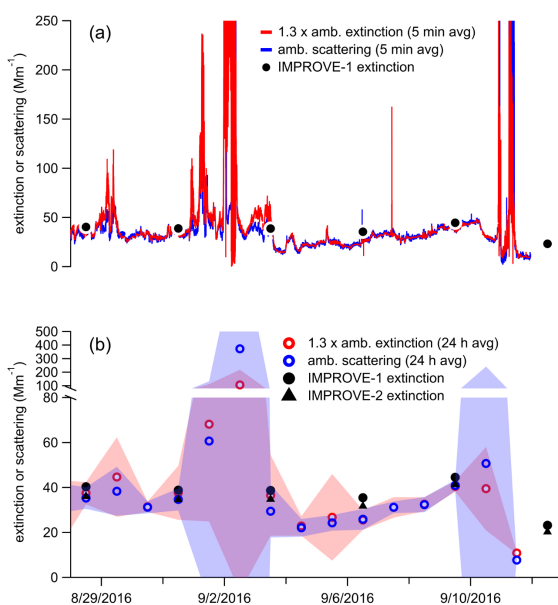


Figure 1. Comparison of aerosol extinction calculated from the original IMPROVE equation and (a) 5-minute average ambient extinction/scattering and (b) 24-hour average ambient extinction/scattering (standard deviations are indicated by the shaded regions) and extinction calculated with the revised IMPROVE equation. IMPROVE-1 extinction values are identical in (a) and (b). IMPROVE data are preliminary and have not been fully validated.

Characterization of Transported Biomass-Burning Smoke from Indochina to Mt. Lulin Based on a Super Event in March of 2009

S.C. Wang¹, N.L.S. Phu¹, B.T. Thuy¹, T.L. Lei¹, H. Huang¹, N. Lin^{1,2}, G. Sheu¹, C. Ou-Yang^{1,2} and C. Lee³

¹National Central University, Department of Atmospheric Sciences, Chung-Li, Taiwan; +886-972881003, E-mail: shenghsiang.wang@gmail.com

²National Central University, Department of Chemistry, Chung-Li, Taiwan

³National Central University, Graduate Institute of Environmental Engineering, Taiwan

Biomass burning (BB) in Indochina during springtime plays a great impact on the air quality of downwind regions, that was continuously obtained at the 2,862 m Lulin Atmospheric Background Station (LABS). In this study, we will combine the data from LABS, Modern-Era Retrospective analysis for Research and Applications (MERRA) reanalysis, and satellites to study the largest BB event (March 17-18, 2009) in the historical record. The event time lasted over 29 hours and the average concentrations of carbon monoxide (CO), ozone (O₃), gaseous elemental mercury (GEM) and PM₁₀ was found to be 586 ± 165 ppb, 105 ± 23 ppb, 2.1 ± 0.2 ng.m⁻³ and 105.2 ± 23.4 µg.m⁻³, respectively. During the event, $\Delta\text{GEM}/\Delta\text{CO}$ ratio significantly decreased from 0.0027 to 0.00079 (ng.m³/ppbv) and the slope of $\Delta\text{O}_3/\Delta\text{CO}$ was calculated to be 0.123 ($r^2 = 0.75$). The carbonaceous contents on 18 March showed high EC1-OP, OC3 concentration which dominated due to the BB aerosols. The aerosol single-scattering albedo and char-EC/soot-EC ratios were 0.87 ± 0.04 and 29.4, respectively, indicating the plume contained high absorption aerosol. All measurements and indexes show that the BB plume experienced weak mixing and chemical transformation before reaching Mt. Lulin. We suggest that this event could be served as a good benchmark for identifying a relatively pure BB long-range transport from Indochina to Mt. Lulin, which would be useful for future event identification.

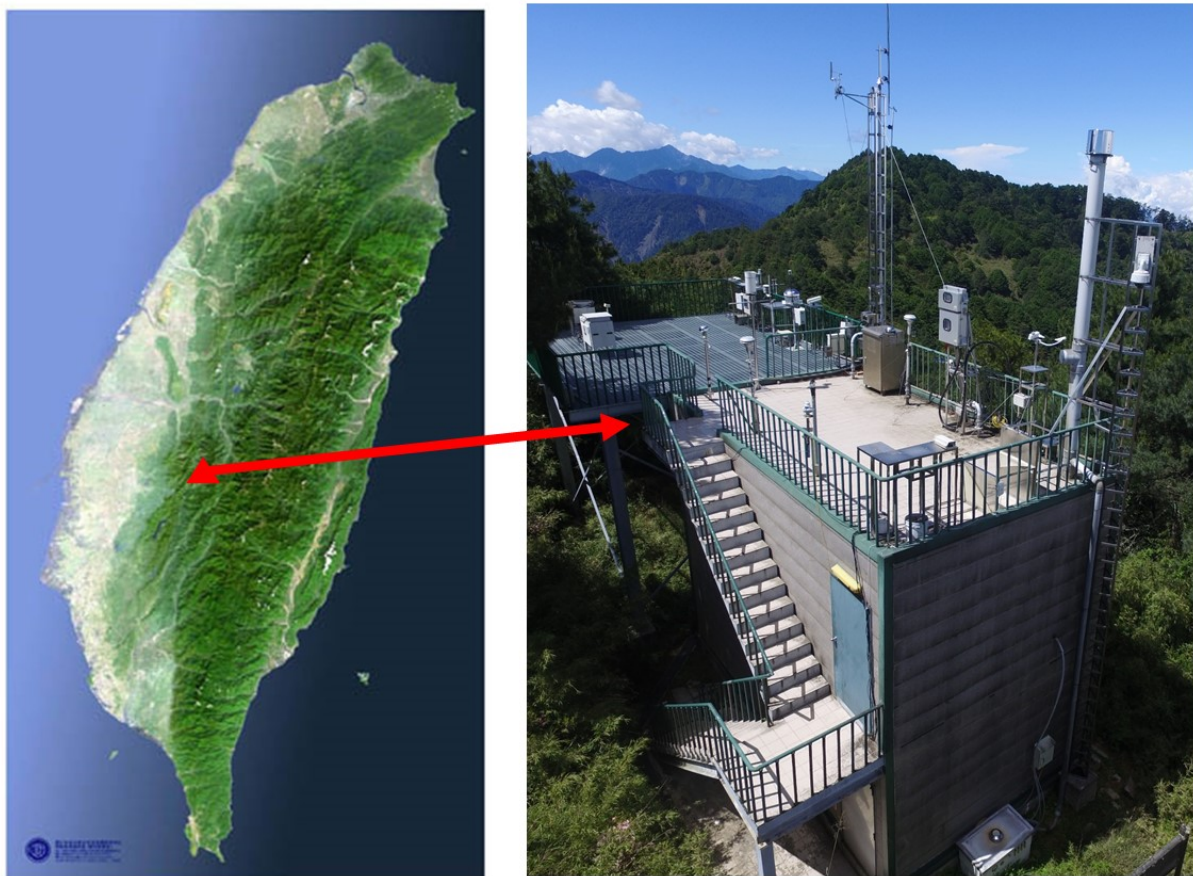


Figure 1. The geographic location and main building of LABS in Taiwan.

Aerosol Measurements Over Mauna Loa Observatory

N.C.P. Sharma¹, J. Barnes^{2,3}, J. Butt⁴, C. Oville⁴ and J. Kulowiec⁴

¹Central Connecticut State University, Department of Physics and Engineering Physics, New Britain, CT 06053; 860-832-2937, E-mail: sharmanim@ccsu.edu

²Cooperative Institute for Research in Environmental Sciences (CIRES), University of Colorado, Boulder, CO 80309

³NOAA Earth System Research Laboratory, Global Monitoring Division (GMD), Boulder, CO 80305

⁴Central Connecticut State University, New Britain, CT 06053

Aerosol measurements were conducted over Mauna Loa Observatory (MLO), an atmospheric baseline observatory, using the CCD Camera Lidar (CLidar) System. The system transmits 532 nm laser pulses vertically into the atmosphere and the side scattered light is detected by imaging using a CCD camera with wide angle optics and laser line filter. The camera is located upslope from the laser-base and 139 m perpendicularly away from the laser-beam. The altitudes of atmospheric constituents scattering laser-light were determined by the bistatic lidar system's geometry. The altitude resolution of the system is sub-meter at ground-level but degrades with increasing altitude. The scattering angle varies with altitude. The returned side-scatter signal is normalized to a molecular scattering model between 10.7 and 14.9 km. The molecular scattering signal component is then removed from the total scattering signal. An aerosol scattering phase function that describes the column average efficiency of aerosol scattering into a particular angle is needed to convert the CLidar derived side scatter to total scatter. Aerosol phase functions used were derived from AERONET sun photometer data taken at MLO during the daytime prior to the evening CLidar data. CLidar data were typically taken starting just after sunset for a duration of several hours on each experimental night, with each data image exposure being 332 seconds. CLidar data were corrected iteratively for transmission and converted to aerosol extinction using a single-scattering albedo of 0.9. Data were examined from 29 dates in 2006-2007 and 2007-2008. Aerosol flows near the 3400 m asl ground level of MLO can be complicated and highly variable. This study focused on MLO aerosol measurements at 4 to 10 km above sea level. The average aerosol extinction above MLO in these data at altitudes from 4 to 10 km ranged from 0.0035 km⁻¹ with a standard deviation of 0.0007 km⁻¹ at 4 km to 0.00033 km⁻¹ with a standard deviation of 0.0002 km⁻¹ at 9.7 km. Figure 1 shows the average aerosol extinction for the combined 2006-2007 and 2007-2008 years, by season. There were a limited number of experimental nights each season. Data show a fairly persistent aerosol layer between 4.7 and 5.5 km above sea level. Yearly average aerosol extinctions varied between years, with extinctions approximately 50% higher in 2007-2008 compared to 2006-2007.

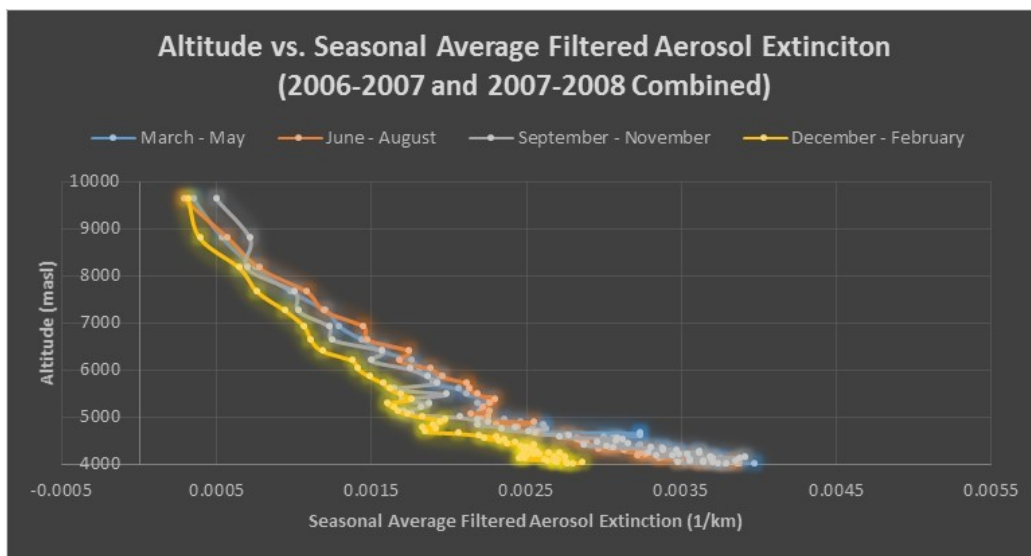


Figure 1. Seasonal trends of 2006-2007 and 2007-2008 CLidar aerosol measurements over MLO.

Calibration and Field Testing of Cavity Ring-down Laser Spectrometers Measuring Methane Mole Fraction and the Isotopic Ratio of Methane, Deployed on Towers in the Marcellus Shale Region

N. Miles¹, D. Martins^{1,2}, S. Richardson¹, C. Rella³, T. Lauvaux¹, K.J. Davis¹, Z. Barkley¹, K. McKain^{4,5} and C. Sweeney^{4,5}

¹The Pennsylvania State University, Department of Meteorology, University Park, PA 16802; 814-880-8087, E-mail: nmiles@met.psu.edu

²FLIR Systems, Wilsonville, OR 97070

³Picarro Inc., Santa Clara, CA 94054

⁴Cooperative Institute for Research in Environmental Sciences (CIRES), University of Colorado, Boulder, CO 80309

⁵NOAA Earth System Research Laboratory, Global Monitoring Division (GMD), Boulder, CO 80305

Four *in situ* cavity ring-down spectrometers (Picarro, Inc.) measuring methane (CH_4), carbon dioxide (CO_2) and the isotopic ratio of methane were deployed at towers with heights between 46 and 61 m a.g.l.. The study is focused on the Marcellus Shale natural gas extraction region of Pennsylvania. The leakage rate of methane determines whether natural gas is useful as a bridge fuel, in terms of greenhouse effects, compared to coal. Sources of methane can be distinguished via the isotopic signature: heavy isotope ratios are characteristic of thermogenic (e.g., oil and gas) CH_4 sources and light isotope ratios are characteristic of biogenic (e.g., landfills, agriculture) sources. The calibration of the isotopic methane instruments is challenging for several reasons, including the need for both a slope/intercept calibration and a mole fraction correction (Fig. 1), and cross-interference from ethane. We describe laboratory and field calibration of the analyzers for tower-based applications, and characterize their performance in the field from January 2016 – November 2016. Prior to deployment, each analyzer was calibrated using high mole fraction bottles with various isotopic ratios from biogenic to thermogenic source values, diluted in zero air. Furthermore, at each tower location, three field calibration tanks were employed, from ambient to high mole fractions, with various isotopic ratios. By testing various calibration schemes, we determined an optimized field calibration method.

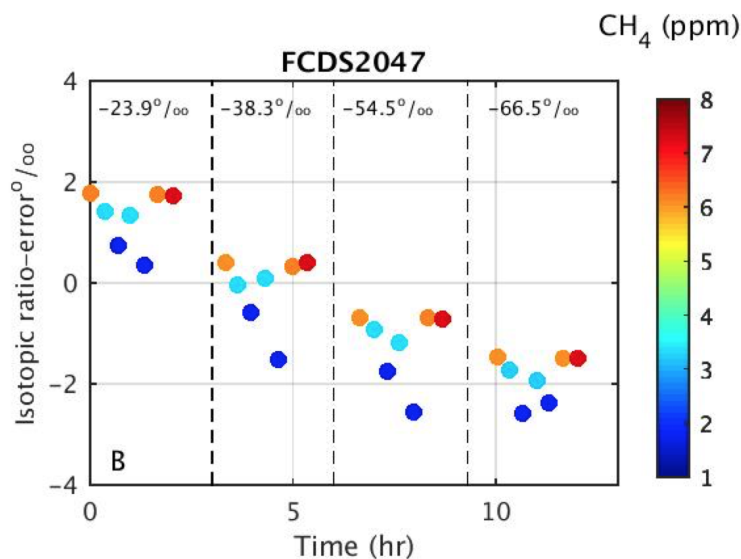


Figure 1. Isotopic ratio error (prior to calibration) as a function of measurement time during the laboratory calibration. For this test, commercially-available isotopic standard bottles (Isometric Instruments, Inc.) were diluted with zero air to produce mixtures with varying CH_4 mixing ratios and $\delta^{13}\text{CH}_4$. The dotted lines separate the four isotopic values tested. The colors indicate the CH_4 mole fraction. The isotopic ratios prior to calibration exhibit both a slope/intercept error and a mole fraction dependence.

Methane Source Attribution in the DJ Basin using Mobile Surveys and Computational Analytics

E. Atherton¹, C. Fougere¹, O.A. Sherwood², D. Risk¹, B. Vaughn² and G. Pétron^{3,4}

¹St. Francis Xavier University, Antigonish, Nova Scotia, Canada; 905-703-9921, E-mail: eatherto@stfx.ca

²Institute of Arctic and Alpine Research (INSTAAR), University of Colorado, Boulder, CO 80309

³Cooperative Institute for Research in Environmental Sciences (CIRES), University of Colorado, Boulder, CO 80309

⁴NOAA Earth System Research Laboratory, Global Monitoring Division (GMD), Boulder, CO 80305

Initiatives aimed at curbing the impacts of climate change by reducing methane (CH_4) emissions require detection and attribution techniques capable of distinguishing between various types of sources, particularly in atmospherically complex multi-use landscapes such as the Denver-Julesburg (DJ) Basin in Colorado. This research applies Emissions Attribution using Computational Techniques (ExACT), proven successful in Canadian oil and gas settings, to Picarro Surveyor high-precision gas data collected in the DJ Basin through the summer of 2014. Throughout the mobile surveys, more than 350,000 geo-located multi-gas [CH_4 , carbon dioxide (CO_2)] measurements were recorded at 1 Hz frequency. ExACT uses super-ambient ratios of $\text{CO}_2:\text{CH}_4$ and geospatial analysis to distinguish point-source emissions from naturally variable background CH_4 concentrations, and attributes these emissions to potential known sources. Based on wind direction and a cut-off distance of 300 m from potential emission sources, 943 wellpads, 34 gas processing facilities, and 23 Concentrated Animal Feeding Operations (CAFOs) were sampled along the survey routes. Wellpads and gas processing facilities related to oil and gas operations had emission frequencies of 31% and 44%, respectively. CAFOs were associated with emissions 48% of the times they were sampled. Based on the high density of oil and gas infrastructure in the area, and relative similarities in CH_4 concentration distributions among the three main sources, oil and gas infrastructure emerged as the primary source of anthropogenic CH_4 emissions in the roughly 40-by-40 mi² study area. Emissions frequency varied significantly by operator, suggesting differences in the effectiveness of emissions mitigation practices. Knowledge of trends among emission sources can ideally be used to inform policy or regulation aimed at curbing greenhouse gas emissions and improving local air quality.

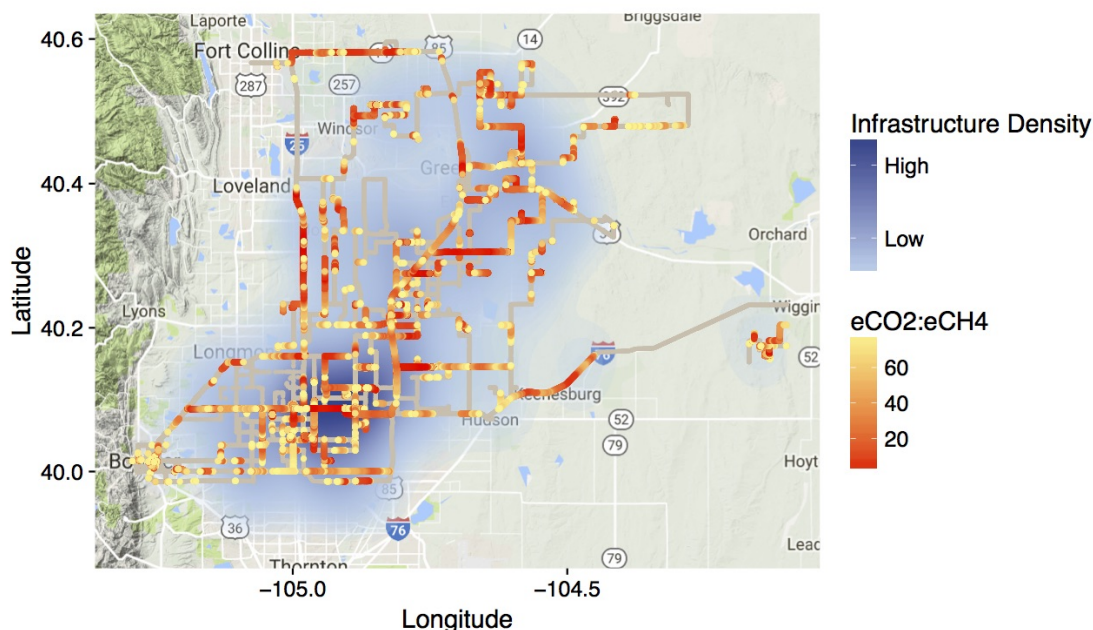


Figure 1. Location of CH_4 -rich plumes defined by values of super-ambient $\text{CO}_2:\text{CH}_4$. Lower values correspond to more CH_4 -rich signatures (red). Infrastructure density (blue) represents the locations of sampled oil and gas wellpads and facilities, and CAFOs.

Temporal Variability in Methane at Indianapolis with Implications for the Urban Methane Flux Estimates

N. Balashov¹, K.J. Davis¹, N. Miles¹, S. Richardson¹, T. Lauvaux¹, Z. Barkley¹ and B.K. Lamb²

¹The Pennsylvania State University, Department of Meteorology, University Park, PA 16802; 814-777-3861, E-mail: nvb5011@psu.edu

²Washington State University, Laboratory for Atmospheric Research, Pullman, WA 99164

As natural gas extraction and use continue to increase, the need to quantify methane (CH_4) emissions, a powerful greenhouse gas, has grown. Large discrepancies in Indianapolis CH_4 emissions are observed when comparing inventory, aircraft mass-balance, and tower inverse CH_4 emissions estimates. The Indianapolis Flux Experiment (INFLUX) tower network is utilized to investigate these discrepancies between bottom-up and top-down CH_4 emission assessments. The INFLUX network includes 9 towers currently hosting continuous, highly-calibrated CH_4 mole fraction measurements to examine the temporal variability in 2012-2016 CH_4 at Indianapolis (see Figure). Three major reasons that may be responsible for the above-mentioned discrepancy are identified: (1) a highly-variable and spatially non-uniform U.S. continental CH_4 background with changes up to 150 ppbv, (2) temporal variability in anthropogenic urban CH_4 sources and (3) an influence of unknown CH_4 sources. To address the first issue, we propose a method for identifying the days with a regionally uniform CH_4 background. With regard to the second issue, we recommend temporal consistency when aircraft mass-balance and tower inverse methods are compared. For the third concern, we investigate the ways to approximate the impact of the unknown sources on the CH_4 flux estimates. Work continues to quantify the implications for total city CH_4 emissions given the regional and local CH_4 temporal variability.

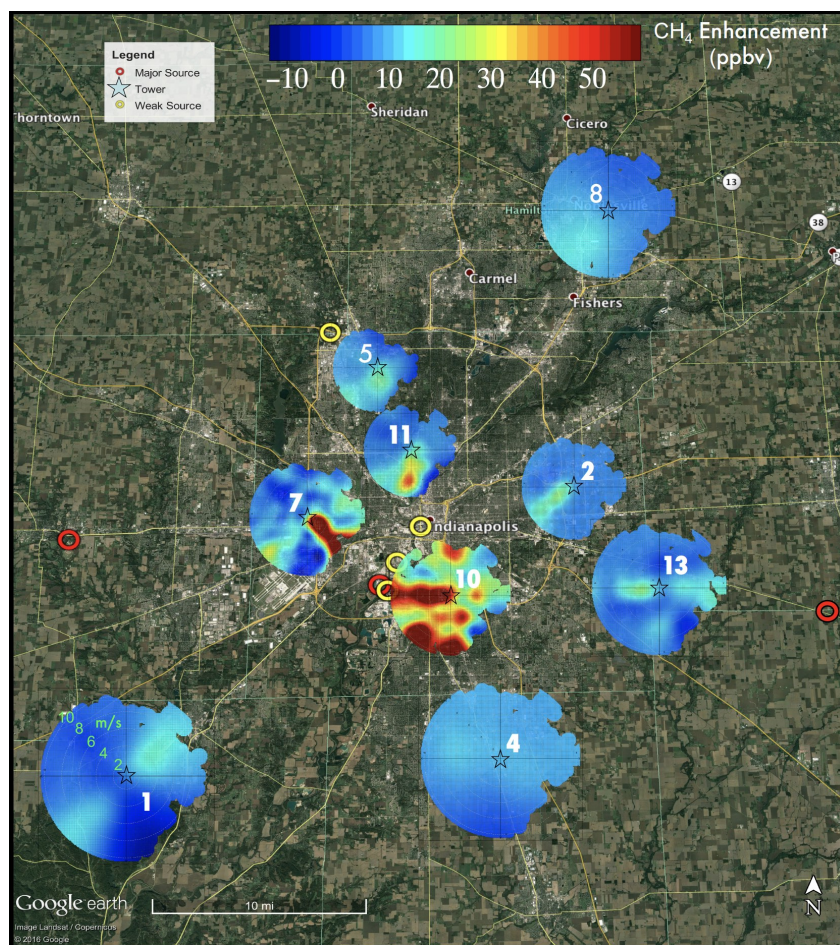


Figure 1. CH_4 enhancements (calculated by subtracting CH_4 background from the tower measurements) using 1500-2200 UTC data for the full year of 2015 as measured by the INFLUX tower network. Bivariate polar plots show CH_4 enhancements as a function of wind direction (degrees) and wind speed (m/s).

Stable Isotopes of Carbon Monoxide during Two Summers at Indianapolis, IN show Significant Influence of Oxidized Biogenic Volatile Organic Compounds on the CO Budget

I. Vimont¹, J. Turnbull^{2,3}, V. Petrenko⁴, P. Place⁴ and A. Karion⁵

¹Institute of Arctic and Alpine Research (INSTAAR), University of Colorado, Boulder, CO 80309; 303-492-5495, E-mail: isaac.vimont@colorado.edu

²GNS Science, National Isotope Centre, Lower Hutt, New Zealand

³NOAA Earth System Research Laboratory, Global Monitoring Division (GMD), Boulder, CO 80305

⁴University of Rochester, Department of Earth and Environmental Sciences, Rochester, NY 14627

⁵National Institute of Standards and Technology (NIST), Gaithersburg, MD 20880

We present carbon monoxide (CO) stable isotopic results from two summers at Indianapolis, as part of the Indianapolis FLUX project (INFLUX). One of the goals of INFLUX is to learn more about the CO budget in urban areas, with particular focus on how CO relates to fossil fuel produced carbon dioxide ($\text{CO}_{2\text{ff}}$). $\text{CO}_{2\text{ff}}$ can be explicitly determined by radiocarbon measurements, but these measurements are too expensive to make at high resolution. CO has been explored as a potential urban tracer for $\text{CO}_{2\text{ff}}$ and has shown promise during the winter months at Indianapolis. However, during the summer months, this relationship breaks down, suggesting non-fossil fuel sources of CO. Here, we use stable isotopes of CO to partition the various sources of CO within the city.

Our results suggest during the summer months around 46% of the CO enhancements (on average) within Indianapolis are due to oxidized volatile organic compounds (VOC's). While our results do not provide information about the exact species of VOC responsible for this large increase, previous work done by numerous groups suggests that isoprene may be the largest, and most likely, source of these summertime CO enhancements within the city. We compare this result to a Congestion Mitigation and Air Quality (CMAQ) chemistry model output for July in Indianapolis, and find reasonable agreement.

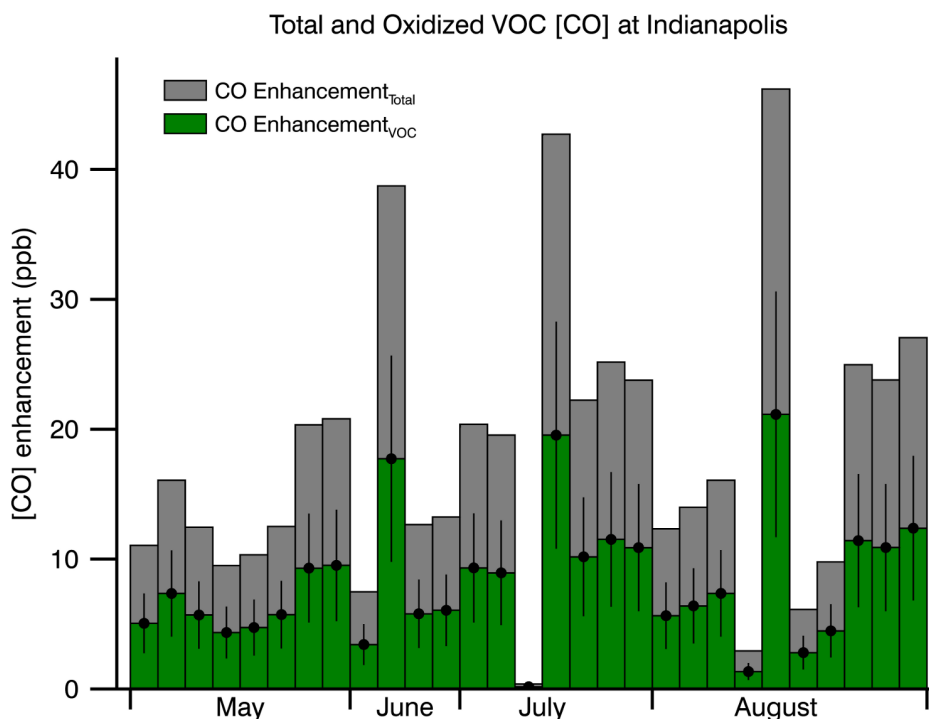


Figure 1. CO enhancements at a tall tower in Indianapolis, IN for the measurements used in this study. Total CO enhancement is shown in grey, and the calculated mean VOC enhancement is overlaid in green. Error bars are 1s of the estimated VOC enhancement.

Chemical Feedback from Decreasing Carbon Monoxide Emissions

B. Gaubert¹, H.M. Worden¹, A.F.J. Arellano², L.K. Emmons¹, S. Tilmes¹, J. Barré¹, S. Martinez-Alonso¹, J.L. Anderson³ and D.P. Edwards¹

¹National Center for Atmospheric Research (NCAR), Atmospheric Chemistry Observations and Modeling Laboratory, Boulder, CO 80307; 303-497-1488, E-mail: gaubert@ucar.edu

²University of Arizona, Department of Hydrology and Atmospheric Sciences, Tucson, AZ 85721

³National Center for Atmospheric Research (NCAR), Computational and Information Systems Laboratory, Boulder, CO 80307

About half of atmospheric carbon monoxide (CO) is from direct emissions that are due to incomplete combustion and are related to both natural (e.g., wildfires) and anthropogenic activities. The remainder of CO in the atmosphere is produced from the chemical oxidation from 1. methane (CH₄) and 2. Non-Methane Organic Compounds (NMVOC's), mainly from biogenic sources (i.e., Isoprene). Since most of the NMVOC's, CO, and CH₄ in the atmosphere are oxidized by the hydroxyl radical (OH), the associated chemical lifetimes of these species are strongly coupled with OH. Understanding changes in the burden and growth rate of atmospheric CH₄ has been the focus of recent studies but still lacks scientific consensus. We quantify the CH₄ loss rate by contrasting two model simulations for 2002-2013: 1) a Measurement of Pollution in the Troposphere (MOPITT) CO reanalysis, and 2) a Control Run without CO assimilation. These simulations are performed with the CESM/CAM-Chem fully-coupled chemistry climate model with prescribed CH₄ surface concentrations. Using the Data Assimilation Research Testbed (DART), the assimilation of MOPITT observations constrains the global CO burden, which significantly decreased over this period. We present a mechanism that link how the reduction of global CO abundance of about 20% results in higher CH₄ oxidation and shorter CH₄ lifetimes (by around 8%). As a direct feedback, there is an increase in the chemical production of CO. We will first present global and annual tropospheric integrated statistics (Figure 1), then, we will zoom in on the tropical region where most of the CH₄ oxidation occurs.

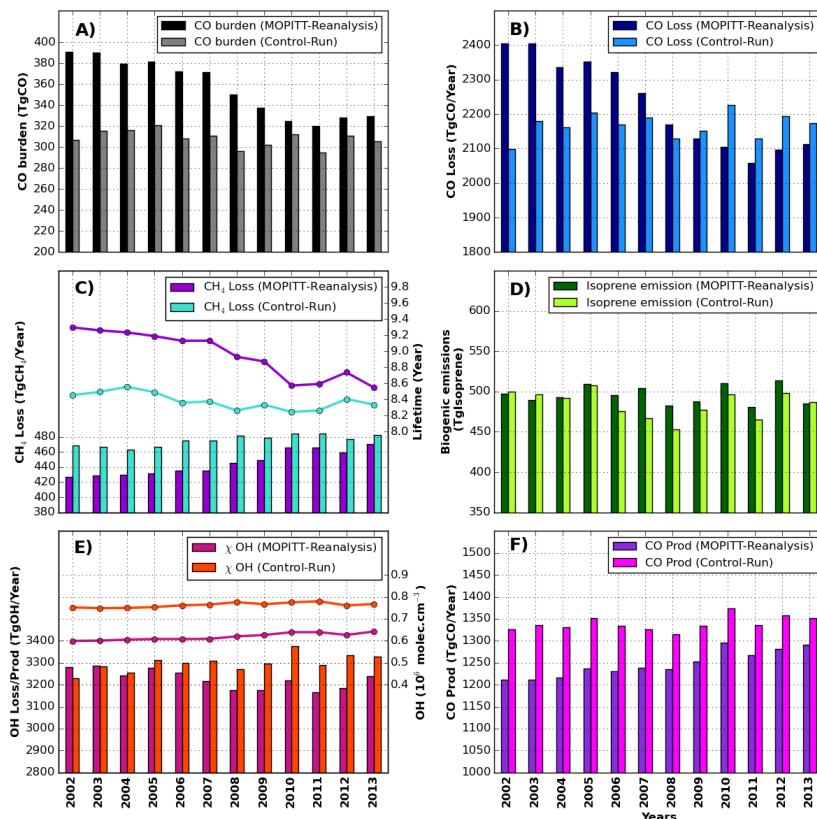


Figure 1. Global, annual and tropospheric integrated CO burden (a, TgCO), CO chemical loss (b, TgCO.yr⁻¹), CH₄ loss (c, TgCH₄.yr⁻¹), Isoprene emissions (d, TgIsoprene.yr⁻¹), OH chemical loss/Production (TgOH.yr⁻¹) and CO chemical production (TgCO.yr⁻¹). The CH₄ lifetime (with regards to OH) is shown on panel D and the airmass-weighted tropospheric mean OH is also plotted on panel E.

NOAA GMD's Global Greenhouse Gas Reference Network Management, Logistics, and Importance

E. Moglia^{1,2}, M.J. Crotwell^{1,2}, E.J. Dlugokencky², P.M. Lang², D. Neff^{1,2} and S. Wolter^{1,2}

¹Cooperative Institute for Research in Environmental Sciences (CIRES), University of Colorado, Boulder, CO 80309; 3034973988, E-mail: eric.moglia@noaa.gov

²NOAA Earth System Research Laboratory, Global Monitoring Division (GMD), Boulder, CO 80305

Beginning in 1967, the NOAA Carbon Cycle Greenhouse Gases (CCGG) group's Greenhouse Gas Reference Network (Figure 1) has provided spatially- and temporally-consistent data for use by scientists, modelers, and organizations around the world. The network focuses on the collection and analysis of background air samples for carbon dioxide (CO₂), methane (CH₄), nitrous oxide, sulfur hexafluoride, carbon monoxide, stable isotopes of CO₂ and CH₄, and volatile organic compounds. Air samples are collected in 2.5 L glass flasks at surface sites and in 0.7 L glass flasks contained in Programmable Flask Packages at aircraft and tall tower network locations.

This extensive global network requires meticulous group oversight including daily preparation and logistical planning, equipment management, quality control, and ongoing international communication. The majority of these daily operations occur in the Flask Logistics Lab. It is here that equipment is prepared for the field and where all of the ~16,000 yearly flask-air samples are received, cataloged, and routed to various analysis laboratories. This presentation will discuss the importance of the network, daily management operations, and logistics.

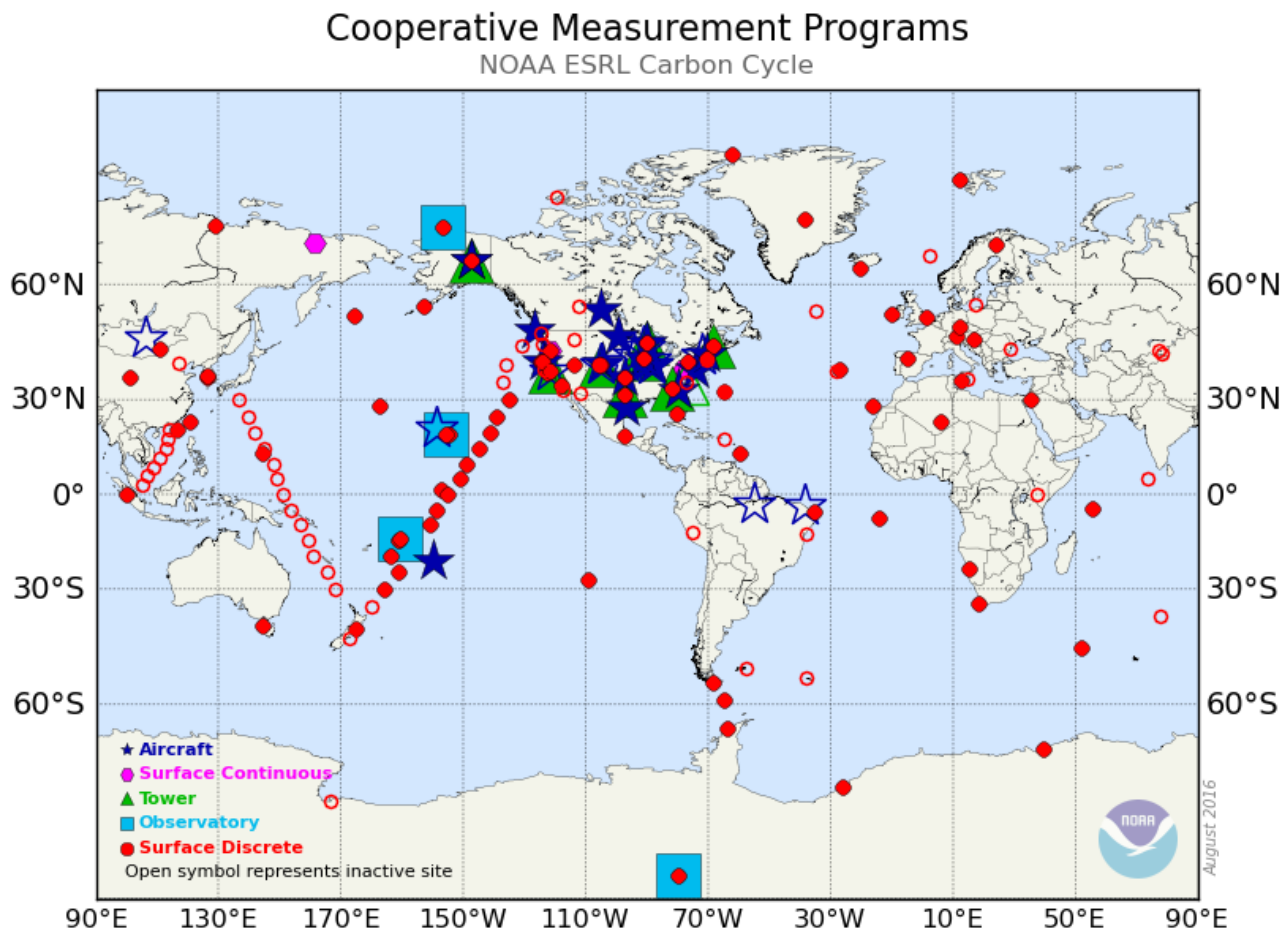


Figure 1. NOAA/ESRL/GMD Global Greenhouse Gas Reference Network site locations including discrete surface network, aircraft network, tall tower network, and observatory sites.

NOAA Flask Measurements of Greenhouse and Trace Gases during the ACT-America Campaign

B. Baier^{1,2}, Y. Choi³, K. Davis⁴, J. DiGangi³, A. Fried⁵, P. Lang², B.R. Miller^{1,2}, T. Newberger^{1,2}, J. Nowak³, S. Pal⁴, C. Sweeney^{1,2}, M.J. Croswell^{1,2}, J. Higgs² and E. Moglia^{1,2}

¹Cooperative Institute for Research in Environmental Sciences (CIRES), University of Colorado, Boulder, CO 80309; 303-497-5769, E-mail: bianca.baier@noaa.gov

²NOAA Earth System Research Laboratory, Global Monitoring Division (GMD), Boulder, CO 80305

³NASA Langley Research Center, Hampton, VA 23681

⁴The Pennsylvania State University, Department of Meteorology, University Park, PA 16802

⁵Institute of Arctic and Alpine Research (INSTAAR), University of Colorado, Boulder, CO 80309

The Atmospheric Carbon and Transport – America (ACT-America) mission studies the transport of atmospheric carbon dioxide (CO₂) and methane (CH₄) in order to reduce uncertainty associated with regional-scale transport and fluxes of carbon in atmospheric inversion models. A series of five, six-week flight campaigns will be conducted over four seasons in three regions of the United States to capture a wide range of ecosystems, carbon sources and sinks, and seasonally-varying weather patterns. NOAA flask measurements of greenhouse and other trace gas species, along with isotopic ratios of CO₂ and CH₄, can help to distinguish regional carbon sources and sinks. We present a brief overview of preliminary observations during the first two summer and winter ACT-America campaigns, along with analyses of regional source/sink tracers to help explain observed CO₂ and CH₄ enhancements.

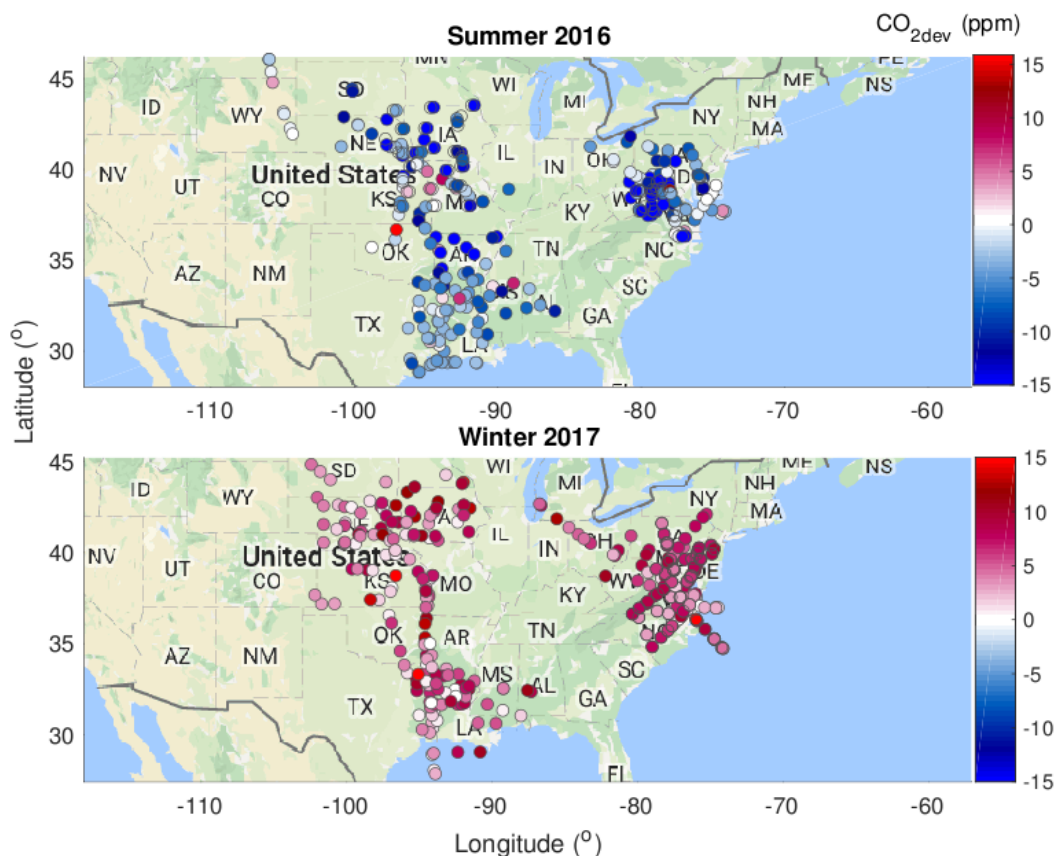


Figure 1. Deviation of NOAA flask CO₂ relative to Mauna Loa background CO₂ levels for the three regions of the ACT-America domain. Top: CO₂ deviation from background levels during summer 2016. Bottom: CO₂ deviation from background levels during winter 2017.

Application of Observations from the Summer 2016 ACT-America Campaign to Constrain Modeled Regional CO₂ Concentrations and Fluxes

B. Gaudet¹, K.J. Davis¹, T. Lauvaux¹, S. Feng¹, S. Pal¹, A. Jacobson^{2,3} and J. DiGangi⁴

¹The Pennsylvania State University, Department of Meteorology, University Park, PA 16802; 814-867-2110, E-mail: bjg20@psu.edu

²Cooperative Institute for Research in Environmental Sciences (CIRES), University of Colorado, Boulder, CO 80309

³NOAA Earth System Research Laboratory, Global Monitoring Division (GMD), Boulder, CO 80305

⁴NASA Langley Research Center, Hampton, VA 23681

While observational constraints on greenhouse gas (GHG) fluxes exist on the local scale (via eddy-covariance flux towers) and the global scale (via remote-site concentration measurements and the conservation of mass), regional-scale observational constraints are relatively deficient. One of the primary goals of the Atmospheric Carbon and Transport – America (ACT-America) project is to increase the understanding of regional-scale GHG fluxes through the use of aircraft, tower and satellite-based measurements over three focus regions (Mid-Atlantic, Midwest and Gulf Coast) during all four seasons. Two airborne platforms, a C-130 Hercules and a B-200 King Air, are equipped with various instruments that sample GHGs as well as other trace gases and meteorological variables. Flight patterns sample the atmosphere at multiple levels (from a few hundred to 8000 meters AGL) that encompass significant portions of weather systems. One flight pattern type focuses on fair-weather conditions with the intent of improving our understanding of seasonal-scale GHG fluxes over spatial scales of order 10⁵ km². A second pattern type samples gradients associated with mid-latitude storm systems.

Here we will compare carbon dioxide (CO₂) concentration observations from the summer 2016 ACT-America campaign to those produced by the CarbonTracker (CT) atmospheric CO₂ inversion system in order to: 1) evaluate the accuracy of the modeled concentrations at various spatial scales; and 2) where practical from the meteorology, infer the accuracy of regional-scale CO₂ flux estimates. We make use of the CarbonTracker Near-Realtime (CT-NRT) product, which uses priors derived from the optimized fluxes of regular CT along with provisional observations to reduce the time required to produce an analysis.

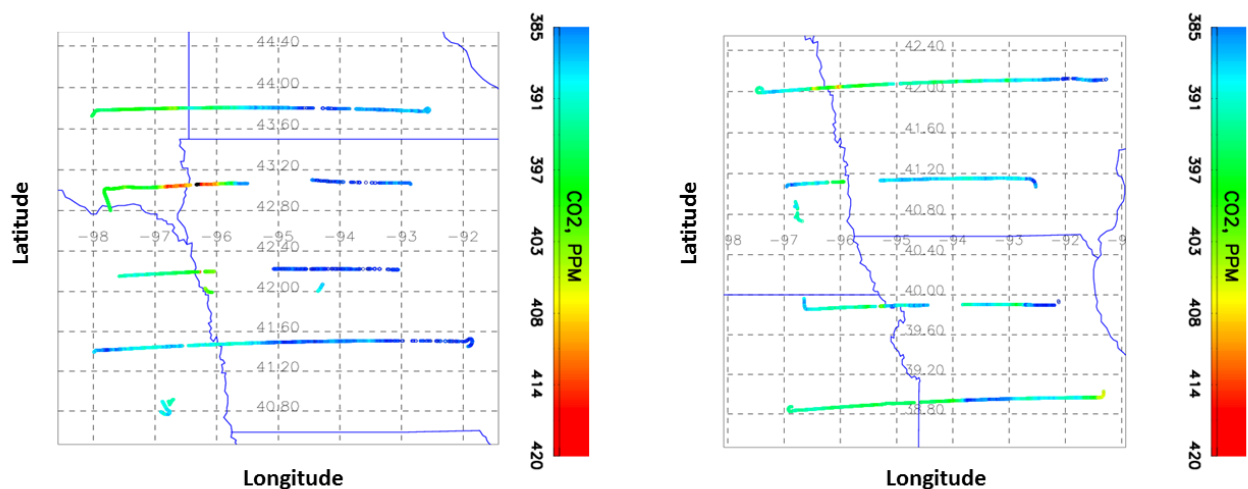


Figure 1. Observed atmospheric boundary layer CO₂ concentrations for both the C-130 and B-200 aircraft for the fair weather cases of 13 Aug 2016 (left panel), and 14 Aug 2016 (right panel).

Comparing Atmospheric CO₂ Measurements from Two Instruments at Baring Head, New Zealand

S. Nichol and G. Brailsford

National Institute of Water and Atmospheric Research (NIWA), Wellington, New Zealand; +64-4-3860396,
E-mail: sylvia.nichol@niwa.co.nz

Measurements of atmospheric carbon dioxide (CO₂) began at Baring Head (41.41° S, 174.87° E) in 1972. From 1986 to December 2016 these measurements were made with a non-dispersive infra-red analyser: the Siemens Ultramat 3. The CO₂ measurements are now made with a Picarro cavity ring down spectrometer. The Picarro ran in parallel with the Siemens from 2011. The Picarro has some advantages over the Siemens: it measures over a wider concentration range, uses less gas, is more stable, is more linear, and also measures CH₄ and H₂O. This paper compares CO₂ measurements made at Baring Head with the Siemens and the Picarro from 2014 to 2016. Eight CCL calibration gases are used in the measuring system as long-term transfer standards to provide a link to the WMO mole fraction scale. The offsets between the Picarro average measured value and the assigned value for each CCL tank lies in the range 0.02 to 0.07 ppm (Figure 1), which is close to the GAW compatibility goal of 0.05 ppm for southern hemisphere stations. The Siemens offsets for six of the CCL tanks (381 to 401 ppm) range from 0.02 to 0.07 ppm, but the values for the 372 ppm and 410 ppm tanks are well outside this range (Figure 1). During steady period events the air arriving at Baring Head has very low CO₂ variability, making these events ideal for comparing the final processed air values from each instrument. A steady interval occurs when the standard deviation of measured values from a single inlet line over a six-hour interval is 0.1 ppm or less. Overlapping “intervals” of steady data are then combined to form steady “periods”. Between 2014 and 2016 the Siemens and the Picarro both measured a steady period at the same time on 82 occasions. For these steady periods, which vary in length from 6 hours to 3 days, the average difference between the two instruments is 0.045 ppm (Figure 2).

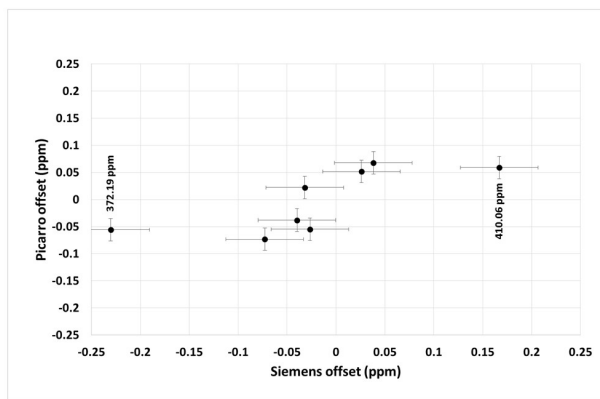


Figure 1. Differences between the average measured values for the CCL tanks and the CCL assigned value. The error bars are the standard deviation.

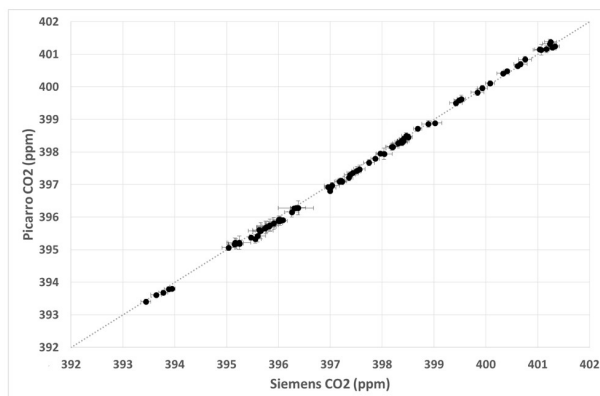


Figure 2. Siemens and Picarro measured CO₂ values for steady period air.

Introduction of the NIMS Activities on a Carbon Cycle Study

T. Goo¹, M. Sun¹, Y. Oh¹, S.T. Kenea¹, G. Kim¹, V.A. Velazco², D.W.T. Griffith², J. Rhee¹ and Y. Byun¹

¹National Institute of Meteorological Sciences, Seogwipo-si, Jeju-do, South Korea; +82-64-780-6653, E-mail: gooty@korea.kr

²University of Wollongong, Wollongong, Australia

The National Institute of Meteorological Sciences (NIMS) has made effort to describe the feature of carbon cycle by means of various kinds of measurements and numerical simulation. In particular, the NIMS has operated a regional Global Atmosphere Watch (GAW) station as well as a designated operational station of Total Carbon Column Observing Network (TCCON) at Anmyeondo, Korea. Total column abundances of carbon dioxide (CO₂) and methane (CH₄) during 2015 are estimated by using GGG v14 and compared with ground-based *in situ* CO₂ and CH₄ measurements at the height of 86 m above sea level. The seasonality of CO₂ is well-captured by both Fourier Transform Spectrometer (FTS) and *in situ* measurements while there is considerable difference on the amplitude of CO₂ seasonal variation due to the insensitivity of column CO₂ to the surface carbon cycle dynamics in nature as well as anthropogenic sources. In addition, the NIMS has a plan for regular CO₂ profile observations by aircraft. The Cavity Ring-Down Spectroscopy (CRDS) analyzer will be used to measure CO₂, CH₄, carbon monoxide (CO) and water vapor (H₂O) up to 5 km once or twice a month. It is expected that the aircraft-based profiling measurements will be used to validate remotely-based column measurement. CO₂ measurements from the various observing instruments are also compared with simulated CO₂ from the CarbonTracker-Asia. Although the feature of CO₂ seasonality is well-captured by both measurement and simulation, the CO₂ amplitudes of pick to pick are considerably different in time and space.



Figure 1. World Meteorological Organization (WMO) regional Global Atmosphere Watch (GAW) station at Anmyeondo, Korea.

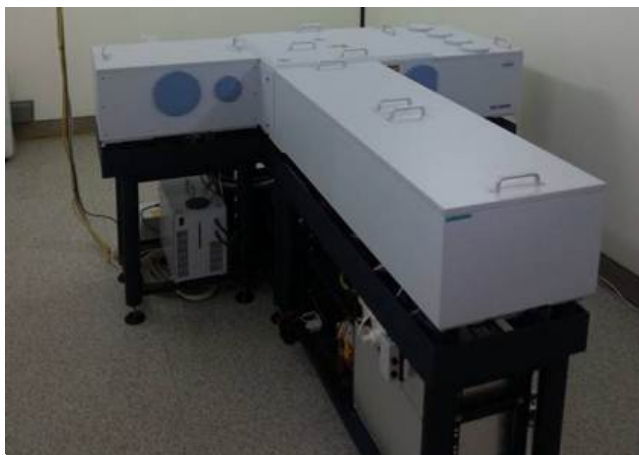


Figure 2. Ground-based Fourier Transform Spectrometer (FTS) at Anmyeondo site of Total Carbon Column Observing Network (TCCON).

A Study of Diurnal and Seasonal Variations of Carbon Dioxide and Methane in the Eastern Highland Rim Region of Tennessee

W.K. Gichuhi and L. Gamage

Tennessee Technological University, Cookeville, TN 38505; 931-372-3499, E-mail: wgichuhi@tntech.edu

Located on the eastern side of the geographically-diverse Highland Rim in Tennessee, the city of Cookeville (36.1628° N, 85.5016° W) has a slightly higher elevation than the surrounding major towns of Nashville and Knoxville, presenting an ideal location for ground-based atmospheric measurements carbon dioxide (CO₂) and methane (CH₄). In this study measurements of CO₂ and CH₄ are made using a Picarro Cavity Ring-Down Spectrometer (CRDS) to gain insights into the atmospheric dynamics contributing to the local and regional methane and carbon cycle within the Eastern Highland Rim region, using Cookeville as a study site. Beginning the summer of 2016 through March 2017, measurements reveal a remarkable seasonal and diurnal variation of CH₄ and CO₂. In a period of one week during the summer of 2016, the respective atmospheric dry molar fractions of CO₂ and CH₄ as measured by the CRDS analyzer were: 400.85 ± 1.67 ppm, and 1.908 ± 0.030 ppb. An increase in the dry mole fractions of the two greenhouse gases was observed during the winter of 2017 where 414.29 ± 1.68 ppm and 2.049 ± 0.026 ppb of CO₂ and CH₄ were recorded in January 2017, respectively. A typical 24-hour continuous monitoring of CO₂ and CH₄ at a height of ~45 m above the ground indicates that the concentration levels increase during night times compared to day times. During the warm, sunny summer months, the presence of sunlight typically decreases the levels of CO₂ as photosynthesis removes CO₂ from the air. At night, the CO₂ levels rises as the plants give off CO₂ during respiration. In the winter months, this daily CO₂ cycle is not as eminent because of the decreased green vegetation in the Cookeville area.

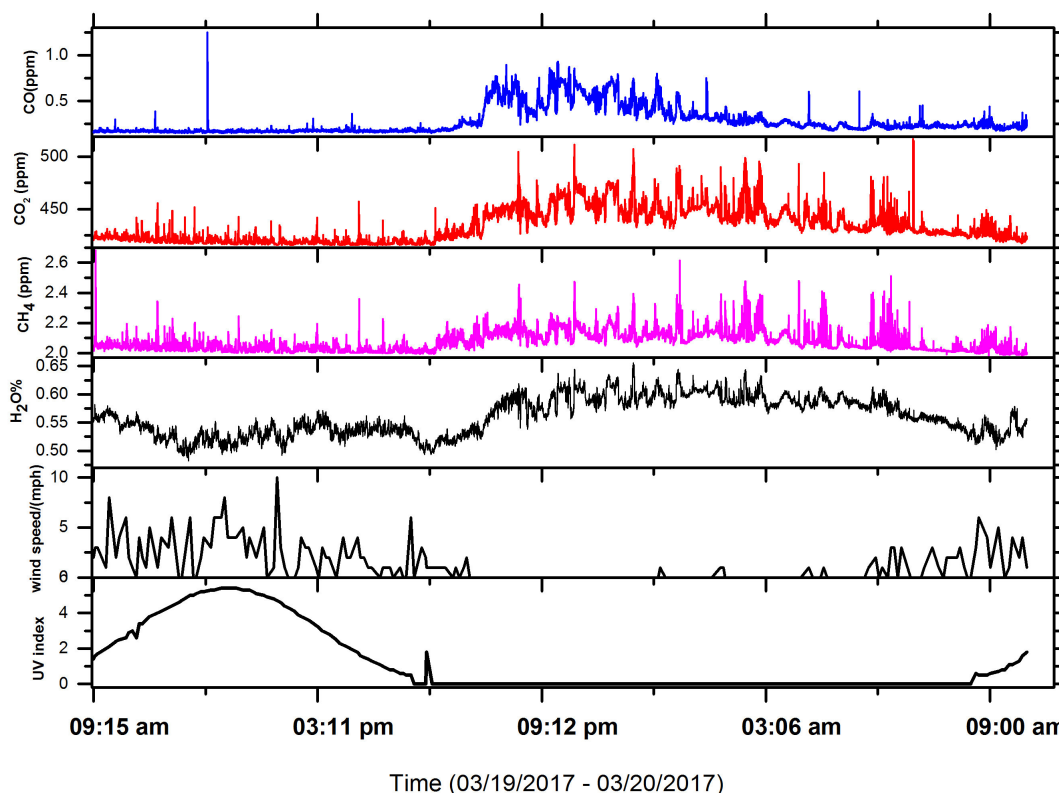


Figure 1. Typical daytime and nighttime CO, CO₂, CH₄, and water vapor dry air mixing ratios in Cookeville, Tennessee during the month of March 2017 as measured using Picarro Cavity-Ring-down Spectrometer accompanied by the corresponding wind speed and UV index.

Can We Detect the Conversion of the Harding Street Power Plant in Indianapolis from Coal to Natural Gas Using Tower-based CO₂ Mole Fraction Data Alone?

N. Balashov, K.J. Davis, N. Miles, S. Richardson and T. Lauvaux

The Pennsylvania State University, Department of Meteorology, University Park, PA 16802; 814-777-3861, E-mail: nvb5011@psu.edu

The atmospheric-based top-down method of determining greenhouse gas emissions is complementary to inventories, allowing an independent assessment of emissions and the ability to quickly detect temporal changes in emissions. Long-term monitoring of urban emissions has typically been focused on areal emission, not point sources, but point sources can be a large fraction of urban emissions. We use carbon dioxide (CO₂) mole fraction data measured on towers in and surrounding Indianapolis as part of the INFLUX project to demonstrate the ability to quantify point source emissions, and their changes. The Harding Street Power Plant in downtown Indianapolis, like many power plants across the country, was recently converted from coal to natural gas, with the conversion being completed in March 2016. The Harding Street Power Plant is in the southwest quadrant of downtown, 6 km to the west of INFLUX Tower 10. Analysis of modeled CO₂ indicates that prior to the conversion of the power plant from coal to natural gas, 47% of the CO₂ mole fraction enhancement at Tower 10 was attributable to the electricity production sector. Emissions from the power plant should drop by roughly a factor of two given the conversion to natural gas. In Figure 1, probability distribution functions of Tower 10 afternoon CO₂ enhancement compared to the background Tower 1 indicate a significant decrease in the enhancements in 2016-2017 dormant time frame (Mar., Nov.-Feb.) compared to previous equivalent time periods, when the winds are from the west. Relatively little change from year to year is found when the winds are from the other directions. We also present progress toward quantifying emissions using plume dispersion modeling by evaluating plume events before and after the conversion as a function of atmospheric stability.

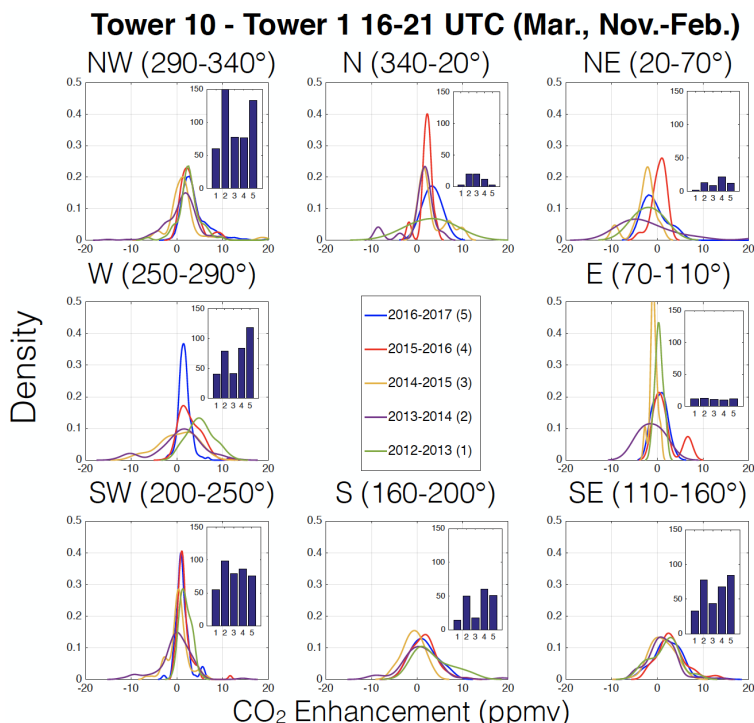


Figure 1. Probability distribution functions of afternoon CO₂ enhancement, segregated into wind direction sectors for the dormant season (Mar., Nov.-Feb.) of each of five time frames. Here CO₂ enhancement is defined as the difference between the CO₂ measured at the predominantly downwind Tower 10 and that measured at the predominantly background Tower 1. The inset plots show the sample size of hourly differences for each time frame. The time frame represented by a number from 1-5 is indicated in the legend.

The Role of Horizontal Grid Spacing on Transport and Mixing of Passive Tracers over Complex Terrain

G. Duine and S.F.J. De Wekker

University of Virginia, Charlottesville, VA 22904; 434-227-0151, E-mail: gd6s@virginia.edu

Both observations and high-resolution modeling have shown that the planetary boundary layer (PBL) depth varies considerably over complex terrain. Currently, regional-to-continental scale carbon dioxide (CO₂) budgets are estimated using coarse global models that have horizontal grid spacings on the order of 50-100 km. Such models lack terrain variability, but a correct simulation of the PBL is crucial for accurate estimates of CO₂ budgets, especially because studies have indicated that a large part of the U.S. gross primary production of CO₂ is from mountainous regions. Duine and De Wekker (2017) showed that convective boundary layer (CBL) depths are overestimated in coarse grid domains over complex terrain (see Figure 1). This is a consequence of the terrain smoothing in the coarse grid, and the poor representation of physical and dynamical processes associated with mountainous terrain. In this poster, we investigate in detail how differences in the representation of physical and dynamical processes in atmospheric models with different horizontal grid spacings affect the mixing transport of passive tracers over complex terrain. In addition, we investigate how these differences may impact the estimation of CO₂ budgets. We use the Weather Research & Forecasting (WRF) model in quasi-idealized simulation settings with prescribed CO₂ surface fluxes. By changing systematically the horizontal grid spacing in terrain with varying complexities, we are able to investigate the relative importance of various physical and dynamical processes in the simulation of carbon budgets in complex terrain. A better understanding and representation of these processes in coarse atmospheric models would lead to an improved quantification of North American and global carbon sources and sinks.

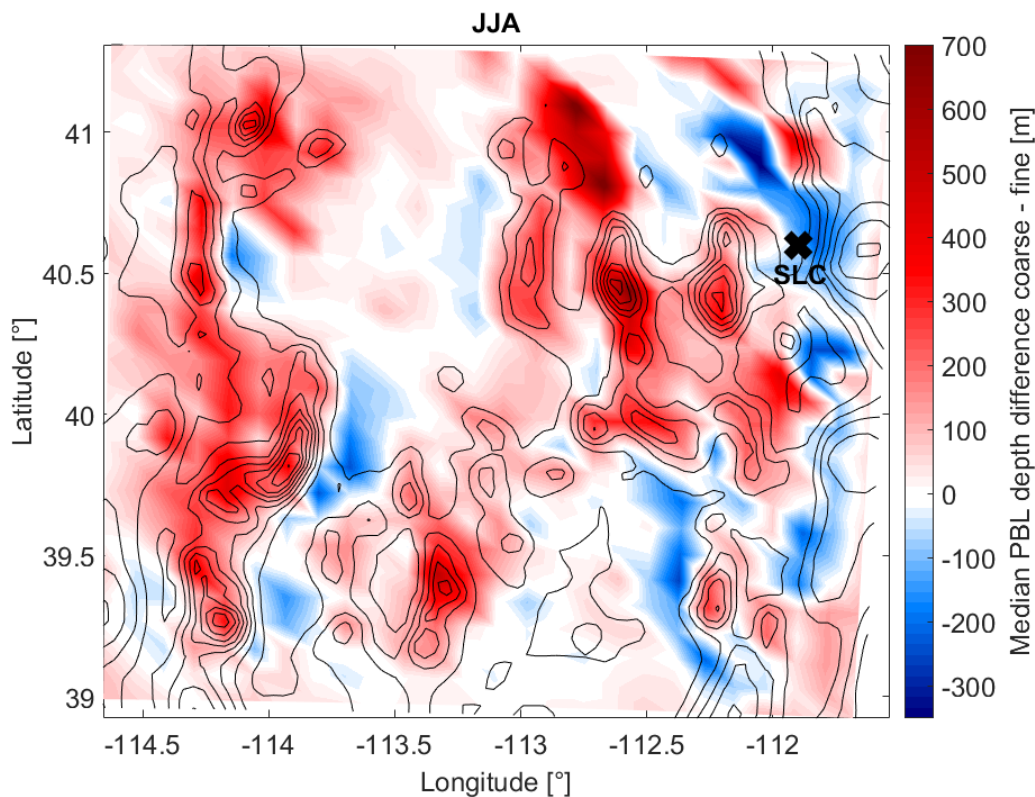


Figure 1. The differences in PBL depths (colors) between simulations with horizontal grid spacings of 10 km (coarse grid) and 3.3 km (fine grid) for Utah and the period of July 2012 – June 2014, summer months only, on top of the fine grid domain terrain elevation (contours). The ‘x’ denotes the location of Salt Lake City (SLC). Adopted from Duine and De Wekker (2017), under review.

Evaluation of the Carbon Cycle in the CMIP5 Earth System Model ESM2G

M. Leonard^{1,2}

¹Science and Technology Corporation, Boulder, CO 80305; 303-497-6823, E-mail: mark.leonard@noaa.gov

²NOAA Earth System Research Laboratory, Global Monitoring Division (GMD), Boulder, CO 80305

Understanding potential carbon cycle climate feedbacks is essential, however future simulations are extremely uncertain. Coupled climate-carbon cycle models project an additional rise in carbon dioxide (CO₂) by year 2100 of between 20 to 200 parts per million (ppm) due to carbon cycle feedbacks. The higher end of this range could have significant additional impacts on global climate. This paper demonstrates methods to improve coupled climate-carbon cycle models by evaluating the models based on NOAA's indispensable and multi-decadal data record. We will focus on the coupled climate-carbon model GFDL ESM2G that is a possible prior flux model for the future NOAA Earth System Analyzer (ESA). The NOAA ESA will be a diagnostic carbon cycle model that will quantify the carbon budget over recent decades covered by the NOAA observational record. Such a model will help improve coupled climate-carbon models by improving their ability to simulate the recent past. This paper investigates global to regional scaled comparisons of the coupled climate-carbon model GFDL ESM2G using two types of data-constrained models: CarbonTracker and SiBCASA-GFED. The former is constrained by atmospheric observations, while the later is constrained by space-based estimates of photosynthesis unlike the GFDL ESM2G, which is purely predictive. We will discuss in detail the following: an early growth seasons in the northern boreal regions, an inverse annual cycle around the Indian and Southern Ocean, and an overestimation of Gross Primary Production in regions near the Inter Tropical Convergence Zone. We present ideas for improving future versions of GFDL ESM2G applicable for other coupled climate-carbon models.

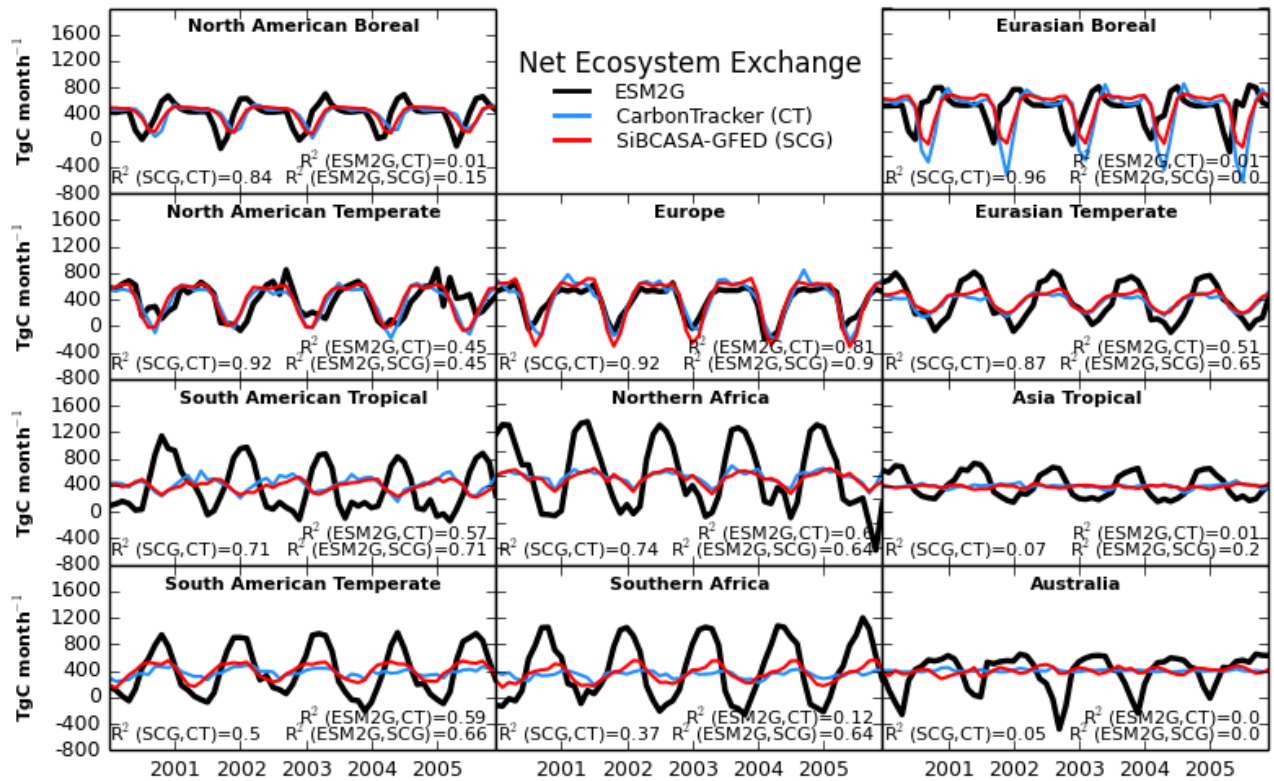


Figure 1. Regional monthly means of net ecosystem exchange of carbon from land fluxes to the atmosphere from years 2001-2005.

The Estimation of CO₂ Fluxes with a Coupled Meteorological and Tracer Transport Model

V. Khade¹, S. Polavarapu², M. Neish², P. Houtekamer² and D. Jones^{1,3}

¹University of Toronto, Department of Physics, Toronto, Ontario, Canada; 416-978-2936, E-mail: vikram.khade@utoronto.ca

²Environment and Climate Change Canada, Toronto, Ontario M3H 5T4, Canada

³Joint Institute for Regional Earth System Science and Engineering (JIFRESSE), UCLA, Los Angeles, CA 90095

An important component of transport model error that is neglected in typical flux inversion systems is due to uncertain wind fields. However with a coupled meteorological and tracer transport model, this component of model error can be accounted for. In this work, we use an operational weather forecast model with coupled greenhouse gas transport as the basis for an ensemble Kalman Filter (EnKF) assimilation system in order to directly simulate all the sources of error: initial states of constituents, meteorological states, fluxes, model formulation and observations. The model is based on the Canadian Global Environmental Multi-scale - Modelling Air quality and Chemistry (GEM-MACH) model with a grid of 400x200 with 74 vertical levels and includes extensions for carbon dioxide (CO₂) simulation (Polavarapu et. al. 2016).

In this work, progress on the adaptation of the EnKF (Houtekamer et. al. 2014) for CO₂ assimilation is reported. The variable localization of Kang et al. (2011) was implemented and simulated flask, tower and aircraft observations of CO₂ are ingested. The meteorological state is constrained with conventional observations and an ensemble size of 64 members is used. Observing System Simulation Experiments (OSSEs) are performed with simulated CO₂ observations in order to determine whether, in the ideal case, true fluxes can be recovered. The OSSEs are also used to tune key parameters of the assimilation system such as localization radius for the CO₂ state and its fluxes as well as inflation factors. In particular, we determine the dependence of localization radius for CO₂ and flux covariances on observation density.

The observations are assimilated every 6 hours. The spread of 6 hours forecast CO₂ ensemble at a particular time is shown in figure 1.

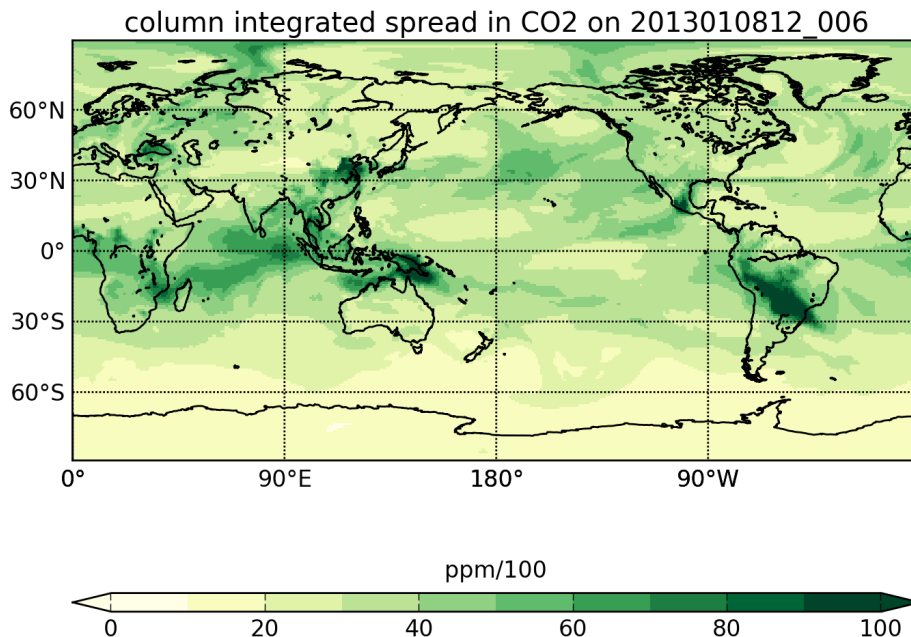


Figure 1. Spread of forecast CO₂ estimated by standard deviation after 48 cycles.

Towards a Novel Integrated Approach for Estimating Greenhouse Gas Emissions in Support of International Agreements

S. Reimann¹, M.K. Vollmer¹, A. Manning², P. deCola³, O. Tarasova⁴ and D. Brunner¹

¹Swiss Federal Laboratories for Materials Science and Technology, Empa, Dübendorf, Switzerland; +41587654638, E-mail: stefan.reimann@empa.ch

²UK Meteorological Office, Exeter, United Kingdom

³Sigma Space Corporation, Lanham, MD 20706

⁴World Meteorological Organisation, Geneva, Switzerland

In the Paris Agreement the community of signatory states has agreed to limit the future global temperature increase compared to pre-industrial times to a maximum of +2.0 °C. To achieve this goal, emission reduction targets have been submitted by individual nations (called Nationally Determined Contributions, NDCs). Inventories will be used for checking progress towards these envisaged goals. These inventories are calculated by combining information on specific activities (e.g. passenger cars, agriculture) with activity-related, typically IPCC-sanctioned, emission factors – the so-called bottom-up method. These calculated emissions are reported on an annual basis and are checked by external bodies by using the identical method.

As second, independent method emissions can be estimated by translating greenhouse gas measurements made at regionally representative stations into regional/global emissions using meteorologically-based transport models. In recent years this so-called top-down approach has been substantially advanced into a powerful tool and emission estimates at the national/regional level have become possible. This method is already used in Switzerland, in the United Kingdom and in Australia to estimate greenhouse gas emissions and independently support the national bottom-up emission inventories within the UNFCCC framework. Figure 1 shows a comparison between emissions of HFC-125 from the Swiss greenhouse gas inventory and from a measurement-based method. Examples of the comparison of the two independent methods will be presented and the added-value will be discussed.

The World Meteorological Organization and partner organizations are currently developing a plan to expand this top-down approach and to expand the globally representative Global Atmospheric Watch (GAW) network of ground-based stations and remote-sensing platforms and integrate their information with atmospheric transport models. This Integrated Global Greenhouse Gas Information System (IG³IS) initiative will help nations to improve the accuracy of their country-based emissions inventories and their ability to evaluate the success of emission reductions strategies. This could foster trans-national collaboration on methodologies for estimation of emissions. Furthermore, real-world information on emissions will build up trust between different countries.

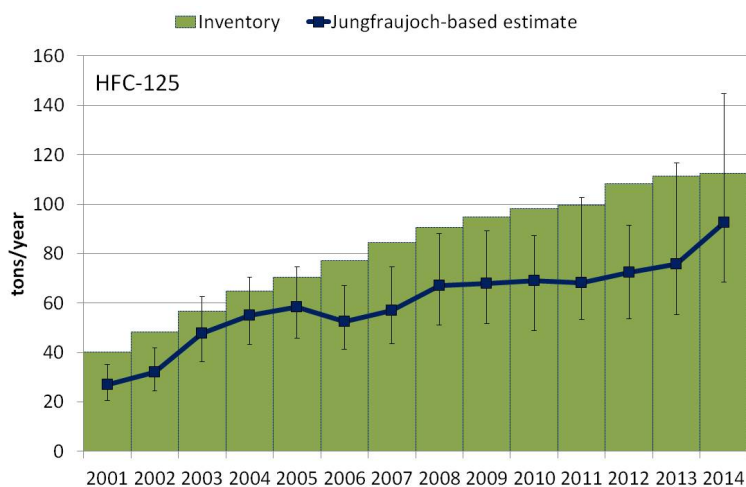


Figure 1. Comparison between emissions of HFC-125 from the Swiss greenhouse gas inventory and from a measurement-based inversion method, using data from Jungfraujoch in conjunction with meteorological transport models.

Quantification of NO_y and CO Emissions from Washington, D.C.-Baltimore during the WINTER Campaign

O.E. Salmon¹, P.B. Shepson², X. Ren^{3,4}, R.R. Dickerson³, B.H. Stirm⁵, S.S. Brown⁶, D.L. Fibiger^{7,6} and E. McDuffie^{7,6}

¹Purdue University, Department of Chemistry, West Lafayette, IN 47907; 920-366-5276, E-mail: osalmon@purdue.edu

²Purdue University, Department of Earth, Atmospheric, and Planetary Sciences, West Lafayette, IN 47907

³University of Maryland, Department of Oceanic and Atmospheric Science, College Park, MD 20742

⁴NOAA Air Resources Laboratory (ARL), Silver Spring, MD 20910

⁵Purdue University, Department of Aviation Technology, West Lafayette, IN 47907

⁶NOAA Earth System Research Laboratory, Chemical Sciences Division (CSD), Boulder, CO 80305

⁷Cooperative Institute for Research in Environmental Sciences (CIRES), University of Colorado, Boulder, CO 80309

Regulations to limit surface-level ozone have successfully targeted emissions of carbon monoxide (CO) and nitrogen oxides (NO_x = NO + NO₂) from combustion sources. Bottom-up inventories are updated periodically to reflect reductions in emissions. However, because emissions of CO and NO_x are highly dependent on equipment age, type, and operating conditions, inventories must be sophisticated to accurately estimate emissions. Similarly, estimating top-down NO_x emissions can be complicated as NO_x readily partitions to other reactive nitrogen species (NO_y; total reactive nitrogen). The Wintertime INvestigation of Transport, Emissions, and Reactivity (WINTER) campaign, conducted in the northeastern U.S. in 2015, investigated NO_y chemistry and transport unique to the cold season.

Airborne mass balance flights conducted around Washington, D.C.-Baltimore allow for the determination of the urban area's NO_y and CO emission rates by calculating the product of the perpendicular wind speed and the downwind enhancement in NO_y and CO, respectively. Here we compare our top-down NO_y and CO emission rate estimates to inventory estimates. Preliminary analyses suggest agreement between top-down and bottom-up NO_y emissions estimates, while our CO emissions estimates are a factor of ~3 lower than inventory estimates. It is possible our preliminary results indicate improvements to the National Emissions Inventory are required to better estimate CO emissions, at least in some regions of the U.S.

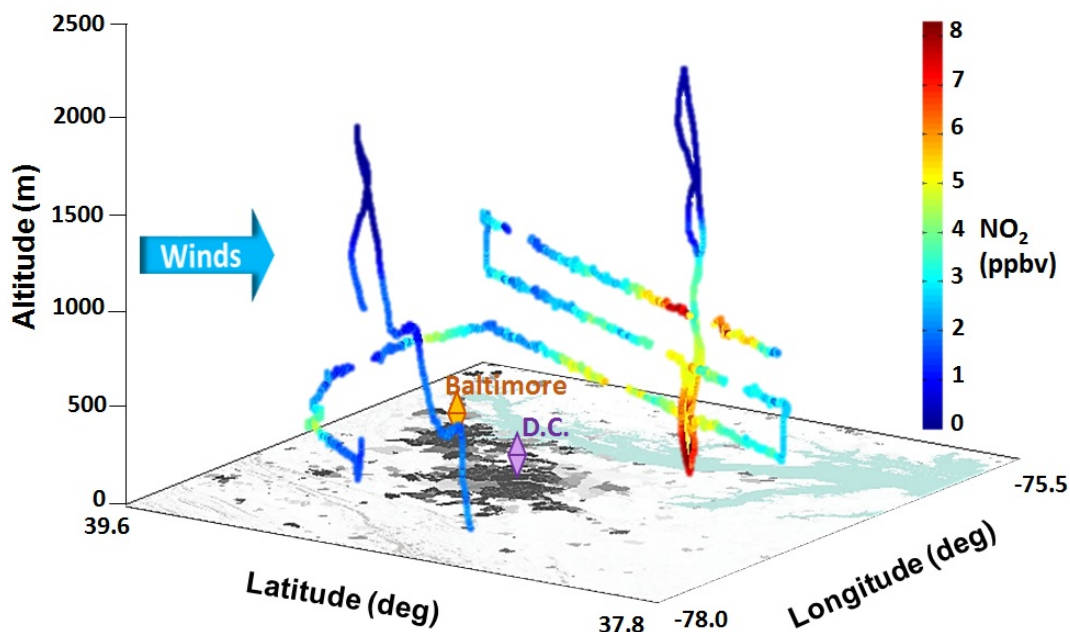


Figure 1. A mass balance flight path on February 27, 2015 around the Washington, D.C.-Baltimore area.

Analysis of Long-term Observations of NO_x and CO in Megacities and Application to Constraining Emissions Inventories

G. Frost¹, B. Hassler² and B. McDonald³

¹NOAA Earth System Research Laboratory, Chemical Sciences Division (CSD), Boulder, CO 80305; 303-497-7539, E-mail: gregory.j.frost@noaa.gov

²Bodeker Scientific, Alexandra, New Zealand

³Cooperative Institute for Research in Environmental Sciences (CIRES), University of Colorado, Boulder, CO 80309

Long-term atmospheric NO_x/carbon monoxide (CO) enhancement ratios in megacities provide evaluations of emission inventories. A fuel based emissions inventory approach that diverges from traditional bottom-up inventory methods explains 1970 – 2015 trends in NO_x/CO enhancement ratios in Los Angeles, CA. Combining this comparison with similar measurements in other U.S. cities demonstrates that motor vehicle emissions controls were largely responsible for U.S. urban NO_x/CO trends in the past half-century. Differing NO_x/CO enhancement ratio trends in U.S. and European cities over the past 25 years highlight alternative strategies for mitigating transportation emissions, reflecting Europe’s increased use of light-duty diesel vehicles and correspondingly slower decreases in NO_x emissions compared to the U.S. A global inventory widely used by chemistry-climate models fails to capture long-term trends and regional differences in U.S. and Europe megacity NO_x/CO enhancement ratios, possibly contributing to these models’ inability to accurately reproduce observed long-term changes in tropospheric ozone.

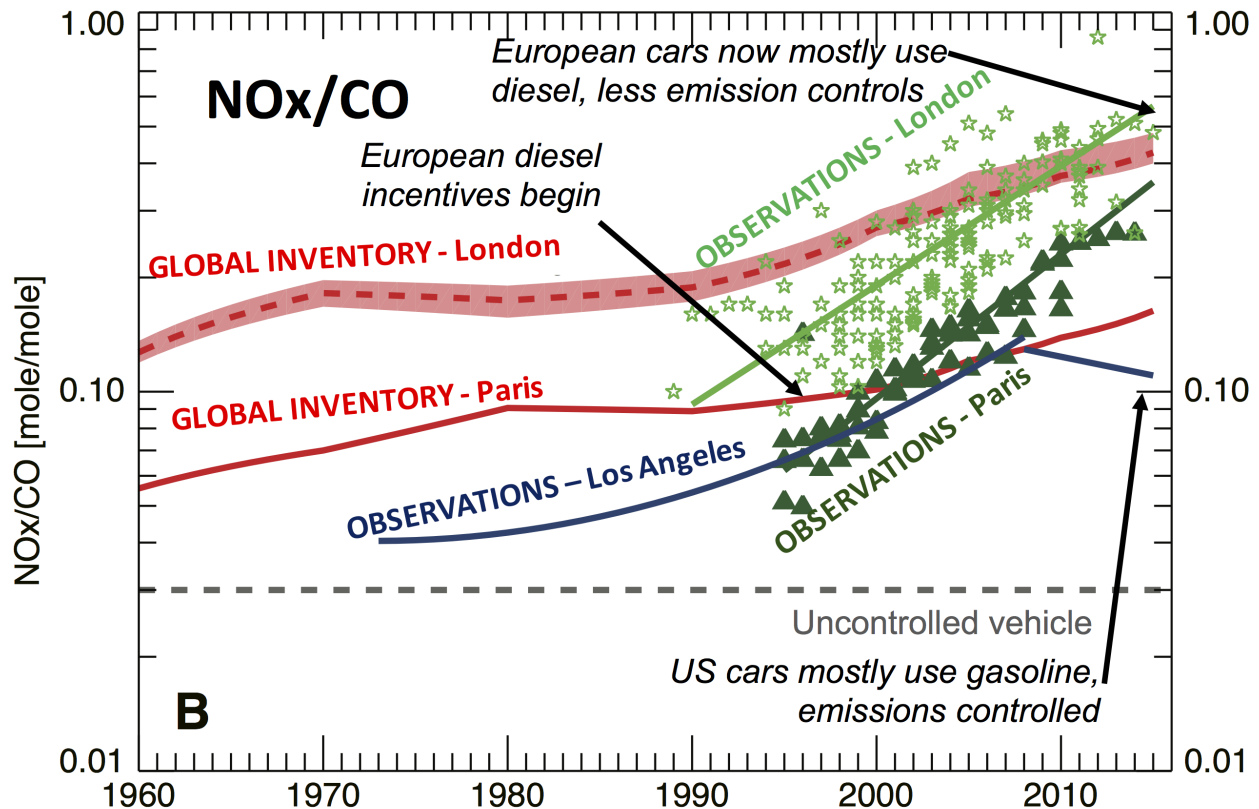


Figure 1. NO_x/CO enhancement ratios from roadside monitor measurements at air quality monitoring stations in Paris (dark green symbols) and London (light green stars), along with log-linear trends for the Paris (dark green line) and London (light green light) monitoring data. The trend for analogous Los Angeles air quality monitoring observations is shown for comparison (blue line). Also shown are the MACCity global inventory’s NO_x/CO emissions ratios for Paris (solid red line) and averaged for all London grid cells (dashed red line) and the range for individual London grid cells (red shading).

Increased Propane Emissions from the United States

L. Hu^{1,2}, S.A. Montzka², A.E. Andrews², J.B. Miller², S. Lehman³, B. Miller^{1,2}, C. Sweeney^{1,2}, D. Helmig³, E.J. Dlugokencky², J.W. Elkins² and P.P. Tans²

¹Cooperative Institute for Research in Environmental Sciences (CIRES), University of Colorado, Boulder, CO 80309; 303-497-5238, E-mail: lei.hu@noaa.gov

²NOAA Earth System Research Laboratory, Global Monitoring Division (GMD), Boulder, CO 80305

³Institute of Arctic and Alpine Research (INSTAAR), University of Colorado, Boulder, CO 80309

Propane (C_3H_8) is the second most abundant non-methane hydrocarbon in the atmosphere. It contributes to photochemical air pollution, including ozone and aerosol formation in the troposphere. It is also commonly used as a tracer for distinguishing fossil fuel emissions from natural and other anthropogenic emissions for methane. Global atmospheric observations of C_3H_8 suggest a recent reversal of its atmospheric trend, that is largely due to U.S. oil and natural gas production [Helmig *et al.*, 2016]. In this study, we analyzed atmospheric C_3H_8 data observed in the U.S. portion of NOAA's Global Greenhouse Gas Reference Network. We further estimated U.S. emissions of C_3H_8 using inverse modeling and a ^{14}C -tracer-ratio-based method. Inverse modeling results confirm an increase of U.S. C_3H_8 emissions from 2008 to 2014 that are primarily from oil and natural gas production regions (Fig. 1). The derived emission increase is comparable to the relative increase of U.S. C_3H_8 production over the same period. A preliminary estimate from a ^{14}C -tracer-ratio-based method for emissions during 2010 – 2012 is consistent with the inversions (within estimated uncertainty) (Fig. 1).

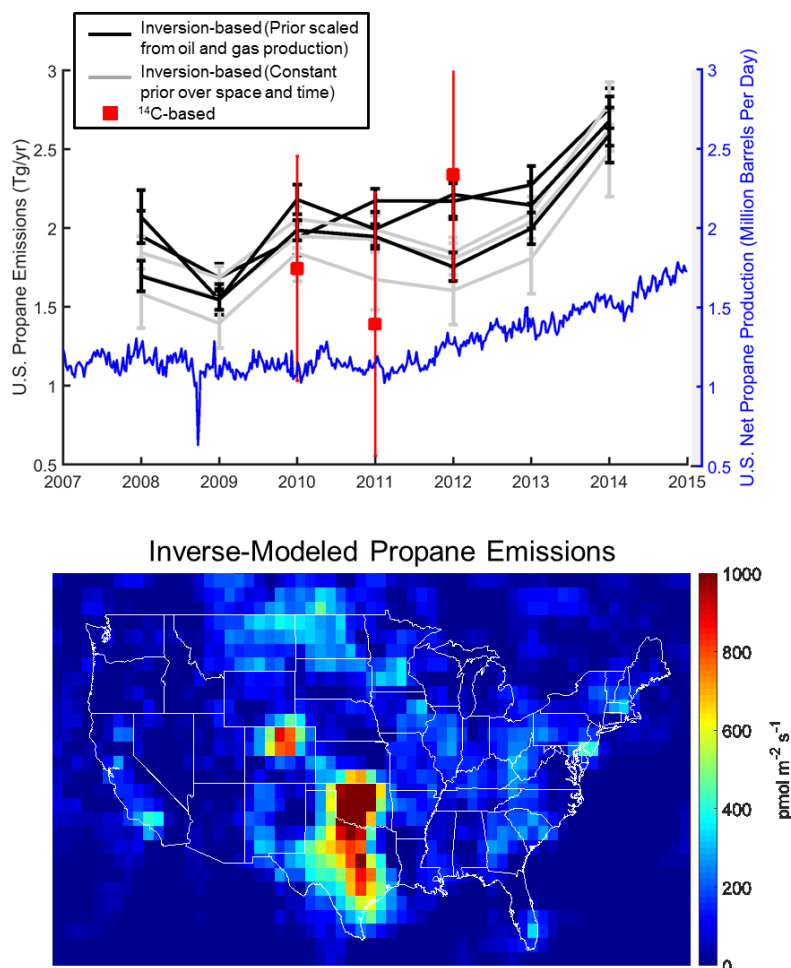


Figure 1. Derived U.S. emissions of propane. (Upper panel) Annual emissions derived from inverse modeling (black and gray lines) and a ^{14}C -based-tracer-ratio method (red squares). Blue line indicates U.S. production of propane reported by U.S. Energy Information Administration. (Lower panel) Average U.S. emissions between 2008 and 2014 derived from inverse modeling with a constant prior over space and time.

A Ten-Year (2006-2016) Record of Non-methane Hydrocarbons (NMHCs) in the Subtropical Marine Boundary Layer at the Cape Verde Atmospheric Observatory

S. Punjabi¹, K.A. Read^{2,1}, L.J. Carpenter¹, A.C. Lewis^{2,1}, J.R. Hopkins^{2,1} and L.N. Mendes³

¹University of York, Department of Chemistry, Wolfson Atmospheric Chemistry Laboratories (WACL), York, United Kingdom; +44-1904-324757, E-mail: shalini.punjabi@york.ac.uk

²University of York, National Centre for Atmospheric Science (NCAS), York, United Kingdom

³Instituto Nacional de Meteorologia e Geofísica (INMG), Mindelo, Republic of Cape Verde

Continuous and *in situ* hourly measurements of more than fifteen Volatile Organic Compounds (VOCs) have been made in the subtropical marine boundary layer at the Cape Verde Atmospheric Observatory (16° 51' N, 24° 52' W, 20m asl) in the east Atlantic Ocean. The observations began in October 2006 and continue today. Typical ambient mixing ratios range from as low as a few parts per trillion for reactive VOCs such as butane and toluene to a few parts per billion for the longest-lived species ethane. Light alkanes have showed well-defined seasonal cycles with winter maximum and summer minimum, consistent with the seasonal variation of the hydroxyl (OH) radical (Fig.1). Upwards trends in ethane and propane have been observed in recent years, consistent with other background locations in the Northern Hemisphere. Detection limits for the Gas Chromatography – Flame Ionisation Detection (GC-FID) system are below 5 ppt for most VOCs except for ethane and propane (around 7 ppt). In addition to using a certified multicomponent laboratory standard, real air monthly target gas measurements are also used to support quality assurance. Measurement uncertainties are below 10% for ethane and propane. The instrument is unusual in that it includes measurements of a small number of oxygenated compounds, although the calibration of these remains a challenge. Relative response factors for acetaldehyde, acetone and methanol have been estimated using two different methods; i) Teflon permeation tube calibration sources and ii) a National Physical Lab (NPL) 5 ppm gas standard in nitrogen. A good agreement has been seen between these two calibration approaches for acetaldehyde and acetone, but not for methanol. A lack of calibration consistency still limits the reporting of some OVOCs to GAW from this station. In addition to performing routine data and instrument checks, a set of additional post-analysis QA tools are now applied to all VOC data before submission to data repositories.

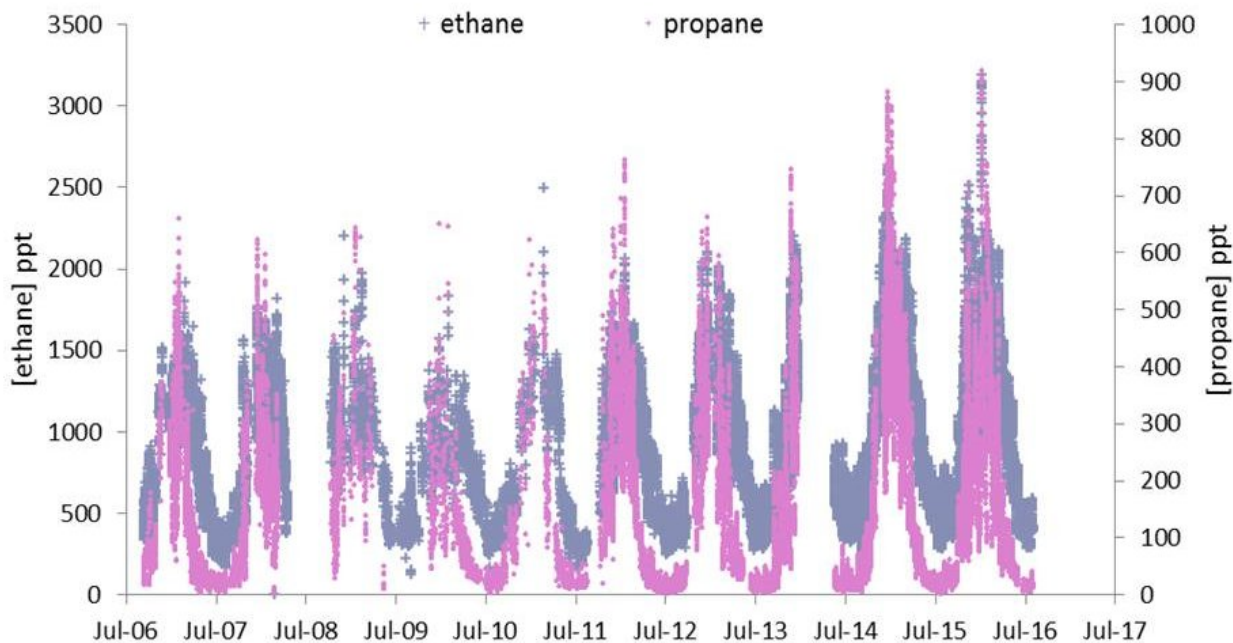


Figure 1. Ethane and propane time series.

Remote Tropical Island Mountaintop Measurements of Halogen Radicals and OVOCs

T. Koenig, B. Dix and R. Volkamer

University of Colorado, Department of Chemistry and Biochemistry, Boulder, CO 80309; 303-735-2235,
E-mail: Theodore.Koenig@colorado.edu

The remote tropical troposphere is responsible for about 75% of the chemical removal of ozone (O_3) and methane (CH_4), two important greenhouse gases. Yet the atmospheric chemistry of tropospheric halogens over remote oceans is largely constrained in the free troposphere (FT), where natural background processes can be probed in absence of local impacts from pollution. Inorganic bromine and iodine radicals from ocean sources are responsible for about 20% of the global tropospheric ozone loss, equivalent to about $900 \text{ Tg } O_x \text{ yr}^{-1}$ [similar to the O_x loss from hydroperoxyl (HO_2)]. Halogens oxidize atmospheric mercury, modify aerosols, and iodine can form new particles.

The Volkamer group at the University of Colorado - Boulder is developing a small network of mountaintop Multiple AXis Differential Optical Absorption Spectroscopy (MAX-DOAS) instruments to probe hemispheric gradients in the remote tropical FT by long-term measurements of trace gases. Since February 2017 we have deployed MAX-DOAS instruments at two sites: 1) Mauna Loa Atmospheric Baseline Observatory (MLO) at 19.5°N , 155.6°W , at 3.4 km altitude in the northern hemisphere tropics, and 2) Maïdo Observatory (Maïdo) at 21.1°S , 55.4°E , at 2.2 km altitude in the southern hemisphere tropics. We measure the halogen oxide radicals bromine monoxide (BrO) and iodine monoxide (IO), small oxygenated volatile organic compounds [OVOC; e.g. formaldehyde (HCHO) and glyoxal (CHOCHO)], as well as total columns of O_3 , and nitrogen dioxide (NO_2), and aerosol optical depth, which can be used for satellite validation. Combining MAX-DOAS measurements that probe the lower troposphere with zenith measurements at twilight to probe the stratosphere, we aim to develop retrievals of vertical columns and atmospheric profiles of trace gases that can have up to 5 degrees of freedom. First results from both sites are presented.

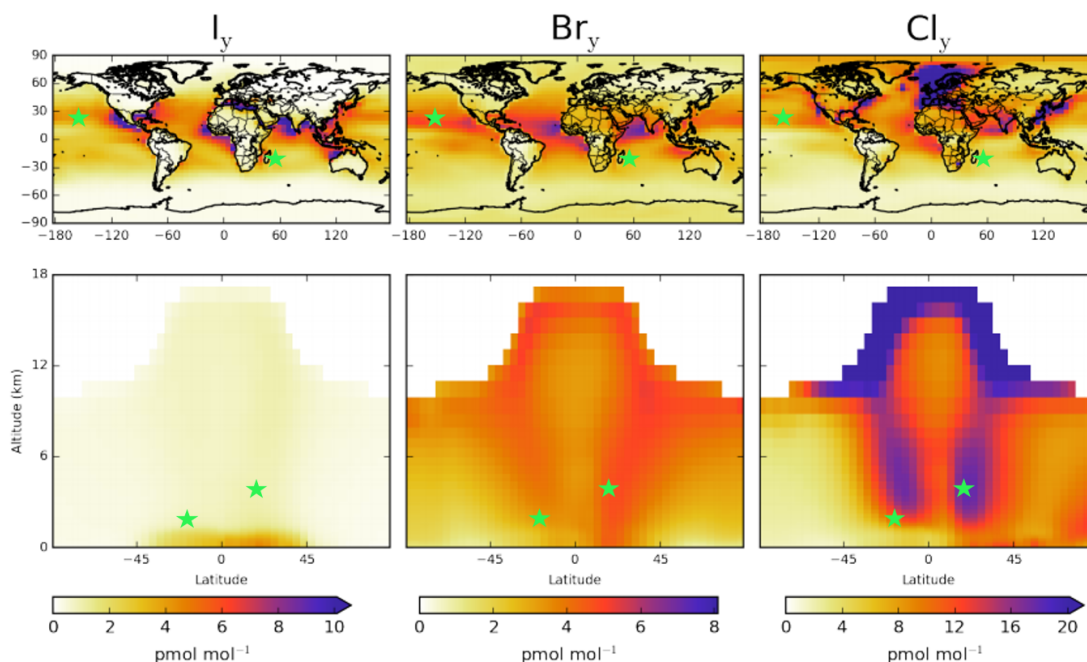


Figure 1. Tropospheric annual average inorganic halogen concentration as modeled in GEOS-Chem from Sherwen et al., 2016. Marked with green stars, the locations of the mountaintop observatories set up. While most apparent in chlorine, all halogens are predicted to be abundant in the tropical FT. Measurements of BrO and IO can be used to constrain the total inorganic bromine and iodine (Br_y, I_y) budget, while measurements of small HCHO and CHOCHO will inform the partitioning of Br_y .

VOC Measurements Using Whole Air Sampling (WAS) During ATom-1

I.J. Simpson, D.R. Blake, N.J. Blake, B. Barletta, S. Meinardi, S. Hughes and N. Vizenor

University of California at Irvine, Department of Chemistry, Irvine, CA 92697; 949-824-1464, E-mail: isimpson@uci.edu

Volatile organic compounds (VOCs) play important roles in atmospheric chemistry and air quality in both remote and polluted environments. The first Atmospheric Tomography field mission (ATom-1) was deployed in summer 2016, using the NASA DC-8 aircraft as a research platform and flying over the Pacific and Atlantic oceans in both hemispheres. The flights performed repeated vertical sampling of the atmosphere, from 0.2 to 12 km, giving a rare three-dimensional view of the remote global troposphere. During the mission UC Irvine collected 1585 whole air samples (WAS) that were analyzed for ~80 C₁-C₁₀ VOCs using multi-column gas chromatography. Ethane (C₂H₆) and propane showed characteristic north-south gradients, with distinct regional sources including biomass burning from Siberia and strong oil and gas signals over the Midwest U.S. Dichloromethane (CH₂Cl₂) and trichloromethane also showed north-south gradients, and CH₂Cl₂ levels were elevated in air masses that appeared to have Asian origins. Conversely, methyl nitrate (MeONO₂) showed a south-north gradient, with higher mixing ratios over the Pacific than the Atlantic. MeONO₂ enhancements were also observed over California, possibly from photochemical production during high nitrogen dioxide conditions. The transition from predominantly oceanic to photochemical alkyl nitrate sources was clear as the alkyl nitrate carbon number increased. Maximum MeONO₂ concentrations were observed over the equatorial Pacific, while maximum *i*-propyl nitrate and 2-butyl nitrate levels were measured over the Midwest U.S. oil and gas regions. These and other results will be presented and discussed.

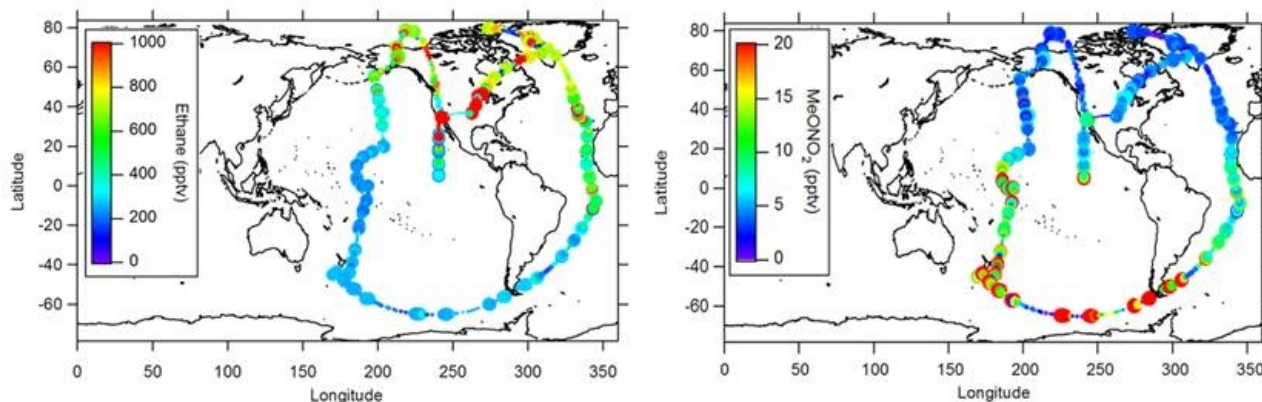


Figure 1. Mixing ratios of C₂H₆ (left panel) and MeONO₂ (right panel) measured during the airborne ATom-1 mission in summer 2016. Bigger markers represent lower altitudes.

First Results of Tall Tower Surface-atmosphere N₂O Flux Measurements over a Mixed Agricultural Region in Central Europe

L. Haszpra^{1,2}, Z. Barcza^{3,4} and D. Hidy⁴

¹Hungarian Meteorological Service, Budapest, Hungary; +36-1-346-4816, E-mail: haszpra.l@met.hu

²MTA Research Centre for Astronomy and Earth Sciences, Sopron, Hungary

³Eötvös Loránd University, Department of Meteorology, Budapest, Hungary

⁴Eötvös Loránd University, Excellence Center, Martonvásár, Hungary

In summer 2015 an eddy covariance (EC) system was put into operation at the Hungarian tall tower greenhouse gas monitoring site (Hegyhátsál - 46°57'N, 16°39'E, 248 m a.s.l.) to monitor the vertical flux of nitrous oxide (N₂O). The N₂O EC system is co-located with a previously installed EC system that monitors the surface/atmosphere exchange of carbon dioxide (CO₂) at 82 m above the ground. The high-elevation, large-footprint EC systems are primarily intended for the monitoring of the net fluxes of the mixed agricultural fields surrounding the tower and characteristic for an extended region. Monitoring of the greenhouse gas exchange of a typical mixture of different agricultural fields might better support the estimation of the regional/national level emission than that of specific ecosystems. It also contributes to the development and validation of ecosystem models. Both EC systems are precisely calibrated and also suitable for the long-term monitoring of the atmospheric concentrations. The poster focuses on the first results of the N₂O flux measurement system describing the setup, presenting the temporal variations in both the concentration and the vertical flux, as well as the upgraded version of Biome-BGCMuSo process oriented biogeochemical model (Hidy et al., 2016) extended for the simulation of the full nitrogen budget of the ecosystems. The available data series (covering the period of Jul, 2015 - Dec, 2016) indicate 0.95 ppb/year concentration trend. The annual N₂O emission for year 2016 was ~340 mg/m².

Hidy, D. et al., 2016: Terrestrial ecosystem process model Biome-BGCMuSo v4.0: summary of improvements and new modeling possibilities. *Geoscientific Model Development* 9, 4405-4437. doi:10.5194/gmd-9-4405-2016

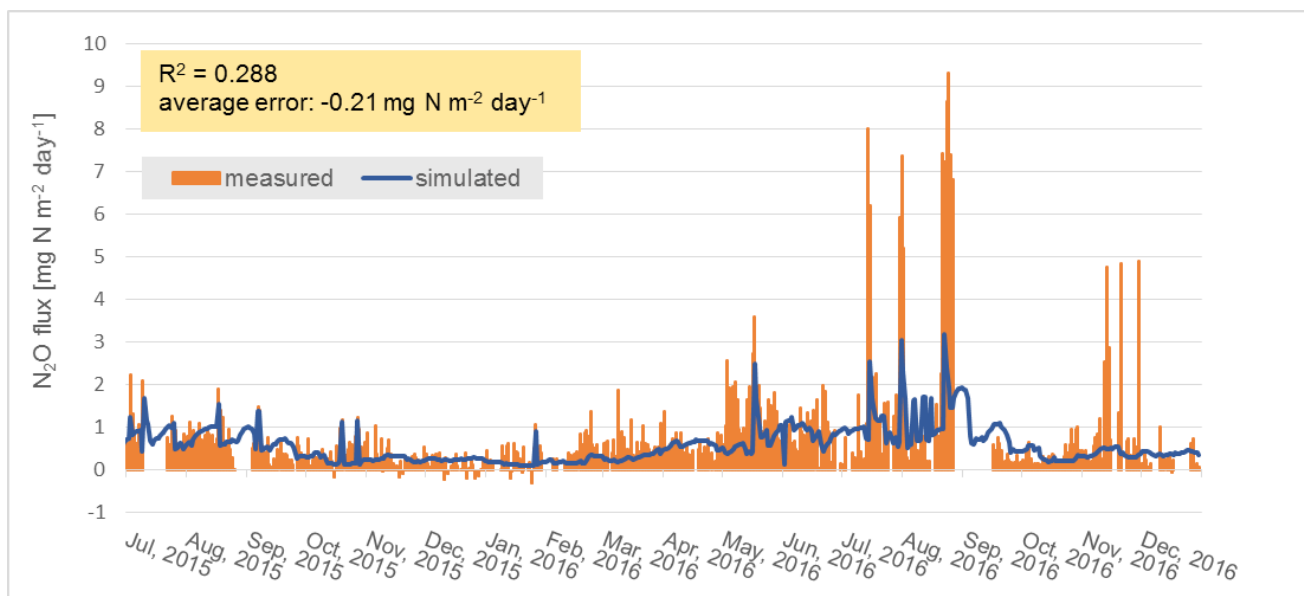


Figure 1. Measured and modelled N₂O flux of the agricultural fields surrounding Hegyhátsál greenhouse gas monitoring site.

The WMO-GAW-VOC Network with Contributions of AGAGE

R. Steinbrecher¹, S. Thiel¹, S. Reimann², M.K. Vollmer² and G. Spain³

¹Institute for Meteorology and Climate Research, Karlsruhe Institute of Technology, Campus Alpin, Karlsruhe, Germany; +49-1715-610-982, E-mail: rainer.steinbrecher@kit.edu

²Swiss Federal Laboratories for Materials Science and Technology, Empa, Dübendorf, Switzerland

³School of Physics, National University of Ireland, Galway, Galway, Ireland

The trace gas composition of the atmosphere is a major driver of climate change and air pollution events. Long-term observations with known quality are crucial for detecting trends of major air constituents. Networks with global coverage such as Global Atmosphere Watch (GAW) and Advanced Global Atmospheric Gases Experiment (AGAGE) work on this. This talk investigates the possibilities of how both networks may combine their activities in analyzing non-methane hydrocarbons (NMHCs) in air.

Recent GAW audits for NMHC analysis at GAW/AGAGE stations Mace Head and Jungfraujoch revealed that up to 80% of NMHCs GAW targets can be reported with data qualities matching data quality objectives of GAW for volatile organic compounds (VOC). Thus, by joining network activities the global coverage for VOC reporting stations could be increased and in consequence better data products developed (Figure 1).

Future challenges exist in developing a joint strategy to create synergies between the GAW-VOC and AGAGE networks. These challenges include: agreeing on a common protocol to establish at the stations, the WMO-GAW scale for selected GAW-VOC targets with appropriate QA/QC measures for maintaining and reporting high quality data, and how regular reporting of NMHCs data from stations can be achieved.

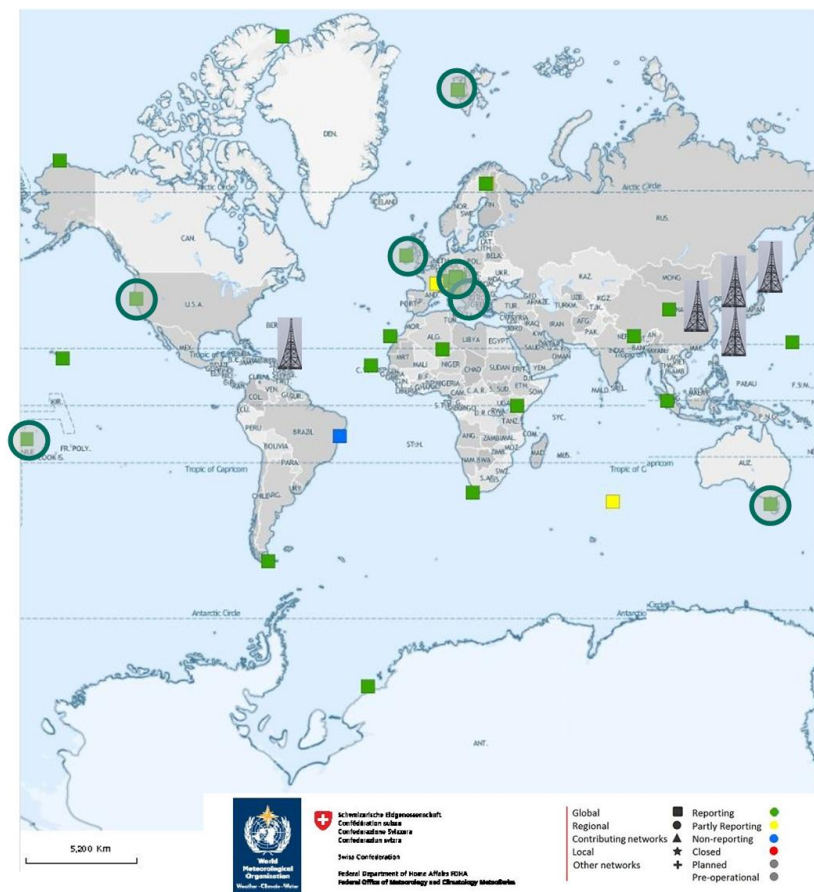


Figure 1. The Network of Global Atmosphere Watch for volatile organic compounds (GAW-VOC; green and yellow squares). The stations of the Advanced Global Atmospheric Gases Experiment (AGAGE) within GAW-VOC are circled. Towers mark further AGAGE and affiliated stations so far not part of the GAW-VOC network.

Twenty-Five Years of Airborne Observations of Ozone-Depleting and Climate-Related Gases in the Upper Troposphere and Lower Stratosphere

J.W. Elkins¹, F.L. Moore^{2,1}, E.J. Hints^{2,1}, J.D. Nance^{2,1}, G.S. Dutton^{2,1}, D.F. Hurst^{2,1} and B.D. Hall¹

¹NOAA Earth System Research Laboratory, Global Monitoring Division (GMD), Boulder, CO 80305; 303-497-6224, E-mail: James.W.Elkins@noaa.gov

²Cooperative Institute for Research in Environmental Sciences (CIRES), University of Colorado, Boulder, CO 80309

Scientists started *in situ* airborne measurements of two strong ozone-depleting gases or chlorofluorocarbons, chlorofluorocarbon-11 (CFC-11) and CFC-113 in 1991 on the NASA ER-2 aircraft with a two-channel gas chromatograph, Airborne Chromatograph for Atmospheric Trace Species (ACATS). We broaden our list of gases to include more ozone-depleting and other climate-related gases. An improved 4-channel gas chromatograph that included nitrous oxide (N₂O), sulfur hexafluoride (SF₆), CFC-11, -12, -113, halon-1211, carbon tetrachloride (CCl₄), methyl chloroform (CH₃CCl₃), methane (CH₄), carbon monoxide (CO), and hydrogen (H₂) was added to the ER-2 aircraft in 1994. In order to study the stratosphere at higher levels to 32 km, we built a 3-channel balloon instrument called the Lightweight Airborne Chromatograph Experiment (LACE). As CFC replacements took hold, we added a 6-channel gas chromatograph-mass spectrometer system, peroxyacetyl nitrate (PAN) and other Trace Hydro-halocarbon Experiment (PANTHER), in 2001 to examine shorter-lived gases mainly in the upper troposphere. These airborne measurements were to complement our ground-based flask and *in situ* measurements from the Halocarbon and other Trace Species Network. This talk will show results from a tropical study, Airborne Tropical Tropopause Experiment (ATTREX) on the NASA Global Hawk aircraft and preliminary results from the Atmospheric Tomography Mission (ATom) conducted in August 2016 on the NASA DC-8 aircraft. A detrended, gridded, latitudinal distribution of SF₆ is shown in the figure below for the years of 1994 through 2014. Such a plot may be useful to atmospheric modelers trying to capture transport or calculate emissions.

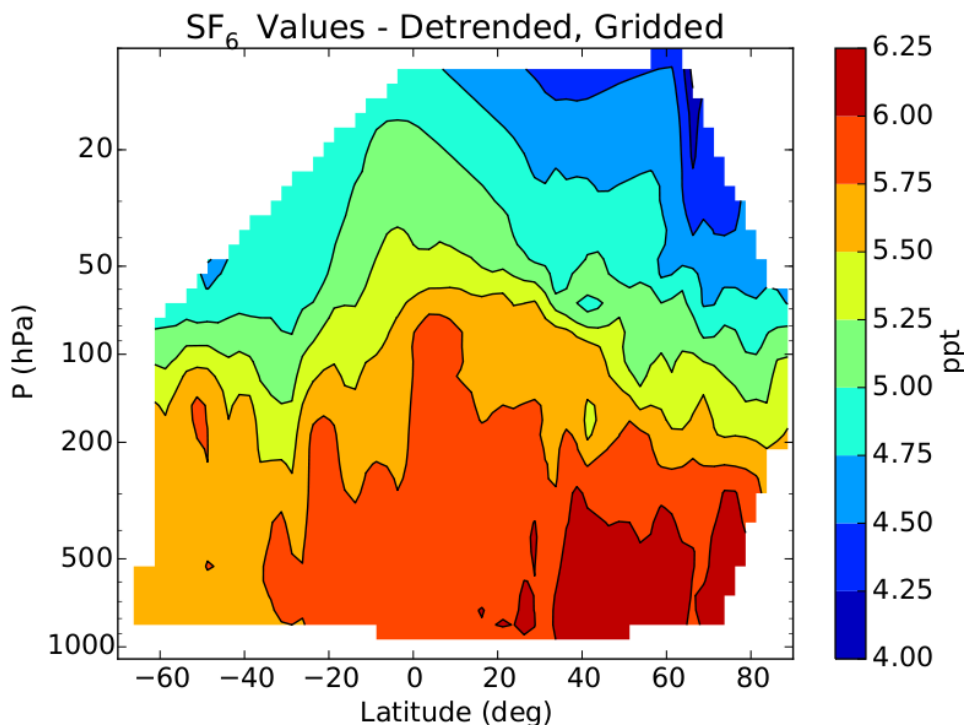


Figure 1. All airborne measurements detrended from 1994 forward for atmospheric SF₆. It was detrended using separate linear fits joining at an inflection point at year = 2006.5.

Sulfuryl Fluoride (SO₂F₂) Atmospheric Abundance and Trend from the GMD North American Tower and Aircraft Programs

B.R. Miller^{1,2}, B. Hall², M.J. Croftwell^{1,2}, C. Siso^{1,2}, S.A. Montzka², A.E. Andrews² and C. Sweeney^{1,2}

¹Cooperative Institute for Research in Environmental Sciences (CIRES), University of Colorado, Boulder, CO 80309; 303-497-6624, E-mail: ben.r.miller@noaa.gov

²NOAA Earth System Research Laboratory, Global Monitoring Division (GMD), Boulder, CO 80305

Beginning in the 1980's, sulfuryl fluoride (SO₂F₂) increasingly replaced methyl bromide (CH₃Br) as the fumigant for structures and postharvest agricultural produce, after the latter came under restrictions by the Montreal Protocol on Substances that Deplete the Ozone Layer and its subsequent amendments. Unlike CH₃Br, SO₂F₂ poses no threat to stratospheric ozone, and despite a global warming potential (GWP) of ~4780 (100-yr horizon), the current global abundance of about 2 ppt means it currently contributes negligible to global warming. The average total global lifetime of SO₂F₂ is 36 ± 11 yrs, and this is dominated by dissolution and hydrolysis in alkaline ocean waters. A previous study (Möhle et al., 2009) found that reported global industrial production of SO₂F₂ averaged ~50% higher than emission estimates derived from modeling atmospheric measurements, suggesting a missing sink that has been hypothesized as a destruction that occurs during the fumigation process. Möhle et al. (2009) estimated a 2005 emission of about 2 Gg/yr and an annual atmospheric abundance growth rate of 5 ± 1% per year. Here we present about 2 years of SO₂F₂ measurements from the GMD Global Greenhouse Gas Reference Network (GGGRN) North American Tower and Aircraft programs, and from the Halocarbons & Other Atmospheric Trace Species (HATS) global flask network.

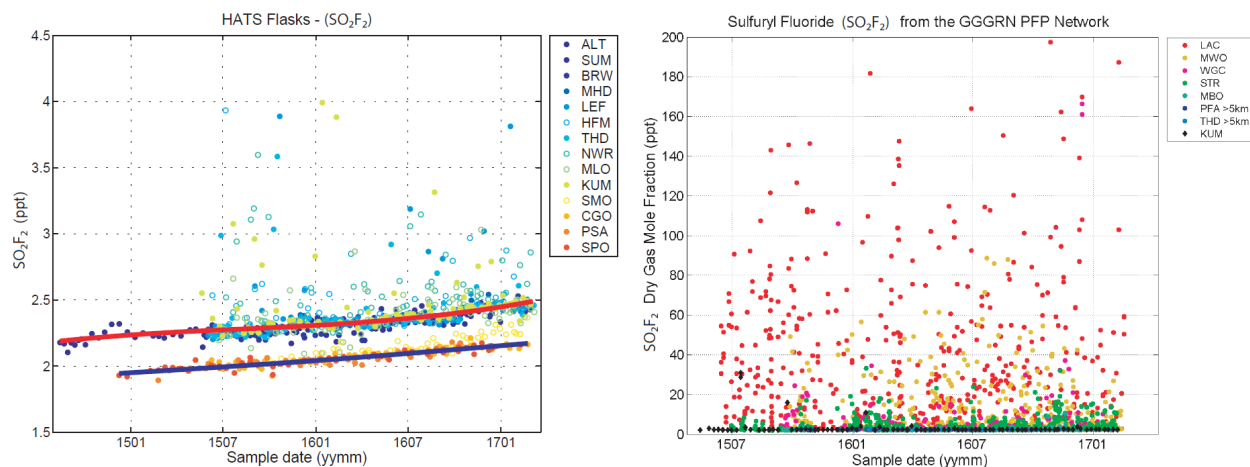


Figure 1. (Left pane) Background SO₂F₂ mole fractions from HATS remote site network. Sites with solid symbols were used to determine the hemispheric trends (red and blue lines), which are about 5% per year in accord with Möhle et al. (2009). Note the enhancements observed at sites such as Trinidad Head Atmospheric Baseline Observatory (THD), Cape Kumakahi (KUM), Mauna Loa Atmospheric Baseline Observatory (MLO) and Niwot Ridge (NWR), indicating influence from regions (California and Hawaii) where SO₂F₂ is used for fumigation. (Right pane) SO₂F₂ mole fractions observed at select North American tower and aircraft sites, with KUM as background reference. The vertical axis has been limited to show 200 ppt maximum, but events with enhancement as high as 500 ppt were observed.

Perfluoro-*N*-methylmorpholine (C₅F₁₁NO), a Persistent Greenhouse Gas: Laboratory Determination of Radiative Efficiency, Atmospheric Loss Processes and Global Warming Potential

F. Bernard^{1,2}, R.W. Portmann² and J.B. Burkholder²

¹Cooperative Institute for Research in Environmental Sciences (CIRES), University of Colorado, Boulder, CO 80309; 303-497-4819, E-mail: Francois.Bernard@noaa.gov

²NOAA Earth System Research Laboratory, Chemical Sciences Division (CSD), Boulder, CO 80305

Perfluoro-*N*-methylmorpholine (PF-*N*-MM, C₅F₁₁NO) belongs to the class of morpholines which are used in heat transfer fluids. Its use and high vapor pressure (~270 Torr at 298 K) may lead to its direct emission into the atmosphere. The atmospheric loss processes and lifetimes for PF-*N*-MM over the different atmospheric regions (troposphere, stratosphere and mesosphere) are not well-defined. PF-*N*-MM is expected to be an atmospherically long-lived compound with a lifetime greater than 500 years. Additionally, PF-*N*-MM is expected to be a potent greenhouse gas due to its strong infrared absorption in the atmospheric window region. Fundamental studies of the environmental impact of PF-*N*-MM are required to identify and quantify its spectroscopic and chemical properties.

In this study, the infrared absorption spectrum of PF-*N*-MM was measured and its radiative efficiency (RE) evaluated. The infrared spectrum was measured using Fourier transform infrared spectroscopy between 500-4000 cm⁻¹ and radiative efficiency was calculated using the Hodnebrog et al. (2013) estimation method. Atmospheric loss processes, O(¹D) reactivity and ultraviolet photolysis, were measured as part of this work, leading to an estimation of the PF-*N*-MM atmospheric lifetime based on 2-D model calculations. Potential atmospheric loss processes, atmospheric lifetime, global warming potential (GWP) of PF-*N*-MM will be discussed.

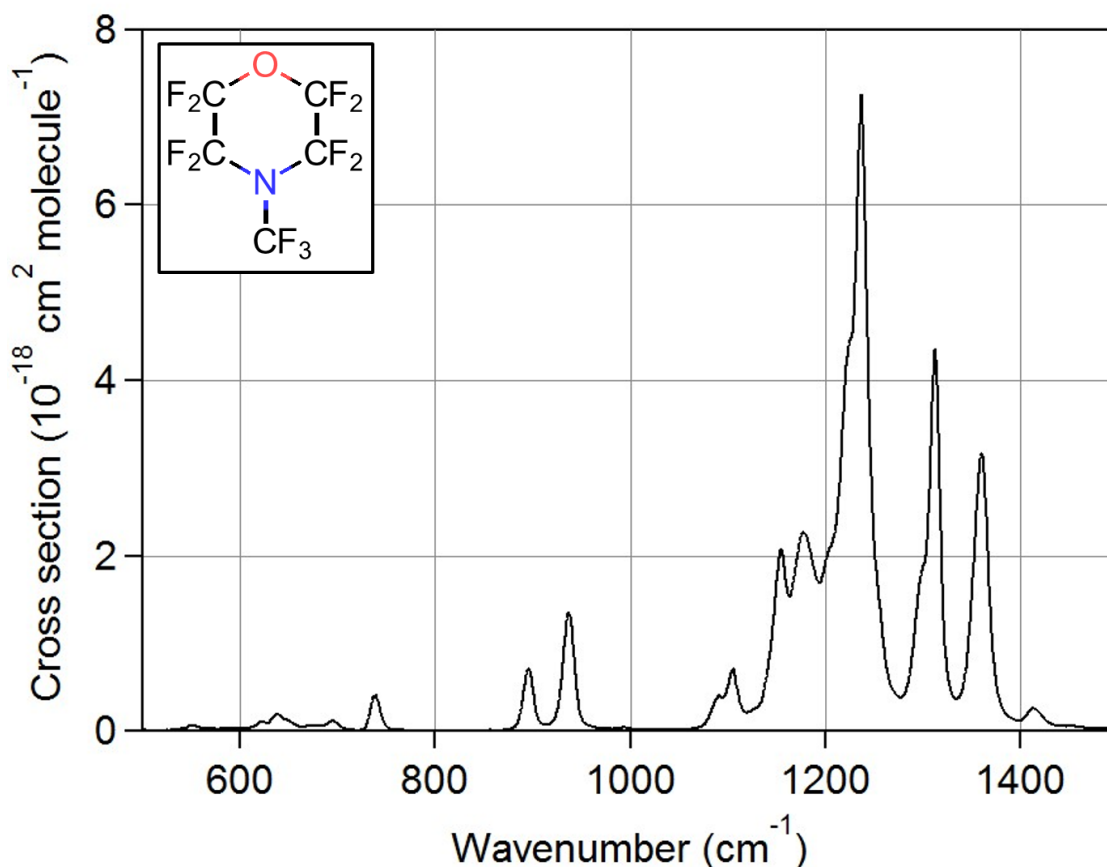


Figure 1. Measured infrared absorption spectrum (base *e*) of perfluoro-*N*-methylmorpholine (PF-*N*-MM).

Development of Traceable Precision Dynamic Dilution Method to Generate Dimethyl Sulphide Gas Mixtures at Sub-nmol/mol for Ambient Measurement

M.E. Kim¹, Y.D. Kim¹, J.H. Kang¹, G.S. Heo¹, D.S. Lee² and S. Lee¹

¹Korea Research Institute of Standards and Science, Center of Gas Analysis, Daejeon, South Korea; +82-4-2868-5864, E-mail: eontree@kriss.re.kr

²Yonsei University, Department of Chemistry, Seoul, South Korea

Dimethyl sulphide (DMS) is an important compound in global atmospheric chemistry and climate change. Traceable international standards are essential for measuring accurately the long-term global trend in ambient DMS. However, developing accurate gas standards for sub-nanomole per mole (nmol/mol) mole fractions of DMS in a cylinder is challenging, because DMS is reactive and unstable. In this study, a dynamic dilution method that is traceable and precise was developed to generate sub-nmol/mol DMS gas mixtures with a dynamic dilution system based on sonic nozzles and a long-term (> 5 years) stable 10 $\mu\text{mol/mol}$ parent DMS primary standard gas mixtures (PSMs). The dynamic dilution system was calibrated with traceable methane PSMs, and its estimated dilution factors were used to calculate the mole fractions of the dynamically generated DMS gas mixtures. A dynamically generated DMS gas mixture and a 6 nmol/mol DMS PSM were analysed against each other by gas chromatography with flame-ionisation detection (GC/FID) to evaluate the dilution system. The mole fractions of the dynamically generated DMS gas mixture determined against a DMS PSM and calculated with the dilution factor agreed within 1% at 6 nmol/mol. In addition, the dynamically generated DMS gas mixtures at various mole fractions between 0.4 and 11.7 nmol/mol were analysed by GC/FID and evaluated for their linearity. The analytically determined mole fractions showed good linearity with the mole fractions calculated with the dilution factors. Results showed that the dynamic dilution method generates DMS gas mixtures ranging between 0.4 nmol/mol and 12 nmol/mol with relative expanded uncertainties of less than 2%. Therefore, the newly developed dynamic dilution method is a promising reference method for generating sub-nmol/mol DMS gas standards for accurate ambient measurements.

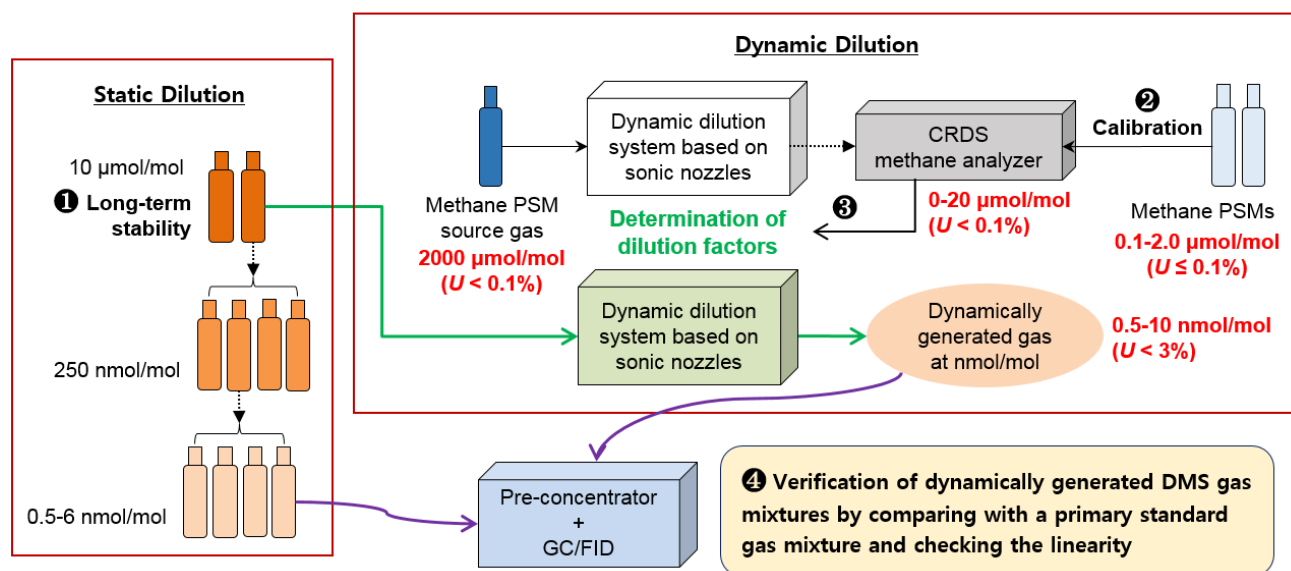


Figure 1. An overview of the research scheme.

Pressure Dependent CO₂ Enrichment in High-pressure Aluminum Cylinders

M.F. Schibig^{1,2}, D. Kitzis^{3,2} and P.P. Tans²

¹Early Postdoc.Mobility Fellow, Swiss National Science Foundation, Bern, Switzerland; 303-497-5468, E-mail: michael.schibig@noaa.gov

²NOAA Earth System Research Laboratory, Global Monitoring Division (GMD), Boulder, CO 80305

³Cooperative Institute for Research in Environmental Sciences (CIRES), University of Colorado, Boulder, CO 80309

The primary standards to maintain the World Meteorological Organization (WMO) carbon dioxide (CO₂) X2007 scale as well as the secondary and the tertiary CO₂ standards to pass the scale down are stored in high-pressure aluminum cylinders. To meet the WMO's accuracy goal of $\pm 0.1 \mu\text{mol mol}^{-1}$, it is crucial that the standards are stable during their whole life time. At field stations but also in laboratory experiments, standard gases showed CO₂ enrichment with decreasing pressure, which was most probably caused by either desorption of CO₂ from the cylinder walls with decreasing pressure or Rayleigh distillation. If these enrichment effects are reproducible, a function could be applied to correct the enrichment effects of the cylinders and improve the accuracy of the CO₂ measurements calibrated with these standards.

To investigate the CO₂ enrichment effects, a batch of eight high-pressure aluminum cylinders is repeatedly filled at NOAA's Niwot Ridge station with pressurized ambient air. After delivery to the laboratory and reaching thermal equilibrium, they are decanted while the CO₂ mole fraction is measured continuously. The obtained data is used to prove whether the CO₂ enrichment is reproducible or not, and to determine whether it is possible to find a useful general correction function.

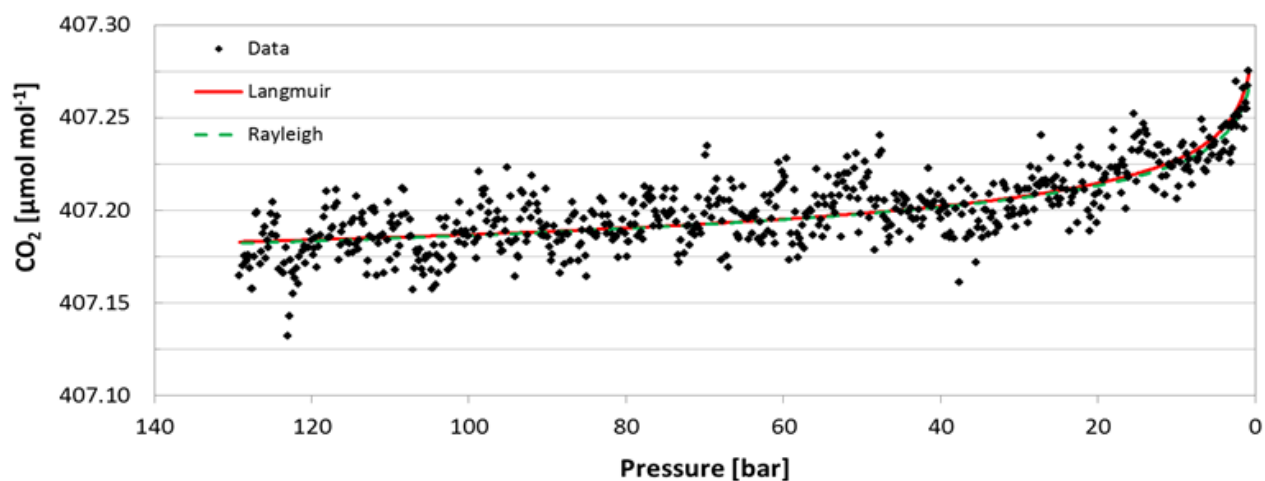


Figure 1. Example for the enrichment of the CO₂ mole fraction with decreasing pressure in air decanted from an aluminum cylinder as used to store CO₂ standards. The black dots represent measurements, the red line corresponds to a best fit according to the Langmuir adsorption/desorption function, and the green dashed line represents a best fit according to the Rayleigh distillation function.

Ensuring High-quality Data from NOAA's GC-MS Perseus Instrument

M.J. Crotwell^{1,2}, B.R. Miller^{1,2}, C. Siso^{1,2}, B.D. Hall² and P.K. Salameh³

¹Cooperative Institute for Research in Environmental Sciences (CIRES), University of Colorado, Boulder, CO 80309; 303-497-4728, E-mail: molly.crotwell@noaa.gov

²NOAA Earth System Research Laboratory, Global Monitoring Division (GMD), Boulder, CO 80305

³Scripps Institution of Oceanography, University of California at San Diego, La Jolla, CA 92037

The NOAA Earth System Research Laboratory Global Monitoring Division collects routine air samples in programmable flask packages (PFPs) from sites across North America and stainless steel and glass flasks across the globe. These sites include atmospheric profiles in small aircraft, stationary locations at tall towers, baseline observatories, and cooperative fixed sites. Starting in 2015, a new gas chromatography-mass spectrometry (GC/MS) analytical system for Preconcentration of Environmentally Relevant Species (or PERSEus) has been making measurements of ~60 halocarbons, hydrocarbons, and sulfur-containing compounds from these PFPs and a subset of flask samples.

Over the past 18 months, more than 15,000 discrete air samples were measured on Perseus for this suite of analytes. Data quality assurance (QA) and quality control (QC) are a fundamental part of these data records. Part of the QA work is performed in the Perseus measurement lab with archive tanks analyzed every 3-5 days, quarterly tertiary and secondary comparisons, bi-annual gravimetric standards comparisons, and routine inter-comparisons among different measurement labs. QC is completed with software developed in GMD and at the Scripps Institution of Oceanography (SIO) to look at raw analysis files, time series plots, and instrument response sensitivities. These tools, and other plotting routines, help us identify sample collection problems and measurement problems (Fig. 1). This presentation will focus on our quality assurance and quality control strategies and findings.

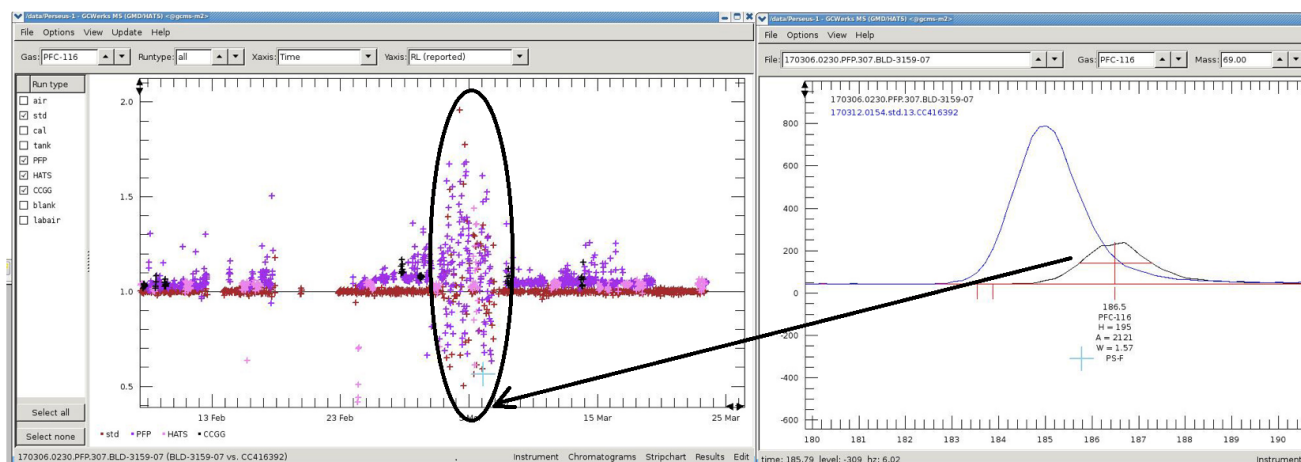


Figure 1. Perseus PFC-116 ratios of sample area/pressure to standard area/pressure are plotted in figure 1 as an analysis date time-series. Standard results are shown in red, PFP results are shown in purple. The results identified with the black circle were determined to have temperature problems during the first trapping phase. The figure to the right shows a PFC-116 chromatogram of detector response vs. retention time (sec) from a “bad” result during this time period (black) compared to a “good” (blue) chromatogram from a later time period.

High-precision, Continuous and Real-time Measurement of Atmospheric Oxygen using Cavity Ring-down Spectroscopy

J. Boulton

Picarro Inc., Santa Clara, CA 94054; 408-962-3946, E-mail: jboulton@picarro.com

Oxygen (O₂) is a major and vital component of the Earth atmosphere representing about 21% of its composition. It is consumed or produced through biochemical processes such as combustion, respiration, and photosynthesis and can be used as a top-down constraint on the carbon cycle. The observed variations of oxygen in the atmosphere are relatively small, in the order of a few ppm's. This presents the main technical challenge for the measurement since a very high level of precision on a large background is required. Only few analytical methods including mass spectrometry, fuel, ultraviolet and paramagnetic cells are capable of achieving it.

Here we present new developments of a high-precision gas analyzer that utilizes the technique of Cavity Ring-down Spectroscopy to measure oxygen concentration and its oxygen isotope ratio ¹⁸O/¹⁶O. Its compact and rugged design, combined with high precision and long-term stability, allows the user to deploy the instrument in the field for continuous monitoring of atmospheric oxygen level. Measurements have a 1-σ 5-minute averaging precision of 1-2 ppm for O₂ over a dynamic range of 0-50%. We will present comparative test results of this instrument against the incumbent technologies such as the mass spectrometer and the paramagnetic cell. In addition, we will demonstrate its long-term stability from a field deployment in Switzerland.

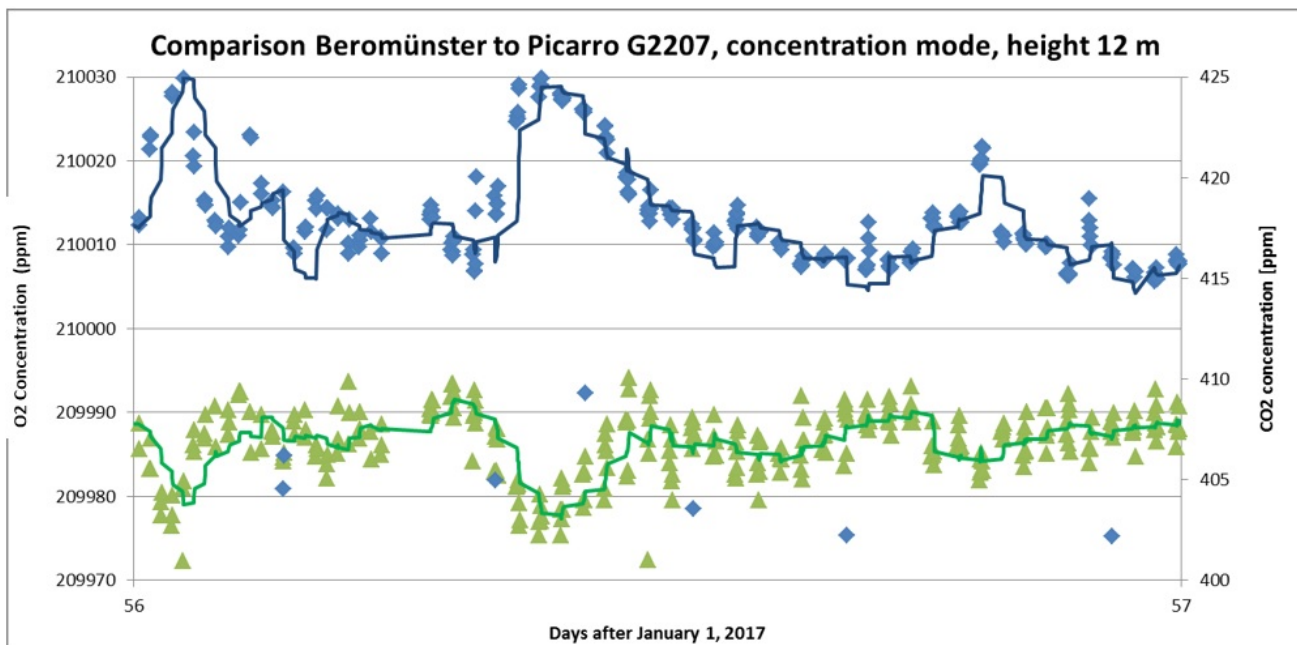


Figure 1. Concentration mode measurements at Beromünster tall tower, in blue carbon dioxide concentration by a Picarro 2401 instrument and in green O₂ values for the inlet at 40 m height, six minute switching. The dark blue and the light green lines correspond to a 10 point running mean of the 30 seconds means, i.e. 5 minute running averages over one day.

Continuous, Regional Approach to Methane Source Detection and Sizing Using Dual Frequency Comb Laser Spectroscopy and Atmospheric Inversions

C. Alden¹, S. Coburn², R. Wright², I. Coddington³, C. Sweeney^{1,4}, A. Karion⁵, S. Ghosh⁵, N. Newbury³, K. Prasad⁵ and G.B. Rieker²

¹Cooperative Institute for Research in Environmental Sciences (CIRES), University of Colorado, Boulder, CO 80309; 719-930-5281, E-mail: aldenc@colorado.edu

²University of Colorado, Department of Mechanical Engineering, Boulder, CO 80309

³National Institute of Standards and Technology (NIST), Boulder, CO 80305

⁴NOAA Earth System Research Laboratory, Global Monitoring Division (GMD), Boulder, CO 80305

⁵National Institute of Standards and Technology (NIST), Gaithersburg, MD 20880

Advances in natural gas extraction technology have led to increased production and transport activity, and, as a consequence, an increased need for reliable monitoring of methane (CH₄) leaks. A gap exists among current methods for leak detection; that is, the ability to provide continuous, time-varying estimates of emissions. For example, satellite observations have day-time and clear sky biases, and also lack the resolution to pinpoint small leaks. Current ground-based and aircraft-based approaches can only collect “snapshots” of emissions in time. These approaches can also require operators and specific atmospheric conditions and/or the use of a tracer gas. Aircraft measurements also have a mid-day bias. The new system that we present here has the potential to offer sensitive, stable, and autonomous coverage of large (5+ km²) areas that can include 10s or 100s of potential source locations. Critically, this system closes the temporal variability information gap. Our system would provide continuous (diurnal, seasonal, interannual) monitoring of emissions from oil and gas operations. We employ a dual frequency comb spectrometer, which offers high stability of trace gas measurements over time, so that concentrations can be compared across different conditions and long periods of time. We situate the spectrometer in the center of a field of well sites. A series of retroreflectors around the perimeter of the field direct light back to a detector co-located with the laser. The beam pitch and catch system sends light between 1620 and 1680 nm, with discrete line spacing of 0.002 nm, resulting in a laser system covers thousands of individual absorption features from multiple species; namely CH₄, carbon dioxide, and water vapor. Field tests demonstrate the ability of the system to identify very small atmospheric methane concentration enhancements (10-20 ppb), leading to the detection and sizing of very small (1.3 g/m) leaks of CH₄, with long-range (>500 m) (see Fig. 1). The demonstration of sensitive CH₄ measurements over kilometer-scale open paths allows for opportunities to monitor CH₄ emissions across large areas of natural gas activity. We will present results of field trials using controlled CH₄ releases in a rural Colorado field site close to the Denver-Julesburg Basin. This work represents the first field use of dual frequency comb spectroscopy to measure long-range, open path atmospheric concentrations of CH₄.

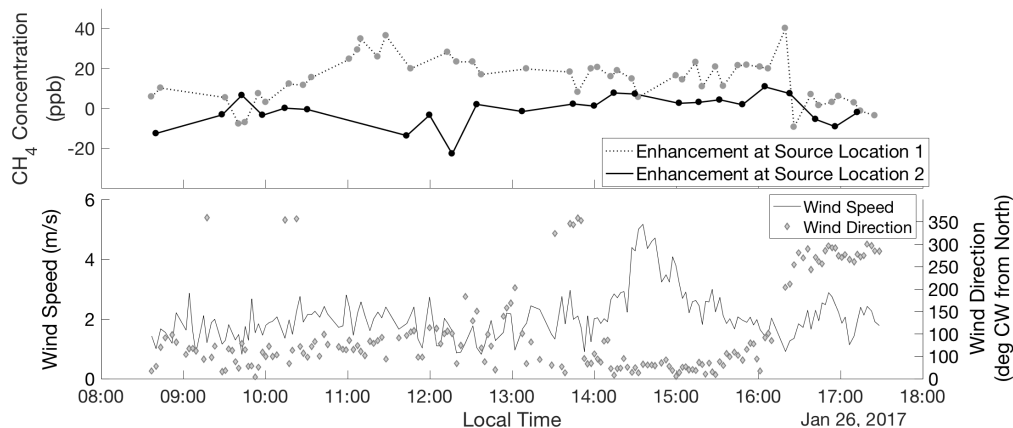


Figure 1. Atmospheric CH₄ enhancements above background along two open-path beams that bound Source Location 1, where a 1.3 g/m controlled release began at 10:00 and ended at 16:30, and non-emitting Source Location 2 (a). Wind speed and wind direction for the measurement period (b).

2017 Cooperative Tower Network Overview and Insights

J. Kofler^{1,2}

¹Cooperative Institute for Research in Environmental Sciences (CIRES), University of Colorado, Boulder, CO 80309; 303 497-4679, E-mail: jonathan.kofler@noaa.gov

²NOAA Earth System Research Laboratory, Global Monitoring Division (GMD), Boulder, CO 80305

Partnerships with external collaborators have enabled the NOAA-ESRL-GMD Tower network to maintain 13 tower sites with regular flask samples and 9 sites with continuous *in situ* carbon dioxide (CO₂), CO sites for nearly a decade. Also, three sites include continuous methane measurements. A summary of the hardware and an overview of the overall trends and some unique characteristics of a few sites is highlighted. Seasonal cycles in CO₂ across the network are shown covering since its inception. Relationships with climate conditions and anomalies such as drought are explored.



Figure 1. Air Intake at West Branch Iowa Tower.

Improvements to UCATS for the Atmospheric Tomography (ATom) Mission and Recent Results

E.J. Hints^{1,2}, F.L. Moore^{1,2}, G.S. Dutton^{1,2}, B.D. Hall², A. McClure-Begley^{1,2}, J.D. Nance^{1,2}, S.A. Montzka², C. Siso^{1,2}, J.W. Elkins², C. Thompson^{1,3}, J. Peischl^{1,3}, T.B. Ryerson³, K. McKain^{1,2}, C. Sweeney^{1,2}, R. Commane⁴, B. Daube⁴, S. Wofsy⁴ and G. Diskin⁵

¹Cooperative Institute for Research in Environmental Sciences (CIRES), University of Colorado, Boulder, CO 80309; 303-497-4888, E-mail: Eric.J.Hints@noaa.gov

²NOAA Earth System Research Laboratory, Global Monitoring Division (GMD), Boulder, CO 80305

³NOAA Earth System Research Laboratory, Chemical Sciences Division (CSD), Boulder, CO 80305

⁴Harvard University, Cambridge, MA 02138

⁵NASA Langley Research Center, Hampton, VA 23681

The NASA Atmospheric Tomography (ATom) Mission is designed to measure vertical cross sections of the atmosphere, to probe methane oxidation and ozone chemistry on large scales, and to challenge chemical transport models. The NASA DC-8 aircraft has been outfitted with a large payload of instruments for reactive and trace gases, aerosols, radiation and meteorology, with flights from north-to-south over the Pacific, returning over the Atlantic. For ATom, we made the following improvements to the UCATS instrument: 1) an upgraded ozone instrument with greater sensitivity and the elimination of artifacts caused by rapid humidity changes on aircraft ascents; 2) a new water vapor instrument for high precision and accuracy measurements from the surface to the stratosphere; and 3) upgrades to the gas chromatograph in UCATS, including improved detector electronics. We purchased a 2B Model 211 ozone instrument with a longer cell, and installed it in a new 3" section at the top of UCATS. To avoid water vapor artifacts, we use Nafion moisture exchangers to maintain sample air at a high enough humidity so the cells never dry out. The Nafion tubes are mounted in a sealed box at the same pressure as the sample gas passing through them, to avoid damage to the Nafion tubes. A new tunable diode laser (TDL) sensor was built by Port City Instruments, using different infrared lines and path lengths to cover the range of water vapor concentrations. For ATom-1, the new ozone instrument was implemented along with faster electronics on the gas chromatograph detectors, but benefits were not obvious because of much lower-than-anticipated pressures at our inlet over the wing. For ATom-2, the inlet was fixed, the new TDL added, and further electronics improvements were made, with much better results. Recent data and a few intercomparisons will be shown, along with future work.

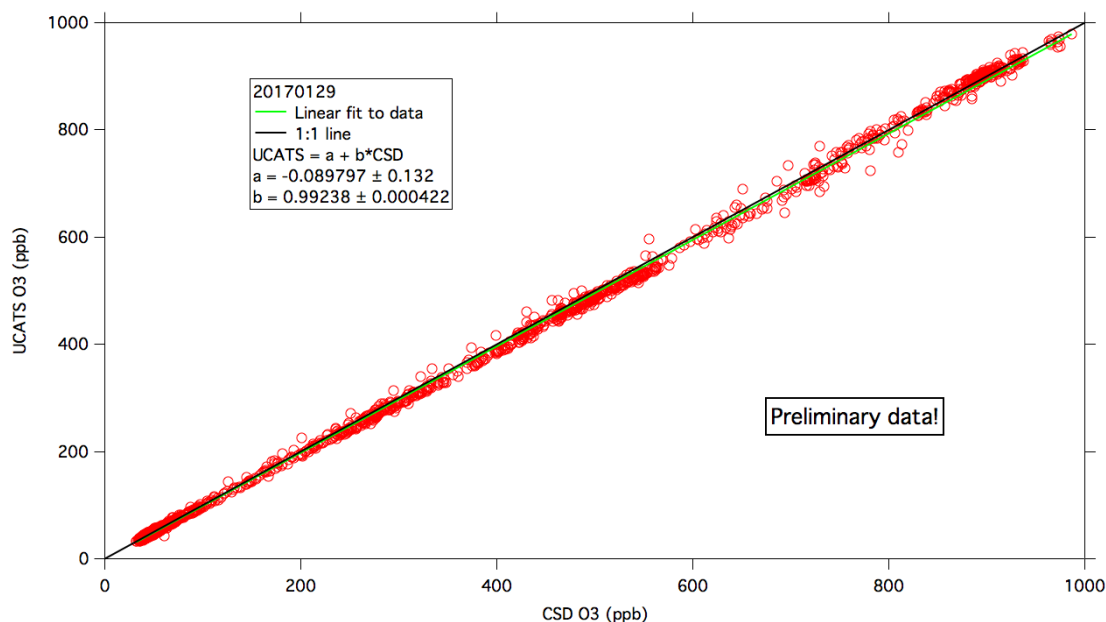


Figure 1. Comparison of preliminary ozone data from UCATS and NOAA Chemical Sciences Division from the DC-8 flight from Palmdale, CA to Anchorage, AK.

Recent Methodological Advancements to the AirCore Atmospheric Profiler

J. Bent^{1,2}, C. Sweeney^{1,2}, P.P. Tans², T. Newberger^{1,2}, J. Higgs² and S. Wolter^{1,2}

¹Cooperative Institute for Research in Environmental Sciences (CIRES), University of Colorado, Boulder, CO 80309; 303-497-8747, E-mail: jbent@ucar.edu

²NOAA Earth System Research Laboratory, Global Monitoring Division (GMD), Boulder, CO 80305

The innovative AirCore atmospheric profiler remains one of the foremost tools for accurately measuring vertical profiles of carbon dioxide (CO₂), methane (CH₄) and carbon monoxide (CO). The 100 m-long passivated stainless steel tubing coil works as a sort of atmospheric “tape recorder”—it is launched on a balloon with one end open, allowing the tube to empty as it ascends, and fill back up with an atmospheric profile as it descends. The resulting “core” provides concentrations of the three gases from 30 km (~12 mbar) to the surface. Metadata and fluid dynamics models map the resulting core to the pressure altitude at which a given parcel of air was sampled. Here, we present recent developments and proposed methodological advancements of the platform, including a new Python code product that allows end users to process the cleaned up data themselves, and a proposed actively-pumped AirCore, “AirCore-Active”, designed to fly on small unmanned aerial system (UAS) platforms as a tool to measure fluxes from CH₄ point sources.

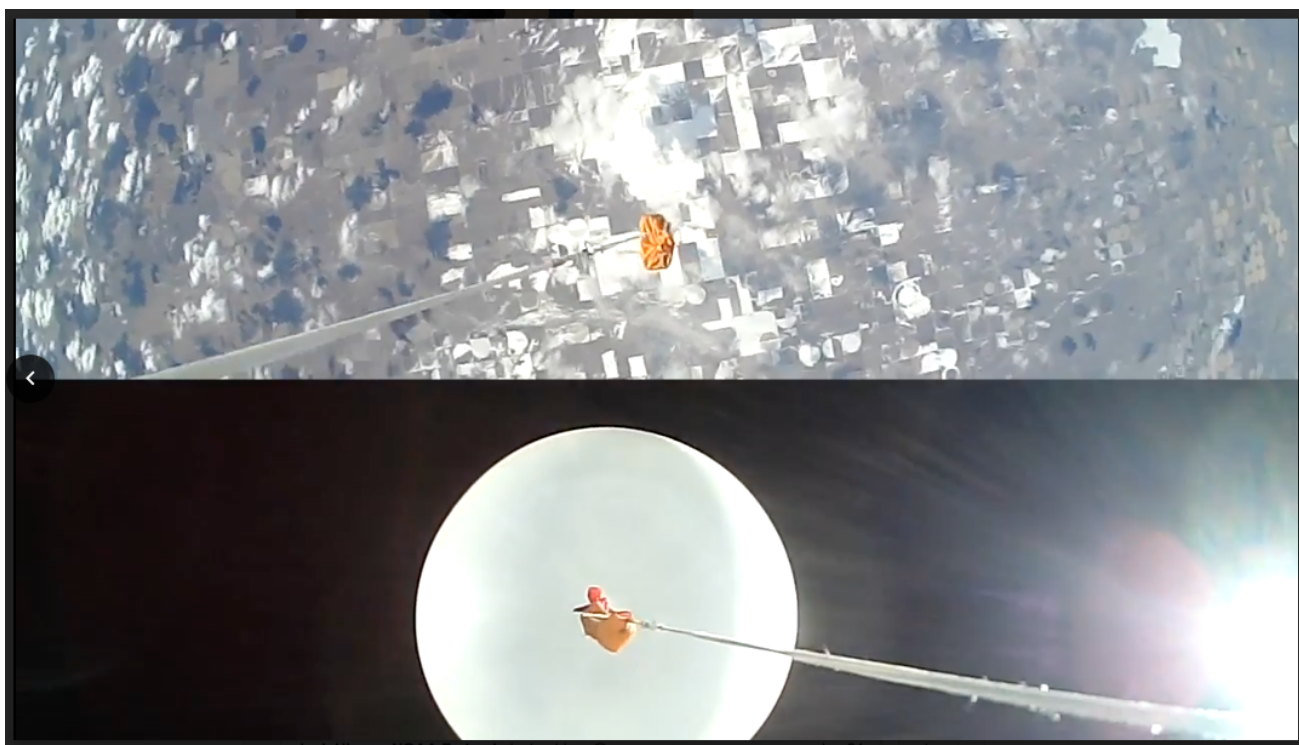


Figure 1. The AirCore profiler at its apex (30 km, ~100,000 ft) immediately before descent: downward and upward views.

NOAA Frost Point Hygrometer (FPH) Comparisons, Measurement Uncertainties and Recent Instrument Improvements

E. Hall^{1,2}, A.F. Jordan^{1,2}, D.F. Hurst^{1,2}, S.J. Oltmans³, H. Vömel⁴, B. Kühnreich^{5,6}, V. Ebert^{7,6}, S. Khaykin⁸, S. Davis^{1,9} and L. Kalnajs¹⁰

¹Cooperative Institute for Research in Environmental Sciences (CIRES), University of Colorado, Boulder, CO 80309; 303-497-4288, E-mail: Emrys.Hall@noaa.gov

²NOAA Earth System Research Laboratory, Global Monitoring Division (GMD), Boulder, CO 80305

³Retired from NOAA Earth System Research Laboratory, Global Monitoring Division (GMD), Boulder, CO 80305

⁴National Center for Atmospheric Research (NCAR), Earth Observing Laboratory, Boulder, CO 80307

⁵Physikalisch-Technische Bundesanstalt, Braunschweig, Germany

⁶Center of Smart Interfaces, Technische Universität Darmstadt, Germany

⁷Physikalisch-Technische Bundesanstalt PTB, Braunschweig, Germany

⁸LATMOS, CNRS, Université de Versailles St. Quentin, Guyancourt, France

⁹NOAA Earth System Research Laboratory, Chemical Sciences Division (CSD), Boulder, CO 80305

¹⁰University of Colorado, Laboratory for Atmospheric and Space Physics (LASP), Boulder, CO 80309

Accurate measurements of upper tropospheric and lower stratospheric water vapor contribute to many processes and feedback mechanisms and play an important role on the radiative forcing of our climate. The NOAA frostpoint hygrometer (FPH) is a balloon-borne instrument flown monthly at three sites to measure water vapor profiles up to 28 km. The ongoing 37-year FPH record from Boulder, Colorado is the longest continuous stratospheric water vapor record.

The NOAA FPH has an uncertainty in the stratosphere that is $< 6\%$ and $< 12\%$ in the troposphere (2σ). In 2008, a digital microcontroller version of the instrument improved upon the older versions by incorporating sunlight filtering along with better frost control. A new thermistor calibration technique was applied in 2014. This decreased the error in the thermistor calibration fit from $0.06\text{ }^\circ\text{C}$ to less than $0.01\text{ }^\circ\text{C}$ over the full range of frostpoint or dewpoint temperatures measured during a profile ($-93\text{ }^\circ\text{C}$ to $+20\text{ }^\circ\text{C}$).

Atmospheric chamber comparisons between the NOAA FPH and the direct tunable diode laser absorption spectrometer MC-PicT-1.4 during AquaVIT-2 in Karlsruhe, Germany are presented. Dual instrument balloon flights comparing vertical profiles between the NOAA FPH and the cryogenic frostpoint hygrometer (CFH) as well as the Lyman-alpha fluorescence hygrometer (FLASH-B) also show good agreement providing confidence in the accuracy of the FPH measurements.

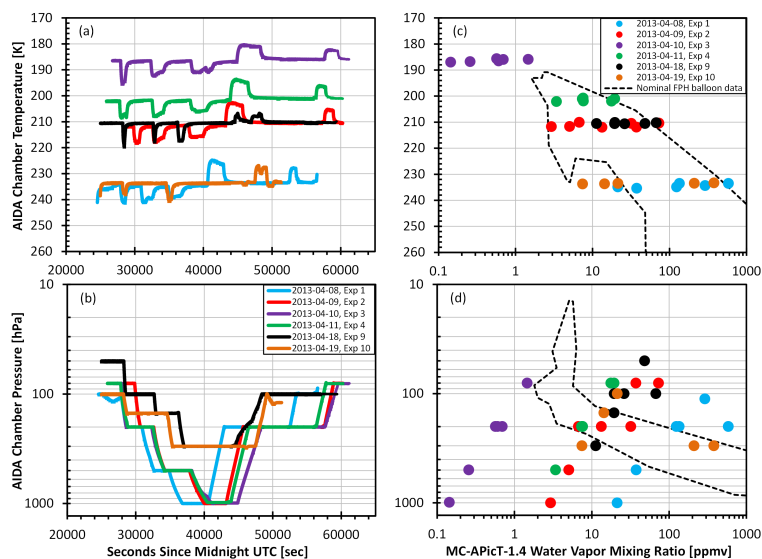


Figure 1. Daily time series of temperatures (a) and pressures (b) for all data during the six non-blind AquaVIT-2 experiments are shown. The relationship between chamber temperature and pressure with 36 individual stable water vapor mixing ratio segments is shown in panels (c) and (d), respectively. Areas contained by dashed lines indicate the range of water vapor and temperature in the actual atmosphere.

Homogenizing NOAA's Ozonesonde Data Set Improves Comparison with Satellite-derived Vertical Ozone Profiles

C.W. Sterling^{1,2}, B.J. Johnson², S.J. Oltmans³, P. Cullis^{1,2}, A. Jordan^{1,2}, E. Hall^{1,2} and D. Hubert⁴

¹Cooperative Institute for Research in Environmental Sciences (CIRES), University of Colorado, Boulder, CO 80309; 303-497-4291, E-mail: chance.sterling@noaa.gov

²NOAA Earth System Research Laboratory, Global Monitoring Division (GMD), Boulder, CO 80305

³Retired from NOAA Earth System Research Laboratory, Global Monitoring Division (GMD), Boulder, CO 80305

⁴Royal Belgian Institute for Space Aeronomy, Brussels, Belgium

NOAA recently completed a long and arduous process of ‘homogenizing’ the 50+ year record of vertical ozone profiles measured by the electrochemical concentration cell (ECC) ozonesonde. The homogenization effort fixed historical data processing errors and derived functions to correct sensing solutions and instrumental biases to an ozone photometer. In this analysis, the vertical ozone profiles of both the homogenized and unhomogenized data sets are compared to a suite of satellite instruments capable of making similar, lower resolution ozone profile measurements. The analysis determined that the three functions derived for the 1% Full Buffer Solution, 2% No Buffer Solution, and the 6A sonde type biases all improved the comparison between the ozonesondes and the satellites. Additionally, the methodology for the individual, unique uncertainty calculations added to each ozonesonde profile is presented here. NOAA’s homogenization effort has removed the largest biases associated with changes in the ozonesonde record, improved comparisons with satellite measurements, and calculated the uncertainty in the ozone partial pressure with a bottom-up approach.

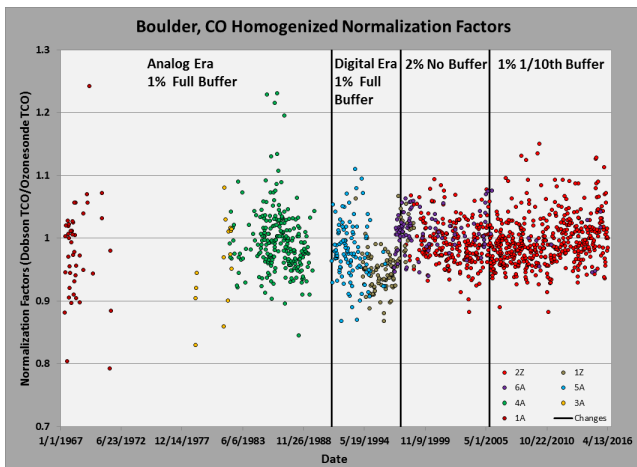


Figure 1. Normalization factors (Dobson Total Column Ozone/Ozonesonde Total Column Ozone) for the 50+ year ECC ozonesonde record in Boulder, Colorado.

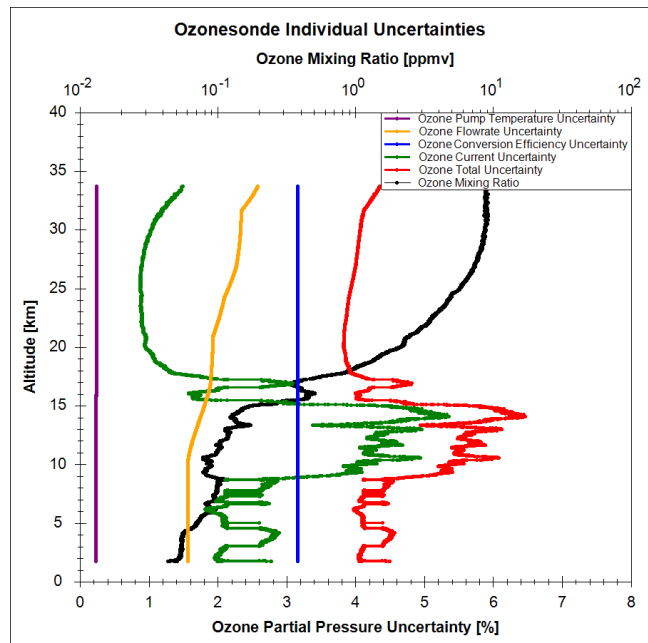


Figure 2. The total and individual components of the uncertainty in the ozone partial pressure vs. altitude.

SHADOZ (Southern Hemisphere Additional Ozonesondes) Network Report: Updates and Station Activities

A.M. Thompson¹, J. Witte^{2,1} and R.M. Stauffer^{3,1}

¹NASA Goddard Space Flight Center (GSFC), Atmospheric Chemistry and Dynamics Laboratory, Greenbelt, MD 20771; 301-614-5905, E-mail: anne.m.thompson@Nasa.gov

²Science Systems and Applications, Inc. (SSAI), Lanham, MD 20706

³Universities Space Research Association (USRA) - NASA Postdoctoral Program (NPP), Columbia, MD 21046

SHADOZ (Southern Hemisphere Additional Ozonesondes) has collected more than 7,000 profile sets from ozonesondes and radiosondes in the tropics and subtropics since 1998. Measurements originate at 14 long-term stations; a map of the operational stations and data are archived at <http://tropo.gsfc.nasa.gov/shadoz>. The NOAA/GMD Ozone and Water Vapor Group is a major part of SHADOZ data collection, training, and data quality assurance protocols. Through affiliation with the Network for Detection of Atmospheric Composition Change (NDACC; www.ndsc.ncep.noaa.gov) and posting of profiles to the NASA Aura Validation Data Center (AVDC) and WMO's World Ozone and UV Data Centre (woudc.org), SHADOZ data are distributed across the satellite, monitoring and modeling communities. We review recent major activities of SHADOZ, including re-activation of several SHADOZ stations. The most significant new SHADOZ activity is the first major reprocessing of the 18-year ozonesonde dataset to account for changes in ozonesonde instrumentation and biases among stations (Witte et al., GMAC Paper; *JGR*, in review). Also significant - we have applied innovative ozone profile classification, e.g., Self-Organizing Maps (Stauffer et al., *JGR*, 2016), to SHADOZ data. SOM climatologies are associated with meteorological variability and offer a value-added alternative to simple monthly means for model evaluation and satellite algorithms.

SHADOZ Sites: <https://tropo.gsfc.nasa.gov/shadoz>



Figure 1. Operational SHADOZ stations in 2016-2017.

Ozone Vertical Profile Measurements in the Northern Front Range of Colorado in July-August 2014 during FRAPPE and DISCOVER-AQ

S.J. Oltmans¹, L. Cheadle^{2,3}, B.J. Johnson³, R.C. Schnell³, C.W. Sterling^{2,3}, A.M. Thompson⁴, E.G. Hall^{2,3}, A. McClure-Begley^{2,3}, A.F. Jordan^{2,3} and J. Wendell³

¹Retired from NOAA Earth System Research Laboratory, Global Monitoring Division (GMD), Boulder, CO 80305; 303-497-6676, E-mail: samuel.j.oltmans@noaa.gov

²Cooperative Institute for Research in Environmental Sciences (CIRES), University of Colorado, Boulder, CO 80309

³NOAA Earth System Research Laboratory, Global Monitoring Division (GMD), Boulder, CO 80305

⁴NASA Goddard Space Flight Center (GSFC), Atmospheric Chemistry and Dynamics Laboratory, Greenbelt, MD 20771

Ozone (O₃) and temperature profiles were measured from tethered ozonesondes, from release ozonesondes, and continuously from a 300 m tower instrumented at two levels during the FRAPPE/DISCOVER-AQ campaigns in summer 2014. Tethersonde measurements were made on 3 days at a site west of Fort Collins typically, between 8:30 AM and 4:30 PM, averaging 40 profiles a day. Forty release ozonesondes were flown from Platteville with multiple profiles on a number of days. Continuous O₃ profiles from a tall tower (6 and 300 m) east of Boulder tracked O₃ variability through the experiment. The release ozonesondes demonstrated the important role of morning mixing from the upper boundary layer or lower free troposphere into the lower boundary layer. This mixing established the mid-morning boundary layer O₃ mixing ratio from which the daily photochemical production progressed. The generally constant mixing ratio with height and highest mixing ratios above the surface seen in the near-continuous tethersonde profiles indicate that photochemical O₃ production was taking place throughout the profile. This suggests that O₃ precursors are mixed through the boundary layer enabling widespread O₃ production. Tethersonde wind measurements on August 3, a high O₃ day at Fort Collins, showed consistent winds out of the southeast indicating a source of O₃ precursors from oil and gas operations. O₃ growth rates on high O₃ days (peak hourly value ≥75 ppb) computed during the time of peak O₃ production (10:00 AM – 3:00 PM) was in the range of 4.5-6 ppbv/hour through the measured profile from both the tethersonde and tower measurements.

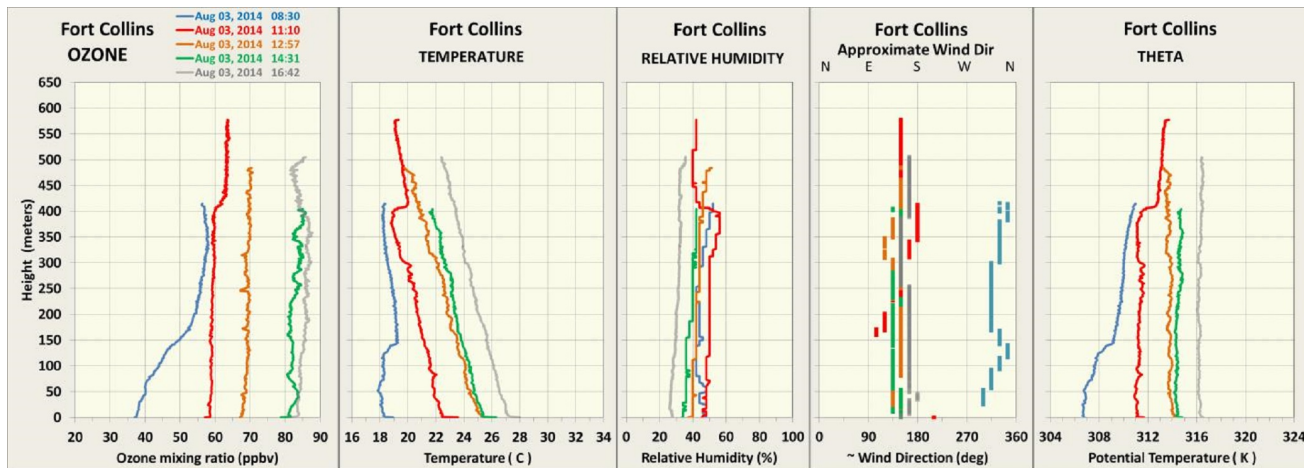


Figure 1. Tethered ozonesonde profiles from Fort Collins on August 3, 2014 showing ozone buildup during the day.

Influence of Stratospheric Intrusions on the Lower Free Tropospheric Ozone at Lulin Atmospheric Background Station

C. Ou-Yang^{1,2}, J. Lee², N. Lin^{1,2}, M. Yen¹ and J. Wang²

¹National Central University, Department of Atmospheric Sciences, Chung-Li, Taiwan; 886-3-4227151 ext. 65543, E-mail: cfouyang@cc.ncu.edu.tw

²National Central University, Department of Chemistry, Chung-Li, Taiwan

Stratospheric intrusions (SI) often bring ozone (O_3) rich air with low humidity from the stratosphere rapidly into the troposphere. Cutoff lows, tropopause folds, frontal passages and surface high-pressure systems are mainly counted for the occurrence of SI. In this study, we present 5 years of O_3 data measured at Lulin Atmospheric Background Station (LABS; 23.47°N, 120.87°E, 2862m a.s.l.) located in the subtropical East Asia from April 2006 to March 2011. The mean O_3 mixing ratio was 32.8 ± 15.2 ppb, whereas the O_3 was enhanced ~ 11.5 ppb on average during the 64 detected SI events over the 5 years. Distinct seasonal variation of O_3 was observed with a springtime maximum and a summertime minimum, which was predominately shaped by the long-range transport of biomass burning air masses from Southeast Asia and oceanic influences from the Pacific, respectively. Diurnal cycles were also observed at the LABS, with a maximum around midnight and a minimum during noontime. The impacts and characteristics of SI events during the measurement period were investigated. Selected SI events were also discussed in associated with Modern Era Retrospective Analysis-2 (MERRA-2) assimilated data provided by NASA/Goddard Space Flight Center in this study.

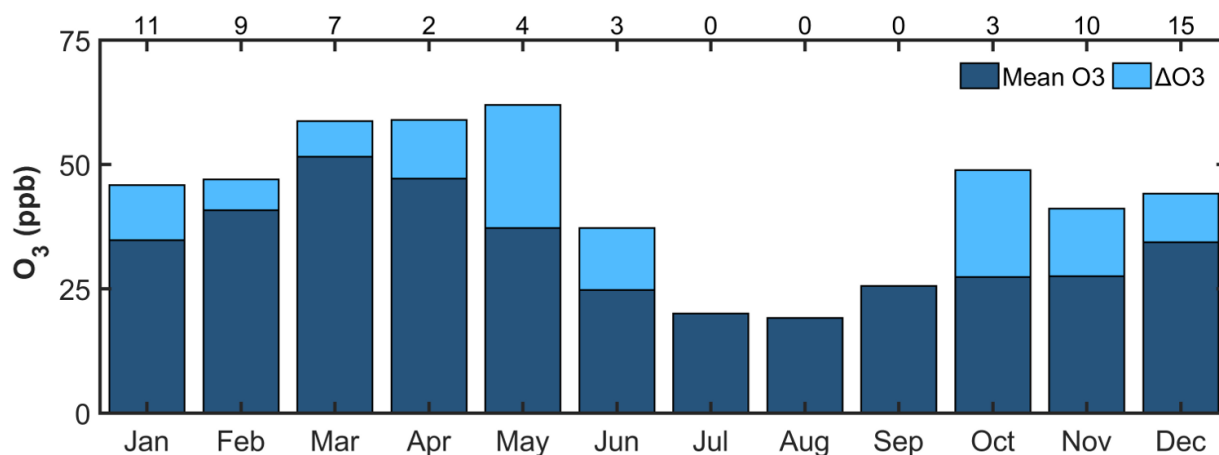


Figure 1. Seasonal variation of O_3 and enhanced levels by SI at Mt. Lulin from April 2006 to March 2011. Numbers of detected events in each month are listed on the top of the figure.

Regional Trend Analysis of Surface Ozone Observations from Monitoring Networks in Eastern North America, Europe and East Asia

K. Chang^{1,2}, I. Petropavlovskikh^{3,2}, O. Cooper^{3,4}, M.G. Schultz⁵ and T. Wang⁶

¹National Research Council Post-Doc, Boulder, CO 80305; 720-243-5287, E-mail: kai-lan.chang@noaa.gov

²NOAA Earth System Research Laboratory, Global Monitoring Division (GMD), Boulder, CO 80305

³Cooperative Institute for Research in Environmental Sciences (CIRES), University of Colorado, Boulder, CO 80309

⁴NOAA Earth System Research Laboratory, Chemical Sciences Division (CSD), Boulder, CO 80305

⁵Institute for Energy and Climate Research, Troposphere IEK-8, Research Center, Juelich, Germany

⁶NASA Jet Propulsion Laboratory, California Institute of Technology, Pasadena, CA 91109

Surface ozone is a greenhouse gas and pollutant detrimental to human health as well as crop and ecosystem productivity. The Tropospheric Ozone Assessment Report (TOAR) is designed to provide the research community with an up-to-date observation based overview of tropospheric ozone's global distribution and trends. We conducted a spatial and temporal trend analysis using the TOAR database of global surface ozone observations for different regions and for several metrics in summertime (April-September) over 2000-2014. The generalized additive mixed model (GAMM) analysis of several ozone metrics indicates that East Asia has the greatest human and plant exposure to ozone pollution under current monitoring coverage, with increasing ozone levels through 2014. The results also show that ozone mixing ratios continue to decline significantly over eastern North America and Europe, however, there is less evidence for decreases of daytime average ozone at urban sites.

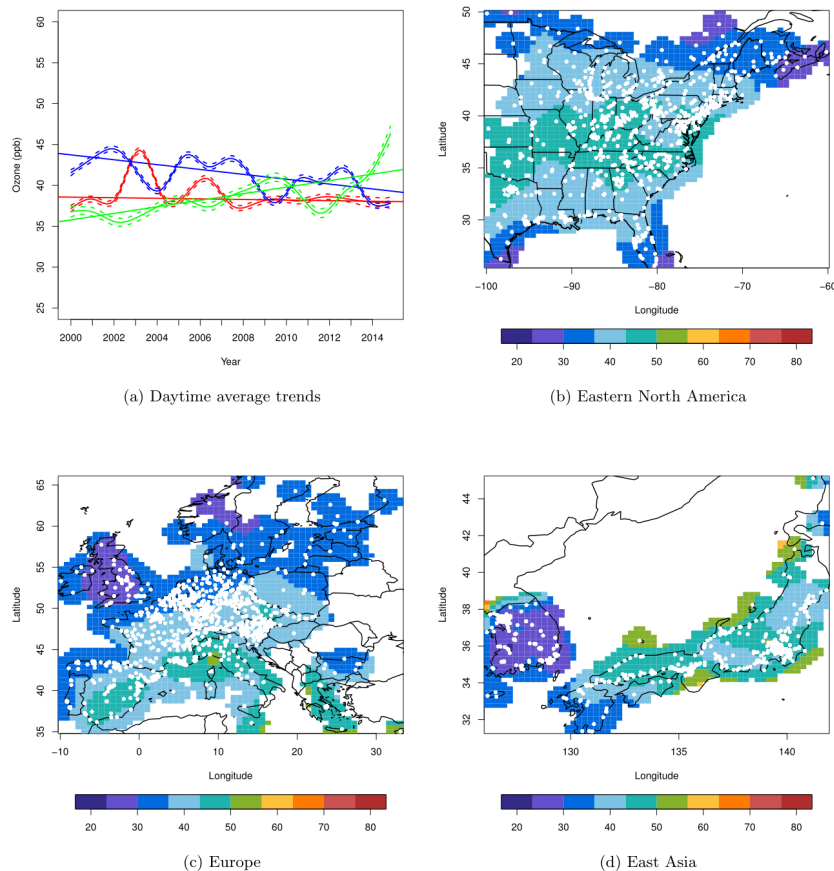


Figure 1. Spatial and temporal trends for summertime mean of daytime average in different regions: estimated long-term changes (ppb) in eastern North America (blue), Europe (red) and East Asia (green), and their spatial distributions. The white points indicate the locations of stations.

Overview of the Long-term Ozone Trends and Uncertainties in the Stratosphere (LOTUS) SPARC Activity

I. Petropavlovskikh^{1,2}, D. Hubert³, S. Godin-Beekmann⁴, R. Damadeo⁵, B. Hassler⁶ and V. Sofieva⁷

¹Cooperative Institute for Research in Environmental Sciences (CIRES), University of Colorado, Boulder, CO 80309; 303-497-6279, E-mail: Irina.Petro@noaa.gov

²NOAA Earth System Research Laboratory, Global Monitoring Division (GMD), Boulder, CO 80305

³Royal Belgian Institute for Space Aeronomy, Brussels, Belgium

⁴Université de Versailles Saint-Quentin en Yvelines (UVSQ), Centre National de la Recherche Scientifique (CNRS), Guyancourt, France

⁵NASA Langley Research Center, Hampton, VA 23681

⁶Bodeker Scientific, Alexandra, New Zealand

⁷Finnish Meteorological Institute, Helsinki, Finland

World Meteorological Organization United Nations Environment Programme (WMO/UNEP) Assessments on the state of the ozone (O₃) layer (aka O₃ Assessments) require an accurate evaluation of both total O₃ and O₃ profile long-term trends. These trend results are of utmost importance in order to evaluate the success of the Montreal Protocol with regards to the recovery of the O₃ layer and the effect of climate change on this recovery, in the main regions of the stratosphere (polar, mid-latitudes, tropics). A previous activity sponsored by Stratosphere-troposphere Processes And their Role in Climate (SPARC), International Ozone Commission (IO₃C), IGACO-O₃ (Integrated Global Atmospheric Chemistry Observations) and NDACC (SI²N) successfully provided estimates of O₃ profile decreasing trend in the period 1979 - 1997 and sign change of the trend in the period 1998 – 2012, from a variety of long-term records, however results on the significance of the trends in the latter period were different from those published in the WMO 2014 O₃ Assessment report. For the WMO/UNEP 2018 O₃ Assessment, a clearer understanding of O₃ trends and their significance as a function of altitude and latitude is needed, nearly 20 years after the peak of O₃ depleting substances in the stratosphere. In recent years, new merged satellite data sets and long awaited homogenized ozonesonde data series have been produced. There is thus a strong interest in the scientific community to understand limitations in determining significance of O₃ recovery. In order to address the issues left pending after the end of SI²N, a comprehensive evaluation of all long term data sets available together with their relative drifts is needed. Evaluation of error propagation in O₃ trend calculation is also required. This presentation will provide an overview of the LOTUS project goals and highlights of the emerging results.



Figure 1. LOTUS activity for SPARC.

Removal of Seasonal Bias from Dobson Spectrophotometer Records using Reanalysis

B. Noiro¹, I. Petropavlovskikh^{1,2}, G. McConville^{1,2}, K. Miyagawa³, B.J. Johnson² and S. Strahan⁴

¹Cooperative Institute for Research in Environmental Sciences (CIRES), University of Colorado, Boulder, CO 80309; 303-497-6279, E-mail: brandon.noiro@gmail.com

²NOAA Earth System Research Laboratory, Global Monitoring Division (GMD), Boulder, CO 80305

³Guest Scientist at NOAA Earth System Research Laboratory, Global Monitoring Division (GMD), Boulder, CO 80305

⁴Universities Space Research Association (USRA), NASA Goddard Space Flight Center (GSFC), Greenbelt, MD 20771

The Dobson spectrophotometer is an ozone-observing (O_3) instrument that has been in operation in the NOAA O_3 -observing network since the early 1960's. Dobson spectrophotometers measure differential absorption in solar ultraviolet (UV) spectrum and use lab-measured O_3 absorption cross sections to derive total column ozone. However, differential absorption in UV spectrum depends on stratospheric temperature. A correction for the historical Dobson dataset is proposed to account for the daily variability of stratospheric temperatures via an O_3 -weighted temperature. Presently, Dobson observations use Bass and Paur (1985) O_3 absorption dataset. Recently, new O_3 cross section lab measurements were acquired and published by Serdyuchenko et al. (2014). Operational O_3 monitoring at all World Meteorological Organization ground-based stations relies on a single static temperature of -46.3°C . Daily stratospheric temperatures deviate from this reference temperature and directly affect the measurement. The difficulty of applying a correction is having a temperature and O_3 profile available at the same time as a Dobson measurement. Ozonesondes are not a daily occurrence and satellites generally pass over a station once every one to two days. Therefore, we propose using a reanalysis product to account for daily variability in O_3 and stratospheric temperatures to correct Dobson historical record. NASA's GMI-MERRA product is used for this project. We will present results of daily corrections for NOAA Dobson total O_3 record and compare against other co-located O_3 measurements, including satellites.

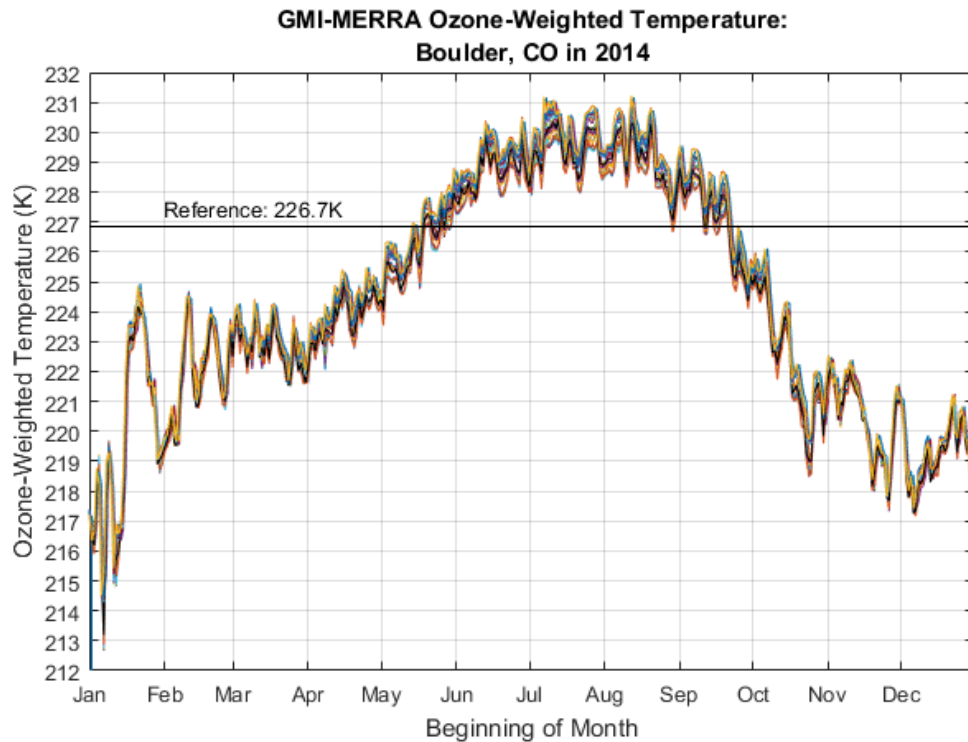


Figure 1. Time series of effective temperatures derived using GMI-MERRA dataset for Boulder, CO. Currently used operational static temperature is shown as reference.

Comparison of Ozone Retrievals from the Umkehr Reprocessing Version and Satellites

K. Miyagawa¹, I. Petropavlovskikh^{2,3}, G. McConville^{2,3}, A. McClure-Begley^{2,3} and R.D. Evans⁴

¹Guest Scientist at NOAA Earth System Research Laboratory, Global Monitoring Division (GMD), Boulder, CO 80305; 303-497-6679, E-mail: miyagawa.koji@noaa.gov

²Cooperative Institute for Research in Environmental Sciences (CIRES), University of Colorado, Boulder, CO 80309

³NOAA Earth System Research Laboratory, Global Monitoring Division (GMD), Boulder, CO 80305

⁴Retired from NOAA Earth System Research Laboratory, Global Monitoring Division (GMD), Boulder, CO 80305

The long-term record of Umkehr measurement by the NOAA Dobson spectrophotometer has been reprocessed by updating calibration procedures and applying new quality-controlled tools under the updated Dobson automation software. In this study we present the comparison of Dobson Umkehr ozone profiles from three NOAA ozone network stations (Boulder, Mauna Loa and Lauder) against satellite overpass data, i.e. Aura Microwave Limb Sounder (MLS) and Ozone Mapping Profiler Suite (OMPS) overpasses. The satellite data are spatially (less than 200 km) and temporally (within 24 hours) matched with Dobson Umkehr measurements at the station. The retrieved individual Umkehr Averaging Kernels (AKs) are applied to smooth the overpass satellite profiles prior to comparisons. Comparisons show good agreement in the middle stratosphere (Umkehr layers 5–7) and in the upper stratosphere (layer 8 and combined layers 8, 9, and 10). However, in the lower stratosphere (Umkehr layers 2-4) a relatively large difference up to 20% is found. In addition, we discuss comparisons with the Suomi-NPP OMPS satellite and other co-located instruments at NOAA stations.

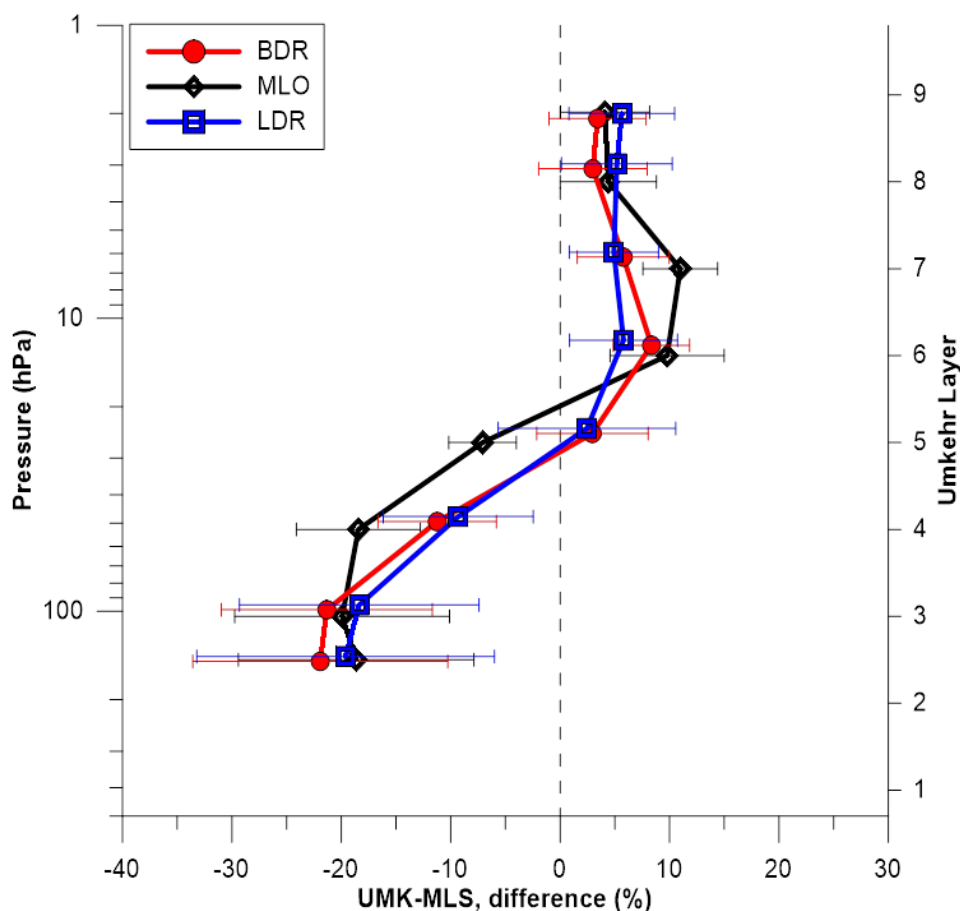


Figure 1. Shown are differences between Umkehr and Aura MLS data matched (200 km less than overpass distance and within 24 hours with Umkehr) from 2004 to 2016 at Boulder, Mauna Loa and Lauder station.

Differences Between the Reprocessed Dobson Total Ozone and Satellite Observation Records

K. Miyagawa¹, I. Petropavlovskikh^{2,3}, G. McConville^{2,3}, A. McClure-Begley^{2,3} and R.D. Evans⁴

¹Guest Scientist at NOAA Earth System Research Laboratory, Global Monitoring Division (GMD), Boulder, CO 80305; 303-497-6679, E-mail: miyagawa.koji@noaa.gov

²Cooperative Institute for Research in Environmental Sciences (CIRES), University of Colorado, Boulder, CO 80309

³NOAA Earth System Research Laboratory, Global Monitoring Division (GMD), Boulder, CO 80305

⁴Retired from NOAA Earth System Research Laboratory, Global Monitoring Division (GMD), Boulder, CO 80305

The entire Level-Zero data record from the NOAA Dobson Ozone Spectrophotometer network has been reprocessed with a new software system, with updated quality control features. The reprocessed new data set from the 1960s will be provided to the World Ozone and Ultraviolet Radiation Data Centre (WOUDC) and Network for the Detection of Atmospheric Composition Change (NDACC) archives.

This study estimates the long-term record difference with various satellite observations for assessment of the reprocessed total ozone (O_3) in sixteen NOAA worldwide stations. For comparison we used the gridded data and overpass data from the NASA Goddard Space Flight Center (Nimbus-4 BUUV, Nimbus-7 SBUV, Nimbus 7 TOMS, Earth Probe TOMS, Aura OMI, NPP OMPS and NOAA SBUV/2). The daily O_3 on a station used the bi-linear interpolation algorithm from the gridded data. Additionally, we surveyed different correlations from the latitude (or longitude) of a station for gridded data matching. The official algorithm for retrieval of O_3 from Dobson measurements includes static absorption coefficients derived using Bass and Paur (1985) cross-sections. We estimated the impact of use of different O_3 absorption coefficients (DBM and IUP) and temperature dependent coefficients using McPeters and Labow 2011 climatology.

In this analysis, OMI (Gridded Level 3e) shows the high overall quality without latitude dependence. The time series comparisons show an agreement within 1% over the past 13 years (Fig. 1). Additionally, high altitude Mauna Loa, Hawaii has good agreement due to the O_3 below the station which the satellite sees.

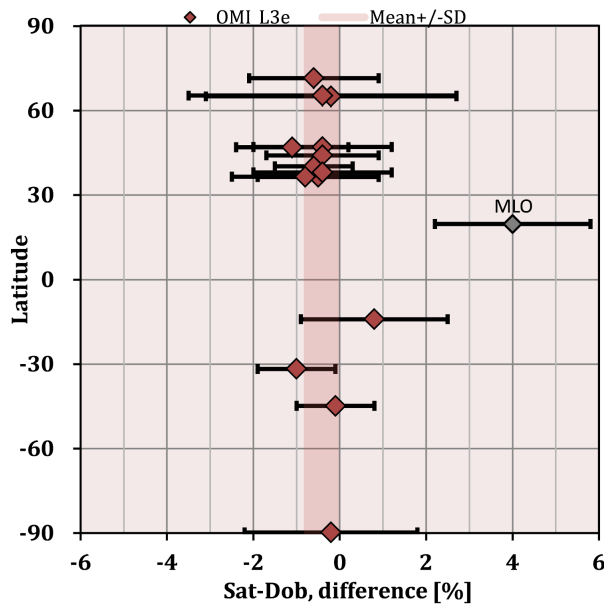


Figure 1. Difference of the total O_3 with Dobson (ADDS matched) and OMI Level 3e satellite (from 2004 to 2016). The error bar shows +/- 1 standard deviation.

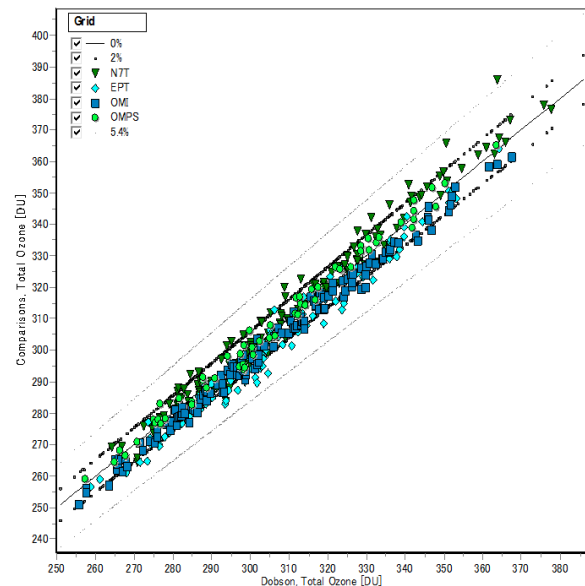


Figure 2. Monthly average scattering of the total O_3 of Dobson and gridded satellites at Boulder. Relation plot period 1979-2016.

Congregation of Vapors: Towards a Synoptic View of Water Vapor in Support of Airborne IR Astronomy

J. Van Cleve^{1,2}, T. Roellig², A. Meyer^{3,2}, D.F. Hurst^{4,5}, E.G. Hall^{4,5} and A.F. Jordan^{4,5}

¹SETI Institute, Mountain View, CA 94043; 650-336-4779, E-mail: jeffrey.vancleve@nasa.gov

²NASA Ames Research Center, Moffett Field, CA 94035

³SOFIA Science Center, Universities Space Research Association (USRA), Moffett Field, CA 94035

⁴Cooperative Institute for Research in Environmental Sciences (CIRES), University of Colorado, Boulder, CO 80309

⁵NOAA Earth System Research Laboratory, Global Monitoring Division (GMD), Boulder, CO 80305

The Stratospheric Observatory for Infrared Astronomy (SOFIA) airborne astronomical observatory operates at the physical boundary between the troposphere and stratosphere, and at the intellectual boundary between atmospheric science and infrared astronomy. Planning and calibration at water-sensitive wavelengths, either in narrow bands at wavelengths $< 28 \mu\text{m}$ or throughout the $28\text{-}300 \mu\text{m}$ range, requires the prediction and measurement of the total precipitable water (TPW) above the aircraft when observing at altitudes between 10.7 and 13.7 km. Nadir sensors, limb sensors and *in situ* radiosonde measurements cannot simultaneously provide the sensitivity and temporal, spatial and vertical resolution required to calibrate SOFIA data. Thus, SOFIA has an on-board 183 GHz radiometer (WVM) to measure TPW. Yet using atmospheric models to convert WVM TPW to infrared radiation (IR) absorption corrections is not straightforward. Even cross-calibration between different bands of the same SOFIA instrument give inconsistent results (Guan et al., 2012). In search of additional data or model insights, we looked for correlations between mass mixing ratio (MMR) and TPW in NOAA frost point hygrometer (FPH) data to assess the degree to which MMR at a given altitude is a good predictor of TPW above that altitude. FPH MMR data is sampled every 0.25 km at altitudes up to 25 km, and collected during monthly balloon flights over Boulder (Colorado), Hilo (Hawaii), and Lauder (New Zealand) under mostly clear sky conditions. TPW is then simply the integral over pressure of MMR, with a small constant offset for the contribution above 25 km. We combined an empirical power-law with the Haas & Pfister (HP98) model to jointly fit data from all 3 launch sites, examples of which are shown in Figure 1. We conclude that an automated atmospheric science research package containing an aircraft FPH (Buck Instruments CR-2) and possibly other instruments, similar to the successful IAGOS-CARIBIC package for commercial airliners, would allow SOFIA to serve atmospheric science as well as astronomy.

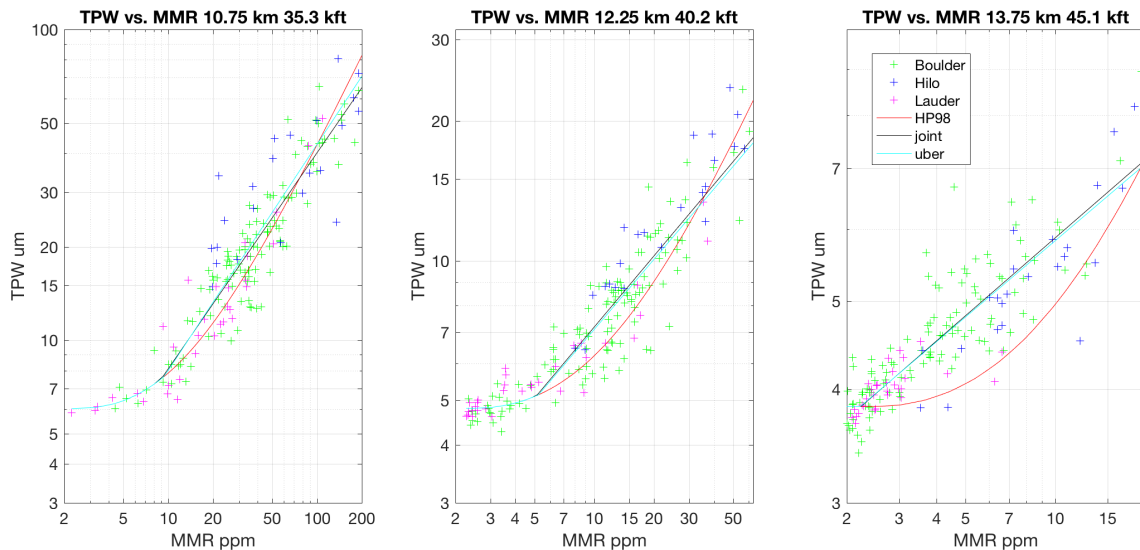


Figure 1. Example plots for various altitudes showing correlation of TPW above altitude vs. Mass Mixing Ratio (MMR) at altitude for all FPH descent data from all 3 stations. The uber fit lets the power-law prefactor and exponent themselves be simple functions of altitude. At the lowest MMRs, the uber, joint, and HP98 fits are indistinguishable.

A New Data Product for the NOAA Environmental UV-ozone Brewer Network (NEUBrew) Aerosol Optical Depth in the UV Spectral Region

P. Disterhoft^{1,2} and S. Stierle^{1,2}

¹Cooperative Institute for Research in Environmental Sciences (CIRES), University of Colorado, Boulder, CO 80309; 303-497-6355, E-mail: patrick.disterhoft@noaa.gov

²NOAA Earth System Research Laboratory, Global Monitoring Division (GMD), Boulder, CO 80305

The Brewer Mark IV spectrophotometer was designed to passively measure the total column ozone using an algorithm specific to its optical geometry. The Brewer makes near-simultaneous measurements of ultraviolet (UV) irradiance at five separate wavelengths. It performs these measurements through a sun-pointing prism that provides an approximate 2.3 degree field of view. The chosen wavelengths also provide for the retrieval of total column sulfur dioxide (SO₂). The Brewer is normally operated in an automated schedule that makes these direct-sun measurements throughout the day, thereby providing narrow field of view irradiance measurements at five UV wavelengths through different slant paths through the atmosphere. These are the exact type of measurements necessary for an aerosol optical thickness or if enough information is available an aerosol optical depth retrieval for one species. In our case, the objective is to retrieve the aerosol optical depth at the five Brewer ozone operational wavelengths, 306.3, 310.1, 313.5, 316.8, and 320.1 nm.

Due to the fact that the Brewer was designed to operate unattended, the data in the direct-sun output files are not raw. They have been corrected for dark count, dead-time, the natural log of the raw signal is taken, the temperature effects on the various neutral density filters, and Rayleigh scattering has been removed. Additionally, the Brewer makes the direct-sun irradiance measurements through a slanted quartz window, which imparts a degree of polarization to the input beam. The magnitude of the S and P polarization is a function of the incident angle to the quartz window, which is dependent on the solar zenith angle. The polarization is not dealt with in ozone retrievals since it is performed using the near simultaneous five irradiance measurements in a relative manner. This works for the ozone retrieval, but does not work for the aerosol optical depth retrievals, because the measurements are made at an individual wavelength over many hours. The time factor changes the incident angle to the quartz window, which in turn changes the throughput, due to polarization effects to the detection electronics.

To achieve the aerosol optical depth retrieval it is first necessary to back out some of the modifications that the Brewer main program applies to the raw data. The Rayleigh effects must first be removed, followed by the temperature corrections. The data are then plotted, the natural log of the adjusted data to the air mass. Perform a linear regression on these data points and extrapolating to zero air mass yields the signal that the Brewer would theoretically measure at the top of the atmosphere. This gives us our calibration factor which is used in the aerosol optical depth retrievals.

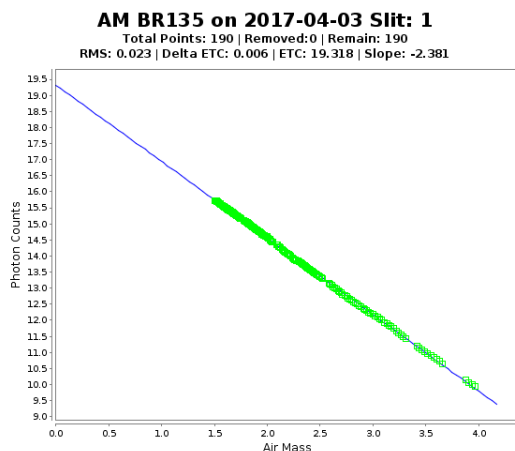


Figure 1. Langley Regression Example.

Significant Improvements in Pyranometer Nighttime Offsets Using High-Flow, DC Ventilation

M.C. Kutchenreiter¹, J.J. Michalsky^{2,3}, C.N. Long^{2,3} and A. Habte¹

¹National Renewable Energy Laboratory (NREL), Golden, CO 80401; 303-384-7900, E-mail: Mark.Kutchenreiter@nrel.gov

²Cooperative Institute for Research in Environmental Sciences (CIRES), University of Colorado, Boulder, CO 80309

³NOAA Earth System Research Laboratory, Global Monitoring Division (GMD), Boulder, CO 80305

Accurate solar radiation measurements using pyranometers are required to understand radiative impacts on the earth's energy budget, solar energy production, and to validate radiative transfer models. The accuracy of measured solar radiation depends on multiple conditions, such as instrument specification, measurement setup, and environmental conditions. Some pyranometers are equipped with ventilators which are used to keep the domes clean and dry; however, they affect instrument thermal offset as well. This poster examines different ventilation strategies. For the several commercial single-black-detector pyranometers and with ventilators examined here, high flow rate (50 cubic feet per minute (CFM) and higher), 12 VDC fans lower the offsets, lower the scatter, and improve the predictability of the offsets during the night compared to lower flow rate 35 CFM, 120 VAC fans operated in the same ventilator housings. Single-black-detector pyranometer nighttime average thermal offsets have reduced from approximately -7 Wm^{-2} using lower CFM AC fans, to -2 Wm^{-2} using higher CFM DC fans at Atmospheric Radiation Measurement (ARM) program Solar Infrared Radiation Station (SIRS) sites.

Black-and-white pyranometers which are mainly used to measure diffuse horizontal irradiance sometimes show improvement with DC fan ventilation, but in some cases the offsets are made slightly worse. Since the offsets for these black-and-white pyranometers are always small, usually no more than 1 Wm^{-2} , whether AC or DC ventilated, changing their ventilation to higher CFM DC fan ventilation is not imperative.

An important outcome of future research should be to clarify under what circumstances nighttime data can be used to predict daytime offsets.

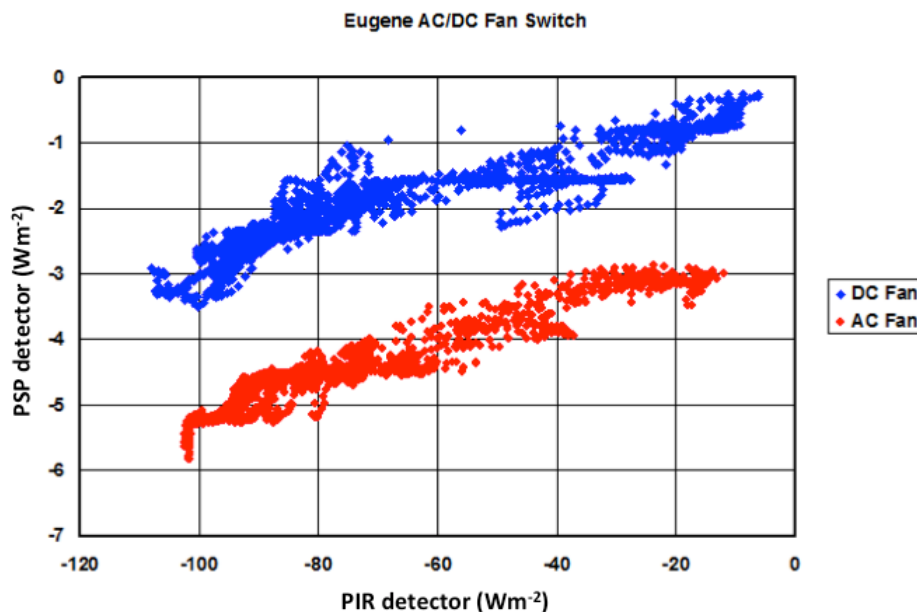


Figure 1. Nighttime thermal offset reduction and improvement is shown for an Eppley Precision Spectral Pyranometer (PSP) operated in a higher flow DC fan ventilator (blue) compared to operation in a lower flow AC fan ventilator (red) during a seven day test period at the University of Oregon.

Analysis of Solar Radiation Measurements at BSRN Lulin Candidate Station

N. Hsueh¹, S. Wang¹, N. Lin^{1,2}, Y. Lee³, S. Chang⁴, H. Huang¹ and C. Yao¹

¹National Central University, Department of Atmospheric Sciences, Chung-Li, Taiwan; +886-3-4227151-65519, E-mail: frankshue@gmail.com

²National Central University, Department of Chemistry, Chung-Li, Taiwan

³Central Weather Bureau, Observation Division, Taipei, Taiwan

⁴Environmental Protection Administration, Taipei City, Taiwan

Solar radiation plays an important role in the global energy balance, and largely determines the climatic conditions of the Earth. In order to better understand the solar radiation reaching Earth's surface, ground-based observations were established at Lulin Atmospheric Background Station (LABS; 23.47°N, 120.87°E; 2,862 m a.s.l.), which is now a Baseline Surface Radiation Network (BSRN) candidate station. This research focuses on the overall climatology of solar radiation at LABS during the period of 2010 to 2016. Previous studies show that from the 1980s to present, global brightening, which refers to a decadal increase in surface shortwave radiation, has been observed in many regions of the world. Equipped with broad-band shortwave and longwave radiometers (Kipp & Zonen CMP21 and CGR4, respectively) at LABS, we can analyze the seasonal variations and long-term trends of solar radiation from 2010 to 2016, and detect the global brightening phenomenon. In addition, comparisons with the solar radiation measurements at Mt. Jade (23.29°N, 120.57°E; 3,850 m a.s.l.) are included, enhancing the knowledge of radiation characteristics for the mountain area in central Taiwan. The long-term changes in aerosol optical depth (AOD) at LABS will also be analyzed, showing whether it accounts for the increasing and decreasing of surface solar radiation.

Keywords:

Surface solar radiation, global dimming/brightening phenomenon, aerosol optical depth



Figure 1. The overall view of Lulin station.



Figure 2. Sun tracker and radiometers used at Lulin station.

A Length-Scale Analysis of Variance for Many Constituents from Aircraft, Satellite and Model Results During the 2013 SENEX Field Study

S. McKeen^{1,2}, R. Ahmadov^{1,3}, N. Smith⁴, A. Gambacorta⁴, G. Frost², S. Kim^{1,2}, Y. Cui^{1,2}, B. McDonald¹, W.M. Angevine^{1,2}, M. Trainer², J. Peischl^{1,2}, T. Ryerson², C. Barnet⁴ and R.B. Pierce⁵

¹Cooperative Institute for Research in Environmental Sciences (CIRES), University of Colorado, Boulder, CO 80309; 303-497-5622, E-mail: Stuart.A.McKeen@noaa.gov

²NOAA Earth System Research Laboratory, Chemical Sciences Division (CSD), Boulder, CO 80305

³NOAA Earth System Research Laboratory, Global Systems Division (GSD), Boulder, CO 80305

⁴Science and Technology Corporation, Boulder, CO 80305

⁵NOAA National Environmental Satellite, Data, and Information Service (NESDIS), Advanced Satellite Products Branch, Madison, Wisconsin 53706

A useful perspective for analyzing the temporal or spatial variance of a time series measurement is by decomposing the signal into orthogonal functions that depend on the sample interval or length-scale. The fractal nature of free atmospheric turbulence is the determining factor in the scale dependence of variance, and has been found in previous studies to affect chemical constituents in the same manner as standard meteorological quantities. Fourier analysis of 8 constituents collected at 1 Hertz by the NOAA W-P3 aircraft during the 2013 Southeast Nexus (SENEX) field campaign are analyzed in terms of slopes of the power spectral density (PSD), focusing on the 25 to 200 km length-scale range. When spectra are averaged over several 500 mb flight legs, a very linear dependence is found on log-log plots of PSD versus inverse length-scale, with slopes varying within $\pm 30\%$, and close to the slope of $-5/3$ predicted from dimensional scaling theory of isotropic turbulence. A similar analysis is applied to WRF/Chem model results and observations derived from NOAA's Cross-track Infrared Sounder (CrIS) and Advanced Technology Microwave Sounder (ATMS) instruments from the Visible Infrared Imaging Radiometer Suite (VIIRS) by NOAA Unique Combined Atmospheric Processing System (NUCAPS), including profiles of temperature, water and several trace gases (e.g. O_3 , CO , CH_4 , CO_2 , HNO_3 , SO_2 , and N_2O). Comparisons with the aircraft data shows the model accounts for variance on length-scales greater than $\sim 6\Delta X$, where ΔX is the model horizontal resolution (12km). The model length-scale dependence of variance in the 200 to 1000 km range is quite similar to that of the NUCAPS retrievals for many variables and is likewise consistent with the expected $-5/3$ power law scaling of isotropic turbulence. Several gas phase species from NUCAPS show a length-scale dependence inconsistent with the model and NUCAPS H_2O and O_3 . A technique is provided to estimate the appropriate horizontal averaging lengths for those species that exhibit this inconsistency.

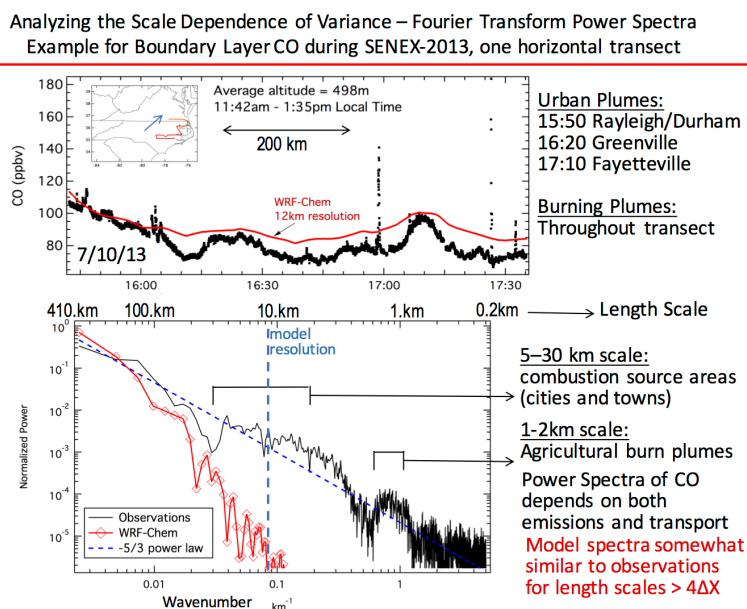


Figure 1. Example of time series and normalized Fourier power of CO from a NOAA-P3 aircraft transect over North Carolina during the 2013 SENEX campaign.

Continuous Long-term Monitoring of Atmospheric Key Species at the GAW Global Station Hohenpeissenberg

D. Kubistin, W. Thomas, B. Briel, A. Claude, T. Elste, J. Englert, H. Flentje, R. Holla, M. Lindauer, J. Muller, M. Schumacher and C. Plass-Duelmer

Meteorological Observatory Hohenpeissenberg, German Meteorological Service, Hohenpeissenberg, Germany; +49-69-80629740, E-mail: dagmar.kubistin@dwd.de

Long-term observations of trace gases, radiation and aerosol are crucial for understanding their impact on human health and climate change. They provide information, e.g. on ozone trends, the self-cleaning capacity and atmospheric processes, as well as being an independent measure on anthropogenic emission regulations. Since 1995, the atmospheric composition, characteristic for central Europe, has been continuously monitored at the global Global Atmospheric Watch (GAW) station Hohenpeissenberg. The tropospheric components include reactive gases such as *in situ* ozone, nitrogen oxides (NO, NO₂, NO_x, PAN), carbon monoxide, sulphur dioxide, anthropogenic and biogenic VOCs, sulfuric acid, radical species (OH, RO_x), total hydroxyl (OH) reactivity and recently the greenhouse gases carbon dioxide, methane and nitrous oxide in the framework of ICOS (Integrated Carbon Observation System). Aerosol parameters are covered by particle number, particle mass, size distribution, scattering and absorption coefficients, spectral AOD measurements, extinction and (attenuated) backscatter profiles from a multi-channel Raman Lidar (Polly^{XT}) and a ceilometer, respectively. The chemical composition of water-soluble aerosols and of precipitation is provided by filter measurements and wet chemical analysis and are further complemented by measurements of an Aerosol Chemical Speciation Monitor.

Here we present the time series of selected trace gases, radiation and aerosol parameters, revealing their evolution over the past two decades at this central European station.

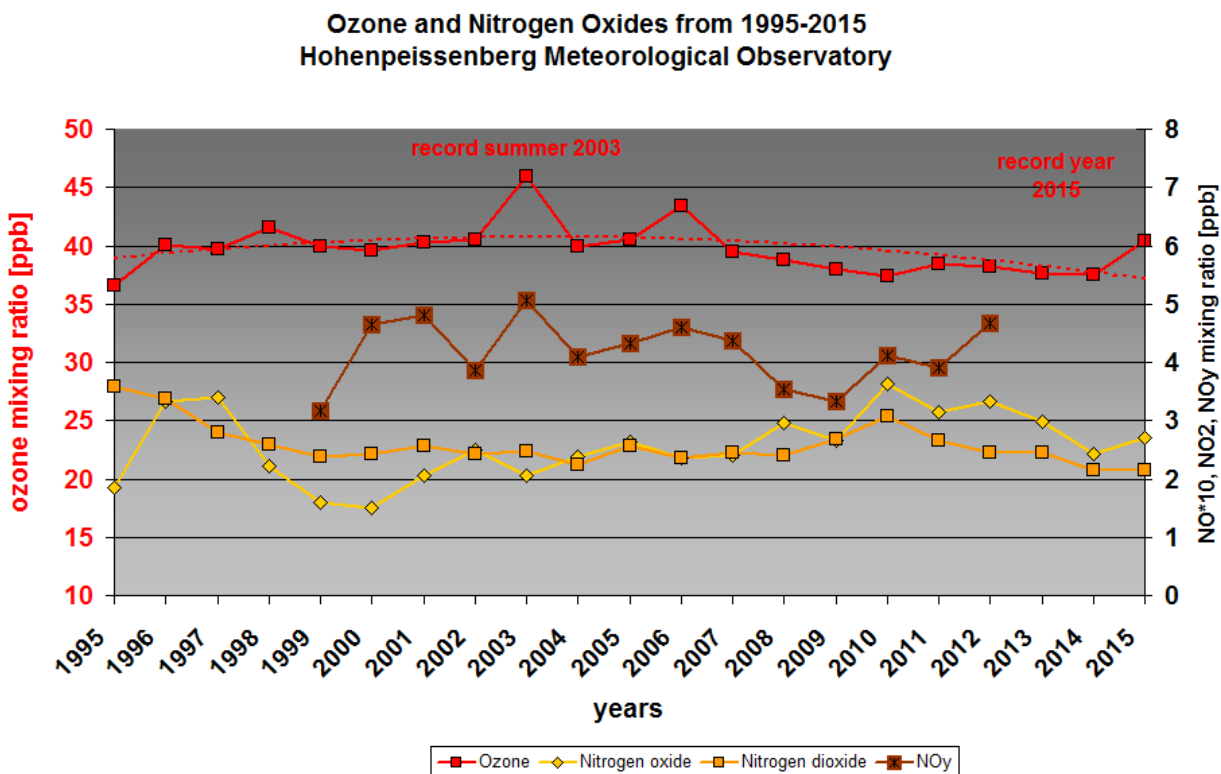


Figure 1. *In situ* ozone and nitrogen oxides mixing ratios at Hohenpeissenberg from 1995 till 2015.

Long-term Measurements from the GAW Cape Verde Atmospheric Observatory (CVAO)

K.A. Read^{1,2}, J.R. Hopkins^{1,2}, S.Punjabi^{2,1}, J.D. Lee^{1,2}, L.M. Neves³, C.Reed⁴, L.J.Carpenter², A.C. Lewis^{1,2} and Z. Fleming⁵

¹University of York, National Centre for Atmospheric Science (NCAS), York, United Kingdom; +44-190-432-2565, E-mail: katie.read@york.ac.uk

²University of York, Department of Chemistry, Wolfson Atmospheric Chemistry Laboratories (WACL), York, United Kingdom

³Instituto Nacional de Meteorologia e Geofísica (INMG), Mindelo, Republic of Cape Verde

⁴Cranfield University, Facility for Airborne Atmospheric Measurements (FAAM), Cranfield, United Kingdom

⁵University of Leicester, National Centre for Atmospheric Science (NCAS), Leicester, United Kingdom

We present over ten years of measurements from the Global Atmospheric Watch (GAW) Cape Verde Atmospheric Observatory (CVAO, 16,848°N, 24.871°W), a subtropical marine boundary layer atmospheric monitoring station situated on the island of São Vicente. Almost continuous measurements of the trace gases, ozone (O₃), carbon monoxide (CO), non-methane volatile organic compounds (NMVOC), nitric oxide (NO), and nitric dioxide (NO₂), along with meteorological parameters, have been obtained. Other data from the CVAO, for example of greenhouse gases, aerosol, halocarbons, halogen oxides, total gaseous mercury (Global Mercury Observation System) are also available over various timescales. This year we add sulfur dioxide (SO₂) to the suite of measurements. Recent published work includes our discovery of nitrate aerosol as a dominant source of NO_x in the remote marine boundary layer, and analysis of our 4-year total gaseous mercury record, which suggests influence from an unregulated source of mercury from West Africa. We also present some early trend analyses and interpretation of our longer datasets. This September the MarParCloud campaign will be taking place at the CVAO, a project concerned with marine biogenic production, organic aerosols and maritime clouds. We also plan to carry out some air pollution measurements in the city of Mindelo alongside the Cape Verde national mobile air pollution monitoring facility. The CVAO has two sampling towers (7.5m and 30m) and additional air-conditioned space to accommodate visiting instrumentation. It is a global GAW station and data is submitted regularly to the World data centres (WDCGG and WDRG) in addition to the Centre for Environmental Data Analysis (CEDA, formerly BADC), along with associated metadata.

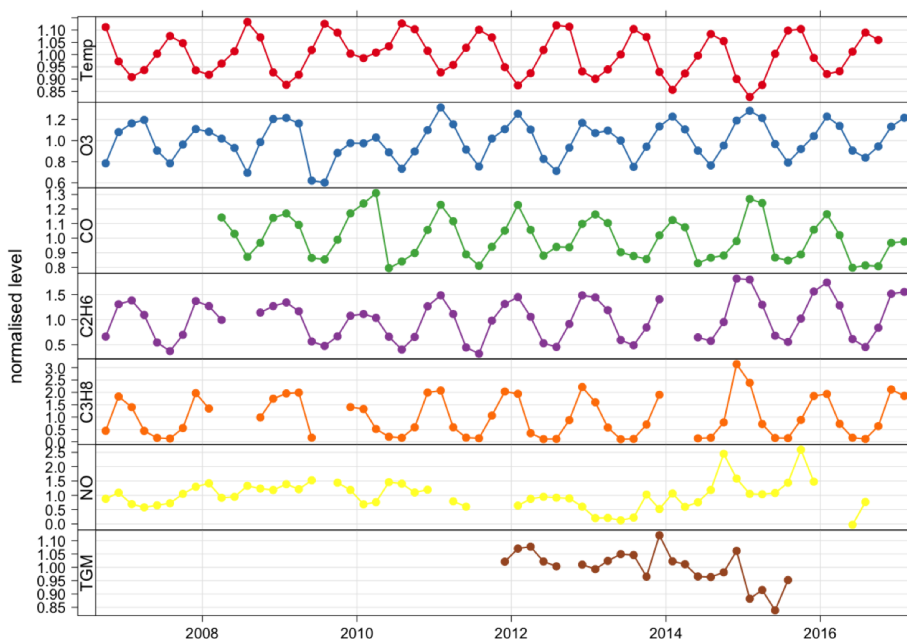


Figure 1. Time-series of species from the CVAO with concentrations normalised to their individual means over the entire time period.

Lanyu (Island) Station – New Horizons of the Western Pacific Ocean in Background Atmospheric Chemistry and Radiation Observations

K. Lin¹, S. Wang², Y. Lee¹, N. Lin^{2,3}, W. Chen¹ and C. Ou-Yang^{2,3}

¹Central Weather Bureau, Observation Division, Taipei, Taiwan; +886-2-23491029, E-mail: adenins@cwb.gov.tw

²National Central University, Department of Atmospheric Sciences, Chung-Li, Taiwan

³National Central University, Department of Chemistry, Chung-Li, Taiwan

The Lanyu meteorological station (22.04°N, 121.56°E; 324 m) is located on the peak of Lanyu Island, approximately 70 km offshore of eastern Taiwan. Because of its special geographic location, the site is characterized by a clean maritime environment and being the front line of the typhoon watch. The weather station was built by the Japanese in 1940 for typhoon monitoring. Later in 1947, the Central Weather Bureau (CWB) started to take routine meteorological observations, which continue to this day. Since 1995, the CWB made initial *in situ* measurements for atmospheric chemical compositions (i.e., carbon dioxide (CO₂), nitrogen oxide, ozone, sulfur dioxide, and carbon monoxide) in order to respond to the WMO's recommendation. The review of the 20-year long data record from the Lanyu site will be presented in this presentation. In general, the data quality is good and the magnitudes are within a reasonable range. The CO₂ trend shows a good agreement with other background stations (i.e. Lulin, Dongsha Island). Occasionally, the influence of anthropogenic sources, such as ship emissions, has also been observed in the data set. In order to remove outliers, we performed a statistical method to remove the contamination from pollution events and calculated the baseline values for each species. The baseline values provide us with the preliminary understanding of background atmospheric conditions in the western Pacific Ocean. For future plans, we propose to upgrade *in situ* measurements and to set up a high quality radiation observation at the Lanyu site. The site will continue provide high standard data and serve as an international collaboration platform in the science community.



Figure 1. Geographic location of Lanyu Island (Captured from Google Maps).



Figure 2. The Lanyu weather station taken from quadcopter.

Variability in the Onset of Summer Monsoon over Vietnam

N.T.L. Anh¹, N.D. Mau² and C.T.T. Huong¹

¹Hanoi University of Natural Resources and Environment (HUNRE), Hanoi, Vietnam; +84-165-868-4842, E-mail: nguyentananh4895@gmail.com

²Vietnam Institute of Meteorology, Hydrology and Climate Change, Hanoi, Vietnam

In this paper, the 850 hPa winds of CFSR (Climate Forecast System Reanalysis) and OLR (Outgoing Longwave Radiation) during the period from 1982-2010 were used for analyzing the onset dates of summer monsoon over Vietnam. The 850 hPa zonal winds of CFSR was used for definition of onset dates; based on the simple yet effective index, the Vietnam summer monsoon index (VSMI) (N.D. Mau et al, 2016), the 850-hPa zonal winds averaged over the southern parts of Vietnam (5°-17°N and 100° - 110°E). The onset pentad of Vietnam summer monsoon is defined as the first pentad of the two consecutive pentads when the 850 hPa zonal wind direction changes from easterly to westerly or from less than 0 m/s to greater than 0 m/s (N.D. Mau et al, 2016). The results showed the climatological onset date of summer monsoon in Vietnam is pentad of 25,5 (7 May), with the standard deviation is 2,4 pentads. During 1981-2010, the pentads of onset summer monsoon were increasing; and it was that the onset of summer monsoon was to be later. In addition, the onset of Vietnam summer monsoon was closed to activities of the El Niño–Southern Oscillation (ENSO) phases; later in the El Niño years; and earlier in the La Niña years (Fig. 1). In addition, there is a clear similarity between the change of direction of the 850 hPa winds and the development of deep convection during the onset of summer monsoon. The onset period of summer monsoons is marked by a suddenly changes in 850 hPa winds (from eastly winds to westly winds), which is reflected by the apparent difference in pentad-1 circulation with pentad-0 (Fig. 2).

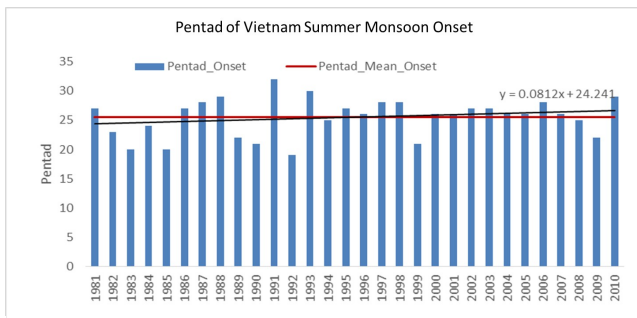


Figure 1. Trends of the onset pentads of Vietnam summer monsoon during 1981-2010.

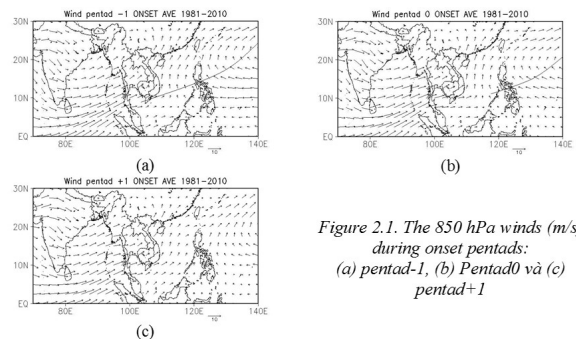


Figure 2.1. The 850 hPa winds (m/s) during onset pentads: (a) pentad-1, (b) Pentad0 và (c) pentad+1

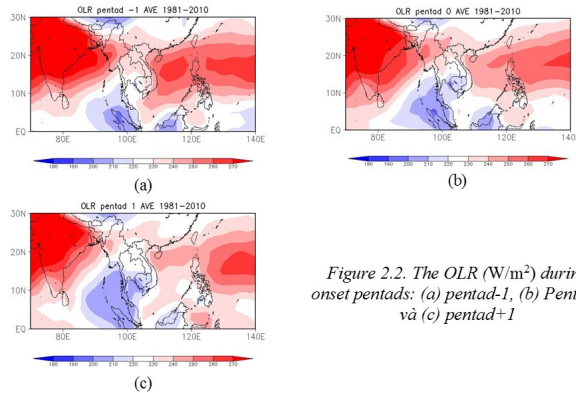


Figure 2.2. The OLR (W/m²) during onset pentads: (a) pentad-1, (b) Pentad0 và (c) pentad+1

Figure 2. Changes in 850 hPa winds (Fig 2.1) and OLR (Fig. 2.2) during onset pentads of Vietnam summer monsoon.

Variability and Trends of Withdraw for the Summer Monsoon over Vietnam

P.T.M. Linh¹, N.D. Mau² and C.T.T. Huong¹

¹Hanoi University of Natural Resources and Environment (HUNRE), Hanoi, Vietnam; 84-1646896516, E-mail: phungmylinh165@gmail.com

²Vietnam Institute of Meteorology, Hydrology and Climate Change, Hanoi, Vietnam

In this paper, the 850 hPa winds of CFSR (Climate Forecast System Reanalysis) and OLR (Outgoing Longwave Radiation) during the period from 1982-2010 were used for analyzing the withdraw dates of summer monsoon over Vietnam. The criteria of withdraw for the Vietnam summer monsoon is defined by the simple index, the Vietnam summer monsoon index (VSMI) (N. D. Mau et al, 2016) or the mean 850-hPa zonal winds over the southern parts of Vietnam (5°-17°N and 100° - 110°E), when the first pentad of the easterly 850 hPa winds in the two consecutive pentads. The results showed that the climatological withdraw date of Vietnam summer monsoon is approximately pentad 65 to 66. The withdraw pentads were increasing during 1981-2010; which means that withdraw dates were trending towards later. The variability of the withdraw pentads was quite large; the latest pentad was 70 in 2009 and the earliest pentad was 61 in 1981 and 1984. The variability of the withdraw summer monsoon was closely related to El Niño-Southern Oscillation (ENSO) activities; with later dates in El Niño phases and earlier dates in La Niña phases (Fig. 1). The results also showed that the changes in 850 hPa winds and OLR was slow with the southwardly movement of the Western Pacific Subtropical High during the withdraw of the summer monsoon. The most prominent feature of the circulation during withdraw of the summer monsoon is the gradual retreat of western winds to the west and the expansion of the Western Pacific Subtropical High pressure to the west (Fig. 2).

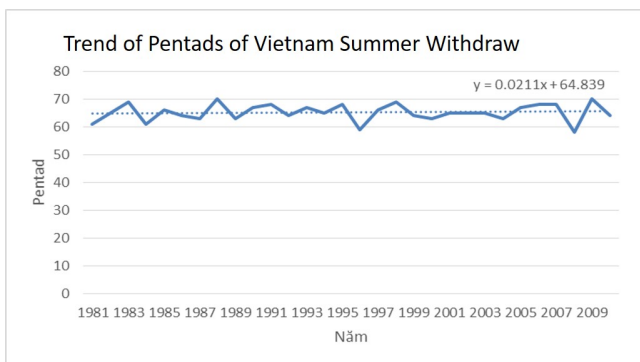


Figure 1. Trends of the withdraw pentads of Vietnam summer monsoon during 1981-2010.

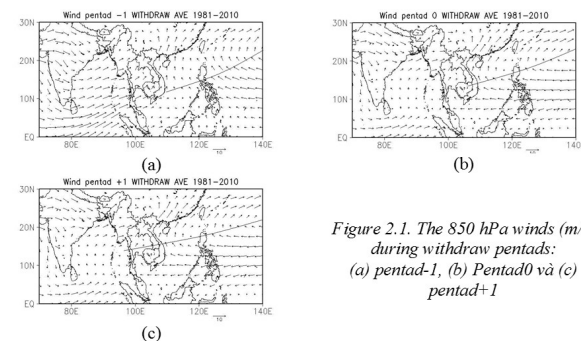


Figure 2.1. The 850 hPa winds (m/s) during withdraw pentads: (a) pentad-1, (b) Pentad0 và (c) pentad+1

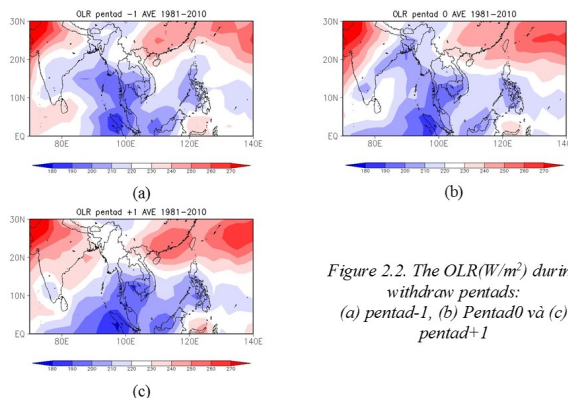


Figure 2.2. The OLR(W/m²) during withdraw pentads: (a) pentad-1, (b) Pentad0 và (c) pentad+1

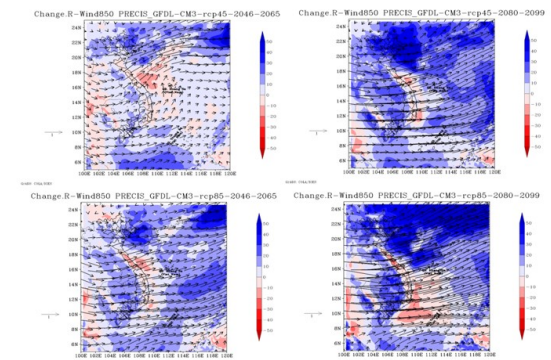
Figure 2. Changes in 850 hPa winds (Fig 2.1) and OLR (Fig. 2.2) during withdraw pentads of Vietnam summer monsoon.

Projections of Variability and Trends of Summer Monsoon Rainfall over Vietnam

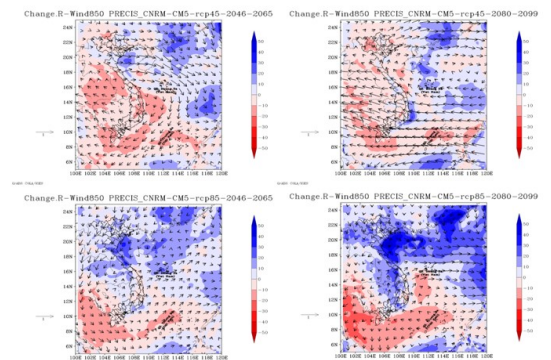
N.D. Mau, N.V. Thang and M.V. Khiem

Vietnam Institute of Meteorology, Hydrology and Climate Change, Hanoi, Vietnam; +84-4-62728299, E-mail: mau.imhen@gmail.com

In this paper, the variability and trends of summer monsoon rainfall of near-future (2046-2065) and far-future (2080-2099) compared with a baseline period (1986-2005) over Vietnam are projected by the PRECIS model under RCP4.5 and RCP8.5 scenarios. In this study, the PRECIS model was driven by the CNRM-CM5 (PRECIS/CNRM-CM5) and GFDL-CM3 (PRECIS/GFDL-CM3) for the baseline simulation (1986-2005) and future projections (2046-2065 and 2080-2099). The variability of summer monsoon rainfall was defined by the standard deviation (SD). The trend analysis shows that the trend of the 21st century average monsoon rainfall is increasing under PRECIS/GFDL-CM3 projections in both RCP4.5 and RCP8.5 scenarios. However, the PRECIS/CNRM-CM5 shows the 21st century average monsoon rainfall is increasing in the RCP8.5 scenarios; and decreasing in the RCP4.5 scenario. The PRECIS/GFDL-CM3 and PRECIS/CNRM-CM5 show the increasing of variability of summer monsoon rainfall during near-future under both RCP4.5 and RCP8.5, with the increasing rate of SD is about 0 to 80% compared with baseline simulation. However, both PRECIS models show the little change and decreasing in SD during far-future compared with baseline simulation.

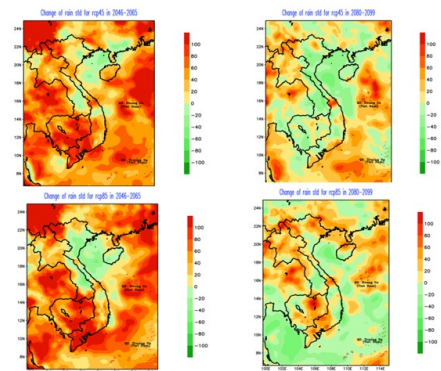


a) Changes in 850 winds (vector, m/s) and summer rainfall (shaded, %) by PRECIS/GFDL-CM3: RCP4.5 (above) and RCP8.5 (below); near future (2046-2065, Left), far future (2080-2099, Right)

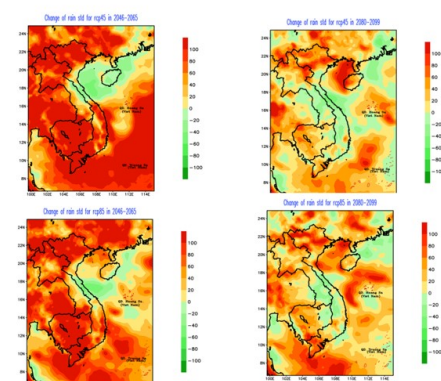


b) Changes in 850 winds (vector, m/s) and summer rainfall (shaded, %) by PRECIS/CNRM-CM5: RCP4.5 (above) and RCP8.5 (below); near future (2046-2065, Left), far future (2080-2099, Right)

Figure 1. Projections of changes in 850 winds (vector, m/s) and summer rainfall (shaded, %) compared with baseline simulation: (a) PRECIS/GFDL-CM3 and (b) PRECIS/CNRM-CM5; RCP4.5 (above) and RCP8.5 (below); near-future (2046-2065; Left), far-future (2080-2099; Right).



a) Changes in SD (shaded, %), by PRECIS/GFDL-CM3: RCP4.5 (above) and RCP8.5 (below); near future (2046-2065, Left), far future (2080-2099, Right)



b) Changes in SD (shaded, %), by PRECIS/CNRM-CM5: RCP4.5 (above) and RCP8.5 (below); near future (2046-2065, Left), far future (2080-2099, Right)

Figure 2. Projections of changes in SD (shaded, %) compared with baseline simulation: (a) PRECIS/GFDL-CM3 and (b) PRECIS/CNRM-CM5; RCP4.5 (above) and RCP8.5 (below); near-future (2046-2065; Left), far-future (2080-2099; Right).

Study of the Diurnal Cycle of Microphysical Properties of Clouds in the Amazon Basin using GOES Measurements

A.C.P. da Silva and A.L. Correia

Institute of Physics, University of São Paulo, São Paulo, Brazil; +55 11 3091-6925, E-mail: andrecps@if.usp.br

The Amazon Basin plays a fundamental role in the hydrological cycle and the energy budget for the planet, since its mass and energy fluxes of water vapor, sensible and latent heat are crucial to global circulation and precipitation patterns. These energy and mass exchanges occur through precipitation, cloud formation and dissipation cycles. Therefore, understanding the formation and evolution of clouds has great importance for the global energy balance. In the case of the Amazon, however, there are still major gaps in the knowledge of the physical processes that affect the life cycle of clouds. For example, models predict precipitation early in the morning, with precipitation events usually being observed early in the afternoon. This occurs due to limitations in representation in hot convective cloud models and the transition to deep convective clouds. In this work, we used a set of radiance measurements performed by channels 1, 2 and 4 (0.63, 3.9 and 11 μm , respectively) of NOAA Geostationary Operational Environmental Satellite (GOES) and radiative transfer codes to obtain estimates of cloud optical depth, as well as the effective radius of droplets and ice particles in convective clouds. We studied how these microphysical parameters vary throughout the day in the Amazon region during the dry and wet seasons. The results will be analyzed and compared, aiming correlating their variation with atmospheric aerosol load and to assess the processes of convective cloud formation and development in the Amazon.

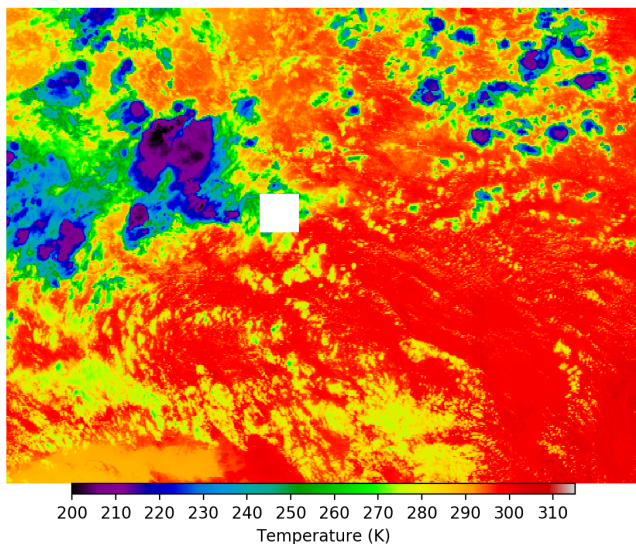


Figure 1. Example of measurement of the brightness temperature obtained through channel 4 of the GOES on the Amazon basin. The white square in the center corresponds to the area used to obtain the data plotted in Figure 2.

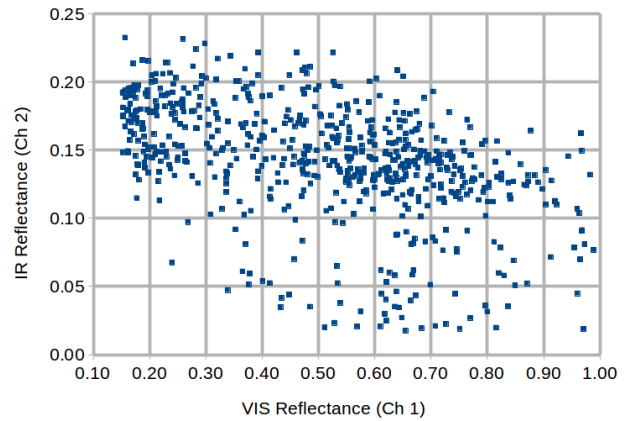
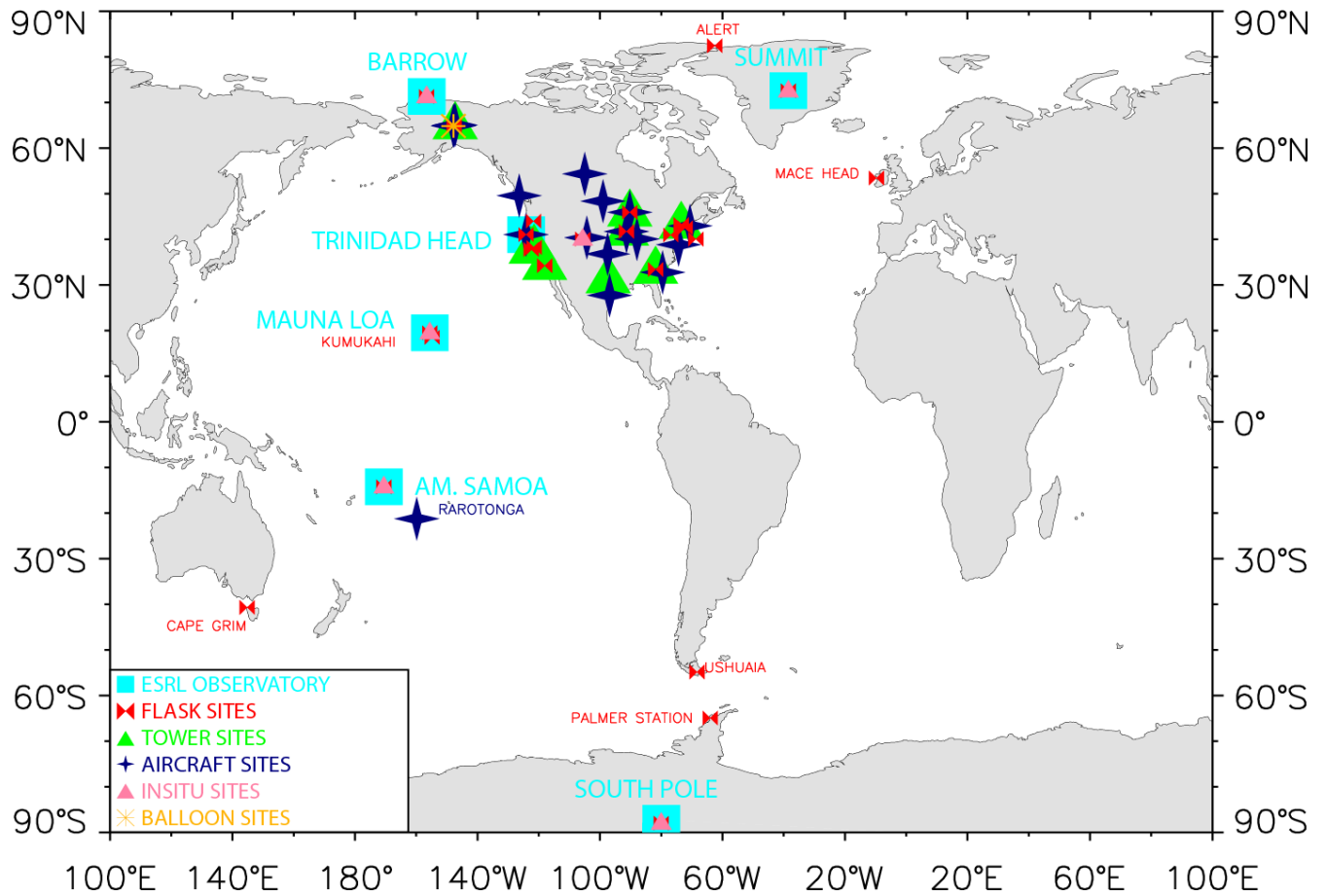


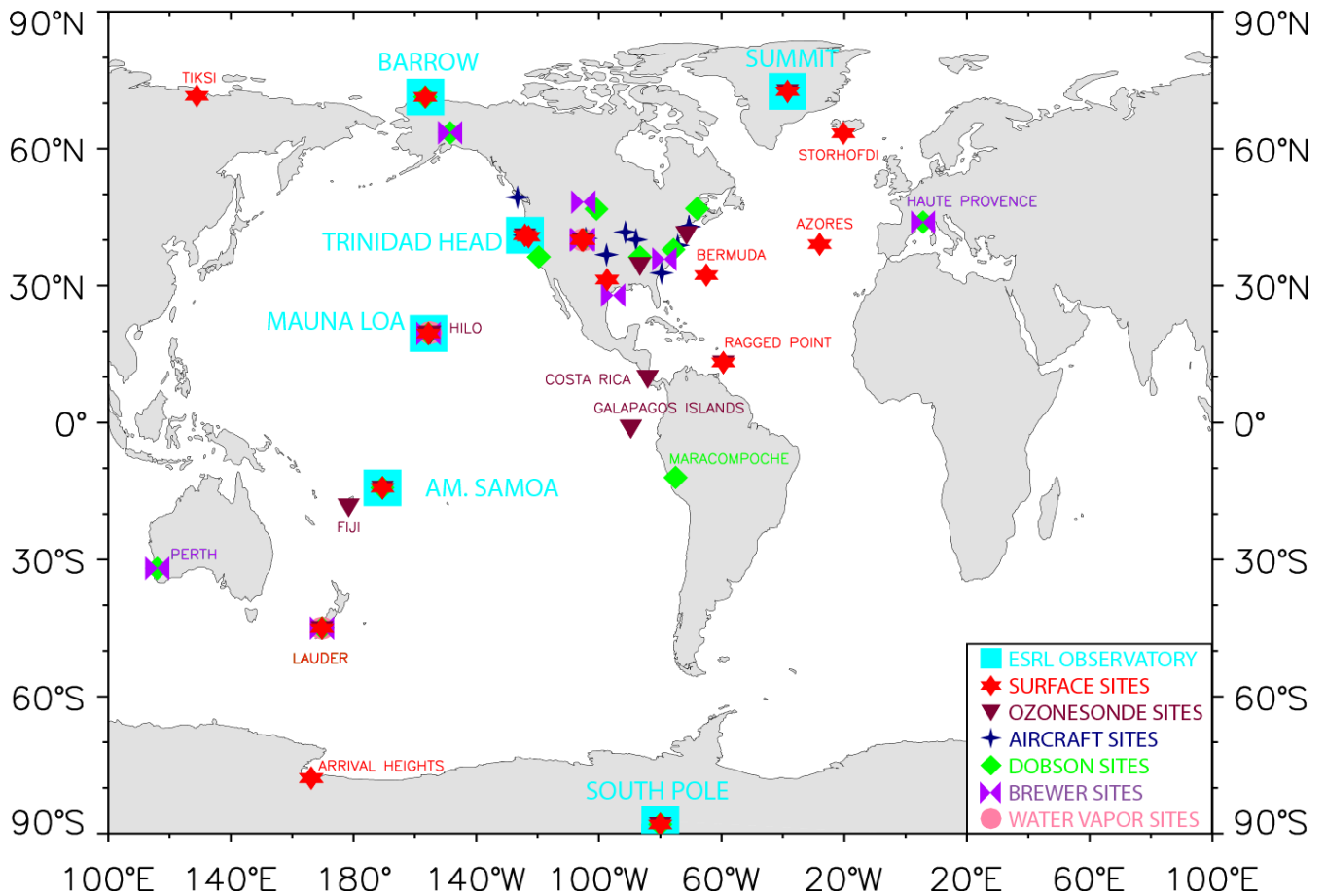
Figure 2. Reflectance values in channel 2 as a function of the reflectance in visible channel, corresponding to the white square of Figure 1.

Notes:

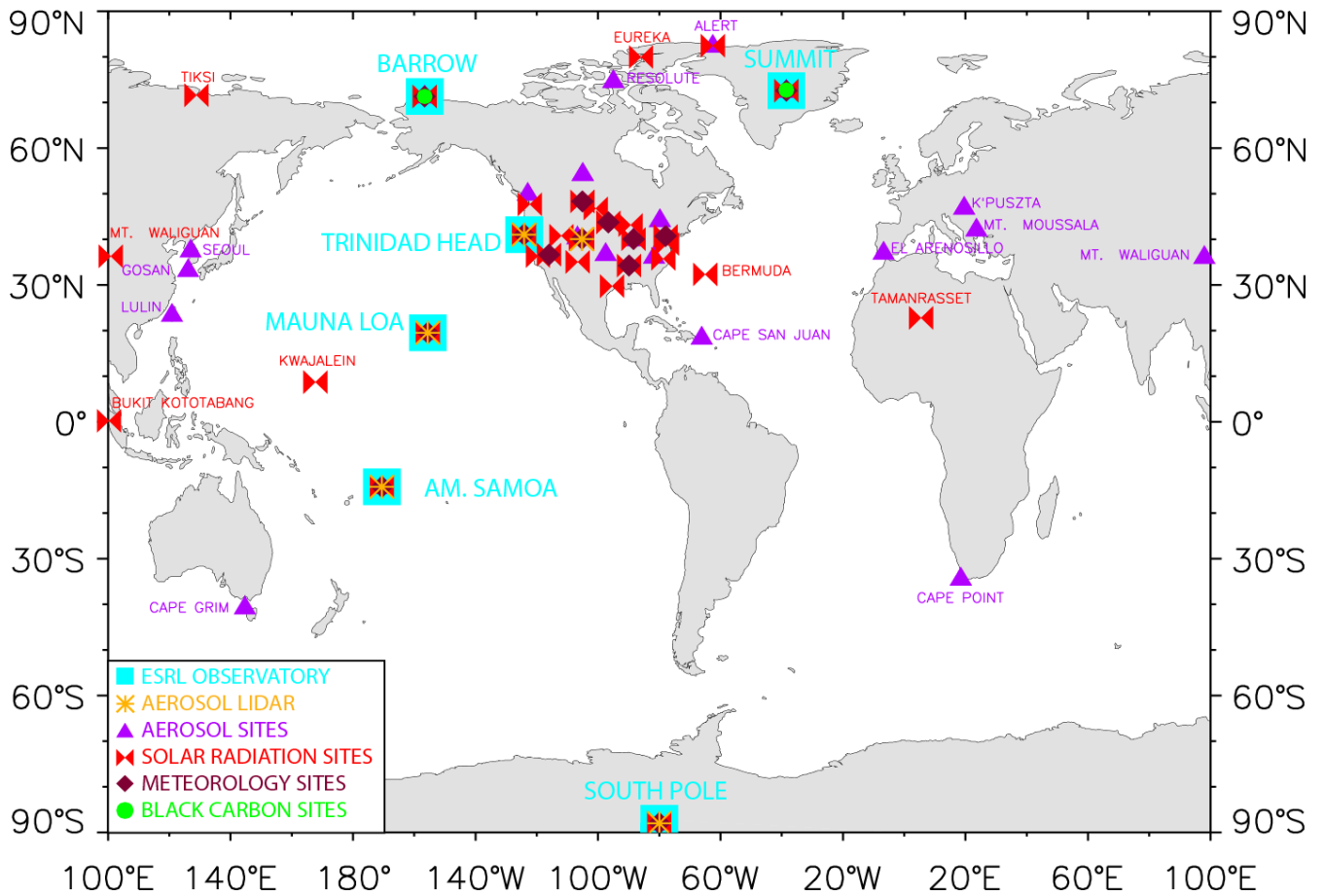
NOAA ESRL Halocarbons and Atmospheric Trace Species Network



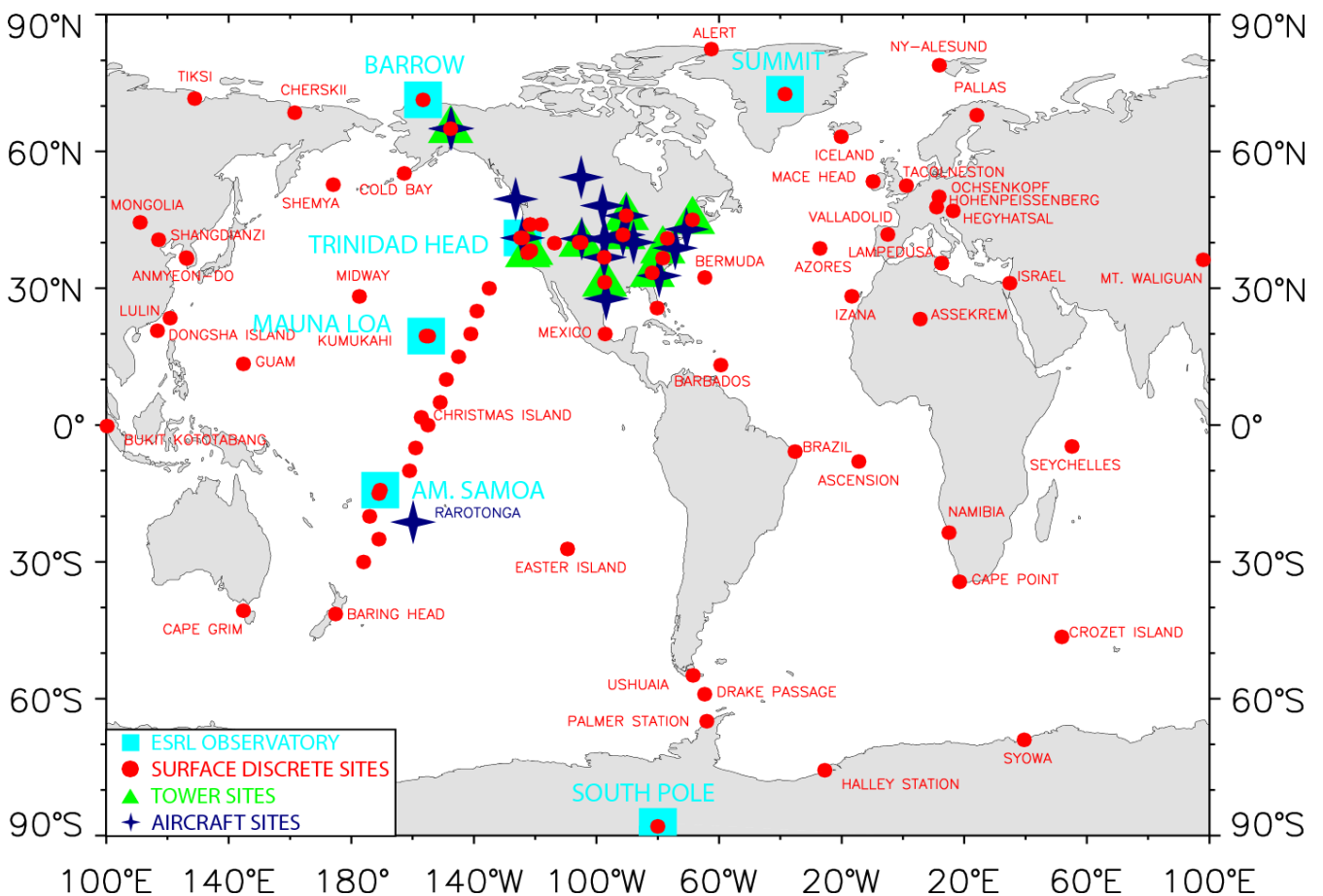
NOAA ESRL Ozone and Water Vapor



NOAA ESRL Aerosols, Solar Radiation, Meteorology and Black Carbon



NOAA ESRL Carbon Cycle Greenhouse Gases





2017 Global Monitoring Annual Conference

